THE ROLE OF THE NUCLEAR ENVELOPE

IN REGULATION OF AGEING

A thesis submitted for the degree of Doctor of Philosophy

Marek Mateusz Drożdż

Sir William Dunn School of Pathology

Lincoln College

University of Oxford

Trinity Term 2015

Abstract

THE ROLE OF THE NUCLEAR ENVELOPE IN REGULATION OF AGEING

Marek Mateusz Drozdz
Sir William Dunn School of Pathology and Lincoln College
University of Oxford

Thesis submitted for the degree of Doctor of Philosophy
Trinity Term 2015
(word count: 48 200)

Cellular senescence is a phenomenon characterised by stable and durable states of proliferative arrest induced by various stress stimuli. The abundance of senescent cells in tissues increases over a lifetime and, among other functions, they have been proposed to play a pivotal role in ageing. Hutchinson-Gilford progeria syndrome (HGPS) is a disease characterised by segmental premature ageing. It is caused by the expression of a persistently farnesylated lamin A isoform. Strikingly, HGPS patients show an increased abundance of senescent cells. Therefore the relationship between the farnesylated lamin A precursor, prelamin A, and senescence was studied in this thesis.

Cellular models of ageing in human dermal fibroblasts were established. They relied on either replicative exhaustion or prelamin A accumulation. An unbiased genome-wide transcript analysis of the ageing models revealed that a significant part of the common senescence programme during cellular ageing can be replicated in young cells by accumulating prelamin A. The most prominent and overlapping expression changes were observed in pathways regulating inflammation, lipid metabolism and cholesterol homeostasis. Six genes, identified as underexpressed consistently across the studied ageing models, were tested functionally in the context of senescence regulation by prelamin A. The ability of prelamin A-accumulating cells to induce inflammation has also been demonstrated by multiplexed detection of secreted cytokines, chemokines and other factors. This confirms that a significant overlap between replicative and prelamin A-induced senescence exists not only at mRNA level changes, but is also observed at the level of secreted proteins. Finally, nuclear morphology was studied in the ageing models, with a particular interest in the formation of a nucleoplasmic reticulum. We identified NOGO/Reticulon-4 as a new protein involved in the process of NR formation, and also demonstrated that new NR channels require incorporation of newly synthesised lipid and protein components. The research presented in this thesis offers a new insight into a role of the prelamin A maturation process in senescence and ageing.

Acknowledgements

There are many people who have played a significant role in my time as a DPhil student, and deserve acknowledgement and gratitude for their part during this process.

I would especially like to thank Prof. David Vaux, not only for his supervision and support, both inside and outside of the laboratory, but also for his guidance and insight into my research. He provided indispensable advice that advanced my work, and gave direction when it was needed.

Dr Ashraf Malhas who first introduced me to experiment set ups and analysis in the Vaux Lab. He instructed me on many techniques utilized in my research, without which, this thesis would not have been possible. He is valued not only for his technical and instructional skills, but also for his intellect, and most importantly, his friendship.

I would also like to thank the members of the Vaux Lab, past and present: Drs Letitia Jean, Ivan Boubriak, Chongsoo Lee, Aileen Moloney, Sameer Sengupta, and Mr Helder Carmen. They have provided endless hours of stimulating discussion over lunches, coffee breaks, as well as in the laboratory. They fostered a collegial work environment and their friendships will be appreciated for a lifetime. Their collective intellect and support have made an arduous process much more enjoyable.

Mr Kurun Kumar and Mr Alessandro Francioni, the students whom I supervised, whose work significantly contributed to the data presented in Chapter 7. Their enthusiasm and excitement in the pursuit of research served to reinvigorate my own path of scientific discovery.

Dr Haibo Jiang, for his analysis of cell samples using nanoSIMS, presented in Chapter 7. Dr Margarita Schlackow, for her help and advice on bioinformatical analysis of microarray data, presented in Chapter 4.

To the Dunn School of Pathology and the EPA Trust for DPhil studentship, without whose funding this research would not have been possible.

And last, but certainly not least, my heartfelt appreciation to my beloved wife Kasia, whom I cannot thank enough for her constant love, support, and belief in me.

Table of Contents

List of Figures

Abbreviations

BSE	back scattered electron microscopy
CaaX	motif cysteine (C), aliphatic (a), aliphatic (a), any amino acid residue (X)
CDK	cyclin-dependent kinase
DAR	darunavir
DDIS	DNA-damage-induced senescence
DDR	DNA damage response
DMSO	dimethyl sulphoxide
ECM	extracellular matrix
EM	electron microscopy
ER	endoplasmic reticulum
FCS	foetal calf serum
FDR	false discovery rate
FTI	farnesyl transferase inhibitor
GMFI	geometric mean fluorescence intensity
GSEA	gene set enrichment analysis
HDFs	human dermal fibroblasts
HGPS	Hutchinson-Gilford progeria syndrome
HIV-PI	HIV protease inhibitor
ICMT	isoprenyl cysteine methyl transferase
IGFBP	insulin-like growth factor binding protein
INM	inner nuclear membrane

KEGG	Kyoto Encyclopedia of Genes and Genomes
MMP	matrix metalloproteinase
NanoSIMS	nano secondary ion mass spectrometry
NCS	nucleolar channel system
NE	nuclear envelope
NF-κB	nuclear factor κB
NLS	nuclear localisation sequence
NPC	nuclear pore complex
NR	nucleoplasmic reticulum
OIS	oncogene induced senescence
ONM	outer nuclear membrane
PBS	phosphate buffered saline
PFA	paraformaldehyde
PNS	perinuclear space
PPAR	peroxisome proliferator-activated receptors
qRT-PCR	quantitative real time polymerase chain reaction
RB	retinoblastoma
Rce1	ras converting enzyme
RD	restrictive dermopathy
ROS	reactive oxygen species
SAHF	senescence associated heterochromatin foci
SAQ	saquinavir
SASP	senescence associated secretory phenotype
SAβGal	senescence associated β-galactosidase

siRNA	small inhibitory RNA
SREBP	sterol regulatory element binding protein
TX-100	triton X-100
UPR	unfolded protein response
WS	Werner syndrome
Zmpste24	mammalian zinc metalloprotease Ste24p

CHAPTER 1

1 Introduction

Cellular senescence is characterised by extremely stable and durable form of proliferative arrest induced by various stress stimuli. Over a lifetime the abundance of senescent cells in tissues increases and, among other functions, they have been proposed to play a pivotal role in ageing. Farnesylated precursor of lamin A, called prelamin A, which is a component of nuclear lamina was also observed to accumulate with ageing. Furthermore, in Hutchinson-Gilford progeria syndrome (HGPS), a disease characterised by segmental premature ageing and caused by the expression of a persistently farnesylated lamin A isoform, an increased abundance of senescent cells has been observed. Therefore, the relationship between prelamin A and senescence was the subject of this thesis and background information about senescence and nuclear lamina is summarised below.

1.1 Concept of cellular senescence

Cellular senescence is a phenomenon characterised by an essentially permanent cell-cycle arrest in response to a range of detrimental stressors in order to limit propagation of damaged cells. Cells can undergo senescence in several different ways (described in more detail below) in response to DNA damage, activation of oncogenes or their telomere attrition after the cells have undergone a large number of cell divisions. Senescence is defined by a number of markers and morphological changes which allow senescent cells to be distinguished from other non-dividing cells, such as quiescent or terminally differentiated cells. Unlike quiescent cells which can re-enter

mitosis, senescence cells lose their proliferative abilities and remain unresponsive to mitogenic stimuli. Although senescence was first observed in primary cell cultures, there is an overwhelming body of evidence demonstrating cellular senescence *in vivo.* Senescence, along with programmed cell death pathways, is primarily recognised as a mechanism preventing tumourigenesis. The complexity of cellular changes associated with the senescent phenotype, including altered gene expression and secretory pathways, implies its role in a broader spectrum of functions and pathologies. Interestingly, senescent cells may exhibit pro-tumorigenic action, depending on the cell-context. It is also believed that senescence plays a major role in tissue remodelling, both in adults and during embryogenesis. Most importantly, however, new reports are continuously emerging linking senescence to the ageing process.

1.1.1 Types of senescence

Senescence was first described over five decades ago when Leonard Hayflick and Paul Moorhead observed that normal human fibroblasts demonstrated limited proliferative capacity in culture (Hayflick, 1965; Hayflick and Moorhead, 1961). When the cell proliferative limit (today referred to as the Hayflick limit) was reached, it resulted in a permanent cell-cycle arrest during which the cells remained viable and metabolically active. Although Hayflick and Moorhead's results were questioned extensively when first published, it is now widely-accepted that normal primary cells do not grow in culture indefinitely. Now we know that this behaviour of cultured human cells is a result of telomere loss following many rounds of DNA replication in the absence of endogenous telomerase activity (Harley et al., 1990; Shay and

Wright, 2000). Indeed, when an exogenous telomerase was introduced into human cells it resulted in delayed onset of senescence (Bodnar et al., 1998).

Senescence caused by telomere attrition and presumably coupled with oxidative damage, is known as replicative senescence. Senescence induction, however, may occur through various other mechanisms (Figure 1.1) (Campisi, 2013; Pawlikowski et al., 2013). It may be triggered by the activation of certain mitogenic oncogenes or the loss of anti-mitogenic tumour-suppressors (e.g., Myc, RAS, B-Raf, PTEN), herein referred to as oncogene-induced senescence (OIS) (Collado et al., 2007; Gorgoulis and Halazonetis, 2010; Kuilman et al., 2010; Serrano et al., 1997). DNA-damaging agents like ionizing radiation and chemotherapeutic drugs can lead to DNA-damage induced senescence (DDIS) that is distinct from telomere loss. In addition, many other senescence stimuli have been identified. Reactive metabolites, like reactive oxygen species (ROS), fatty acids, ceramides, elevated glucose levels or the proteotoxic stress caused by protein aggregation and unfolded protein response (UPR) can also induce a senescent state (d'Adda di Fagagna, 2008; Passos et al., 2010; Rodier and Campisi, 2011; Saretzki and Von Zglinicki, 2002; Sitte et al., 2000; Weyemi et al., 2012). Inadequate cell culturing condition is recognised as a factor that may lead to stress-induced senescence, also referred as a cell culture shock (Sherr and DePinho, 2000). Indeed, cell culture conditions differ in many aspects from tissue environment. Disruption of cell-cell contacts, lack of interactions with different cell types and absence of appropriate survival factors, hyperoxia, and growing cells on plastic are likely to induce senescence to explanted cells. Despite the seemingly broad range of senescence stimuli, their signalling is transduced through an integrated network

of effector pathways that ultimately leads to the establishment of a stable growth arrest rather than cell death.

Senescence, in principle, is a mechanism that fulfills a similar function

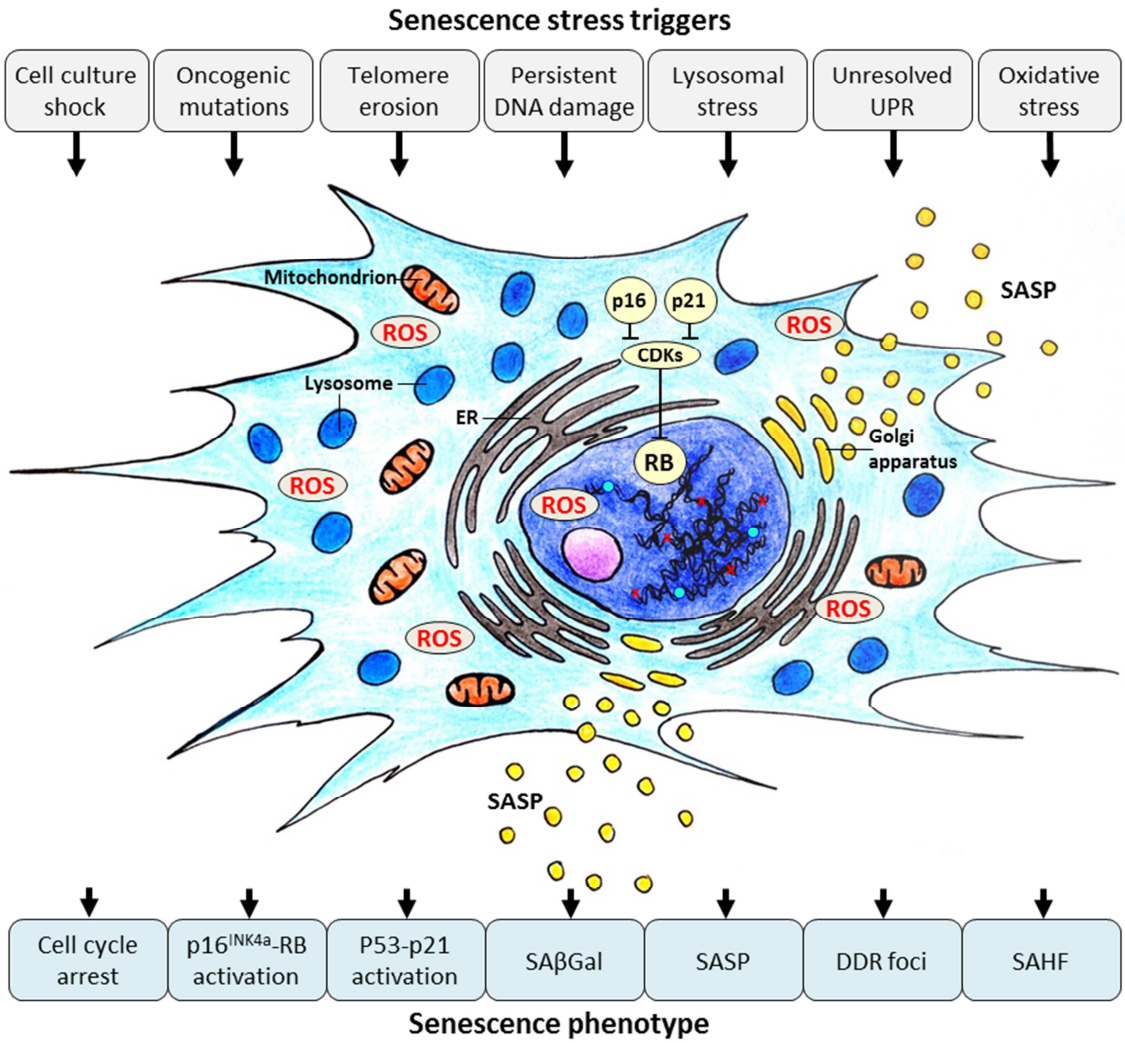

Figure 1.1. Senescent cell characteristics.

Multiple stress signals can trigger senescence and induce a stable cell-cycle arrest, accompanied by senescence biomarkers. Both $p16^{INK4a}$ and p21, through inhibition of specific cyclin-dependent kinases (CDKs) in the cytoplasm, prevent phosphorylation of RB hence enforcing proliferation arrest. In the nucleus DNA damage is depicted by red x, while the SAHF by blue circles. Cytoplasm is abundant in lysosomes containing SAβ-Gal. Senescent cell contains elevated ROS levels and is secreting a range of factors, collectively known as SASP, which exhibit both autocrine and paracrine effects. SAβGal, senescence-associated β-galactosidase; SASP, senescence associated secretory phenotype; DDR, DNA damage response; SAHFs, senescence-associated heterochromatic foci; ROS, reactive oxygen species; UPR, unfolded protein response.

to apoptosis, the prevention of proliferation of damaged cells. Apoptosis has been classified into several subtypes, depending on the cell death modalities observed under varying stimuli (Galluzzi et al., 2012). Similarly, the exact mechanisms that ultimately lead to the senescent phenotype may vary between species, cell types, and the response to different cellular stresses.

1.1.2 Senescence biomarkers

Senescence is identified by a collection of cellular characteristics (Figure 1.1) (Collado et al., 2007; Salama et al., 2014; Sharpless and Sherr, 2015). Morphologically, in *in vitro* culture, senescent cells become enlarged, flattened, vacuolated, and sometimes demonstrate multinucleation (Hayflick, 1965). These changes may be absent in *in vivo* senescence, however, because tissue architecture may dictate cell morphology.

The most widely used biomarker of senescent cells is senescence-associated β-galactosidase (SAβGal) activity measured at suboptimal pH 6.0 (Dimri et al., 1995). Endogenous β-galactosidase is a lysosomal enzyme showing optimal activity at pH 4.0-4.5 and is normally not detected when assays are run at a neutral pH. Senescent cells demonstrate enlargement of the lysosomal compartment and overexpress β-galactosidase. It is therefore possible to detect the enzyme's activity at suboptimal pH 6.0 in these cells (Kurz et al., 2000; Lee et al., 2006). Autophagy observed in senescent cells likely further contributes to increased lysosomal content and SAβGal activity (Ivanov et al., 2013; Young and Narita, 2010; Young et al., 2009). The assay for SAβGal detection utilises an artificial substrate of β-galactosidase, the X-Gal, which is hydrolysed by the enzyme, and produces a blue precipitate (Itahana et al., 2007).

Due to the convenience of this method and its ability to distinguish between senescent and non-senescent cells (e.g., quiescent) in a mixed population, both in culture and in tissues, the SAβGal assay is the most commonly used for determination of the senescent state. This method has limitations though, and requires fresh or frozen samples for the enzymatic reaction to occur.

Another emerging marker of senescent cells that can overcome these limitations is histochemical Sudan Black B stain specific to lipofuscin, a lysosomal aggregate of oxidised proteins, metals, and lipids (Georgakopoulou et al., 2013). Lipofuscin, also known as an "age pigment", is considered a hallmark of ageing as it accumulates progressively in aged post-mitotic tissue (Jung et al., 2007; Terman and Brunk, 2004). Histochemical staining of lipofuscin has been demonstrated to work with formalin-fixed and paraffin-embedded tissue, as well as with fresh samples (Georgakopoulou et al., 2013). More importantly, the Sudan Black B stain co-localises with SAβGal-positive cells.

Many common mediators of senescence, involved in regulation of cell-cycle progression, are recognised as canonical senescence markers (Kuilman et al., 2010; Muñoz-Espín and Serrano, 2014; Sharpless and Sherr, 2015). Among them are p53, p21, p15, p27, hypophosphorylated Retinoblastoma (RB), ARF, and probably the second most widely used senescence marker, $p16^{INK4a}$ (Campisi and d'Adda di Fagagna, 2007; Chandler and Peters, 2013). $p16^{INK4a}$ is a tumour suppressor that selectively inhibits cyclin-dependent kinase CDK4 and CDK6 (Serrano et al., 1993). It is expressed at very low levels or is undetectable in most cells and tissues under normal conditions. Senescence induction, however, achieved through multiple pathways, leads to a significant increase in $p16^{INK4a}$ expression and cell-cycle arrest (Alcorta et al.,

1996; Brenner et al., 1998; Collins and Sedivy, 2003; Hara, 1996; Jacobs and de Lange, 2004; Le et al., 2010; Ohtani et al., 2004; Serrano et al., 1997; Stein et al., 1999). Moreover, $p16^{INK4a}$ expression steadily increases with physiological ageing in multiple tissues in both mice and humans (Krishnamurthy et al., 2004; Liu et al., 2009; Nielsen et al., 1999; Ressler et al., 2006; Waaijer et al., 2012; Zindy et al., 1997). Activity of $p16^{INK4a}$ has also been shown to negatively impact progenitor cell renewal capacity. This capacity for renewal declines with ageing in multiple tissues (Janzen et al., 2006; Krishnamurthy et al., 2006; Molofsky et al., 2006).

Expression of $p16^{INK4a}$ may contribute to the formation of senescence-associated heterochromatin foci (SAHF), another marker of senescence (Chandra et al., 2012; Narita et al., 2003; Zhang et al., 2005). These foci are characterised by the presence of heterochromatin markers including trimethylation at Lys9 of histone 3 (H3K9me3), binding of heterochromatin protein 1 (HP1), high-mobility group A (HMGA) proteins, and macroH2A histone variant. SAHF formation is mediated through activation of the RB tumour suppressor and subsequent silencing of critical pro-proliferative genes. The SAHF marker is not a common feature in all types of senescence though. SAHF are predominantly formed during OIS, but are dispensable for replicative senescence, and occur in a cell-type specific manner (Di Micco et al., 2011; Kosar et al., 2011). They also appear to be absent in organismal ageing (Scaffidi and Misteli, 2006). Other alterations in chromatin structure that are observed in senescence are persistent DNA damage foci, termed DNA-SCARS. DNA-SCARS are DNA segments with chromatin alterations reinforcing senescence (Rodier et al., 2011). They differ in composition from transient DNA damage foci that mark repairable DNA lesions. For example, they lack the DNA repair proteins RPA and RAD51, but accumulate the DNA damage

response (DDR) mediators, phospho-CHK2 and p53. DNA-SCARS have been identified in tissues under genotoxic stress (Rodier et al., 2009) and in ageing tissues, both mouse and primate (Herbig et al., 2006; Sedelnikova et al., 2004; Wang et al., 2009).

Despite the cessation of proliferation, senescent cells remain viable and metabolically active. One of the hallmarks characterising this state is the senescence-associated secretory phenotype (SASP) (Coppé et al., 2008; Tchkonia et al., 2013). Secretion of a broad range of pleiotropic factors, including immune modulators and inflammatory cytokines, extracellular matrix proteases, and growth factors is increased in senescence. This is largely in response to the activation of nuclear factor-κB (NF-κB) signalling (Chien et al., 2011). The exact composition of SASP factors may vary between cell types and the severity of senescence-inducing stimuli (Coppé et al., 2010a). It is regulated, at least partially, by persistent DDR signal. The depletion of the DDR mediators, such as ATM, CHK2 and NBS1, abates secretion of the key SASP components, like interleukin 6 (IL6) (Rodier et al., 2009). Furthermore, SASP is not only a downstream result of senescence, but also an effector mechanism that reinforces proliferative arrest by enhancing the DDR. This can occur through the binding of several ligands (IL8, GROα, ENA78, for example) to chemokine receptor 2 (CXCR2) (Acosta et al., 2008; Kuilman et al., 2008). This activity may occur in autocrine and paracrine manners, hence the SASP has the potential to co-ordinate the behaviour of a local field of cells. Due to a broad spectrum of SASP factors, their pleiotropic nature, and context-dependence of their functions, the SASP has been shown to play a role in multiple processes in both an autocrine and paracrine manner. Some of them include chronic inflammation and activation of innate immune response, alteration of tissue architecture, and stimulation of wound healing (Demaria

et al., 2014; Krizhanovsky et al., 2008; Lujambio et al., 2013; Xue et al., 2007). Surprisingly, SASP may contribute to both tumour promotion (Demaria et al., 2014; Krtolica et al., 2001) and tumour suppression (Acosta et al., 2013; Kang et al., 2011; Lujambio et al., 2013; Xue et al., 2007). Effects mediated through SASP factors, mainly attributed to their role in maintaining sterile chronic inflammation and its consequences, have also been argued to contribute to the ageing process (Chung et al., 2009; Franceschi and Campisi, 2014; Rodier and Campisi, 2011).

Several other markers associated with senescence have also been proposed. Loss of lamin B1 is a common feature observed in multiple types of cellular senescence, and in the tissue context (Freund et al., 2012; Shah et al., 2013; Shimi et al., 2011). The presence of decoy receptor 2 (DCR2, encoded by TNFRSF10D gene) and DEC1 (encoded by TNFRSF10C) was shown to be specific to senescent cells, at least in OIS (Collado et al., 2005). Since senescence is characterised by a stable cell-cycle arrest, the absence of proliferative markers, like 5-bromodeoxyuridine (BrdU) incorporation or Ki67 protein, may also complement the identification of senescent cells.

Senescence is defined by a collection of these hallmarks. It is clear however, that none of them is completely unique to the senescence programme (Sharpless and Sherr, 2015). As a result, senescent cells are identified by multiple phenotypic characteristics, rather than by a single biomarker. It has been demonstrated that despite the presence of various biomarkers of senescence, each individual biomarker may be dispensable. For example, some types of *in vitro* senescence lack $p16^{INK4a}$ expression, which can be compensated through other mechanisms and upregulation of other cell-cycle inhibitors (Beauséjour et al., 2003; Herbig et al., 2004; Yamakoshi et

al., 2009). Even the most definitive feature of senescence, the lack of proliferation, may be absent. This is seen in senescent hematopoietic stem cells in ageing. They display multiple senescence markers, and yet they retain at least partial proliferative capacity (Chen, 2011).

1.1.3 Molecular pathways in senescence

1.1.3.1 Retinoblastoma and p53, the two master regulators

Despite the diversity of senescence-inducing stimuli, the stable proliferation arrest appears to be achieved by the activation of either or both of the two gatekeeper tumour suppressors, p53 and RB (Ben-Porath and Weinberg, 2005; Campisi, 2005). Both are potent transcriptional regulators and central players in multiple pathways, with a variety of upstream regulators and downstream effectors (Sherr and McCormick, 2002). Their equally important role in the execution of cell-cycle arrest in senescent human cells is further highlighted by the fact that inactivation of both p53 and RB pathways is required in order to bypass senescence (Bond et al., 1999; Hahn et al., 2002; Shay et al., 1991; Smogorzewska and De Lange, 2002). However, preferential differences exist, both cell-type-specific and species-specific, with which either pathway is engaged. While the p53 pathway seems to be more often engaged in the early stages of senescence, activation of the RB pathway is thought to be more important for the later stage and maintenance of senescence.

The p53 pathway is primarily engaged in senescence induced by persistent DNA damage, for example by telomere attrition or ionizing radiation (Campisi and d'Adda di Fagagna, 2007). One of the upstream regulators of p53 in humans is the E3 ubiquitin-

protein ligase HDM2 (MDM2 in mice) that targets p53 for degradation. Alternate reading frame (ARF) protein may inhibit HDM2 activity, thereby enhancing signalling through p53 (Sherr and McCormick, 2002). p21, a downstream transcriptional target of p53, has been shown to mediate p53-dependent senescence (Brown et al., 1997). Indeed, reduction of p53, p21 or DDR mediators (such as ATM or CHK2) has been shown to prevent DNA damage-induced senescence (d'Adda di Fagagna, 2003; Di Micco et al., 2006; Gire et al., 2004).

The second main mediator of senescent proliferative arrest is RB and its upstream regulator $p16^{INK4a}$. Increased $p16^{ink4a}$ activity results in hypophosphorylation of RB, a state in which this master regulator enforces cell-cycle arrest (Chicas et al., 2010). Notably, $p16^{INK4a}$ is both a tumour suppressor and a biomarker of ageing (Kim and Sharpless, 2006; Ohtani et al., 2004). Similar to the p53-p21 axis, the $p16^{INK4a}$-RB pathway can also be engaged by the DDR, although it seems secondary to the activation of p53 signalling (Jacobs and de Lange, 2004; Stein et al., 1999). In addition, expression of $p16^{INK4a}$ can be directly induced by a variety of stimuli, including overexpression of oncogenes such as RAS (Lowe and Sherr, 2003). The $p16^{INK4a}$-RB pathway is essential for the formation of SAHF in OIS, which in turn leads to transcriptional silencing of E2F-responsive promoters. This action blocks expression of multiple pro-proliferative genes and results in cell-cycle arrest that, once established, does not require $p16^{INK4a}$ or RB for maintenance (Narita et al., 2003). This suggests that the senescence-associated repressive chromatin, induced by the $p16^{INK4a}$-RB pathway, could be a self-maintaining mechanism. It may further explain why senescence induced by engaging $p16^{INK4a}$-RB signalling appears to be a more stable

proliferative arrest than the one mediated through the p53-p21 axis (Beauséjour et al., 2003).

The senescent phenotype is achieved by a complex network of interactions rather than a simple, linear signal transduction. Therefore, both $p16^{INK4a}$-RB and p53-p21 pathways have many branching signal transduction routes, upstream and downstream, which intersect and can affect each other. $p16^{INK4a}$ and p21 are both CDK inhibitors that can prevent phosphorylation of RB, keeping it in an active form that blocks proliferation (Sherr and McCormick, 2002). Additionally, the loss of $p16^{INK4a}$-RB activity may lead to increased expression of p53 and p21. This could be attributed to the deregulation of E2F activity in the absence of $p16^{INK4a}$-RB-mediated control, which in turn, stimulates ARF expression and protects p53 from degradation (Bates et al., 1998; Zhang et al., 2006). As with many other pathway engagements in senescence, it appears that this is a cell-type specific mechanism.

It is worth noting that both $p16^{INK4a}$ and ARF are encoded by the same genomic locus CDKN2A (Gil and Peters, 2006). The CDKN2A (also called INK4a-ARF) locus normally remains transcriptionally inactive in young tissues, but it is activated with ageing and in senescent cells (Krishnamurthy et al., 2004). The mechanism behind derepression of this locus appears to rely largely on the disassociation of Polycomb repressive complexes from the locus, which results in senescence (Bracken et al., 2007; Jacobs et al., 1999).

1.1.3.2 *DNA-damage response (DDR)*

DNA damage is often produced by many of the senescence inducers like ROS, radiation, UV exposure, or chemotherapeutic drugs, which in turn leads to activation

of the DDR. The DDR is mainly mediated through the DNA damage kinases ATM, ATR, CHK1, and CHK2, leading to phosphorylation and activation of cell cycle proteins. Among them is p53 that stimulates expression of p21, which in turn inhibits CDK-cyclin complexes and enforces cell cycle arrest (Campisi and d'Adda di Fagagna, 2007).

Telomere shortening associated with replicative senescence is also sensed by the DDR (d'Adda di Fagagna, 2003; Herbig et al., 2004; Takai et al., 2003). Moreover, poor accessibility of the DNA damage repair machineries to telomeres makes them even more prone to external damaging agents. This contributes to persistent DDR and senescence induction (Fumagalli et al., 2012; Hewitt et al., 2012). However, persisting DNA damage foci can be also observed in senescent cells at non-telomeric sites, indicating that the initiation of the senescence programme is not telomere-damage specific (Fumagalli et al., 2014; Nakamura et al., 2008). The DDR response leading to activation of the p53-p21 pathway is also engaged in senescence caused by oncogenic activation. This is presumably due to hyper-replication of DNA resulting in replication fork collapse and DNA double-strand breaks (Bartkova et al., 2006; Di Micco et al., 2006). Moreover, telomere attrition has also been observed in OIS, highlighting the hypersensitivity of telomeric repeats to the DNA replication stress observed after oncogenic activation (Hewitt et al., 2012; Suram et al., 2012). In addition, inactivation of the DDR mediators not only prevents senescence induction by RAS oncogene activation, but also promotes cellular transformation. Therefore, intact DDR appears to be crucial for OIS establishment (Di Micco et al., 2006).

A persistent DNA-damage response is also important for expression of the SASP, one of the senescence hallmarks (Rodier et al., 2009). Compromising activity of the DDR mediators such as ATM, NBS1, and CHK2 can abolish secretion of SASP

components by senesced cells. Thus, it highlights a possible means by which senescent cells not only block their proliferation when they encounter irreparable DNA damage, but also communicate their compromised status to neighbouring cells.

1.1.3.3 Chromatin remodelling

It has long been noted that senescence is accompanied by substantial changes in chromatin organisation (Adams, 2009; Ryan and Cristofalo, 1972). It appears to be a widespread feature that contributes to the establishment of replicative block and may involve both chromatin relaxation and heterochromatin formation, depending on the context and affected genes. Formation of heterochromatin in the form of SAHF at multiple genomic loci can repress expression of E2F-dependant pro-proliferative genes as observed in oncogene-induced senescence (Narita et al., 2003). Conversely, senescence can also be induced by global chromatin relaxation, as observed in cells treated with broad-acting inhibitors of histone deacetylase (Munro et al., 2004). Chromatin relaxation leads to derepression of the CDKN2A genomic locus, expression of $p16^{INK4a}$ and ARF tumour suppressors, and hypophosphorylation of RB. $p16^{INK4a}$ acts through inhibition of the cyclin-dependent kinases CDK4 and CDK6 and prevents them from assembling into functional holoenzymes, rendering them unable to phosphorylate RB. Whereas, the ARF acts through regulation of p53 stability (Gil and Peters, 2006; Kim and Sharpless, 2006).

A similar mechanism is engaged by other senescence inducers, like suboptimal c-MYC or p300 histone acetyltransferase (Bandyopadhyay et al., 2002; Guney et al., 2006). They appear to enforce the senescent phenotype by epigenomic perturbations that lead to $p16^{INK4a}$ derepression. In some instances, chromatin remodelling may also

trigger the DDR, even without DNA damage. This is observed in the activation of the DDR protein ATM in cells treated with histone deacetylase inhibitors (Bakkenist and Kastan, 2003; Pazolli et al., 2012).

1.1.3.4 Role of oncogenes

Oncogenes play an important role in the senescence induction process by engaging various signalling pathways (Kuilman et al., 2010). It is well recognised that this process also occurs *in vivo*, and serves as a protective mechanism against tumourigenesis (Collado and Serrano, 2010). Oncogene-induced senescence (OIS) was first observed for oncogenic RAS expressed in human fibroblasts (Serrano et al., 1997). Hyperproliferation observed in oncogene-stimulated cells often leads to DNA damage and is recognised as a mechanism triggering senescence. As a result, it prevents unrestricted growth of potentially neoplastic cells (Di Micco et al., 2006). Since the discovery of the ability of RAS to induce senescence, the list of oncogenes able to exhibit a similar action has risen to about 50 (Gorgoulis and Halazonetis, 2010). It is apparent though, that senescence can also be triggered by loss of tumour suppressors as demonstrated with PTEN (Alimonti et al., 2010), NF1 (Courtois-Cox et al., 2006) or VHL (Young et al., 2008). In addition to engaging the DDR (Bartkova et al., 2006), there are other mechanisms involved in the establishment of OIS which can be simultaneously triggered. For example, $BRAF^{V600E}$-mediated senescence leads to direct activation of $p16^{INK4a}$ (Lin et al., 1998; Zhu et al., 1998), suppression of pyruvate dehydrogenase (Kaplon et al., 2013), and upregulation of pro-inflammatory SASP factors (Kuilman et al., 2008). Senescence due to the loss of PTEN is mediated through mTORC pathway, and DNA damage does not appear to be important for this process

(Alimonti et al., 2010). Derepression of the CDKN2A locus can also occur in some cell types in OIS (Gil and Peters, 2006; Kim and Sharpless, 2006).

These observations again highlight that oncogenic stimuli also act through different signalling pathways in the process of establishing an irreversible senescent state. Ultimately common effectors of senescence, like $p16^{INK4a}$ and p53 are activated (Nardella et al., 2011), although with variations across cell types and species. For example, activation of p53 in mice seems to depend largely on the ARF action (Efeyan and Serrano, 2007), whereas in humans the DDR plays a more prominent role in p53 activation (Halazonetis et al., 2008). In addition, while $p16^{INK4a}$ readily promotes OIS in humans, it plays only a modest role in this process in mice (Evan and d'Adda di Fagagna, 2009).

1.1.3.5 *Reactive oxygen species in senescence*

As cells progress through their replicative lifespan, the mitochondrial functions change. This leads to metabolic inefficiency, and is accompanied by elevated intracellular ROS levels (Allen et al., 1999; Hutter et al., 2004; Passos et al., 2007). However, multiple other types of senescence, whether induced by loss of telomeres, persistent DNA damage, oncogene activation or chemotherapeutic drugs are also accompanied by increased ROS levels (Passos et al., 2009). In fact, senescence onset can be delayed, or even prevented, with antioxidant treatment (Chen et al., 1995; Lee et al., 1999; Macip et al., 2002).

Mechanistically, increased intracellular ROS levels lead to activation of p38 MAPK that stimulates p53-p21 signalling in the establishment of senescence (Sun et al., 2007). It has also been demonstrated that the p16-RB pathway, when

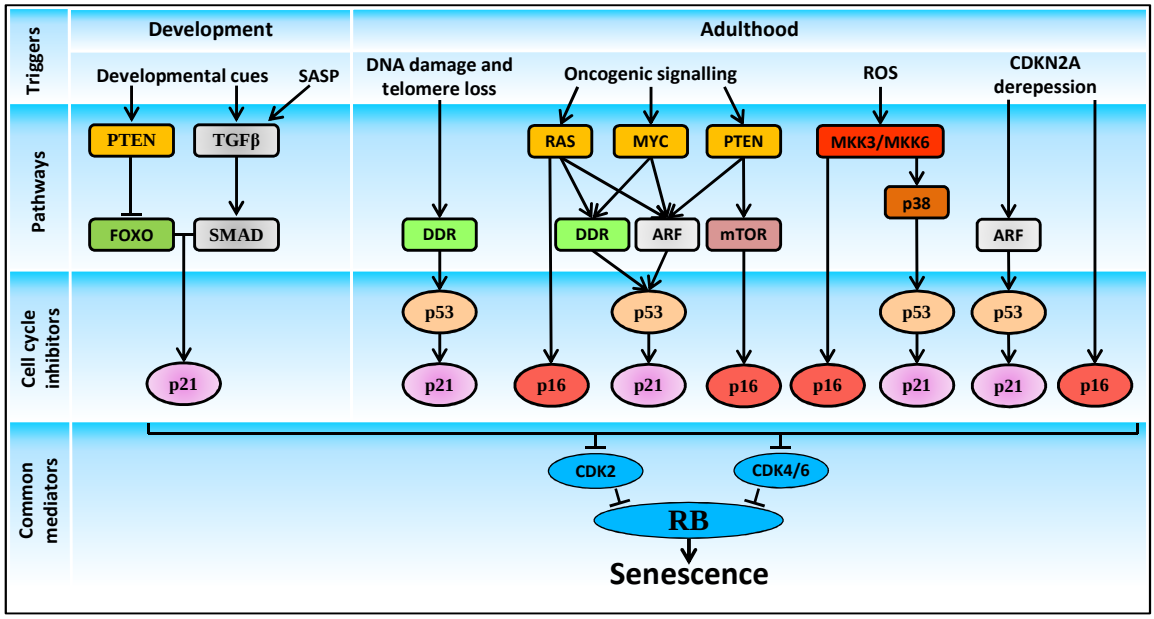

Figure 1.2. Senescence pathways.

Induction of senescence can be triggered by various stimuli, engaging distinct signalling pathways that converge on the cell cycle arrest by activation of the tumour suppressor RB. Developmental senescence is mediated via different signalling cascades than stress induced senescence in adulthood. See text for details.

activated upon senescence, not only leads to increased ROS levels, but also establishes a ROS-generating positive feedback loop mediated by proteinase kinase C (PKC), which reinforces senescence by blocking cytokinesis (Takahashi et al., 2006). Thus it could be a factor contributing to the often observed multinucleated state in senescent cells (Hayflick, 1965). Furthermore, oxidative stress, by causing DNA lesions and accelerating telomere attrition, can potentiate the DDR (Sedelnikova et al., 2010; von Zglinicki, 2002).

1.1.3.6 Summary of senescence effector pathways

The $p16^{INK4a}$-RB and/or p53-p21 pathways regulate most features of senescent cells (Figure 1.2). Generally overexpression or chronic activation of RB, p53, $p16^{INK4a}$ or p21 is sufficient to enforce growth arrest (Beauséjour et al., 2003; McConnell et al.,

1998). Persistent DDR signalling is responsible for the initiation of proliferation arrest. This may be assisted later by additional signals from, for example, stress-responsive p38 MAPK, PKC, and increased intracellular ROS (Freund et al., 2011; Iwasa et al., 2003; Passos et al., 2010; Takahashi et al., 2006). These pathways contribute to stimulation of $p16^{INK4a}$ expression, followed by RB hypophosphorylation which results in essentially irreversible proliferation arrest (Beauséjour et al., 2003).

1.2 Role of senescence

Senescence can be activated by a plethora of stimuli, but ultimately results in a stable proliferative arrest. Unlike apoptosis, senescence does not lead to cell death. In fact, senescent cells remain viable for an extended time, even after growth arrest is in place. They continue to communicate with their surroundings, for as long as they persist. Therefore, depending on the context, they may affect a variety of functions, both cellular and organismal.

1.2.1 Cellular senescence during development

Since the first report of programmed cell death during *Caenorhabditis elegans* development (Sulston et al., 1983), apoptosis has been a well-recognised process essential during embryogenesis (Czabotar et al., 2014; Fuchs and Steller, 2011; Lettre and Hengartner, 2006). Interestingly, recent studies have demonstrated that the senescence programme is also activated during development (Muñoz-Espín et al., 2013; Rajagopalan and Long, 2012; Storer et al., 2013). Senescent cells have been identified at multiple structures of mouse, human, chicken (Muñoz-Espín et al., 2013; Storer et al., 2013), and quail embryos (Nacher et al., 2006), suggesting that it is

a conserved mechanism in vertebrates. Senescent cells in embryos can either be cleared by macrophages or overgrown by surrounding cells, hence contributing to tissue patterning. A secretory phenotype of embryonic senescent cells, similar, but not identical to the SASP of adulthood senescence, can offer another means of tissue remodelling during embryogenesis. Interestingly, developmental senescence relies on p21 as the key mediator of the proliferation arrest, whereas $p16^{INK4a}$ and p53 activation seems dispensable (Muñoz-Espín and Serrano, 2014; Storer and Keyes, 2014). This suggests that while senescence is a common feature of many structures in the developing embryo, it has distinctive characteristics when compared to stress-induced senescence in adulthood (Figure 1.2).

1.2.2 Tumour suppression

It is well established that senescence plays a role in tumour suppression by restricting uncontrolled growth of damaged and potentially precancerous cells (Campisi and d'Adda di Fagagna, 2007; Prieur and Peeper, 2008). Indeed, many of the stimuli inducing senescence are cancer-associated, and establishment of the senescent phenotype makes cells resistant to oncogenic transformation (Campisi, 2013; Kim and Sharpless, 2006; Kuilman et al., 2010). This occurs at the benign stage of tumourigenesis and is supported by studies *in vivo* (Collado and Serrano, 2010). For example, it has been observed that premalignant human nevi and colon adenomas contain senescent cells (Bartkova et al., 2005; Michaloglou et al., 2005). Upon malignant transformation however, senescent cells become scarce. Similar observations were reported for mouse models of oncogenesis depending on RAS activation or PTEN deletion. Senescent cells were abundant in premalignant lesions,

but their number was markedly decreased in the cancers that develop from these lesions (Braig et al., 2005; Chen et al., 2005; Collado et al., 2005). A compelling body of evidence shows that these senescent cells in premalignant lesions are cleared by the immune system (Hoenicke and Zender, 2012). The clearance can be achieved either by T-cell-mediated recognition of senescent cells (Kang et al., 2011) or by recruitment of inflammatory phagocytes (Xue et al., 2007). This process is most likely mediated by the secretion of SASP factors (Campisi, 2013; Kuilman and Peeper, 2009).

In some cases, established cancers may be eradicated by senescence-induction. This process can be driven *in vivo* by immune cells secreting cytokines (e.g., interferon γ and tumour necrosis factor) that act on tumour cells in a paracrine manner enforcing senescence (Braumuller et al., 2013). Tumour cells can also senesce *in vivo* in response to chemotherapy (Coppé et al., 2010b; Schmitt et al., 2002), or acute reactivation of p53 (Ventura et al., 2007; Xue et al., 2007), followed by tumour regression. In addition, pharmacological inhibition of CDK4 and/or CDK6, which results in hypophosphorylation and activation of RB, can also induce senescence in cancer cells (Michaud et al., 2010; Rader et al., 2013; Thangavel et al., 2011). Such inhibitors are currently being tested in human clinical trials and showing promising results (Dickson et al., 2013; Guha, 2013; Leonard et al., 2012). Regressing tumours, similar to premalignant senescent cells, evoke an inflammatory response and are eliminated by the activation of the innate immune system.

1.2.3 Tumour promotion

It is seemingly contradictory that senescence, a tumour-suppressive mechanism, may actually contribute to the development of malignancy. This activity is mainly

attributed to one of the hallmarks of senescent cells, the SASP. It consists of a plethora of secreted factors, some of which exhibit tumour-promoting activities and, in a permissive context, can contribute to tumourigenesis, particularly with advanced age (Campisi, 2013; Rodier and Campisi, 2011).

There is no evidence that senescent cells occurring *in vivo* can stimulate progression of naturally occurring cancer cells in their vicinity. It has been shown, however, that coinjection of senescent fibroblasts and epithelial tumour cells into immunocompromised mice significantly enhanced proliferation of the tumour cells (Coppé et al., 2006; Krtolica et al., 2001; Liu and Hornsby, 2007). This effect was absent when non-senescent fibroblasts were used. Tumour growth was stimulated by the SASP components, MMP3 (stromelysin) and VEGF in particular, which promote tumour invasiveness and angiogenesis, respectively. In addition to studies in mice, SASP factors (like IL6 and IL8) secreted by senescent fibroblasts were shown to induce epithelial-to-mesenchymal transition (EMT) in premalignant epithelial cells as well as in non-aggressive cancer cells (Coppé et al., 2008; Ksiazek et al., 2008; Parrinello et al., 2005; Pricola et al., 2009). This behaviour *in vivo* could be a factor leading to the loss of tissue integrity and the increased migratory capacity of malignant cells. Moreover, several other SASP factors have been demonstrated to mediate not only tumour development, but also offer protection from chemotherapeutic agents to pre-malignant neighbouring cells (Bavik et al., 2006; Coppé et al., 2010a; Gilbert and Hemann, 2010; Sun et al., 2012).

1.2.4 Tissue repair

A growing body of evidence supports the role of senescence and its accompanying SASP in the repair of damaged tissue (Adams, 2009; Campisi et al., 2011; Kortlever et al., 2006; Rodier and Campisi, 2011). It has been demonstrated that the repair of liver injury in a mouse model is assisted by senescence and, as a result, prevents fibrosis (Krizhanovsky et al., 2008). Initially, in response to liver damage, activated hepatic stellate cells proliferate and form the fibrotic scar in place of the injury. During this process they undergo senescence and are cleared by the immune system (primarily by natural killer cells), which reduces liver fibrosis and restores tissue homeostasis. When liver injury was induced in mice deficient in the $p16^{INK4a}$-RB and p53-p21 pathways, therefore unable to trigger the senescence response, healing of the liver damage was characterised by excessive fibrosis (Krizhanovsky et al., 2008). This further supports the beneficial role of senescence in limiting the fibrogenic response. It is in concordance with previous studies reporting reduced fibrosis and increased inflammation in the presence of senescent hepatic stellate cells (Schnabl et al., 2003). Presumably, SASP components, particularly the matrix metalloproteinases, secreted by senescent cells help to resolve fibrotic deposition. The role of senescence in tissue homeostasis is not only limited to the liver. It has also been demonstrated to reduce fibrosis in the kidney and heart (Wolstein et al., 2010; Zhu et al., 2013), as well as in other organs, like the skin.

Skin wounding in mouse models induces surrounding fibroblasts and myofibroblasts to senesce (Jun and Lau, 2010b). The ECM protein CCN1, which is highly expressed at the sites of skin injury, has been demonstrated to induce senescence of fibroblasts through integrin-mediated oxidative stress. In mice depleted

of the functional CNN1 protein, the wounds were excessively fibrotic. Fibrosis was however resolved upon topical application of functional CCN1 protein in these mice. This was accompanied by senescence induction and the SASP. In concordance with prior studies, a recent study in mice demonstrated that skin wound healing is accompanied by a transient outburst of senescent cells that disappear upon wound closure (Demaria et al., 2014). When execution of the senescence response was blocked, it translated into a significant delay in wound healing. This was because senescent fibroblasts and epithelial cells at the site of the injury were needed for secretion of platelet-derived growth factor AA (PDGF-AA), which stimulates myofibroblast differentiation and wound closure.

These studies suggest that tissue repair is also dependent on senescence and the SASP. Efficient clearance of senescent cells by the immune system, however, is important for regaining tissue homeostasis.

1.2.5 Senescence in ageing

It is well established that senescent cells accumulate in multiple mitotically-competent tissues during organismal ageing and in progeroid syndromes (Baker et al., 2008; Burton and Krizhanovsky, 2014; Campisi et al., 2011; Hasty et al., 2003; Herbig et al., 2006; Ohtani et al., 2010; Waaijer et al., 2012). This may happen as a result of several factors: declining functions of immune system and delayed clearance of senescent cells (Solana et al., 2012), inability to stabilise p53 to a high-enough level required for apoptotic cell death (Feng et al., 2007), or slow accumulation of damage that remains below the threshold that triggers apoptosis

(Van Deursen, 2014). The exact mechanism, whether it is increased generation, inefficient elimination, or both, remains unknown.

Many age-associated degenerative diseases and phenotypes have been linked to the increased abundance of senescent cells and accompanying SASP (Ovadya and Krizhanovsky, 2014). The hypothesis that senescent cells are indeed the drivers of age-related pathology was demonstrated by studies in transgenic mice (Baker et al., 2011). Baker and colleagues generated mice in which senescent cells can be eliminated by synthetic drug (AP20187) administration. The drug induces dimerization of a membrane-bound myristoylated FK506-binding-protein–caspase 8 that leads to apoptosis of cells expressing this fusion protein. To achieve clearance of senescent cells, the fusion protein was under $p16^{INK4a}$ promoter. It is well accepted that high levels of $p16^{INK4a}$ expression is a marker of senescent cells, both *in vitro* and *in vivo* (Martin et al., 2014). Therefore, in this model, the assumption that senescent cells were targeted and subsequently eliminated by apoptosis is justified. By using this inducible senescence-to-apoptosis system in progeroid *BubR1*$^{H/H}$ mice, they showed that clearance of $p16^{INK4a}$-expressing cells decreased the overload of senescent cells in tissues in which senescence is primarily triggered by $p16^{INK4a}$. These included skeletal muscle, adipose tissue and eye. Remarkably, clearance of $p16^{INK4a}$-positive cells attenuated some of the advanced progeric pathologies, such as sarcopenia, cataracts, and kyphosis. This is consistent with the observation that inactivation of *p16*^{Ink4a} in *BubR1*$^{H/H}$ mice selectively delays the onset of age-related pathologies such as loss of adipose tissue or muscle function (Baker et al., 2008). However, cardiac arrhythmias and arterial wall stiffening were not alleviated by clearance of $p16^{Ink4a}$-positive senescent cells in these mice, because they arise in these tissues in

a $p16^{Ink4a}$-independent fashion (Matsumoto et al., 2007). Therefore, despite of the clearance of $p16^{Ink4a}$-positive senescent cells in *BubR1*$^{H/H}$ mice, the overall survival was not substantially extended, because cardiac failure is presumably responsible for death of these mice. Nevertheless, work of Baker and colleagues strongly supports the hypothesis that lack of efficient clearance of senescent cells and their resultant accumulation in ageing can aggravate tissue dysfunction and drive age-related pathology. Their work also showed that tissues of some organs, such as heart or liver, do not express $p16^{Ink4a}$, despite the fact that cells from these organs still can undergo senescence. This could suggest that senescence in certain tissues is p53-dependant, while in others $p16^{Ink4a}$ plays a more vital role.

A wealth of data supports the contribution of senescent cells to age-related diseases, often by secretion of certain SASP components. For example, neurodegenerative diseases such as Alzheimer's and Parkinson's diseases are accompanied by senescent astrocytes that were suggested to promote the age-associated neurodegeneration and cognitive impairment (Bhat et al., 2012; Bitto et al., 2010; Chinta et al., 2013; Salminen et al., 2011b). Senescent chondrocytes were proposed to underlie age-related changes observed in pathologies like osteoarthritic joints and degenerated intervertebral discs, thereby contributing to pathogenesis (Anderson and Loeser, 2010; Roberts et al., 2006). Similarly, deterioration of the cardiovascular system with age has been linked to senescent endothelial and smooth muscle cells, implying their role in both the genesis and promotion of the pathologic state (Erusalimsky and Kurz, 2005; Gorenne et al., 2006). Type 2 diabetes has been linked to the accumulation of senescent adipocytes, suggesting their role in the pathogenesis of this condition (Markowski et al., 2013;

Minamino et al., 2009). Many other age-related conditions have been linked to senescence, postulating a role for senescent cells either in their pathogenesis or at least in contribution to the process (Ovadya and Krizhanovsky, 2014; Zhu et al., 2014). They include, among others, macular degeneration, sarcopenia, and chronic obstructive pulmonary disease, etc. Age-associated dermal and epidermal thinning was also proposed to arise from increased frequency of senescent cells in ageing skin (Dimri et al., 1995; Herbig et al., 2006; Ressler et al., 2006; Velarde et al., 2012), possibly resulting in increased secretion of MMPs and collagen loss.

The aforementioned studies, and many others support the concept that some features of organismal ageing can arise from increased frequency of senescent cells as they accumulate in tissues over a lifetime (Martin et al., 2014; Muñoz-Espín and Serrano, 2014; Sharpless and DePinho, 2007; Signer and Morrison, 2013). Therefore, understanding the full extent of senescence characteristics will most likely assist in making predictions about physiological age and longevity determinants. Furthermore, it should also contribute to the discovery of efficient anti-ageing therapies, extending the period of time that an individual remains healthy, the so called 'healthspan'. Such therapies are already being tested with promising results, and a new group of therapeutics called 'senolytic' drugs is emerging (Zhu et al., 2015). These agents selectively target senescent cells, trigger their clearance, and may reverse some aspects of ageing.

1.3 Architecture and function of the Nuclear Envelope

The nuclear envelope (NE) constitutes a boundary between two very different compartments within a cell, the cytoplasm and nucleoplasm (Figure 1.3). In metazoans, the most prominent structural features of the NE are the outer nuclear membrane (ONM) and the inner nuclear membrane (INM) with a perinuclear space (PNS) between them, which ranges from 30 to 50 nm in dimension (Prunuske and Ullman, 2006; Stewart et al., 2007). Underlying the INM is the nuclear lamina, a proteinaceous meshwork of intermediate filament proteins. The NE is pierced with highly structured nuclear pore complexes (NPC) spanning across the two membranes. These structures are involved in trafficking of molecular cargo in and out of the nucleus (Grossman et al., 2012b). The ONM is connected with the endoplasmic reticulum (ER), thus making the PNS continuous with the ER lumen. Although the INM and ONM meet at the periphery of each NPC, they each retain a fairly distinctive protein composition. The ONM, due to its continuity with the ER is enriched in ER components, while the INM retains its own distinctive array of integral membrane proteins (Schirmer and Foisner, 2007). The NE often shows multiple invaginations of the nuclear membrane into the nucleus, forming an often elaborate network of tubules and INM sheets continuous with the NE. This feature is termed nucleoplasmic reticulum (NR), so named for its structural resemblance to the ER (Malhas et al., 2011).

Functionally, the NE determines global nuclear architecture. In addition, as an interface between nucleoplasm and cytoplasm, it is involved in selective bidirectional transport of macromolecules and ions, regulation of gene expression, mechano-signal transduction between nucleoskeleton and cytoskeleton, and serves

as a signalling platform. Nuclear lamins, in addition to their role in maintaining nuclear structure, are involved in most nuclear activities, either directly or through the array of interactions with their associated proteins (Ho and Lammerding, 2012).

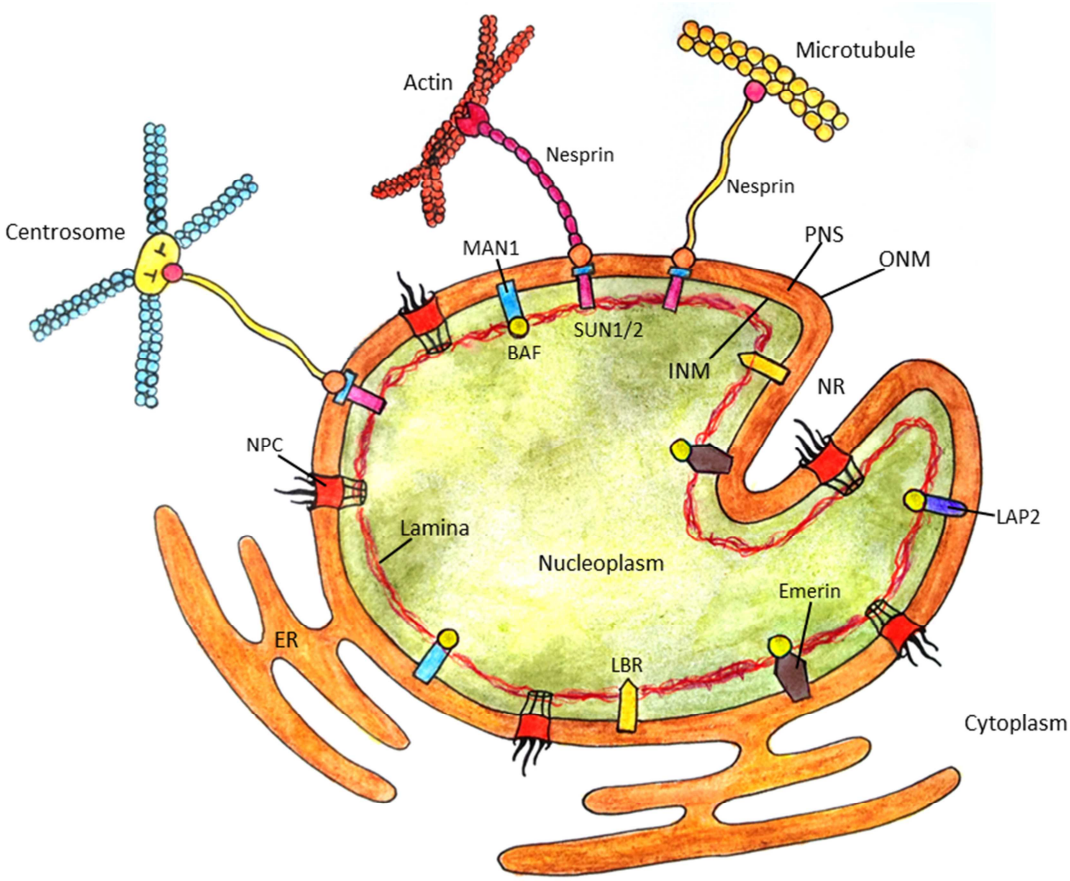

Figure 1.3. Architecture of the Nuclear Envelope.

Schematic representation of the nucleus, showing several NE proteins and associated structures. The nuclear phospholipid bilayer consists of outer nuclear membrane (ONM) and inner nuclear membrane (INM) separated by perinuclear space (PNS). The ONM is contiguous with the endoplasmic reticulum (ER). The NE forms invaginations termed the nucleoplasmic reticulum (NR). Through Linker of Nucleoskeleton and Cytoskeleton (LINC) complex (consisting of SUN1/2 proteins, nespirns and associated proteins), nuclear cytoskeleton communicates with cytoplasmic intermediate filaments, actin filaments, microtubules and connects to centrosome. Several (of many) other NE-associated proteins are also depicted. LBR, lamin B receptor; BAF, barrier to autointegration factor 1; LAP2, lamin associated protein 2; NPC, nuclear pore complex.

1.3.1 The nuclear lamins

The nuclear lamina is predominantly a feature of metazoan NE, however, lamin-like protein NE81 has also been identified in the lower eukaryote *Dictyostelium* (Amoebozoa) (Krüger et al., 2012). It appears that during evolution, the number of lamin-encoding genes and the complexity of the lamina structure increased (Fuchs and Weber, 1994; Weber et al., 1991), with metazoans outside the vertebrate lineage having generally only a single lamin gene (Peter and Stick, 2012, 2015).

In humans and other mammals, the major components of the lamina structure are A-type and B-type lamins (Burke and Stewart, 2013; Gerace and Blobel, 1980; Gerace et al., 1978). A-type lamins are all encoded by a single gene LMNA, and through alternative splicing give rise to four main isoforms: lamin A, AΔ10, C, and C2 (Fisher et al., 1986; Furukawa et al., 1994; Lin and Worman, 1993; Machiels, 1996; McKeon et al., 1986). While lamins A and C are the two most widely expressed A-type lamins in somatic cells, lamin C2 is specifically expressed in testes only. Lamin AΔ10 appears in somatic cells as well, but is far less abundant. Moreover, A-type lamins are developmentally regulated and while maternally derived A-type lamin pool disappears during the first 2-4 cleavage divisions, endogenously encoded A-type lamins reappear much later at the developmental stage (Machiels, 1996; Rober et al., 1989; Stewart and Burke, 1987). B-type lamins are encoded by two separate genes LMNB1 and LMNB2, and give rise to lamin B1 and lamin B2, respectively (Lin and Worman, 1995; Peter, 1989; Vorburger et al., 1989). They are widely expressed with at least one B-type lamin present in every somatic cell in the body. The third lamin B variant, lamin B3, is also encoded by LMNB2 gene and is derived by alternative splicing (Furukawa and Hotta, 1993). Similar to lamin C2, lamin B3 is a testis-specific protein.

The nuclear lamins belong to the type V intermediate filament protein family (Parry et al., 1986). The structure of each lamin is characterised by a small N-terminal head domain of about 33 residues, followed by a central α-helical rod domain that contains four coiled-coil regions (Figure 1.4; lamin A as an example). The C-terminal domain ('tail') includes an immunoglobulin (Ig)-like β-fold and a nuclear localisation sequence (NLS) that facilitates nuclear import of the lamins (Dhe-Paganon et al., 2002; Fisher et al., 1986; Krimm, 2002; McKeon et al., 1986; Stuurman et al., 1998). At the C-terminus, B-type lamins and lamin A harbour a CaaX motif (C is cysteine, a is an aliphatic residue, and X is variable, but usually represents methionine) that is modified post-translationally by farnesylation, endoproteolysis, and carboxymethylation (Beck et al., 1990; Kitten and Nigg, 1991; Sinensky, 1994; Wolda and Glomset, 1988).

Formation of lamin intermediate filaments (IF) is a hierarchical process (Aebi et al., 1986; Foeger, 2006; Heitlinger, 1991; Kapinos et al., 2010; Strelkov et al., 2004). *In vitro* and *ex vivo* studies have demonstrated that lamins can self-associate to form filaments (Ben-Harush, 2009; Grossman et al., 2012a). First, a formation of parallel coiled-coil homodimers occurs, followed by their association into head-to-tail strings through electrostatic interactions. These molecular strings then assemble laterally, in an antiparallel fashion, forming protofilaments. Protofilaments are the basic assembly units and they can associate further, in many conformations, to form thicker filaments and higher order structures, thus providing greater mechano-stability of a nucleus.

A-type and B-type lamins in cells appear to form distinct, albeit interacting, networks at the NE (Goldberg et al., 2008; Shimi et al., 2008). Moreover, lamins A and C, both A-type lamins, appear to segregate in living cells to some extent (Kolb et al., 2011). This and recent report from Goldman group further suggest that *in vivo,* each

lamin subtype forms separate polymers, although some degree of co-localisation is being observed (Shimi et al., 2015). However, in pathological condition when aberrantly processed lamin A variant was expressed, it perturbed lamin B1 and lamin A segregation and a mixed heteropolymers were detected *in vivo* (Delbarre et al., 2006). How new lamin copies assemble into the existing lamina meshwork is elusive though, and whether they form new layers of intermediate filaments or integrate into pre-existing structures is not yet fully understood.

Although the majority of nuclear lamin copies are incorporated into the peripheral nuclear lamina meshwork, a subset is also present within the nucleoplasm (Butin-Israeli et al., 2012; Dechat et al., 2000; Dyer et al., 1997; Goldman et al., 1992; Moir et al., 1994). Nucleoplasmic lamins seem to form functional complexes, rather than only being transiently present in the nucleoplasm before their assembly into the peripheral structure. Indeed, a stable pool of incompletely processed lamin B1 that did not chase away after blocking protein synthesis has been observed (Maske et al., 2003). Presence of the nucleoplasmic lamin A depends on binding to lamin associated protein 2α (LAP2α), through which it interacts with RB. LAP2α knock-out mice showed loss of soluble and nucleoplasmic lamin A (Naetar et al., 2008). This suggests that soluble lamin A is organised in functional proteinaceous networks within the nucleus, rather than just at the nuclear periphery. Moreover, it has been suggested recently that phosphorylation of lamin A at Serine 22 and Serine 392 is responsible for solubilizing lamin A (Kochin et al., 2014). Interestingly, a small, highly immobile nucleoplasmic fraction of B-type lamins has also been identified (Moir et al., 2000). It interacts with proliferating cell nuclear antigen (PCNA) and is needed for DNA replication (Moir et al., 1994; Shumaker et al., 2008).

1.3.2 The nuclear lamina and its binding partners

The nuclear lamina is a vast structure at the interface between the cytoplasm and nucleoplasm, with additional lamin presence within the nucleoplasm. Therefore it is not surprising that multiple lamin-binding partners (>100), involved in various cellular processes, have been identified (de Las Heras et al., 2013; Simon and Wilson, 2013). Moreover, a more recent study identified over 600 binding partners of various lamin A mutants associated with laminopathies by performing yeast two-hybrid tests (Dittmer et al., 2014), suggesting that the array of lamina-interacting proteins is likely to grow further. These interactions can be stable or transient, direct or through additional factors, and are often cell-type specific (Korfali et al., 2012). The full extent of lamin-interacting proteins is still under investigation and new partners are being continually identified (Ahmady et al., 2011; Gudise et al., 2011; Roux et al., 2012). Sometimes they share common protein domains, for example the LEM domain (Lin et al., 2000) or the SUN domain (Tzur et al., 2006). In general, lamin-binding partners may be assigned to two categories: structural proteins (e.g., actin, SUN proteins, nesprin, titin, etc) (Crisp and Burke, 2008; Starr and Fridolfsson, 2010) and regulatory molecules such as transcription factors (e.g., ERK1/2, c-FOS, RB, Oct-1, SREBP) (Dorner et al., 2007; González et al., 2008; Ivorra, 2006; Lloyd et al., 2002; Malhas et al., 2009). Several binding partners may fall into both categories (Simon and Wilson, 2013). In addition, lamins can also interact with DNA, either directly (Luderus, 1992; Shoeman and Traub, 1990; Stierlé et al., 2003) or through histones (Mattout et al., 2007; Taniura et al., 1995).

1.3.3 Lamin A in pathology

Lamin A is first translated into a 74 kDa precursor protein, called prelamin A, that requires several posttranslational modifications before yielding a mature lamin A (Figure 1.4). Similar to B-type lamins, prelamin A harbours the C-terminal CaaX motif that is the primary site for such modifications (Kitten and Nigg, 1991; Sinensky, 1994). Since lamin C, derived through an alternative splicing from the LMNA gene, lacks the CaaX box, it does not require these additional steps for maturation. Initially, the

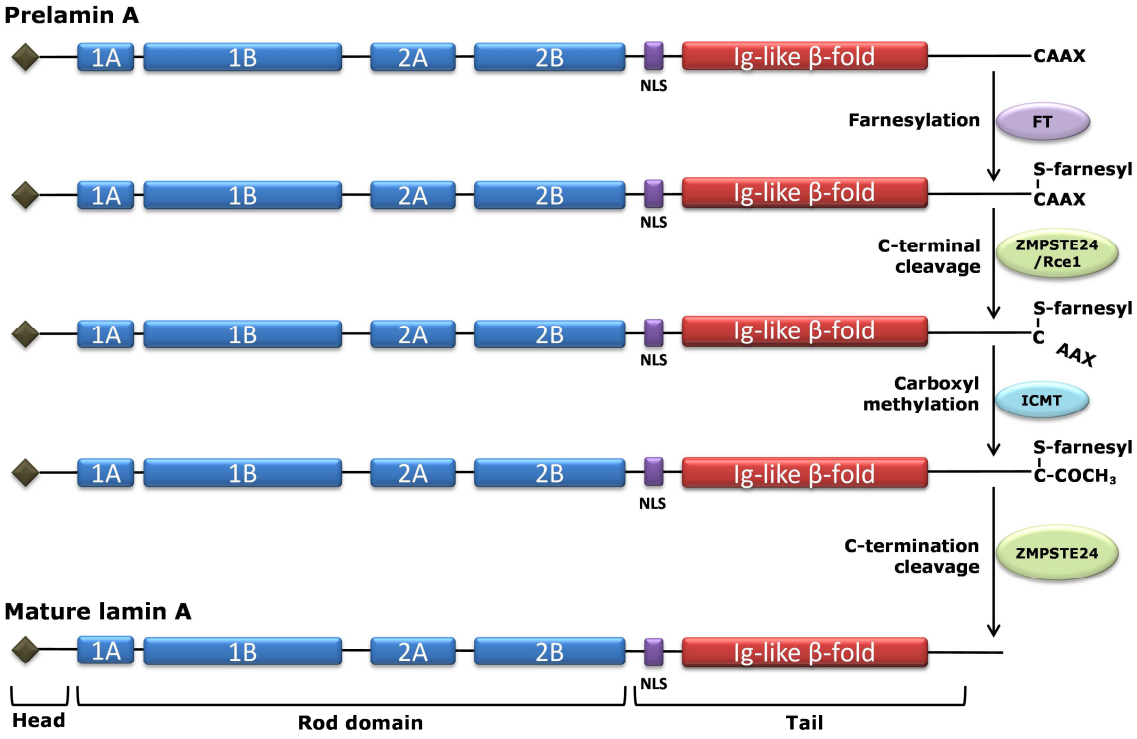

Figure 1.4. Maturation process of prelamin A.

Prelamin A undergoes several posttranslational modifications. First, the precursor protein is farnesylated by farnesyl transferase (FT) shortly after being synthesised, followed by cleavage of the three terminal residues in the CaaX motif either by Zmpste24 or Rce1. The exposed cysteine at the C-terminus is then carboxymethylated by isoprenylcysteine carboxyl methyltransferase (ICMT). In the final maturation step, Zmpste24 endoprotease removes the carboxyl terminal 15 amino acid residues, yielding a mature lamin A. Both head and tail form globular domains, while the central α-helical rod domain contains four coiled-coil regions (1A, 1B, 2A, 2B); NLS, nuclear localisation sequence.

cysteine in the CaaX motif is modified by adding a farnesyl isoprenoid group, a step mediated by farnesyltransferase. Next, a prenyl-CaaX specific endoprotease removes the three C-terminal amino acid residues. In the case of prelamin A it can be mediated either by RAS converting enzyme 1 (Rce1) or the Zn metallopeptidase Zmpste24, also known as FACE1. The farnesylcysteine is then subject to methylation by an isoprenylcysteine carboxyl methyltransferase (ICMT). In the final step, which is absent in B-type lamins, prelamin A undergoes additional cleavage by Zmpste24, which removes the carboxyl terminal 15 residues, including farnesylated and methylated cysteine. This produces the 72 kDa mature lamin A (Corrigan, 2005; Pendas, 2002; Weber et al., 1989). These posttranslational modifications commence soon after lamin synthesis. While B-type lamins retain farnesylated cysteine permanently, it is lost from prelamin A within 2-3 hours.

The precise role of these processing events in the maturation of prelamin A is not fully understood. It has been shown that farnesylation helps to target newly synthesised prelamin A to the NE, because it enhances hydrophobicity of the protein. This presumably facilitates accurate targeting to the nuclear periphery and the INM (Holtz et al., 1989). Studies in mice with reduced ICMT enzyme activity, also support the role for carboxymethylation in the targeting of prelamin A to the nuclear periphery (Ibrahim et al., 2013). However, experiments in which the mature form of lamin A was expressed, thus bypassing the maturation steps, demonstrated normal incorporation of the protein into the nuclear lamina, albeit with varying kinetics, probably due to interactions with chromatin, NE transmembrane proteins, and other NE components (Candelario et al., 2011; Hennekes and Nigg, 1994; Lutz et al., 1992). Although the reason for the farnesylation of prelamin A remains elusive (Davies et al.,

2011), the final cleavage step by Zmpste24 in the prelamin A maturation process is clearly important for proper lamin A behaviour. The fact that many pathologies are associated with abnormal prelamin A processing or loss of Zmpste24 function further supports this assumption.

1.3.3.1 Laminopathies

At least 15 pathologies have been associated with various mutations in LMNA gene, which is more than for any other known human gene (Figure 1.5) (Schreiber and Kennedy, 2013). Together with other diseases caused by dysfunctional nuclear envelope proteins, these pathologies are jointly termed laminopathies (Capell and Collins, 2006).

The first human disease linked to LMNA mutation was Emery-Dreifuss muscular dystrophy (EDMD) (Bonne, 1999; Emery and Dreifuss, 1966). This autosomal dominant disease is characterised by progressive muscle weakness of the lower legs and upper arms, early contractures, and dilated cardiomyopathy that may present itself at later stages (Emery, 2000). Another muscular dystrophy caused by mutations in LMNA gene is limb girdle muscular dystrophy type 1B (LGMD1B) (Muchir et al., 2000). It is also characterised by dilated cardiomyopathy and striated muscle loss. In contrast, dilated cardiomyopathy type 1A (DCM1A), linked to LMNA mutations as well, does not affect skeletal muscles (Fatkin et al., 1999). More recently, a new form of congenital muscular dystrophy has been shown to be caused by LMNA mutations (Quijano-Roy et al., 2008). Additionally, Heart-hand syndrome is characterised by a range of symptoms including cardiomyopathy and shortening of toes and fingers (Renou et al., 2008).

Surprisingly, it has been discovered that other tissues may also be severely affected by LMNA mutations. Various syndromes characterised by loss of adipose tissue were linked to abnormalities in lamin A, including Dunnigan-type familial partial lipodystrophy (FPLD), generalized lipodystrophy (GLD) (Caux et al., 2003), atypical forms of lipodystrophy (Vigouroux and Capeau, 2005), Mandibuloacral dysplasia (MAD) (Novelli et al., 2002), and other overlapping syndromes. Moreover, MAD is also characterised by underdeveloped clavicles and congenital bone abnormalities. Homozygous loss of lamin A function can also lead to demyelination in peripheral nerves and axonal degradation, which is observed in Charcot-Marie-Tooth syndrome

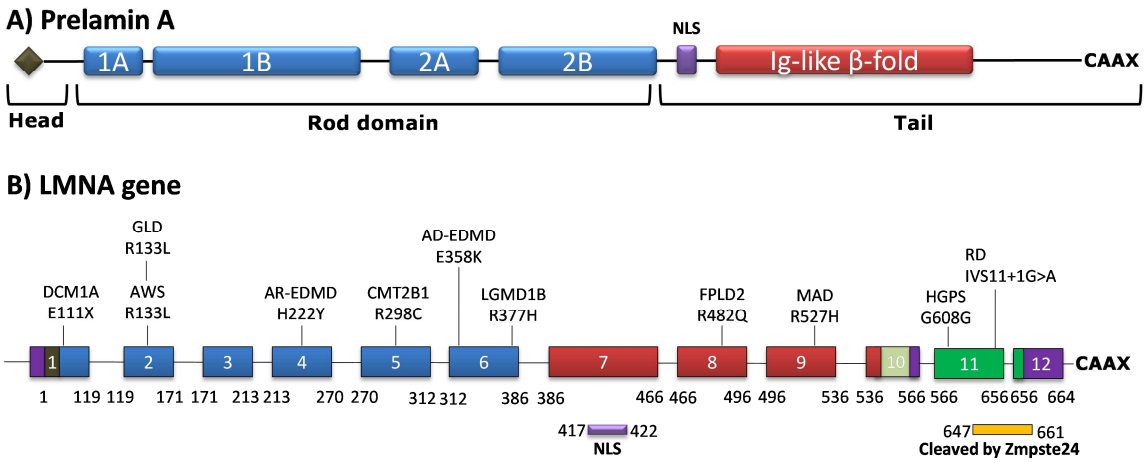

Figure 1.5. The most common mutations in LMNA gene causing laminopathies.

A) Schematic representation of prelamin A structure. **B)** Schematic representation of LMNA gene organisation. Twelve exons of the LMNA gene are depicted with examples of the main mutations causing specified laminopathies (indicated above). A complete list can be obtained from OMIM. For disorders such as DCM1A, AWS, AD-EDMD, GLD, and LGMD1B multiple mutations can underlie the disease and only a representative ones are shown. AD-EDMD, autosomal dominant Emery–Dreifuss muscular dystrophy; AR-EDMD, autosomal recessive Emery–Dreifuss muscular dystrophy; AWS, atypical Werner syndrome; CMT2B1, Charcot–Marie–Tooth disorder, type 2B1; DCM1A, dilated cardiomyopathy, type 1A; FPLD, Dunnigan familial partial lipodystrophy; GLD, generalized lipodystrophy; HGPS, Hutchinson–Gilford progeria syndrome; LGMD1B, limb girdle muscular dystrophy, type 1B; MAD, mandibuloacral dysplasia; RD, restrictive dermopathy. UTR regions are indicated in purple. Pale region within exon 10 indicates lamin C-specific region, followed by lamin C-specific 3'UTR (in purple).

(De Sandre-Giovannoli et al., 2002).

Probably the most striking phenotypes caused by LMNA mutations are the progeroid disorders, which are characterised by segmental premature ageing. One of the best studied is Hutchinson-Gilford progeria syndrome (HGPS), caused by a mutation in LMNA that results in a lamin A variant, progerin. Progerin lacks 50 amino acid residues close to the C-terminus (De Sandre-Giovannoli et al., 2003; Eriksson et al., 2003). Within the absent region is the cleavage site for Zmpste24, therefore progerin remains farnesylated. This is believed to cause a dominant gain-of-function toxicity. Interestingly, a similar observation was made for restrictive dermopathy (RD) in which a larger region of 90 amino acids, including the Zmpste24 cleavage site, was missing (Navarro et al., 2004). This resulted in several more severe HGPS-like pathologies, with a lethal early neonatal course. In addition, RD can be caused by the loss of function of Zmpste24, resulting in prelamin A accumulation. This further emphasises the importance of adequate processing of lamin A. Other mutations in LMNA, causing less severe progeroid pathologies, have also been identified (Chen et al., 2003; Verstraeten et al., 2006).

Despite the fact that lamin A is widely expressed in somatic cells, some of the mutations affect only specific tissues, while others have a broader spectrum (Carboni et al., 2013). While many pathologies associated with LMNA mutations demonstrate overlapping characteristics, they can be broadly categorised into diseases affecting: (i) striated muscle, (ii) adipose tissue, (iii) peripheral nerves, (iv) bones or (iv) multiple tissues leading to a progeroid phenotype. Such a variation in the spectrum of pathology most likely arises from the fact that lamin A, among other nuclear envelope proteins, forms complexes with other components that include tissue-specific factors.

As a result, some mutations may only affect interactions occurring in a tissue-specific manner (Worman and Schirmer, 2015).

In addition to LMNA-linked mutations, laminopathies also include diseases caused by aberrations in other lamins (Méndez-López and Worman, 2012). For example, a mutation in LMNB1 causes dominant leukodystrophy (Padiath, 2006), and a different mutation in LMNB2 causes partial lipodystrophy (Hegele et al., 2006). Mutations in many lamin-binding partners can also lead to laminopathies. Homozygous mutations in the lamin B receptor (LBR), an integral INM protein that binds to B-type lamins, cause Greenberg skeletal dysplasia (Waterham et al., 2003). Heterozygous LBR mutations, however, are linked to the Pelger-Huet anomaly, which is characterised by altered chromatin organisation and dysmorphic nuclei in granulocytes (Hoffmann et al., 2002). Another example is seen in mutations in the integral INM protein-coding genes interacting with lamin A, like emerin (EMD), which leads to X-linked EDMD (Bione, 1994). Mutations in MAN1, which is encoded by the LEMD3 gene, and binds emerin, and A-type and B-type lamins, result in pathologies defined by increased bone density (Hellemans et al., 2004). Mutations in multiple genes encoding proteins that form and interact together as part of the linker of nucleoskeleton and cytoskeleton (LINC) complex are associated with muscular dystrophy and cardiomyopathy. These include SYNE1 (nesprin 1), SYNE2 (nesprin 2), TMEM43 (LUMA) and TMPO (LAP2α) (Liang et al., 2011; Taylor et al., 2005; Zhang et al., 2007). Interestingly, when barrier-to-autointegration factor 1 (BAF) is mutated, it leads to atypical progeria (Puente et al., 2011). BAF interacts with emerin, and is also involved in chromatin organisation and nuclear envelope assembly. These are just a

few examples of the many diseases associated with the nuclear envelope. The list is very likely to grow further as new discoveries continue to emerge.

1.4 The nuclear lamina and ageing

The ageing process can be broadly described as overall, progressive deterioration of the physical and physiological abilities of an organism. It is accompanied by a decline in proper tissue function and a reduced capability to counteract the threats and damage that an individual is exposed to during their lifetime. A great deal of understanding of the ageing process has come from studies of premature ageing, as observed in progeroid syndromes. As mentioned earlier, these rare genetic disorders can arise from mutations in either LMNA or Zmpste24 genes which affect normal prelamin A processing, as is the case in HGPS and RD. Several other progeroid syndromes caused by mutations in separate genes have also been described (Coppedè and Migliore, 2010; Navarro et al., 2006). Some of the most recognised are, for example, mutations in RecQ protein-like helicases (RECQL) causing Werner syndrome, Bloom's syndrome and Rothmund–Thomson syndrome. Defects in nuclear excision repair (NER) proteins underlie Cockayne syndrome, xeroderma pigmentosum, and trichothiodystrophy. Although all of these disorders display many symptoms of physiological ageing with several tissues affected, not all features of the normal ageing process are present (Puzianowska-Kuznicka and Kuznicki, 2005). Thus, they are also known as segmental ageing syndromes.

The lack of full recapitulation of the physiological ageing process in progeroid syndromes questions their value as useful models for studying ageing because they

may represent an effect of highly specialised physiological conditions (Dreesen and Stewart, 2011; Kipling et al., 2004). Studies continue to emerge, however, in favour of the fact that progeroid syndromes represent the natural ageing process, only at an accelerated speed (Burtner and Kennedy, 2010). For example, progerin, a farnesylated prelamin A variant expressed in HGPS patients, has also been found in older individuals, albeit at lower levels (Scaffidi and Misteli, 2006). Interestingly, accelerated cardiovascular disease is the primary cause of death in HGPS, and progerin has also been found to gradually accumulate in the coronary arteries in the normal ageing process (Olive et al., 2010).

1.4.1 Hutchinson-Gilford progeria syndrome

HGPS was first reported by Jonathan Hutchinson in 1886, and subsequently in an independent report by Hastings Gilford in 1897, hence the syndrome's name. HGPS is a rare autosomal dominant syndrome with an early onset of progeroid symptoms. As of September 2015, there were 103 children diagnosed with HGPS worldwide (www.progeriaresearch.org), making it one of the rarest described syndromes. Despite its rarity, HGPS is widely recognised due to its peculiarity. Individuals diagnosed with this devastating disease suffer from sclerotic skin, bone abnormalities, joint contractures, alopecia, and growth impairment. Cognitive development, however, is normal. These patients generally die in their teens as a result of cardiovascular complications associated with atherosclerosis, like myocardial infarction and stroke (DeBusk, 1972; Merideth et al., 2008; Pereira et al., 2008).

Progeria is predominantly caused by a *de novo* point mutation in the LMNA gene (C1824T) within exon 11 (De Sandre-Giovannoli et al., 2003; Eriksson et al., 2003). This

single base substitution activates a cryptic splice site, which results in a truncated version of prelamin A. It is missing internal 50 amino acid residues yielding a protein termed progerin. Within that missing region lays a recognition site for the second cleavage by Zmpste24 protease. As a result, progerin retains farnesylation and carboxymethylation at its C-terminal cysteine, which is considered toxic to the cells. Progerin leads to various cellular abnormalities, both morphological and molecular (Ghosh and Zhou, 2014; Gonzalo and Kreienkamp, 2015; Prokocimer et al., 2013). Among the most prominent effects of progerin expression is nuclear lobulation and altered nuclear architecture, mitochondrial dysfunction, release of heterochromatin from the nuclear periphery, altered epigenetic regulation and signalling, and gene expression. It also leads to genome instability, telomere aberrations, impaired DNA repair, compromised cell-cycle regulation, and increased senescence (Cao et al., 2011; Goldman et al., 2004; Hernandez et al., 2010; Liu et al., 2005; Osorio et al., 2012; Shumaker et al., 2006; Viteri et al., 2010).

Multiple tissues, mainly of mesenchymal origin, are affected in individuals suffering from HGPS. In contrast to normal ageing, HGPS is not associated with central nervous system (CNS) pathology and cognitive function deficit. This appears to be an effect mediated by the microRNA miR-9 that is highly expressed in the CNS (Jung et al., 2012). Based on mouse model, it has been shown that miR-9 regulates the levels of lamin A mRNA in the brain and as a result, this protein is absent. Lamin C, however, remains expressed because miR-9 recognition sequence is localised to the C-terminal region of LMNA transcript, absent in lamin C mRNA. The target sequence for miRNA-9 is preserved in the progerin transcript though. Therefore, the down-regulation of progerin expression in the brain mediated by miR-9 could explain why HGPS patients

are free of cognitive impairment, as continuous miR-9 expression would offer protection from any detrimental toxicity caused by progerin in the CNS.

1.4.2 Lamin B in ageing/senescence

Recent reports have implied a role for lamin B in ageing and/or cellular senescence, although the emerging picture is complex. *In vitro* studies on fibroblasts from patients with the progeroid syndrome ataxia telangiectasia (AT), which is characterised by impaired DDR, lamin B1 levels were significantly increased (Barascu et al., 2012). It was proposed that increased ROS levels observed in AT mediated lamin B1 overexpression via the p38 MAPK pathway leads to cellular senescence. By contrast, lamin B1 loss was demonstrated to affect senescence of normal human fibroblasts in *in vitro* cultures. Both replicative and oncogene-induced senescence led to decline in lamin B levels in response to activation of either p53 or RB, but not ROS (Freund et al., 2012; Shimi et al., 2011). In addition, loss of B-type lamins in mouse knock-out models had no effect on embryonic stem cells, hepatocytes or keratinocytes (Kim et al., 2011). Multiple pathways converge on the NE and the lamina (Dauer and Worman, 2009; Simon and Wilson, 2011), and the ROS-mediated damage to lamin A was also observed in senescence (Pekovic et al., 2011). It has therefore been proposed that nuclear lamina perturbation could trigger senescence via different pathways in a context-dependent manner (Hutchison, 2012).

Moreover, it has been shown that lamin B1 can indirectly influence expression of $p16^{INK4a}$, a key effector of the senescence programme. This occurs via lamin B1-mediated regulation of Oct1 transcription factor activity that in turn regulates microRNA miR-31 expression. MiR-31 has been demonstrated to target $p16^{INK4a}$ mRNA

(Malhas et al., 2010). Thus it is another example of the signalling pathway that can link perturbations in the NE to regulation of senescence.

1.5 Aims of the thesis

Senescence is increasingly appreciated as a phenomenon accompanying physiological ageing and underlying many pathologies associated with advanced age. Increased frequency of senescent cells has also been observed in premature ageing syndromes, including HGPS. Given that HGPS is caused by improperly processed progerin, retaining posttranslational modifications at its C-terminus, it was hypothesised that farnesylated prelamin A could induce cellular senescence and contribute to normal physiological ageing. Indeed not only progerin, but also prelamin A levels progressively increase during the ageing process. Several mRNA profiles have been reported for HGPS and replicative senescence, however none have been described for cells accumulating prelamin A. Moreover, senescence is characterised by the SASP, which can have detrimental effects on tissue homeostasis in late age. No broad SASP characterisation has ever been carried out for cells accumulating prelamin A. Additionally, progerin and prelamin A expression heavily impacts nuclear architecture, altering chromatin organisation, gene expression and cellular signalling. It is accompanied by the formation of an extensive tubular structure within the nucleus termed the NR. Although the NR has been linked to regulation of gene expression and nuclear import/export, its role and formation process remain elusive.

The thesis therefore aims to:

- Determine phenotypical characteristics of prelamin A accumulation and its impact on senescence.

- Characterise the transcriptome profile of cells accumulating prelamin A and how it compares to a profile of physiologically aged cells by replicative senescence.
- Identify potential candidates and explore mechanisms linking the nuclear envelope to ageing via prelamin A accumulation.
- Characterise the Senescence Associated Secretory Phenotype of cells accumulating prelamin A in reference to replicative senescence.
- Investigate mechanisms of Nucleoplasmic Reticulum formation, under both pathological conditions when the prelamin A maturation process is affected, as well as under physiological conditions when NR formation is a part of the natural cellular response.

CHAPTER 2

2 Materials and Methods

2.1 Reagents

2.1.1 Chemicals

Chemicals used for buffer preparations were obtained from Sigma or BDH, except where otherwise stated.

2.1.2 Plasmid DNA

Plasmid DNA vectors used in this thesis were either constructed by myself (Vaux Lab) as described in 2.2.4 or acquired from other researchers as indicated in Table 2.1.

Table 2.1. Plasmid DNA constructs used in the thesis and their origin.

Plasmid name	Gene encoded	GFP location	Promoter driving expression	Origin	Antibiotic resistance
pEGFP_AQP1	Aquaporin 1	N-terminus	CMV	Vaux Lab	Kanamycin
pEGFP_CLDN11v1	Claudin 11 variant 1	N-terminus	CMV	Vaux Lab	Kanamycin
pEGFP_CAV1alpha	Caveolin 1 α	N-terminus	CMV	Vaux Lab	Kanamycin
pEGFP_CAV1beta	Caveolin 1 β	N-terminus	CMV	Vaux Lab	Kanamycin
pEGFP_F3	Thromboplastin (long isoform)	N-terminus	CMV	Vaux Lab	Kanamycin
pEGFP-N1_ADAM12L	Adam12 (long isoform)	N terminus	CMV	U. Wewer (Hougaard et al., 2000)	Kanamycin
pcDNA3.1_tPA-GFP	Tissue plasminogen activator	C-terminus	CMV	Y. Suzuki (Suzuki et al., 2009)	Ampicillin
pEGFP-Tub	Tubulin	N-terminus	CMV	BD Biosciences Clontech	Kanamycin

2.1.3 DNA purification

DNA purification products were obtained from Qiagen unless otherwise stated.

2.1.4 Cell culture products

Media and cell culture products were obtained from PAA. Heat inactivated Foetal Bovine Serum (FBS) was purchased from Sigma. Sterile cell culture plastic ware was purchased from Appleton Woods. It included various formats of cell culture plates and tissue culture flasks with vented caps.

2.1.5 Antibodies

Antibodies used in this thesis are listed in Table 2.2.

Table 2.2. List of antibodies. WB, Western Blotting, IF, Immunofluorescence, FACS, Fluorescence-Activated Cell Sorting.

Antibody	Source	Supplier	Conjugate	Dilution
Anti-GLB1 (EPR8250)	Rabbit monoclonal	Abcam	-	1:10000 WB 1:50 FACS
Anti-IL6	Mouse monoclonal	Abcam	PE	1:10 FACS
Anti-IL6	Mouse monoclonal	ImmunoTools	FITC	1:20 FACS
Anti-IL6	Mouse monoclonal	ImmunoTools	APC	1:20 FACS
Anti-lamin A/C (4C11)	Mouse monoclonal	Active Motif	-	1:2000 WB 1:100 IF
Anti-lamin B1	Rabbit polyclonal	Abcam	-	1:100 IF
Anti-lamin B1 (C-20)	Goat polyclonal	SantaCruz	-	1:200 WB 1:50 IF
Anti-lamin B1 (8D1)	Mouse monoclonal	Own	-	undiluted hybridoma cell culture supernatant
Anti-NOGO A+B (ab47085)	Rabbit polyclonal	Abcam	-	1:1000 WB
Anti-p16 (F-12)	Mouse monoclonal	SantCruz	-	1:200 WB 1:20 FACS
Anti-prelamin A (C-20)	Goat polyclonal	SantaCruz	-	1:50 IF 1:20 FACS

Antibody	Source	Supplier	Conjugate	Dilution
Anti-progerin (13A4)	Mouse monoclonal	Active Motif	-	1:10 IF
Anti-SREBP1 (H-160)	Rabbit polyclonal	SantaCruz	-	1:200 WB
Anti-Zmpste24 (H-170)	Rabbit polyclonal	SantaCruz	-	1:200 WB
Anti-β actin	Mouse monoclonal	Abcam	-	1:3000 WB
Anti-goat	Donkey polyclonal	Molecular probes	Alexa 647	1:300 IF, FACS
Anti-mouse	Donkey polyclonal	Molecular probes	Alexa 488	1:300 IF, FACS
Anti-mouse	Donkey polyclonal	Molecular probes	Alexa 594	1:300 IF, FACS
Anti-mouse	Donkey polyclonal	Jackson ImmunoResearch	Cy3	1:300 IF, FACS
Anti-mouse	Donkey polyclonal	Sigma	HRP	1:5000 WB
Anti-rabbit	Donkey polyclonal	Abcam	Alexa 405	1:300 IF, FACS
Anti-rabbit	Donkey polyclonal	Molecular probes	Alexa 488	1:300 IF, FACS
Anti-rabbit	Donkey polyclonal	Abcam	Alexa 405	1:300 IF, FACS
Anti-rabbit	Donkey polyclonal	Sigma	HRP	1:5000 WB

2.2 DNA amplification, purification and cloning

2.2.1 Bacterial cell culture

Escherichia coli was cultured in sterile Luria-Bertani (LB) medium (170 mM NaCl, 1% tryptone, 0.5% yeast extract) supplemented with appropriate antibiotics using aseptic techniques. Bacterial cells were cultured in a rotary shaker at 220 rpm at 37°C. Antibiotics used: kanamycin at 50 μg/ml, ampicillin at 100 μg/ml.

Bacterial strains were kept long term as glycerol stocks in -80°C. The stocks were prepared by supplementing liquid cell culture with 15% glycerol and transferring to -80°C in cryotubes.

2.2.2 Bacterial cell transformation

NEB 5-α competent *E. coli* (*fhuA2 Δ(argF-lacZ)U169 phoA glnV44 Φ80 Δ(lacZ)M15 gyrA96 recA1 relA1 endA1 thi-1 hsdR17*) (New England Biolabs), a derivative of DH5-α, was used for most transformations unless there was requirement for unmethylated plasmid DNA, in which case *dam*$^{-}$*/dcm*$^{-}$ competent *E. coli* (*ara-14 leuB6 fhuA31 lacY1 tsx78 glnV44 galK2 galT22 mcrA dcm-6 hisG4 rfbD1 R(zgb210::Tn10)* Tet^{S} *endA1 rspL136* (Str^{R}) *dam13::Tn9* (Cam^{R}) *xylA-5 mtl-1 thi-1 mcrB1 hsdR2*) (New England Biolabs) was used.

For a single transfection, 50 µl of competent *E. coli* were thawed on ice and 1 to 5 µl containing 1 pg – 100 ng of plasmid DNA was added to the cell mixture, gently mixed and incubated on ice for 30 minutes. Cells were then heat shocked at 42°C for 30 seconds and placed on ice for five minutes. In the next step, 950 µl of pre-warmed LB medium at 37°C were added, and bacteria were cultured for one hour at 37°C. One hundred µl of the culture were spread on pre-warmed agar plates supplemented with an appropriate antibiotic. The remaining culture was centrifuged (5000 rpm for 1 minute) and the bacterial cell pellet was spread on another selective plate.

2.2.3 Purification of plasmid DNA from bacterial cells

A single transformant colony was used to inoculate 5 ml LB medium supplemented with the appropriate antibiotic and grown at 37°C on a rotor shaker overnight. For small scale plasmid preparation, PureYield Plasmid Miniprep System kit

(Promega) was used for purification of high-quality plasmid DNA suitable for eukaryotic cell transfection. Three ml of the starter culture were used following manufacturer's protocol. The kit relies on alkaline lysis of bacteria cells, followed by column-based DNA purification, and a unique Endotoxin Removal Wash designed to remove contaminants such as RNA, proteins, and lipopolysaccharides (LPS).

For large scale plasmid purification, the Qiagen Midiprep kit (Qiagen) was used according to the manufacturer's guidelines. Briefly, 50 µl of the starter culture were added to 50 ml of selective LB and grown at 37°C at 220 rpm overnight. The next day, bacteria were harvested by centrifugation at 6000g for 15 minutes at 4°C. The cells were then resuspended in 4 ml of buffer P1 and lysed by the addition of 4 ml of buffer P2. The tube containing the lysate was thoroughly mixed by inversion and incubated for five minutes at room temperature. Four ml of chilled buffer P3 were subsequently added to precipitated genomic DNA, proteins, and cell debris, mixed vigorously and incubated on ice for 15 minutes. The mixture was centrifuged at 20000g for 30 minutes at 4°C, the supernatant was transferred to a new tube and centrifuged again for 15 minutes at 4°C. A Qiagen-tip 100 was equilibrated with 4 ml of buffer QBT and the supernatant containing plasmid DNA was allowed to filter through the equilibrated tip by gravity flow. The tip was washed twice with 10 ml of buffer QC. The plasmid DNA was eluted by adding 5 ml of buffer QF and collected in a new tube. DNA precipitation with 3.5 ml of isopropanol followed, and the mixture was centrifuged at 15000g for 30 minutes at 4°C. The supernatant was discarded, and the DNA pellet was washed with 2 ml of room temperature 70% ethanol (70% ethanol:30% water by volume) and centrifuged again at 15000g for 10 minutes. The supernatant was removed; the DNA pellet was air-dried and resuspended in 1 ml of ultrapure water (18

MΩ water from a Millipore Elix water purification system). The concentration of DNA was measured on Nanodrop ND 1000 spectrophotometer.

2.2.4 DNA cloning

2.2.4.1 Template cDNA synthesis

Total RNA from primary Human Dermal Fibroblasts was isolated as in 2.5.1 using the mirVANA Isolation Kit (Life Technologies) according to the manufacturer's guidelines, followed by cDNA synthesis using SuperScript III Reverse Transcriptase (Invitrogen) as recommended by the manufacturer.

2.2.4.2 Oligonucleotide design

Primers were designed to amplify target genes from cDNA with the addition of XhoI and XbaI restriction sites at the N- and C-termini respectively, making sure that ligation into the pEGFP-Tub Vector would result in in-frame product with EGFP at the C-terminus of the target gene.

2.2.4.3 PCR conditions

Two µl of total cDNA were used as a template in PCR reaction using 1.25 units of Taq Polymerase (New England Biolabs) and 200 nM primers in 50 µl total reaction volume. The temperature of melting and annealing for oligonucleotide pairs was calculated in the T_M calculator tool available from New England Biolabs (http://tmcalculator.neb.com/#!/). The first five cycles of DNA amplification were performed at the annealing temperature calculated for the part of the oligonucleotide sequence fully hybridising with the target sequence (shown in upper case in the Table 2.3) followed by 30 cycles at the annealing temperature calculated for the entire

primer sequence (including restriction site overhangs). Extension time was calculated as one minute per 1 kb of target sequence.

Thermocycling conditions were as follows:

- Initial denaturation at 95°C for 30 seconds.
- Five cycles of: (i) 95°C for 30 seconds; (ii) annealing at lower temperature (calculated as described above) for 60 seconds; (iii) 68°C for variable times depending on the sequence length of the target gene (1 min / 1 kb).
- Thirty cycles of: (i) 95°C for 30 seconds; (ii) annealing at higher temperature (calculated as described above) for 60 seconds; (iii) 68°C for variable times depending on the sequence length of the target gene (1 min / 1 kb).
- Final extension at 68°C for five minutes.
- Hold at 4°C.

Table 2.3. List of primers used in the DNA cloning.

Gene name	Primer name	Sequence	T_M (°C)
F3	Marek_F3_F	tactcgagAC**ATG**GAGACCCCTGCCTG	(60), 67
	Marek_F3L_R	gtctagaTTATGAAACATTCAGTGGGGAGTTCTC	(57), 60
Aquaporin 1	Marek_AQP1_v1_F	tactcgagGC**ATG**GCCAGCGAGTTCA	(59), 67
	Marek_AQP1_v1_R	gtctagaCTATTTGGGCTTCATCTCCACCC	(58), 63
Claudin 11	Marek_CLDN11_v1_F	tactcgagCC**ATG**GTGGCCACGTGCCT	(65), 71
	Marek_CLDN11_R	cgtctagaTTATACGTGGGCACTCTTCGCATGAGTC	(63), 66
Caveolin 1 α	Marek_CAV1_v1_XhoI_F	tactcgag GC**ATG**TCTGGGGGCAAATAC	(57), 65
	Marek_CAV1_XbaI_R	cgtctagaTTATATTTCTTTCTGCAAGTTGATGCGG	(56), 61
Caveolin 1 β	Marek_CAV1_v2_XhoI_F	tactcgagCC**ATG**GCAGACGAGCTGAG	(59), 67
	Marek_CAV1_XbaI_R	cgtctagaTTATATTTCTTTCTGCAAGTTGATGCGG	(56), 61

2.2.4.4 Cloning strategy

Five µl of the PCR reaction were run in the 0.8% agarose gel to assess the quality and size of the PCR product. Upon the completion of electrophoresis, the gel was immersed in SYBR Gold Nucleic Acid Gel Stain solution (Molecular Probes), followed by DNA visualisation with UV light. If the quality of the PCR product was satisfactory, appropriate restriction enzymes were added to the remaining PCR reaction volume, followed by incubation at 37°C for two hours. The DNA was then purified with QIAquick PCR Purification Kit (Qiagen) and used for ligation. The acceptor plasmid vector originated from pEGFP-Tub (BD Biosciences Clontech) and was cut with XhoI and XbaI endonucleases to remove the tubulin encoding region. It was subsequently dephosphorylated with alkaline phosphatase (New England Biolabs) and purified from the 0.8% agarose gel with the QIAquick Gel Extraction Kit (Qiagen) following the manufacturer's instructions. The PCR product was then ligated into the acceptor vector for one hour at room temperature using T4 DNA ligase (New England Biolabs) and the ligation solution was used for transformation of competent *E. coli* cells as described in 2.2.2. Kanamycin resistant colonies were screened, plasmid purification followed, and the accuracy of cloning was confirmed by sequencing.

2.3 Mammalian cell culture

2.3.1 Cell lines and their origin

Human dermal fibroblast (HDF) primary cells (De Vos et al., 2011) from healthy volunteers were kindly provided by Dr Winnok De Vos, Department of Molecular Cell

Biology, CARIM-School for Cardiovascular Diseases, Maastricht University, The Netherlands, and supplied by Promocell, Heidelberg, Germany.

Dermal fibroblasts from a classical Hutchinson-Gilford Progeria Syndrome (HGPS) patient, sample AGO 1972, were kindly provided by Dr Joanna Bridger, Brunel University, UK.

HeLa cells were obtained from laboratory stocks. Ishikawa cell line, traceable to ATCC stock, was part of laboratory collection. Whereas mouse preadipocytes (3T3-F442A) were supplied by the Public Health Protection England from the European Collection of Authenticated Cell Cultures (ECACC).

2.3.2 General cell culture technique

Cell culture and passaging was performed in a category two laminar flow hood using sterile techniques. Cells were incubated at 37°C in the presence of 5% CO_2 in a humidified atmosphere.

Most cell lines were cultured in Dulbecco's Modified Eagle Medium (DMEM) supplemented with 10% foetal calf serum (FCS), 1% non-essential amino acids, and penicillin and streptomycin antibiotics (100 units/ml). The exception was HGPS AGO1792 cell line medium, which was supplemented with 15% foetal calf serum and Ishikawa cell line medium in experiments investigating effect of oestrogen. In these experiments, the growth medium was prepared using charcoal-stripped serum (Sigma-Aldrich) at 10% concentration.

Typically, cells were passaged when they reached 80-90% confluency by trypsinisation with TrypLE Express (Gibco) at 37°C. The trypsinisation was subsequently inactivated by the addition of warm growth medium at a ratio of 1:5,

and cells were seeded at the required density. If needed, cells were centrifuged at 300 g for five minutes. For freezing purposes, cells were pelleted, supernatant removed, and cells resuspended in FCS supplemented with 10% DMSO. The cells were then transferred to cryotubes and placed in a polystyrene holder at -80°C overnight before transferring to liquid nitrogen the next day.

2.3.3 Drug treatment of cells in culture

Drug stocks were added to CO_2 and temperature equilibrated cell culture medium to the required concentration. Daily growth medium change with the addition of fresh drug followed unless otherwise stated. Saquinavir (Sigma) and Darunavir (Sigma) were prepared in the same way, by dissolving in DMSO. Both were kept as 5 mM stocks at -20°C. Cells were typically treated with 20 μM saquinavir or darunavir for 48 hours. Farnesyl transferase inhibitor FTI-277 (Calbiochem) was dissolved in DMSO and used at 8 μM for the indicated period of time. Campothotecin was dissolved in DMSO and used at 4 μg/ml for a period of five days. Cyclohexamide (Sigma) was dissolved in ethanol and used at 50 μg/ml, as indicated. Rotenone (Sigma) was dissolved in DMSO and used at 0.5 μM for 48 hours. Negative controls were incubated with the appropriate volume of the corresponding vehicle alone (either DMSO or ethanol).

2.3.4 Plasmid transfection of mammalian cells in culture

The day before transfection, cells were passaged and transferred to antibiotic-free growth medium. Transfection was performed with Lipofectamine 2000 (Invitrogen) following the manufacturer's recommendations. Briefly, DNA and Lipofectamine were diluted separately in DMEM serum-free medium, then mixed

together and incubated for 15 minutes to allow complex formation. For 1 µg DNA, 1 µl Lipofectamine was used. Finally, the mixture was added dropwise to cells. Normally, cells were analysed 48 hours post-transfection unless indicated otherwise.

2.3.5 Plasmid electroporation of primary cells

Human dermal fibroblasts were transfected by electroporation using an Amaxa Nucleofector I device (Lonza). Either Amaxa Human Dermal Fibroblast Nucleofector Kit (Lonza) or Ingenio Electroporation kit (Mirus Bio) was used, following the manufacturer's instructions. Briefly, cells were passaged six days prior to electroporation, and at the time of harvest they were reaching 80-90% confluency. 10^6 cells were resuspended in electroporation solution, combined with 2-3 µg of plasmid DNA, mixed and transferred into a 0.2 cm cuvette. Cells were electroporated using U-23 program on the device designed for high transfection efficiency. The cells were subsequently transferred into pre-equilibrated growth medium and left to recover for 48 hours before gene expression analysis.

2.3.6 siRNA transfection of mammalian cells in culture

Cells were passaged the day before transfection and seeded in antibiotic-free medium. SiRNA transfection was performed with Lipofectamine RNAiMAX reagent (Invitrogen) following the manufacturer's protocol. Briefly, the optimal siRNA amount and Lipofectamine RNAiMAX were diluted separately in serum-free DMEM, combined at a 1:1 ratio, and incubated at room temperature for 15 minutes, followed by the addition of siRNA-lipid complexes to cells. The next day, the procedure was repeated and the cells were analysed 48 hours from the first transfection. For most experiments 20 nM siRNA concentration was used, unless otherwise stated.

2.4 qRT-PCR

The Cells-to-cDNA II Kit (Life Technologies) was used for cDNA synthesis directly from cell lysate without the RNA purification step, following the manufacturer's instructions. Quantitative PCR was performed using a StepOne Plus Real-Time PCR Sytem (Applied Biosystems) and the Fast SYBR Green master mix (Applied Biosystems) according to the manufacturer's instructions. qPrimerDepot database was used for selecting primers (http://primerdepot.nci.nih.gov/). β-actin (Actb) gene was used as an internal control for all qPCR reactions and the relative gene expression values were calculated based on the Formula method $2^{-\Delta\Delta C(T)}$ (Livak and Schmittgen, 2001).

Table 2.4. List of primers used in qRT-PCR. Oligonucleotide primers were obtained from Sigma. F and R in the ending of primer names stand for forward and reverse, respectively.

Gene Name	Primer Name	Sequence	RefSeq
Actβ	Marek_Human_ActB_F	GTTGTCGACGACGAGCG	NM_001101
	Marek_Human_ActB_R	GCACAGAGCCTCGCCTT	
ADAM12	Marek_Human_ADAM12L_2F	ACCGTGTAATTTCGAGCGAG	NM_003474
	Marek_Human_ADAM12L_2R	ACGGGAAAGCAAAGAACTGA	
AIMP3	Marek_Human_AIMP3_F	GAATGTGACAAAACCAGCGA	NM_004280
	Marek_Human_AIMP3_R	TTGTACTATGGACTTCATCGCTTT	
AQP1	Marek_Human_AQP1_2F	CCCGAGTTCACACCATCAG	NM_198098
	Marek_Human_AQP1_2R	CTCATGTACATCATCGCCCA	
CAV1	Marek_Human_CAV1_F	CAAATGCCGTCAAAACTGTG	NM_001753
	Marek_Human_CAV1_R	CGACCCTAAACACCTCAACG	
CLDN11	Marek_Human_CLDN11_2F	GCCTGCATACAGGGAGTAGC	NM_005602
	Marek_Human_CLDN11_2R	TGGTGTTTTGCTCATTCTGC	
DAG1	Marek_Human_DAG1_F	AAGTGACTTGGTCCCAGAGC	NM_004393
	Marek_Human_DAG1_R	AGGAGGAGCGAACACCTG	
EGFR	Marek_Human_EGFR_F	TCCTCTGGAGGCTGAGAAAA	NM_201283
	Marek_Human_EGFR_R	GGGCTCTGGAGGAAAAGAAA	
ELDT1	Marek_Human_ELDT1_F	CTCAGTCCTGTGGCGAAAATG	NM_022159
	Marek_Human_ELDT1_R	GGTTACTGCTGGATCTGAAGC	
F3	Marek_Human_F3_2F	ACAATCTCGTCGGTGAGGTC	NM_001993
	Marek_Human_F3_2R	CCAAACCCGTCAATCAAGTC	
FAS	Marek_Human_FAS_F	TCCTCAATTCCAATCCCTTG	NM_000043
	Marek_Human_FAS_R	GCATCTGGACCCTCCTACCT	
GLB1	Marek_Human_GLB1_F	GGAGTCCCGGCTATAGTCAA	NM_000404
	Marek_Human_GLB1_R	CTCCTTCTGCTGCTGGTTCT	

Gene Name	Primer Name	Sequence	RefSeq
GM-CSF	Marek_Human_GM-CSF_F	GTCTCACTCCTGGACTGGCT	NM_000758
	Marek_Human_GM-CSF_R	ACTACAAGCAGCACTGCCCT	
INFG	Marek_Human_IFNG_2F	GTATTGCTTTGCGTTGGACA	NM_000619
	Marek_Human_IFNG_2R	GAGTGTGGAGACCATCAAGGA	
IGFBP1	Marek_Human_IGFBP1_F	TTATCTCCGTGCTCTCTGGG	NM_000596
	Marek_Human_IGFBP1_R	GGAGCAGCAACCTCTGCAC	
IGFBP3	Marek_Human_IGFBP3_F	GACGGGCTCTCCACACTG	NM_000598
	Marek_Human_IGFBP3_R	AACGCTAGTGCCGTCAGC	
IGFBP5	Marek_Human_IGFBP5_F	GAGTAGGTCTCCTCGGCCAT	M_000599
	Marek_Human_IGFBP5_R	GGTTTGCCTCAACGAAAAGA	
IGFBP6	Marek_Human_IGFBP6_F	GCCTGCTTGGGGTTTACTCT	NM_002178
	Marek_Human_IGFBP6_R	ATCCGCCCAAGGACGAC	
IL1α	Marek_Human_IL1a_F	CCGTGAGTTTCCCAGAAGAA	M_000575
	Marek_Human_IL1a_R	ACTGCCCAAGATGAAGACCA	
IL6	Marek_Human_IL6_F	GTCAGGGGTGGTTATTGCAT	NM_000600
	Marek_Human_IL6_R	AGTGAGGAACAAGCCAGAGC	
IL8	Marek_Human_IL8_F	AAATTTGGGGTGGAAAGGTT	NM_000584
	Marek_Human_IL8_R	TCCTGATTTCTGCAGCTCTGT	
IRAK1	Marek_Human_IRAK1_F	CTTCTCAAAGCCACTCCAGC	NM_001569
	Marek_Human_IRAK1_R	GAGACCTTGGCTGGTCAGAG	
ME1	Marek_Human_ME1_F	GGAGACGAAATGCATTCACA	NM_002395
	Marek_Human_ME1_R	ACGAATTCATGGAGGCAGTT	
MMP3	Marek_Human_MMP3_F	CAATTTCATGAGCAGCAACG	NM_002422
	Marek_Human_MMP3_R	AGGGATTAATGGAGATGCCC	
MYO1D	Marek_Human_MYO1D_F	GACGTTCACTTGAAGGTGGC	NM_015194
	Marek_Human_MYO1D_R	ACAGCCAACCCATGAGAGTC	
NOD2	Marek_Human_NOD2_F	TAGAAGGAAGGCAGCCAATC	NM_022162
	Marek_Human_NOD2_R	GATGAAATCAGGTTGCCGAT	
OPN3	Marek_Human_OPN3_F	TAGGGTGGCAATGGAAACA	NM_014322
	Marek_Human_OPN3_R	TTTACCTTCGTGTCCTGCCT	
p16	Marek_Human_p16_F	GTGAGAGTGGCGGGGTC	NM_000077
	Marek_Human_p16_R	GTTACGGTCGGAGGCCG	
PAI1	Marek_Human_PAI1_F	AGCTCCTTGTACAGATGCCG	NM_000602
	Marek_Human_PAI1_R	ACAACAGGAGGAGAAACCCA	
PLAT	Marek_Human_PLAT_F	GCAGAGCCCTCTCTTCATTG	NM_000930
	Marek_Human_PLAT_R	CTGGAGAGAAAACCTCTGCG	
REL	Marek_Human_REL_F	CCATGTTCATCAGGGAGAAA	NM_002908
	Marek_Human_REL_R	GCAGGAATCAATCCATTCAA	
TAF10	Marek_Human_TAF10_F	AATTATGCGTGGGTCTGAGG	NM_006284
	Marek_Human_TAF10_R	TGGTGGACTTCTTGATGCAG	
TRAF6	Marek_Human_TRAF6_F	GCCACACAGCAGTCACTTTC	NM_004620
	Marek_Human_TRAF6_R	TCCCCGCGCACTAGAAC	
UBE2D1	Marek_Human_UBE2D1_F	TGCCAGTGGAACAAGTCATC	NM_003338
	Marek_Human_UBE2D1_R	ATGGCGCTGAAGAGGATTC	

2.5 Microarray analysis of gene expression

2.5.1 RNA isolation

Six biological replicates were prepared for each comparison tested. RNA was extracted using mirVANA Isolation Kit (Life Technologies) allowing for preparation of both total RNA and small RNA, following the manufacturer's instructions. Briefly, cells were disrupted in a denaturing lysis buffer before they were subjected to Acid:Phenol:Chloroform extraction (Chomczynski and Sacchi, 1987). In the final step, total RNA was immobilised on a Filter Cartridge containing a glass-fibre filter, washed several times, and eluted with a low ionic-strength buffer. The concentration of RNA was quantified on a Nanodrop spectrophotometer, and its integrity was confirmed on a 2100 Bioanalyzer (Agilent Technologies) using Nanochips, according to the manufacturer's instructions. Only RNA samples with RIN index above 9 were used, with the majority ranging from 9.7 to 10.

2.5.2 cDNA preparation and labelling

A 3DNA dendrimer-based system was used for RNA labelling with two dye swaps. 0.5 µg of total RNA was labelled using the 3DNA Array 900 kit (Genisphere), using Superscript III reverse transcriptase (Invitrogen) in the first strand cDNA synthesis, following the manufacturer's instructions.

2.5.3 Hybridisation to microarray slides

HS1200 Human OpArray microarrays, containing 35035 oligonucleotide probes that represented approximately 25100 unique genes and 39600 transcripts, were purchased from Microarray Inc.

The hybridisation was performed in the SDS-based hybridisation buffer on a SlideBooster SB400 (Advalytix AG, Munich) using a LifterSlip (Erie Scientific Company) for an even cDNA transfer across the microarray slide. Power of 27 and a pulse:pause ratio of 3:7 was applied for 16 hours at 55°C. After the first hybridisation, the microarrays were washed at 55°C in 2xSSC/0.2% SDS, then at room temperature in 2xSSC, followed by 0.2xSSC, each wash for ten minutes, with shaking at 150 rpm. The slides were then dried and subjected to the second hybridisation with the 3DNA dendrimer capture reagents supplied with the kit for four hours at 50°C, using the same settings. The slides were then washed and dried as above.

2.5.4 Microarray slides scanning

Hybridised microarray slides were scanned on the ScanArray ExpressHT Scanner (PerkinElmer). The TIFF images for analysis were acquired using autocalibration with 100% laser power and a variable photomultiplier tube setting with a signal target saturation of 90%.

Quality of spots was assessed in the analysis software BlueFuse Version 3.2 (BlueGnome). Manual flagging and automatic exclusion of artifacts, irregular spots, or spots with insufficient signal above background was applied. Additionally, spots with BlueFuse pON score below 0.05 and grid offset above 8.94 were removed from the data set. The intensity values for the remaining spots were extracted and analysed further.

2.5.5 Data normalisation and analysis using BASE

Data output from BlueFuse was imported into the BASE tool (Saal et al., 2002). In order to correct spot intensities with a one-channel bias, the cross-channel

correction (developed by the Computational Biology Research Group, CBRG Oxford; http://www.molbiol.ox.ac.uk/CBRG_home.shtml) was applied by subtracting 2% intensity of one channel from the other and vice versa. Data within each comparison were globally normalised using Lowess normalisation (Yang et al., 2002b), and the overall median fold change for the normalised data from biological replicates was calculated with the fold change algorithm within BASE. The BASE Cyber-T plug-in was used to perform statistical testing using a sliding window size of 101 and a Bayes confidence estimate of ten.

2.5.6 Functional microarray data analysis

Only median fold ratio values with $P < 0.05$ were analysed unless otherwise indicated. Gene Set Enrichment Analysis (Broad Institute) (Subramanian et al., 2005), Gene Ontology (The Gene Ontology Consortium, 2010), Reactome (Joshi-Tope et al., 2005), String (Snel et al., 2000), and WEB-based GEne SeT AnaLysis Toolkit (WebGestalt) (Wang et al., 2013a) were used as indicated. Color-coded clustered image maps ("heat maps") were created using the CIMminer tool (Weinstein et al., 1997) developed by the Genomics and Bioinformatics Group at the National Cancer Institute (http://discover.nci.nih.gov/cimminer/home.do).

2.5.7 qRT-PCR validation

Microarray data was validated by qRT-PCR as described in 2.4.

2.6 Protein analysis by Western blotting

2.6.1 Sample preparation

Cells were washed twice in PBS, trypsinised, and pelleted by centrifugation at 1000g for five minutes. Equal numbers of cells were resuspended in sample lysis buffer (Thermo Scientific) supplemented with 10 mM DTT, followed by a five minute incubation at 90°C. Cell lysates were centrifuged, separated from the pellet, and either analysed immediately or stored at -20°C.

2.6.2 One dimensional SDS polyacrylamide gel electrophoresis (SDS-PAGE)

SDS polyacrylamide gel electrophoresis was performed using either Bio-Rad Miniprotean 3 system (Bio-Rad) for homemade 10% SDS-PAGE gels or XCell SureLock Mini-Cell apparatus (Life Technologies) for precast 4-12% NuPAGE Bis-Tris gels (Novex).

The 10% gels were prepared by casting a resolving gel (10% acrylamide/bisacrylamide 37:5:1, 375 mM Tris-Cl pH 8.8, 0.1% SDS (w/v), 0.1% TEMED (v/v), 0.1% APS (w/v)) with a stacking gel (4% acrylamide/bisacrylamide 37:5:1, 125 mM Tris-Cl pH 6.8, 0.1% SDS (w/v), 0.1% TEMED (v/v), 0.1% APS (w/v)) overlaying it. At least 30 minutes were allowed for polymerisation. Electrophoresis was performed in SDS running buffer (25 mM Tris, 250 mM glycine, 0.1% SDS) at constant voltage of 140V.

Electrophoresis in the 4-12% gradient gels was run using MOPS buffer (50 mM MOPS, 50 mM Tris Base, 0.1% SDS, 1 mM EDTA, pH 7.7) (Novex) with the addition of NuPAGE Antioxidant (Novex) at a constant voltage of 200V for one hour.

2.6.3 Protein transfer to nitrocellulose membrane

Proteins from the gels were transferred to nitrocellulose membrane using the Mini Trans-Blot Electrophoretic Transfer (Bio-Rad). The membrane and gel were apposed and sandwiched between two Whatman 3 mm papers and sponge pads on either side. Protein transfer was achieved in transfer buffer (25mM Tris, 145mM glycine, 20% methanol) at constant 200 mA for one hour. The transfer apparatus was placed in a bucket filled with ice for the entire duration of the process. The transfer quality was assessed by staining the membrane with Ponceau S solution (Sigma) that was then washed off extensively with PBST (PBS, 0.05% Tween) before immunolabelling the membrane.

2.6.4 Western blot analysis of proteins

Destained membrane was blocked in 5% non-fat dried milk in PBST for 30 minutes at room temperature on a rocker. Immunolabelling with primary and secondary antibodies was performed in the blocking solution at the recommended concentrations (see 2.1.5 for details) with rocking. Incubation with primary antibody was done either for one hour at room temperature, or overnight at 4°C, while the secondary antibody was left for one hour at room temperature. Each of the antibody incubations was followed by 3 five-minute washes with PBST buffer. The membrane was then developed with the Immobilon™ Western Chemiluminescent HRP Substrate (Merck Millipore); the signal was detected by exposure to an x-ray film and developed on a Kodak X-OMAT 2000 processor.

2.7 Secretory phenotype analysis using Luminex bead-based assay

2.7.1 Conditioning of cell culture medium

Early passage primary Human Dermal Fibroblasts (HDFs) (passage 22 and below) were seeded in a 24-well plate. Treatment with Saquinavir, Darunavir or DMSO control followed as described in section 2.3.3. Another batch of early passage HDFs was transfected with 20 nM Zmpste24 siRNA (Dharmacon) or control siRNA (Dharmacon) as described in paragraph 2.3.6. Forty-eight hours later, the growth medium was changed, supplemented with drugs where appropriate, and conditioned for five days (120 hours). The medium was also conditioned for five days with untreated early passage HDFs or late passage HDFs (passage 40 and over). For camptothecin-induced apoptosis, 150 000 cells were seeded in a 24-well plate and treatment followed at 4 μg/ml concentration for five days.

HGPS AGO1972 fibroblasts (passage 23) were treated with 8 mM FTI-277 (Calbiochem) for 48 hours, followed by growth medium conditioning for five days in the presence of FTI-277. DMSO control and untreated cells were also included in the comparison.

Conditioned media were collected, centrifuged at 15000 rpm at 4°C, aliquoted and instant-frozen in liquid nitrogen. The volume recovered and cell number from the corresponding samples were recorded. The presence of prelamin A in cells was assessed by immunolabelling. Each condition was prepared in at least three biological replicates.

2.7.2 Luminex Screening multiplex assay

Custom-made, premixed multiplex bead pools for Luminex bead-based Screening Assay was supplied by R&D Systems. It allowed measurement of 34 analytes simultaneously in the same sample and was used according to the manufacturer's instructions. Briefly, the microparticle cocktail was incubated with undiluted conditioned culture supernatant in the filter-bottom microplate on a horizontal orbital shaker for two hours. It was subsequently treated with Biotin Antibody Cocktail for one hour and lastly with Streptavidin-PE for 30 minutes, with three washes following each incubation. Microparticles were then resuspended in 100 µl of Wash Buffer and analysed on the Bio-Rad Bio-Plex 200 System with Bio-Plex Manager operating software. Doublet discriminator gates were set at 4300 and 10000, with 50 events per region and an automatic flow rate.

2.7.3 Data analysis

Median Fluorescence Intensity (MFI) was measured for each analyte in the samples and for standards. Standards were run in replicates and a standard curve was created for each analyte using a five parameter logistic (5-PL) curve-fit in the Bio-Plex Manager. Based on the standard curve, concentration was calculated for the analytes and normalised to the cell number and volume recovered specific to the sample. Calculations and graphs were created in Excel and GraphPad Prism 6.

2.8 ELISA analysis of selected proteins in conditioned cell culture medium

2.8.1 Preparation of conditioned cell culture medium

Conditioned cell culture supernatant was prepared as described in section 2.7.1.

2.8.2 ELISA procedure

Enzyme-Linked Immunosorbent Assay (ELISA) was used for quantitative measurement of specific proteins in the cell culture supernatant following protocols specific for a given kit. ELISA employed an antibody-coated 96-well plate for a specific analyte. Standards and samples were added to the wells and bound by the immobilised antibody, followed by washes and incubation with biotinylated antibody specific to the analyte. Unbound biotinylated antibody was washed away and HRP-conjugated Streptavidin was added to the wells. After another wash step, a TMB substrate solution was added and blue colour developed in proportion to the amount of analyte bound. The reaction was then stopped with the Stop solution, changing the colour from blue to yellow, and the intensity of the colour was measured at 450 nm on a BMG Polarstar plate reader (BMG Labtech). The absorbance was also measured at 570 nm to account for optical imperfections in the plate.

ELISA assay kits used are listed in Table 2.5. All additional reagents were included in the kit, except for assays purchased from ImmunoTools that required additionally: 96 well EIA/RIA plate (Corning), TMB solution (Fisher Scientific), HRP-Streptavidin (ImmunoTools), and Stop solution (2 M H_2SO_4).

Table 2.5. List of ELISA kits and their origin.

Analyte	ELISA origin	Culture supernatant dilution
IL-1 α	R&D Biosystems (DLA50)	-
GM-CSF	R&D Biosystems (DGM00)	-
MMP-3	RayBio (ELH-MMP3)	1:10
PLAT	Abcam (AB119563)	1:10
PAI-1	Invitrogen (KHC3071)	1:10
FAS	Abcam (AB100513)	-
IL-6	ImmunoTools (31670069)	-
IL-8	ImmunoTools (31670089)	-
TNFα	ImmunoTools (31673019U1)	-

2.8.3 Data analysis

Raw data was exported to an Excel file using BMG Mars software (BMG Labtech). Absorbance readings at 570 nm were subtracted from the 450 nm readings to correct for optical imperfections in the plate. After correction, a standard curve was created in GraphPad Prism 6 by generating a four parameter logistic (4-PL) curve fit, and concentration of analytes in the samples was determined. It was then normalised to the cell number and the volume of growth medium recovered to allow comparison across different samples.

2.9 Immunofluorescence light microscopy

2.9.1 Immunolabelling of cultured cells

Cells were seeded on glass coverslips and grown as a monolayer. They were washed in PBS prior to fixation with 4% paraformaldehyde (Electron Microscopy Sciences) in PBS for ten minutes at room temperature. Free aldehyde groups were subsequently quenched with 25 mM glycine in PBS for five minutes. Cell permeabilisation in 0.5% Trition X-100 in PBS followed for five minutes. Cells were blocked in 0.5% fish skin gelatin in PBS for either 30 minutes at room temperature or overnight at 4°C. Antibodies were diluted in blocking solution. Immunolabelling with primary and secondary antibodies followed, each for one hour at room temperature, with three PBS washes after each antibody. Antibodies used and their dilution are listed in section 2.1.5. Coverslips with immunolabelled cell monolayer were then dipped in ultrapure water and immediately mounted on glass microscopy slides with

Mowiol mounting solution supplemented with DAPI (0.2 µg/ml). Slides were left at 4°C in the dark overnight to allow the Mowiol to set.

2.9.2 Light microscopy

Immunostained cells were imaged on the LSM5 Zeiss Inverted 510 META laser scanning microscope (Zeiss) using a Plan Apo 63x 1.4 NA oil immersion lens. Images were acquired using either LSM 5 acquisition software or Zen2009 operating software. Chromatic aberrations were automatically corrected by the acquisition software, without use of TetraSpeck beads (Life Technologies).

2.9.3 Image analysis and processing

Collected images were analysed in Zeiss LSM Image browser and ImageJ (Wayne Rasband, NIH, USA).

2.10 Structured illumination microscopy with 3D reconstruction (3D-SIM)

2.10.1 Immunolabelling of cultured cells

High precision coverslips (22 x 22mm), thickness no. 1.5H (170 µm ± 5 µm) (Marienfeld) were washed for 30 min in diluted HCl (4 ml of HCl 12N in 250 ml H2O) on a shaker, then rinsed thoroughly in deionised water and sterilised in ethanol.

Primary human dermal fibroblasts (HDF) were seeded on the coverslips in 6-well plates and returned to the incubator to allow time to adhere and spread. Saquinavir treatment followed. At the time of fixation, cells were reaching 80% confluency. HDFs were washed twice with 2 ml of PBS for five minutes each time and fixed in 4% paraformaldehyde (Electron Microscopy Sciences) in PBS for ten minutes. Fixative was

aspirated and 2 ml of 25 mM glycine solution in PBS per well were added for five minutes to quench free aldehyde groups. Cells were permeabilised by replacing the glycine solution with 2 ml of 0.5% Triton X-100 in PBS and incubating for five minutes before blocking with 2 ml of 0.5% Fish Skin Gelatin (FSG) in PBS for 30 min at room temperature or overnight at 4°C. Primary and secondary antibodies were diluted in blocking solution and incubation for each was one hour, followed by 3 five-minute washes with PBST (PBS 0.05% Tween). A list of antibodies and their dilution is shown in section 2.1.5. DNA was labelled with 1 ml of 2 µg/ml DAPI in PBS for five minutes before transferring the coverslips to deionised water for five minutes. Coverslips were mounted in 13 µl of Vectashield H-1000 (Vector Laboratories) and sealed with nail polish immediately.

2.10.2 3D-SIM

Slides were imaged on OMX V3 Blaze microscope (GE Healthcare, UK) equipped with a 60x/1.42 oil UPlanSApo objective (Olympus), 405 nm, 488 nm, 593 nm diode lasers, and sCMOS cameras (PCO). The instrument permitted acquisition of 3D-SIM image stacks with five phases, three angles per image plane, and 0.125 µm z-distance between sections. To minimise spherical aberrations, immersion oil of pre-selected refractive indices (RIs) was selected to match the respective optical transfer functions (OTFs) used. For imaging thick specimens, best results were typically obtained with RI 1.514 for depth adjustment in the region of optimal reconstruction a few µm into the sample. The raw data was computationally reconstructed with SoftWoRx 6.0 (Applied Precision). Wiener filter settings 0.002 and channel specifically measured OTFs were applied to generate a super-resolution 3D image stack, obtaining lateral (x-y)

resolution of up to 100-130 nm and an axial (z) resolution of ~300 nm. For multi-colour images, images from the different colour channels were registered with the alignment parameter obtained from calibration measurements with 0.2 µm diameter TetraSpeck beads (Life Technologies) using the OMX Editor software.

2.10.3 Image analysis and processing

Reconstructed images were analysed in Volocity and Imaris software.

2.11 Correlative backscattered electron microscopy and NanoSIMS imaging

2.11.1 Pulse labelling of cells in culture with ^{2}H stearate

2.11.1.1 Deuterated stearic acid D35 preparation

One mM Stearic Acid D35 stock solution was prepared by dissolving 3.2 mg of Stearic Acid D35 (Sigma) in 2 ml of ethanol. It was then complexed with 400 µl of 100 mM solution of NaOH in ethanol. Alcohol was evaporated with nitrogen gas obtaining fatty acid soaps. They were dissolved in 0.5 ml of hot ultrapure water and kept in a 55°C water bath for ten minutes. One gram of fatty acid-free bovine serum albumin (Sigma) was dissolved in 9.5 ml DMEM, warmed to 55°C, added to the dissolved fatty acid soaps, and vortex mixed for ten seconds, followed by a further ten minute incubation at 55°C. The 1 mM deuterated Stearic Acid D35 stock solution was sterilised by filtration, aliquoted and kept at -20°C. Upon thawing, the stearic acid sample was warmed to 55°C to dissolve the precipitate (if formed) and subsequently cooled to 37°C before adding to cells.

2.11.1.2 Cell treatment

Mouse preadipocytes were seeded on 13 mm plastic coverslips (Thermanox) in 24-well plates at 50% confluency and left overnight in the cell culture incubator. The next day, cells were treated with 20 µM saquinavir for 12 hours and with 10 µM Stearic Acid D35 for the last six hours of saquinavir treatment.

2.11.2 Cell fixation and specimen preparation for imaging

Upon treatment completion, cells on coverslips were washed with PBS and fixed at room temperature for 20 minutes by adding 500 µl of fixative warmed to 37°C. Solution of 4% paraformaldehyde and 1% glutaraldehyde in 100 mM PIPES pH 7.4 was used as the primary fixative. Secondary fixation in 2.5% glutaraldehyde in 100 mM PIPES pH 7.4 followed. The cells were incubated for one hour at room temperature, then transferred to 4°C and left overnight.

The next day, samples were washed three times for ten minutes each with 100 mM PIPES pH 7.4, followed by osmication with 1% osmium tetroxide in 100 mM PIPES pH 7.4 for one hour and washed in deionised water for 20 minutes. The cells then went through a graded ethanol series, first at 50% ethanol for 15 minutes, then 70% ethanol overnight at 4°C, then 90% ethanol for 15 minutes, then 95% ethanol for 15 minutes, and finally 100% ethanol for two hours with three solution changes during this time. Gradual infiltration with Agar 100 epoxy resin (Agar Scientific) followed, starting with 25% resin for one hour, then 50% resin for two hours, then 75% resin for one hour, and 100% resin overnight. The next day, samples were transferred twice to fresh 100% resin for three hours each time. The cells were resin-embedded by inverting the coverslips, cells facing down, onto an embedding capsule (BEEM) filled

with fresh resin and left for 24 hours at 60°C for polymerisation. Polymerised blocks were then submerged in liquid nitrogen and the coverslips were snapped off to leave the cells embedded as a monolayer in the resin. The resin blocks were trimmed with a razor blade and glass knife to generate a trapezoid end containing the specimen. The specimen was cut to obtain semi-thin sections of 0.5-1 μm using a Leica UC7 ultramicrotome with a diamond knife (Diatome). Each section was floated on a droplet of water on a 15 nm platinum coated coverslip. These were placed on a 60°C heating block and allowed to dry for a few minutes.

2.11.3 Backscattered scanning electron microscopy imaging

Before starting backscattered electron (BSE) imaging, areas of interest were recorded by optical microscope. Sections were then transferred to the NVision FIB scanning electron microscope and BSE images were acquired with a 2 kV incident beam with a standard aperture (30 μm) and 5-mm working distance.

2.11.4 Nano Secondary Ion Mass Spectrometry

Upon the completion of BSE imaging, the sections were coated with 5 nm of platinum in a Cressington 208HR high-resolution sputter coater to provide the surface conductive for Nano Secondary Ion Mass Spectrometry (NanoSIMS) imaging.

First, the Cs^+ primary beam was used to remove the platinum on the surface at selected locations, simultaneously implementing a low Cs^+ dose of 6.5 x 10^{15} ions/cm^2 to ensure that as small as possible of the section surface was removed before imaging. Small apertures (D1 = 3 or D1 = 4) were used for imaging a single cell in order to match the size of primary beam to the pixel size. The instrument was tuned for $^2H^-$ and $^1H^-$ to give morphological information and allow calculation of the $^2H/^1H$ ratio. The

NanoSIMS images were acquired with a dwell time of 30,000 µs per pixel for 256 x 256 pixel images. A median filter with radius of 3 pixels was applied to the Hue Saturation Intensity (HSI) image.

2.11.5 Image analysis and processing

The BSE and NanoSIMS images were aligned, and the local $^{2}H/^{1}H$ ratio quantified in ImageJ software. Data from ImageJ was then imported to GraphPad Prism 6 and Excel for further analysis.

2.12 Flow cytometry

2.12.1 Cell sample preparation

Cells were treated as described in sections 2.3.3 and 2.3.6. 10^{6} cells were harvested and washed in PBS, followed by centrifugation at 300g for five minutes. The supernatant was discarded and cells were resuspended in 0.5 ml of PBS before adding 4.5 ml of ice cold methanol. The cell suspension was transferred to -20°C and fixed overnight. The sample was then centrifuged at 200g for five minutes and the cell pellet was washed in 5 ml of PBS for five minutes at room temperature, followed by another centrifugation step. Secondary fixation was performed with 4% paraformaldehyde in PBS for ten minutes at room temperature, before quenching with 25 mM glycine for five minutes at room temperature and cell membrane permeabilisation with 0.5% Triton X-100 for five minutes at room temperature. The cells were then pelleted at 200g for five minutes and blocked in 0.5% FSG in PBS for 30 minutes at room temperature with gentle agitation.

2.12.2 Immunolabelling of mammalian cells

Primary and secondary antibodies were diluted in the blocking solution and used as recommended by the manufacturers. In general, 1 µg of primary antibody was used per 10^6 cells to provide saturating antibody concentration in 100 µl of blocking solution. The cells were then washed twice in 1 ml of PBST with five minute incubation time and pelleted (200g for five minutes) before the addition of the secondary antibody. Secondary antibody was diluted 1:300 (6.66 µg / ml) in 100 µl of blocking solution and incubated with cells for one hour at room temperature in the dark. Cells were washed twice again in PBST, before being resuspended in 1 ml of PBS supplemented with 100 µg of DNase free RNase. When indicated, 5 µg of Propidium Iodide was also added to the cell suspension. After one hour incubation at room temperature in the dark, cells were analysed by flow cytometry. In each experiment, unlabelled cell sample and cells immunolabelled with secondary antibodies were always included to determine background fluorescence and to correct for the fluorescence coming from the unspecific binding of the secondary antibodies. This also served to normalise across different experiments.

2.12.3 Flow cytometry

Fluorescence-Activated Cell Sorting (FACS) was performed on a Dako Cyan Flow Cytometry Analyser. Distant channels were utilised to minimise the need for compensation and laser power was adjusted to the unlabelled cell population.

2.12.4 Data analysis and processing

FlowJo V10 software (Tree Star) was used for data analysis from FACS experiments and dot plots creation. Gates were set using relevant control cell samples

and geometric mean fluorescence intensity was calculated. Statistical analysis and graphs were produced in GraphPad Prism 6 and Excel.

2.13 Senescence associated β-galactosidase assay

Cells were seeded on glass coverslips at 50-60% confluency, allowed to adhere overnight, and stained with the Senescence β-Galactosidase Staining Kit (Cell Signalling Technology) following the manufacturer's protocol. Briefly, cells were washed, fixed and incubated with X-gal, a substrate that converts into a blue insoluble precipitate upon cleavage by β-galactosidase. The kit is designed to detect only β-galactosidase activity at pH 6 which is a hallmark of senescent cells. Development of blue colour was monitored under a microscope. When visible signal was detected, coverslips were washed with PBS, then mounted on microscopy slides in Mowiol mounting solution and allowed to set overnight. The slides were then scanned using the Nikon 'Coolscope' Slide Scanner and TIFF images were analysed in Matlab R2012a to quantify senescence associated β-galactosidase activity using QBGAL application (Shlush et al., 2011).

CHAPTER 3

3 Prelamin A accumulation is sufficient to induce senescence

3.1 INTRODUCTION

Cellular senescence is a process in which cells cease dividing and enter stable cell cycle arrest. It is accompanied by profound phenotypic changes, including chromatin alterations, activation of tumour suppressors, and distinctive metabolic and secretory profiles. The term senescence was first introduced by Hayflick and Moorhead who observed that after a series of passages, human diploid cell strains had entered irreversible growth arrest, a state in which cells may survive for a long period of time (Hayflick and Moorhead, 1961). This phenomenon is now referred to as replicative senescence and is attributed to telomere attrition and resultant genomic instability (Bodnar et al., 1998). Telomere erosion, however, is not the only factor involved in the induction of senescence. There are many interactions within the cellular system, as well as a variety of stressors that engage different effector pathways. This results in a complex mechanism leading to cellular senescence.

Similar to telomere shortening, other specific DNA lesions and increase in reactive oxygen species (ROS) may lead to senescence via the same DNA damage response (DDR) pathway (Nair et al., 2015; Sedelnikova et al., 2004). Another potent group of senescence-inducers are oncogenes. Deregulation of their function, whether by activation (RAS, E2F3, BRAF) (Denchi et al., 2005; Di Micco et al., 2006; Kaplon et al., 2013) or by inactivation (RB, PTEN, NF1, VHL) (Nardella et al., 2011) is a potent means of senescence induction. There is a growing body of evidence that

demonstrates how other stressors may be involved in the process of blocking the cell cycle and leading to senescence. Examples include prolonged exposure to interferon β (Moiseeva et al., 2006), epigenetic stressors, like exposure to histone deacetylase inhibitors (Romanov et al., 2010), derepression of the INK4a/ARF locus (LaPak and Burd, 2014), as well as mitotic spindle stressors (Schmidt et al., 2010). Each of these can promote senescence. Some of these stressors operate in a DDR-dependent manner; and others in a DDR-independent manner, engaging p53-p21 and/or $p16^{INK4a}$-RB effector pathways, depending on the cause, context, exposure duration, cell type, etc. These variables form a complex picture of senescence induction mechanisms and their roles.

The primary role of senescence is believed to be the prevention of unrestricted growth of damaged cells in order to safeguard against the development of cancer (Braig and Schmitt, 2006; Collado and Serrano, 2010). This mechanism exists in tandem with apoptosis. Which pathway is followed, senescence or apoptosis, appears to depend largely on the particular wiring of each cell type (Childs et al., 2014). While apoptosis represents a cell-autonomous mechanism with rapid elimination by phagocytes (Erwig and Henson, 2007), senescent cells survive for a long period of time and remain metabolically active. During the period of senescence, cells continue to secrete a range of growth factors and cytokines which allow for communication with neighbouring cells (Young and Narita, 2009). Senescence can be beneficial in the context of living tissue, leading to repair and regeneration (Jun and Lau, 2010a, b; Kong et al., 2012; Krizhanovsky et al., 2008), rather than the abrupt cell loss that is observed in apoptosis. The major impact of senescence however, is on ageing (Baker et al., 2011; Dimri et al., 1995).

Ageing is a multimodal process in which homeostasis and an organism's ability to cope with stress deteriorate over time. This ultimately leads to stem cell exhaustion and reduction of self-regenerative capabilities. As an organism ages, its cells accumulate macromolecular damage, leading to genomic instability, heterochromatin changes, and alterations in normal cellular signalling, often terminating in senescence (Kirkwood, 2008). Over a lifetime, repair mechanisms become less efficient and cannot compensate for the damage. As a result, senescence at the cellular level can lead to tissue decline, deterioration, and ultimately ageing of the organism as a whole. The study of progeroid syndromes, which are considered to be accelerated forms of human ageing, has led to many advances in ageing research (Ghosh and Zhou, 2014). This assumption has been challenged, and the concept of multiple forms of tissue ageing has been proposed and doubted. Other than Werner Syndrome (Yu et al., 1996), it is likely that the most well recognised and best studied is Hutchinson-Gilford progeria syndrome (HGPS) (Gonzalo and Kreienkamp, 2015). It is a severe premature ageing syndrome, caused by a point mutation in the lamin A gene (LMNA) that activates a cryptic splice site (De Sandre-Giovannoli et al., 2003; Eriksson et al., 2003). As a result, progerin, an alternatively spliced lamin A form is expressed. Progerin lacks the cleavage site for Zmpste24 proteinase and as a result is unable to undergo a final maturation step in which the farnesylated C-terminus of the lamin A protein is removed. Expression of farnesylated progerin alters several nuclear functions and leads to a very distinctive phenotype, both at the cellular and organismal levels. Affected nuclear processes include impaired DNA repair, disregulated cell cycle, and elevated senescence (Burtner and Kennedy, 2010; Mehta et al., 2011; Merideth et al., 2008).

In recent years, it has also been shown that healthy ageing individuals accumulate the farnesylated form of lamin A. This occurs either as a result of activation of the cryptic splice site in the LMNA transcript resulting in accumulation of progerin (Scaffidi and Misteli, 2006, 2008) or due to downregulation of the Zmpste24 proteinase, which is responsible for the final maturation cleavage, resulting in accumulation of prelamin A (Ragnauth et al., 2010). Prelamin A shares many similarities with progerin in terms of structure and posttranslational modifications. Both forms are associated with ageing and increased senescence. We therefore decided to determine if prelamin A alone is a sufficient factor to induce cell senescence. Additionally, we sought to determine if the induction of prelamin A accumulation is a good cell model for studying mechanisms linking the nuclear envelope to ageing. Serial passage of matching primary Human Dermal Fibroblasts (HDFs) was used for establishing a physiological model of ageing relying on replicative senescence for a direct comparison with prelamin A accumulating cells.

3.2 RESULTS

3.2.1 Characterisation of replicative senescence in Human Dermal Fibroblasts

Primary Human Dermal Fibroblasts (HDFs) were cultured continuously, with regular 1:2 passaging whenever cells reached 90% confluency. During the culture process, cells were analysed to assess their morphology and expression of senescence markers. HDFs had already begun to demonstrate a significantly slower growth rate, increased cell area, and an inability to form a continuous cell monolayer by passage 35

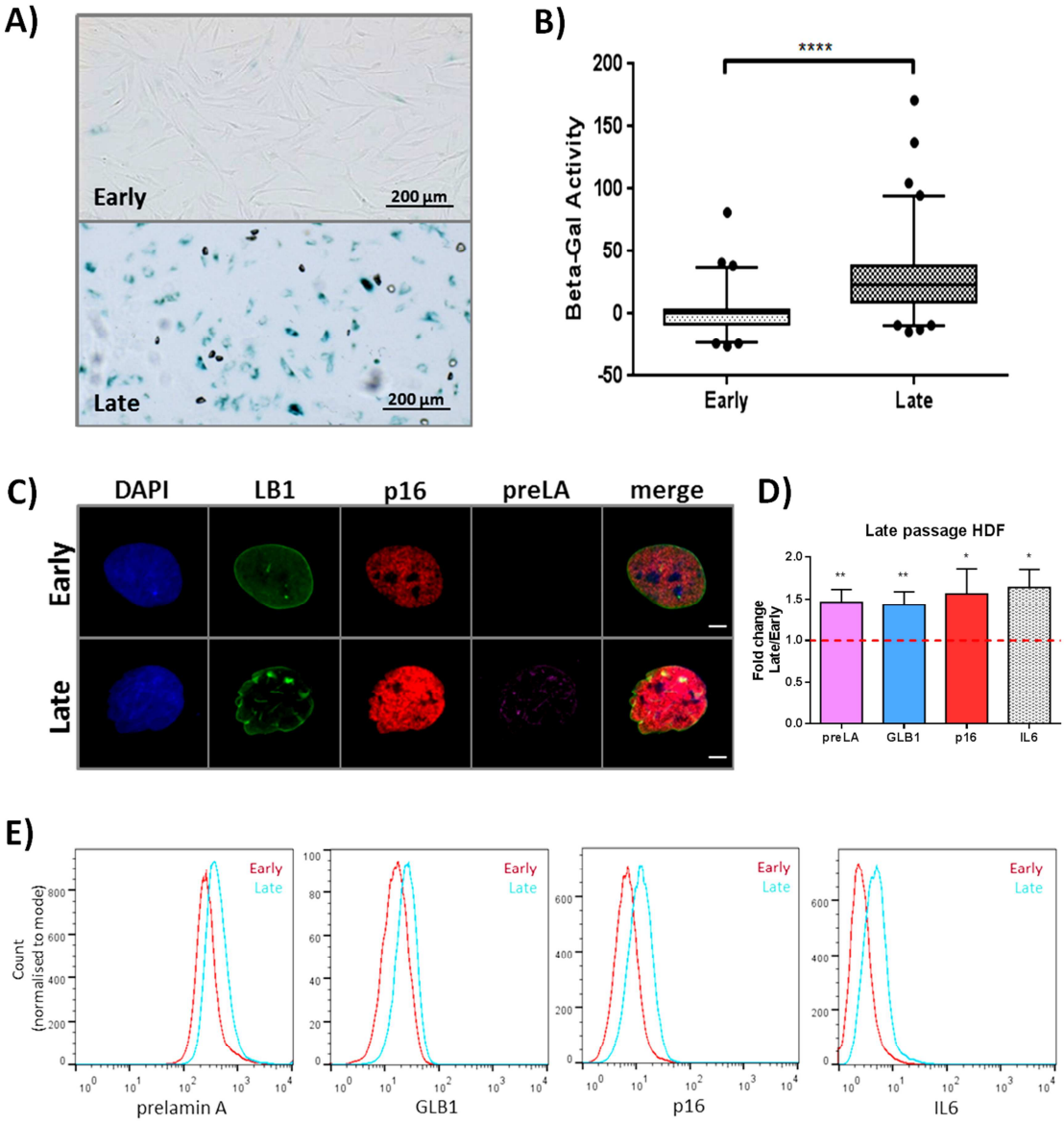

Figure 3.1. Characterisation of replicative senescence in Human Dermal Fibroblasts (HDFs).

A) Detection of Senescence Associated β-Galactosidase (SA β-Gal) activity in early and late passage HDF cells. **B)** Quantification of the SA β-Gal Activity in arbitrary units called β-Galactosidase Assay Values. **C)** Immunofluorescence microscopy on different age HDFs; LB1, lamin B1, p16, p16^{INK4a}; pre LA, prelamin A; scale bar, 5 µm. **D)** Fold change of geometric mean fluorescence intensity measured by flow cytometry for various senescence markers in late passage HDFs and normalised to early passage HDFs (base level of 1 indicated by the red line); preLA, prelamin A; GLB1, β-galactosidase; p16, p16^{INK4a}; IL6, interleukin 6; error bars indicate SD. **E)** Examples of flow cytometry histograms showing fluorescence intensity (in logarithmic scale) measured for selected proteins in a pairwise comparison for early and late passage HDFs. Asterisks above bars represent P value as follows: * $P < 0.05$; ** $P < 0.01$; **** $P < 0.0001$.

under our culturing conditions. They also demonstrated elevated staining for Senescence Associated β-Galactosidase (SAβGal) activity. Detection of this activity in an assay at an enzyme-suboptimal pH (6.0) is a widely accepted hallmark of senescent cells (Dimri et al., 1995). Quantification of the SAβGal signal (Shlush et al., 2011), which is proportional to the intensity of the developed blue colour, revealed a significant difference between early ("young") passage HDFs and late ("old") passage HDFs (Figure 3.1 A, B). Passages below 22 were considered early passage HDFs while passages 39 and over represented late passage HDFs.

Some cell types have been shown to accumulate prelamin A as part of their natural ageing process (Ragnauth et al., 2010). We therefore set out to determine if this is also the case for HDFs. Late passage HDFs in pairwise comparison by immunofluorescent microscopy with early passage HDFs detected modest expression of prelamin A, yet detectably higher than in early passage cells. This was accompanied by clear nuclear shape abnormalities visualised by anti-lamin B1 labelling (Figure 3.1 C). Flow cytometry was employed analysing a population of at least 20k cells per experiment. It demonstrated that there was approximately a 50% increase in geometric mean fluorescence intensity (GMFI) specific for prelamin A in late passage cells, when compared to early passage HDFs. A similar level of increase was detected for SAβGal in the same assay (Figure 3.1 D E).

Replicative senescence is often linked to CDKN2A locus derepression, leading to expression of two tumour suppressors, $p16^{INK4a}$ and ARF (Gil and Peters, 2006). Expression of $p16^{INK4a}$, an inhibitor of cyclin-dependent kinases 4 and 6 (CDK4 and CDK6), leads to proliferative arrest in which hypo-phosphorylation of the retinoblastoma gene (RB) is the crucial element (Chicas et al., 2010). Late passage

HDFs demonstrated elevated $p16^{INK4a}$ immunolabelling as revealed by fluorescent microscopy detection, and significant increase of $p16^{INK4a}$ GMFI when analysed by flow cytometry (Figure 3.1 D, E).

Interleukin-6 (IL6), another marker of senescence, and a prominent component of the Senescence Associated Secretory Phenotype, was also investigated. Late passage cells demonstrated nearly a 60% increase in the GMFI specific for IL6 immunolabelling (Figure 3.1 D, E).

3.2.2 Prelamin A-induced senescence after saquinavir treatment

A number of HIV protease inhibitors (HIV-PIs) have been shown to interfere with the maturation process of prelamin A by blocking activity of Zmpste24 protease, the enzyme responsible for the final cleavage of prelamin A (Coffinier et al., 2007; Hudon et al., 2008). The effect of saquinavir, one of these HIV-PIs, was tested on HDFs. At a physiologically relevant concentration, saquinavir induced prelamin A accumulation (Figure 3.2). Cells responded very quickly to saquinavir treatment and accumulation of prelamin A was detected already after three hours of drug exposure, as demonstrated by immunofluorescent microscopy and Western blotting data. There was little increase in prelamin A levels beyond 48 hours (data not shown). As the level of prelamin A increased in early passage HDFs, their nuclear morphology became distorted (shown with anti-lamin B1 labelling) and the level of $p16^{INK4a}$ increased. These observations are similar to changes found in HDFs reaching replicative senescence.

When the proliferation of HDFs was examined, it was observed that saquinavir has different effects on the cells, depending on the number of times that they had

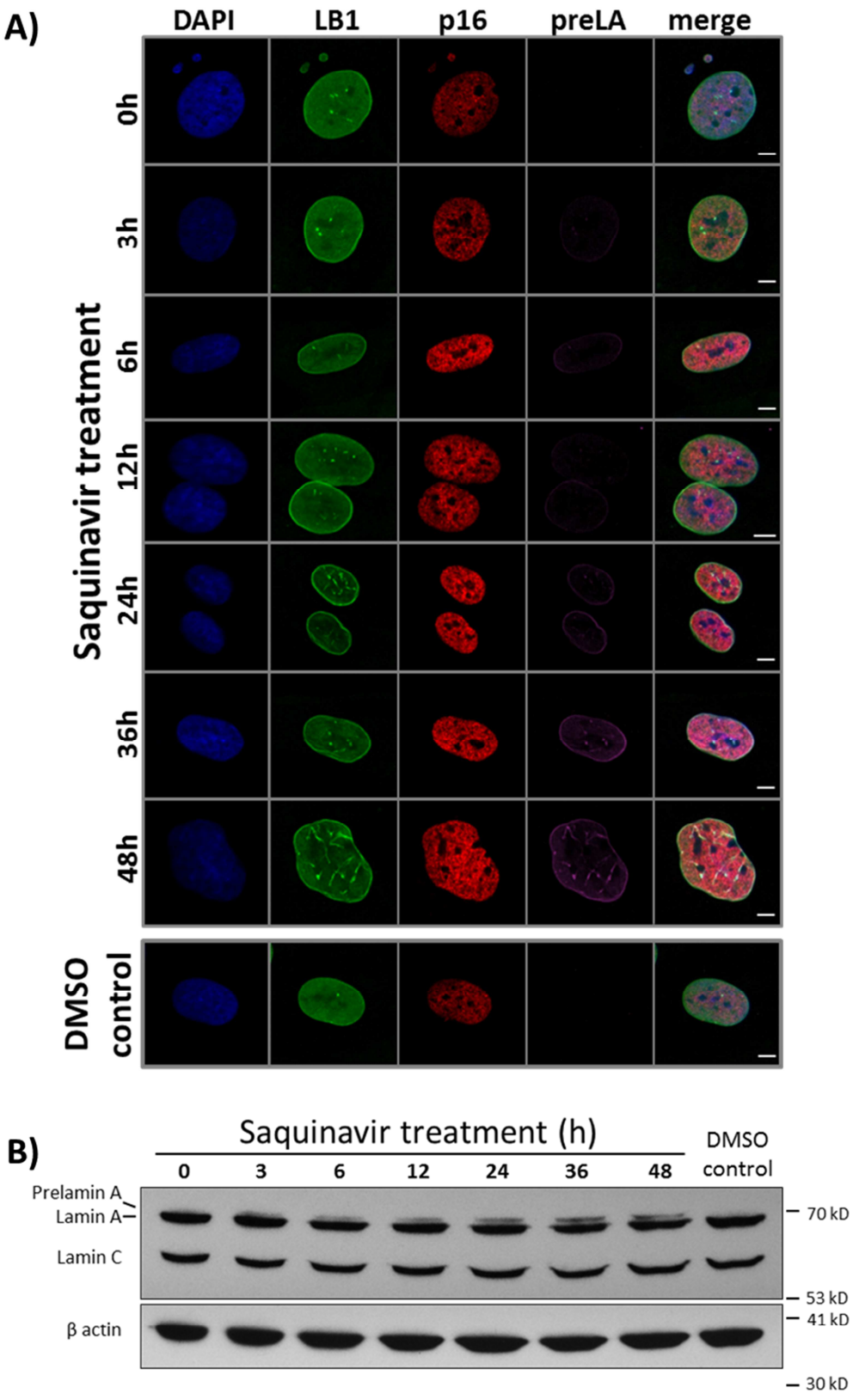

Figure 3.2. Prelamin A accumulation in response to saquinavir.

A) Immunofluorescence microscopy on HDFs treated with saquinavir over 48 hours period; DMSO control cells were imaged at 48 hours time point; LB1, lamin B1; p16, $p16^{INK4a}$; pre LA, prelamin A; scale bar, 5 µm**. B)** Western Blot analysis of whole cell lysates prepared at different time points of saquinavir treatment; DMSO control cells were lysed at 48 hour time point.

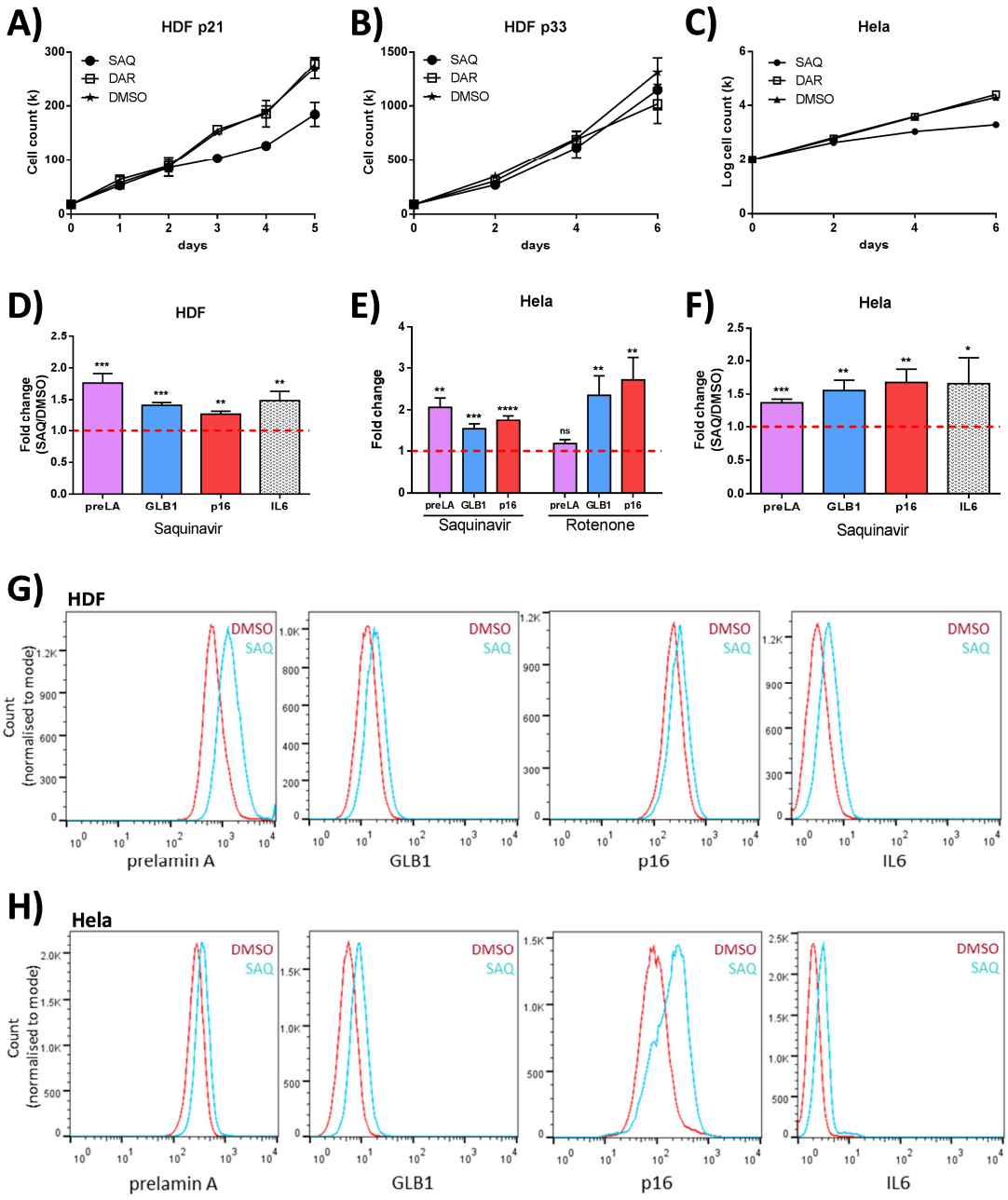

Figure 3.3. Cell response to prelamin A accumulation upon saquinavir treatment.

Growth curves of cells cultured in the presence of saquinavir (SAQ), darunavir (DAR) and vehicle control (DMSO): early passage HDFs (**A**), presenescent passage HDFs (**B**) and HeLa (**C**). Fold change of geometric mean fluorescence intensity measured by flow cytometry for various senescence markers and normalised to DMSO control cells (base level of 1 indicated by the red line) in: (**D**) early passage HDFs in response to saquinavir; (**E**) HeLa in response to either saquinavir or rotenone; (**F**) HeLa in response to saquinavir. Examples of flow cytometry histograms showing fluorescence intensity (in logarithmic scale) measured for selected proteins in a pairwise comparison for HDFs (**G**) and HeLa (**H**); preLA, prelamin A; GLB1, β-galactosidae; p16, $p16^{INK4a}$; IL6, interleukin 6. P value as follows: * $P < 0.05$; ** $P < 0.01$; *** $P < 0.001$; **** $P < 0.0001$

been passaged. The growth rate of early passage cells, continuously exposed to saquinavir, decreases after 48 hours. This was not observed in the DMSO control (vehicle) or in darunavir treated cells (Figure 3.3 A). Darunavir is a newer generation HIV-PI that, unlike saquinavir, does not block Zmpste24 activity (Coffinier et al., 2008). It was observed, however, that presenescent HDFs at passage 33 demonstrated little to no difference in growth rates in any of these three conditions (Figure 3.3 B). This may suggest that presenescent HDFs already suffer from cellular defects and therefore it is likely that prelamin A accumulation does not impair their proliferative capacity further. Conversely, HeLa cells, an immortal cell line, do not demonstrate senescence even on prolonged passage. They do however respond to saquinavir exposure with growth inhibition. A similar 48 hour delay in growth inhibition that had been observed in early passage HDFs was also noted in this cell line (Figure 3.3 C).

Expression analysis of senescence markers by flow cytometry has shown that saquinavir treatment of early passage HDFs leads not only to prelamin A accumulation, but is also accompanied by an elevated level of β-galactosidase, $p16^{INK4a}$, and IL6 (Figure 3.3 D, G). HeLa cells were also tested for the expression of senescence markers either by inducing accumulation of prelamin A with saquinavir or by treating with rotenone. Rotenone is a drug that interferes with the electron transport chain in mitochondria, leading to the production of excess intracellular reactive oxygen species (ROS). These in turn cause DNA damage and promote senescence (Noppe et al., 2009). In concordance with literature, rotenone-exposed HeLa cells demonstrated strong upregulation of SA β-Galactosidase and $p16^{INK4a}$, but, as expected, without affecting lamin A maturation (Figure 3.3 E). HeLa cells treated with saquinavir accumulated prelamin A and demonstrated upregulation of these two

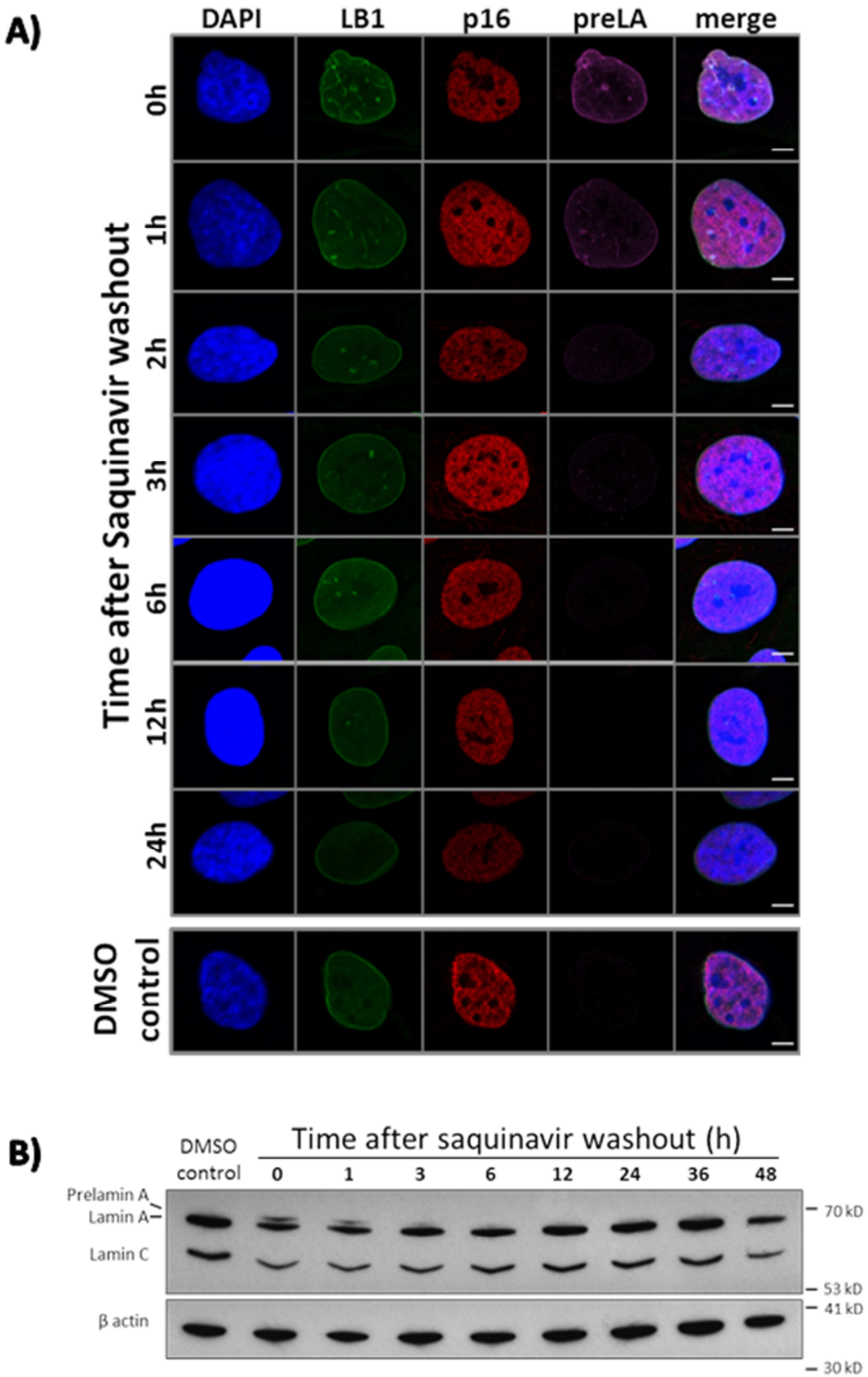

Figure 3.4. Prelamin A is rapidly processed upon saquinavir removal.

A) Immunofluorescence microscopy on early passage HDFs upon saquinavir washout, images were taken at the indicated time points; LB1, lamin B1; p16, p16^{INK4a}; pre LA, prelamin A; scale bar, 5 µm. **B)** Western Blot analysis of HDF cell lysates prepared at indicated time points after saquinavir removal from culture medium.

senescence markers, albeit at lower levels. Furthermore, IL6 was also elevated in such treated HeLa cells (Figure 3.3 F, H).

Removing saquinavir from the growth medium leads to a rapid maturation of accumulated prelamin A which is processed within 2-3 hours upon drug washout (Figure 3.4 A, B). This raises the question whether Zmpste24 inhibition by saquinavir is transient and can be reversed by removing the interfering drug or if it is a permanent effect that can only be reversed by production of newly synthesised Zmpste24 that has had no contact with the inhibitor. To address this point, HeLa cells were treated with saquinavir for 24 hours to accumulate prelamin A. The growth medium was then

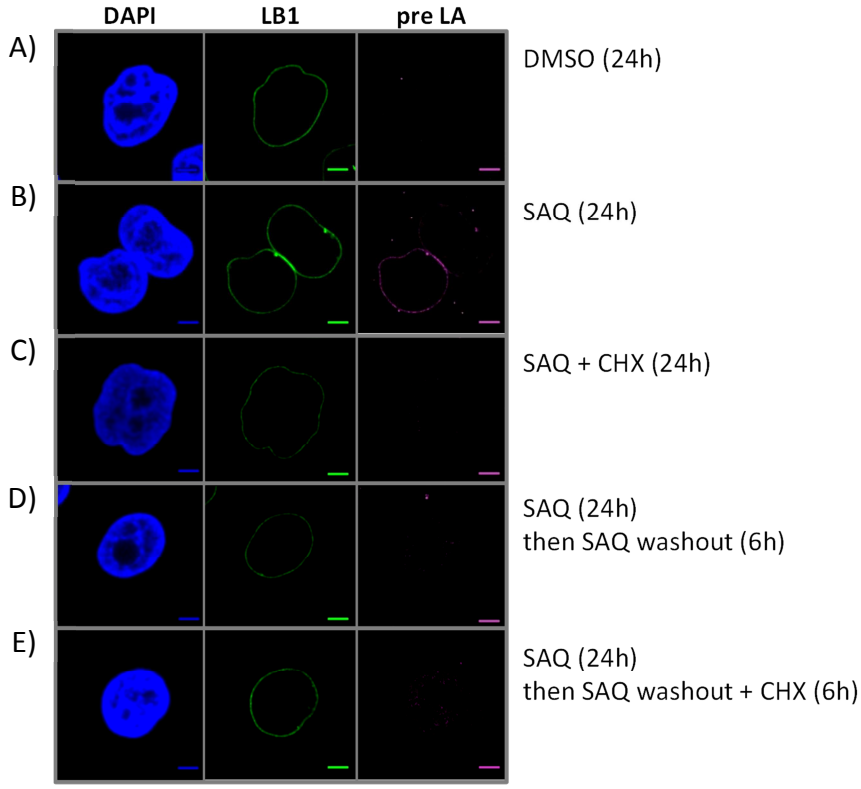

Figure 3.5 Zmpste24 inhibition by saquinavir is reversible.

HeLa cells were cultured for 24 hours in the presence of (**A**) vehicle control (DMSO) or (**B**) saquinavir (SAQ) to accumulate prelamin A. (**C**) When cyclohexamide (CHX) was added at the same time (SAQ+CHX) no prelamin A accumulation was observed because new protein synthesis was blocked by CHX. **D)** 24 hour saquinavir incubation followed by 6 hours in saquinavir-free medium removes Zmpste24 inhibition and results in prelamin A processing. **E)** Addition of CHX during washout period does not affect prelamin A processing despite blocking synthesis of new proteins, including Zmpste24.

changed to saquinavir-free with or without cyclohexamide, an inhibitor of translation. As shown in Figure 3.5, HeLa cells treated for 24 hours with saquinavir accumulated prelamin A, but not in the presence of cyclohexamide which blocked synthesis of new prelamin A copies (Figure 3.5 A-C). Upon saquinavir washout, HeLa cells that accumulated prelamin A, processed the protein to its mature form, both in presence and absence of cyclohexamide (Figure 3.5 D, E). This indicates that clearance of prelamin A upon saquinavir washout is catalysed by the pool of Zmpste24 already present in the cell. Thus the Zmpste24 inhibition by saquinavir is a transient process and the enzyme does not lose its activity permanently upon saquinavir interference with its active centre.

Rapid processing of prelamin A upon saquinavir washout indicated that continuous presence of the drug is required to maintain Zmpste24 inhibition longer term. Hence for most of this research, saquinavir was replenished daily in cell culture to ensure complete inhibition of Zmpste24. With the knowledge that for some experiments (e.g., accumulating secretory products over long periods of culture) daily

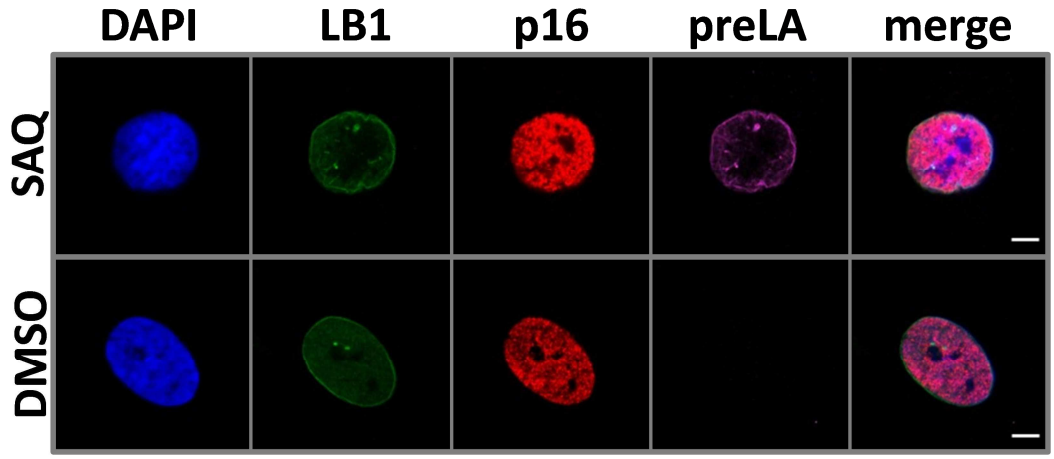

Figure 3.6 Saquinavir stably inhibits Zmpste24 over a longer period.

Immunofluorescence microscopy on HDFs treated with saquinavir with a single dose of the drug and no medium change during 5 day period. LB1, lamin B1; p16, $p16^{INK4a}$; preLA, prelamin A; scale bar, 5 µm.

growth media change with fresh drug supplementation would not be possible, the effect of a single dose of saquinavir over a longer time period was tested. As shown in Figure 3.6, Zmpste24 activity was persistently blocked over five day period with a single dose of saquinavir, as judged by the continued presence of a strong prelamin A signal. This was despite the possibility of drug loss through instability or cellular metabolism.

3.2.3 Zmpste24 knock-down leads to prelamin A accumulation

Prelamin A accumulation achieved with saquinavir treatment is a potent means of inducing senescence in the entire cell population. However, its effect on Zmpste24 is a side reaction, as saquinavir is as a potent HIV-PI. Thus it is possible that the drug has additional cellular targets. To overcome this issue, an alternative strategy to drive prelamin A accumulation was developed. By using Zmpste24 siRNA, gene expression was knocked-down. Since prelamin A is the only known substrate of this protease, it was assumed that such an approach would address the off-target effects of saquinavir. Cell transfection with Zmpste24 siRNA reduced Zmpste24 mRNA level and in turn, prelamin A accumulation (Figure 3.7 A, C). All consecutive experiments used 20 nM siRNA concentration with a 48 hour incubation time to allow the knock-down. Despite the substantial drop in the Zmpste24 mRNA level and detection of prelamin A in the cells, there was no reduction in immunodetectable Zmpste24 protein presumably due to poor quality of anti-Zmpste24 antibody and unspecific binding in Western blot analysis (Figure 3.7 B).

Similar to the saquinavir model, for some experiments (e.g., accumulating secretory products over long periods of culture; described in Chapter 6)

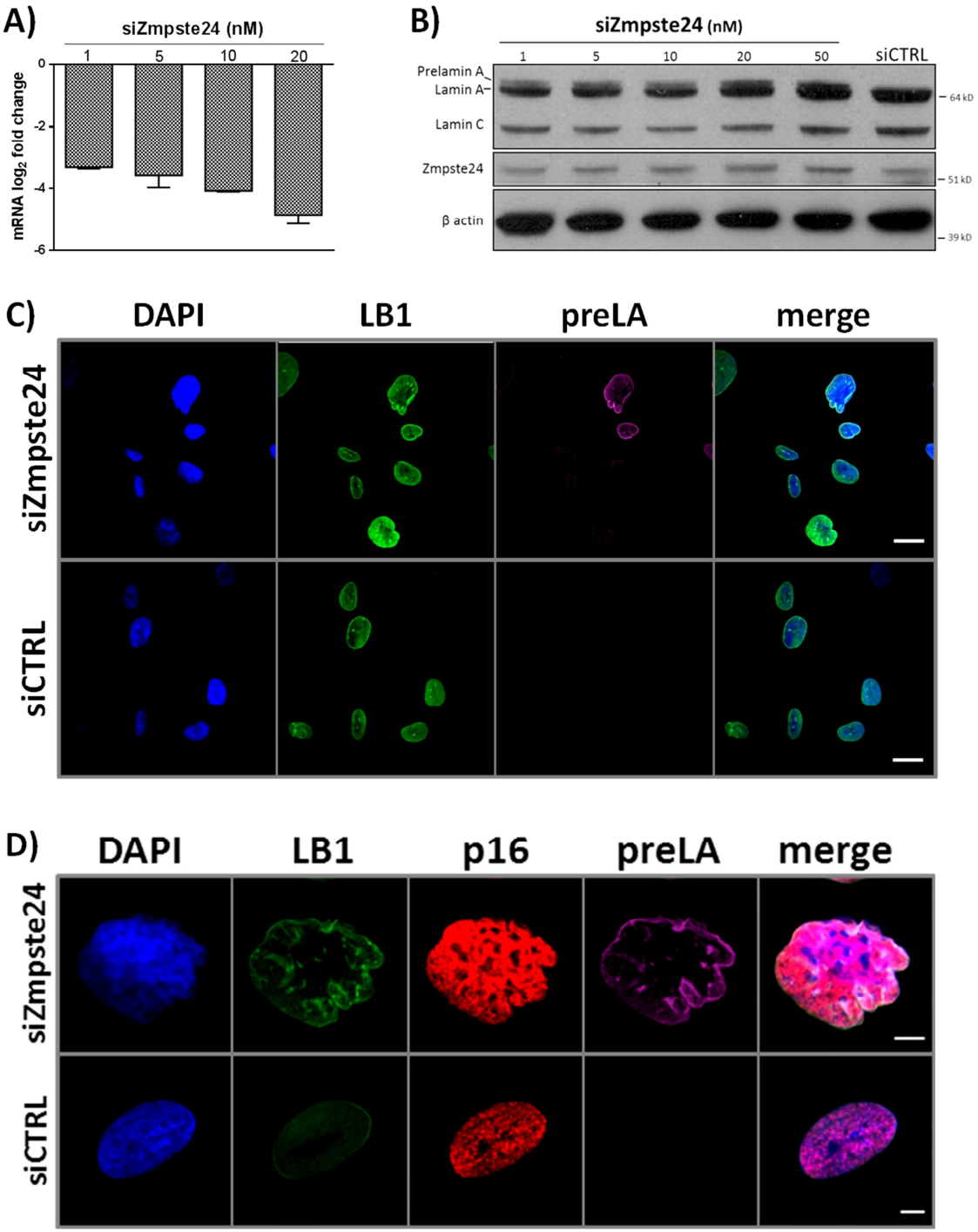

Figure 3.7. Prelamin A accumulation after Zmpste24 knock-down.

A) qRT-PCR analysis of ZMPSTE24 mRNA level 48 hours post-transfection of early passage HDFs with indicated concentrations of Zmpste24 siRNA. **B)** Western Blot analysis of whole cell lysates of early passage HDFs 48 hours post-transfection with indicated concentrations of Zmpste24 siRNA. **C)** Immunofluorescence microscopy on early passage HDFs transfected with 20 nM Zmpste24 siRNA and imaged 48 hours after transfection; LB1, lamin B1; pre LA, prelamin A; scale bar, 20 µm **D)** Immunofluorescence microscopy on early passage HDFs transfected with 20 nM Zmpste24 siRNA and imaged 120 hours (5 days) after transfection; LB1, lamin B1; p16, $p16^{INK4a}$; pre LA, prelamin A; scale bar, 5 µm.

re-transfection with fresh Zmpste24 siRNA would not be possible, the duration of Zmpste24 knock-down over a longer time period was tested. Depletion of Zmpste24 activity by siRNA knock-down was demonstrated to be a stable process. It was noted that at five days post-transfection, the prelamin A signal remained strong, nuclei showed distorted morphology, and $p16^{INK4a}$ expression increased (Figure 3.7 D).

3.3 DISCUSSION

Senescence appears to be a complex cellular mechanism, implicated in multiple functions with perhaps the most significant role in ageing. It is suggested that an organism's frailty and age-associated diseases result from the accumulation of senescent cells which in turn reduces tissues' regenerative capacities leading to functional deterioration (Ovadya and Krizhanovsky, 2014). Many well characterised causes of senescence have been described thus far. Telomere attrition, DNA damage beyond repair, oncogene dysfunction, oxidative stress resulting from reactive oxygen species represent just a few (Pawlikowski et al., 2013). With the expansion of the field, there is a growing body of research reporting new senescence-inducers, however the uniformity of the senescence response to this diversity of triggers is not yet fully characterised.

Here we show evidence that acute prelamin A accumulation is a potent means of senescence induction in early passage Human Dermal Fibroblasts (HDFs). Cell treatment with saquinavir, an older generation HIV-PI, leads to the inhibition of Zmpste24, the proteinase responsible for the final maturation step in lamin A posttranslational processing (Corrigan, 2005). Cells exposed to the drug, over time

undergo substantial alterations in nuclear morphology proportional to the level of prelamin A accumulation. Similar distortion of nuclear shape is observed in HGPS cells that express a mutant form of lamin A, called progerin (De Sandre-Giovannoli et al., 2003; Eriksson et al., 2003). It is believed that progerin is the dominant cause of the severe premature ageing phenotype observed in HGPS syndrome (Gonzalo and Kreienkamp, 2015). Upon prelamin A accumulation, HDFs increase expression of several senescence markers, such as SA β-galactosidase, $p16^{INK4a}$, and IL6. It is possible that prelamin A accumulation upon saquinavir treatment alters chromatin organisation and affects expression of these markers. Indeed, it has been reported that prelamin A can lead to derepression of $p16^{INK4a}$ locus (conference report from Shanahan Laboratory), which in turn could lead to execution of senescence program. Changes in transcriptional landscape upon prelamin A accumulation is going to be discussed in Chapter 4 in more detail. Similar to HDFs, HeLa cells induced to accumulate prelamin A also demonstrated a substantial rise in all three markers tested. This is the same response as observed in ROS induced senescence after rotenone treatment. Importantly, replicative senescence in HDFs shares many similarities with prelamin A-induced senescence. Late passage HDFs show defects in nuclear morphology, as shown by immunofluorescence data. Additionally, they begin to express a modest level of prelamin A, and other expected senescence markers.

It could be argued that the observed effect of saquinavir treatment on cell proliferation is a result of apoptosis rather than senescence. This would be a serious concern if cells were over-treated with high drug doses. Indeed, it has been shown before for several senescence-inducing factors (such as doxorubicin, etoposide, UVB, H_2O_2) that al low doses they promote senescence, while at higher they lead to

apoptosis (Altieri et al., 2012; Chen et al., 2000; Debacq-Chainiaux et al., 2005; Probin et al., 2006; Song et al., 2005; Spallarossa et al., 2009). The presence of senescence hallmarks upon prelamin A accumulation in our experimental set-up argues against apoptosis. Furthermore, when cell viability was assessed during continuous cell culture it oscillated around 95% for both drug treated and control samples. This suggests that cell number reduction upon saquinavir treatment is a result of cell cycle arrest rather than cell death. Additionally, the loss of prelamin A on drug washout is far too rapid to represent the appearance of new cells by proliferation. This confirms the reversibility of the drug effect, which would not be possible if the cells were lost to apoptosis.

A more specific approach to induce prelamin A accumulation was also employed by the use of Zmpste24 siRNA. This proteinase has no reported substrates other than prelamin A (Barrowman and Michaelis, 2009), therefore targeting Zmpste24 specifically should reduce off-target effects. Transfection of primary cells however, is challenging, and what this model offers in terms of specificity, it lacks in robustness of response. This is because the cell populations will exhibit different efficiencies of Zmpste24 knock-down due to variability in transfection rates. As a result, the execution of senescence will not be synchronous. Alternatively, it may offer a more tissue-like environment, where the cell population is heterogeneous, with only a subset of cells undergoing senescence upon ageing. In our experimental set-up, reduction of Zmpste24 protein levels was not observed in the siRNA knock-down experiments. This was despite clear evidence of transcript depletion and resultant accumulation of uncleaved lamin A, the only known Zmpste24 substrate. Poor

antibody quality or unspecific binding to other proteins present in the lysate may explain these findings.

This chapter characterises three laboratory models of cellular ageing that were established for the purpose of this research. The first is physiologic, and was achieved by passaging HDFs until replicative senescence was reached. The two other models relied on prelamin A accumulation as a stress signal inducing senescence. The second, a pharmacologic model, induced prelamin A accumulation with drug treatment. The third, a genetic model, employed Zmpste24 siRNA to induce premature ageing. Despite the fact that these three models operate *in vitro* at the cell autonomous level without tissue context, they should help to gain further understanding of the molecular mechanisms of senescence, especially in the context of abnormal prelamin A maturation resulting in perturbed nuclear envelope structure.

Large scale profiling with transcriptomics, proteomics, and metabolomics, among others, has provided great insights into molecular mechanisms that drive changes in cellular signalling in response to various stimuli. Having established the three laboratory models of ageing, further characterisation of the similarities and differences between senescence induced by proliferative exhaustion and acute prelamin A accumulation was undertaken. Genome wide mRNA profiles for each model were studied by microarrays in the next step.

CHAPTER 4

4 Global transcriptional analysis of the ageing models

4.1 INTRODUCTION

A great insight into a biological state and the significance of cellular processes can come from analysis of the cell transcriptome. The transcriptome is the entire repertoire and quantity of transcripts present in a cell at a specific developmental stage, or under particular physiological conditions. For years, techniques like Northern blots or reverse-transcription PCR have been employed to gain more information about the expression of specific RNA messages. The later development of expressed sequence tags (ESTs) libraries (Adams et al., 1991), and serial analysis of gene expression (SAGE) techniques offered more robust tools (Velculescu et al., 1995) in cell transcriptome characterisation. The real break-through in transcriptome profiling however, came with the development of high-throughput quantification methods such as gene expression microarrays (Schena et al., 1995) and, more recently, RNA-Seq (Mortazavi et al., 2008).

Gene expression microarray is a hybridisation-based method. It requires a chip with immobilised short oligonucleotides, designed based on the current knowledge of the genome sequence, aiming at representation of all mRNA transcripts. Usually, multiple oligonucleotide probes per gene are printed on the chip. Transcripts are extracted from the investigated organism or cells and labelled with one or two colours of fluorescent dye. Usually one fluorochrome is used per cellular condition. Often pairwise comparison of two states is done using two fluorochromes to distinguish

different RNA pools. Next, labelled transcripts are hybridised to the array. Transcribed RNA, if present in the sample, will bind to its complementary sequence, derived from the target genes. The array is washed and scanned with a laser. Detection of the light coming from fluorescent dye indicates not only the presence of the transcript, but also its expression level, which is proportional to the intensity of the light.

An alternative to microarrays is the RNA-Seq method, which is a sequencing-based approach (Martin and Wang, 2011; Mortazavi et al., 2008). The starting transcript material is directly sequenced. Subsequently, the resulting sequence reads are individually mapped back to a reference genome or used for *de novo* assembly. The number of mapped reads is then used as a measure of the level of expression of the reference region. The advantage of RNA-Seq is that it may not require prior knowledge of the genomic sequence and therefore is not limited by the availability of fully sequenced genomes. Not being limited by a specified set of oligonucleotides supports discovery of new candidate genes and expression from genomic regions that appear to be transcriptionally inactive. Furthermore, RNA-Seq allows for detection of new exon junctions, RNA editing events, as well as allele-specific expression.

Both microarrays and RNA-Seq have been used extensively for transcriptome characterisation in various samples. As is the case with large-scale profiling studies, neither of these techniques is flawless. Therefore the study design, objectives, and available budget will often determine which method is used. RNA-Seq offers a clear advantage with regard to the detection of unmapped transcripts, whether it is a new gene, alternatively spliced mRNA, or non-coding RNAs. It can however lead to biased expression estimates if the depth of sequencing is uneven along the transcript length. Additionally, RNA-Seq output files require substantially more memory space. Also,

data analysis may be much more challenging because improvements in the normalisation methodology are still being developed. Alternatively, microarray technology has been available far longer than RNA-Seq. This has allowed for a more extensive understanding of the method, and greater knowledge of its inherent biases. A broad range of analysis tool packs and mature strategies have been developed to deal with errors and artifacts produced by microarrays. Additionally, despite decreasing costs of high-throughput sequencing, microarrays are still significantly less expensive. Therefore, study conditions can be designed without compromising the number of replicates or putting too much strain on the project budget. Furthermore, data gathered with microarrays demonstrates good concordance with RNA-Seq. Microarrays demonstrate only a slightly lower detection of low abundance transcripts than does RNA-Seq (Mooney et al., 2013; Wang et al., 2014).

Regardless of the technique employed, microarrays or RNA-Seq, understanding the transcriptome aids in the interpretation of the changes and mechanisms cells activate in response to various stimuli, developmental changes, and disease. It is important though, to note that the outcome of these analyses is measurement of the population average, rather than a single-cell's response. Thus only the biggest and most common changes across the population will be detected and the results will not account for heterogeneity within the population. In an effort to overcome this limitations, strategies are currently being developed that aim at spatially resolved characterisation of the transcriptome (among other –omes, like the proteome, metabolome, etc.) that allow for single-cell level studies (Crosetto et al., 2015).

Broad availability of technology for genomewide RNA expression profiling shifts the challenge from data acquisition to understanding the biological meaning of the

information. Typically, transcriptome analysis of two different conditions will result in a list of hundreds of differentially expressed genes. The fundamental aim is to reduce that data to a smaller and more comprehensive set of affected pathways and networks. While a pathway defines a more linear process that is fairly well understood, networks are proving to be more challenging to understand and visualise. Networks may consist of many pathways that can intersect and exhibit a broad spectrum of interactions, both stimulatory and inhibitory, depending on the context. These changes get to the very heart of homeostatic network control mechanisms, but are only a snapshot of dynamic regulatory processes, including negative and positive feedback as well as feedforward. Databases with annotated gene sets which comprise all known genes involved in a particular pathway or process provide significant assistance in the analysis and understanding of biological mechanisms behind the observed changes in gene expression. Perhaps one of the most recognised is the Gene Ontology initiative which groups related genes into annotated sets. They are classified into three main categories: biological processes, molecular functions, and cellular locations, based on multiple types of evidence (The Gene Ontology Consortium, 2010). There is, however, a long list of available resources and gene set databases, listing pathways and network interactions (Bader et al., 2006) that are helpful when analysing changes in genome wide profiles. Analysis usually involves the use of a wide range of these tools because each is made in a different way and for a distinct purpose.

Different approaches can be undertaken to investigate the biological meaning behind transcriptional profiling with a variety of available software tools (Creixell et al., 2015). Often, the starting point is the gene enrichment analysis which helps to

identify pathways, networks, processes, or functional groups, etc. that are enriched in differentially expressed genes from the dataset. This approach allows for the identification of overrepresented pathways (or networks, processes, etc.). It also provides the statistical significance of the findings with multiple testing correction. This gives a measure of the false discovery that would occur by chance, because it accounts for the number of differentially expressed genes in the list, as well as for the number of gene sets (pathways) tested. Many web services provide such analysis tools, for example DAVID (Huang et al., 2007), WEB GESTALT (Wang et al., 2013a), g:Profiler (Reimand et al., 2007). The GSEA software from the Broad Institute (Cambridge, USA) is also widely used for such a purpose (Subramanian et al., 2005). Gene set enrichment analysis provides the first insight into affected biological processes. In the next step, already having some clues for the pathway enrichment analysis, the differentially expressed genes can be used to build a network of interactions *de novo*, based on the information available from various resources about the potential or proven interplay between them. ReactomeFIViz (Wu et al., 2014), STRING (Franceschini et al., 2013), and GeneMANIA (Warde-Farley et al., 2010) are just few examples of the many algorithms available for network construction.

There has been a substantial effort put into understanding the transcriptional changes that occur in physiological ageing and in the HGPS premature ageing syndrome, with multiple studies performing genome-wide analysis. Cellular senescence has also received significant attention, but there has not been a study specifically comparing senescence induced by prelamin A accumulation and replicative senescence though. This chapter provides a description of the microarray analysis of the three ageing models described in the previous chapter. Transcriptional profiling

was characterised for replicative senescence and for the two models with acute prelamin A accumulation: (i) the pharmacological, induced by saquinavir treatment, and (ii) the genetic, by siRNA knock-down of Zmpste24. In this chapter an unbiased genome-wide transcript analysis was performed separately for each model. Despite different senescence-inducing stimuli (proliferative exhaustion over multiple passages versus acute prelamin A accumulation over 48 hour-period) similarities between models were identified and described here.

4.2 RESULTS

4.2.1 An overview of the microarray data

To study the effects of senescence on gene expression, genome-wide microarray experiments were performed (see Figure 4.1 for the overview). Six biological replicates of RNA preparations for pairwise comparisons were prepared for:

- late (p39) and early (p15) passage HDFs (Late/Early) to analyse transcriptome changes in replicative senescence that developed continuously over an extended period of time allowing for potential compensation mechanisms to be triggered
- saquinavir or DMSO (vehicle) treated early passage HDFs (SAQ/DMSO) to study effects of acutely induced senescence in response to prelamin A accumulation
- darunavir or DMSO treated early passage HDFs (DAR/DMSO) to account for the effects of HIV-PI that are unrelated to prelamin A accumulation, but might overlap with the SAQ/DMSO comparison

- siZmpste24- or siCTRL-transfected early passage HDFs (siZmpste24/siCTRL) to study the specific effects of depletion of Zmpste24 activity and hence reducing the off-target impact of saquinavir.

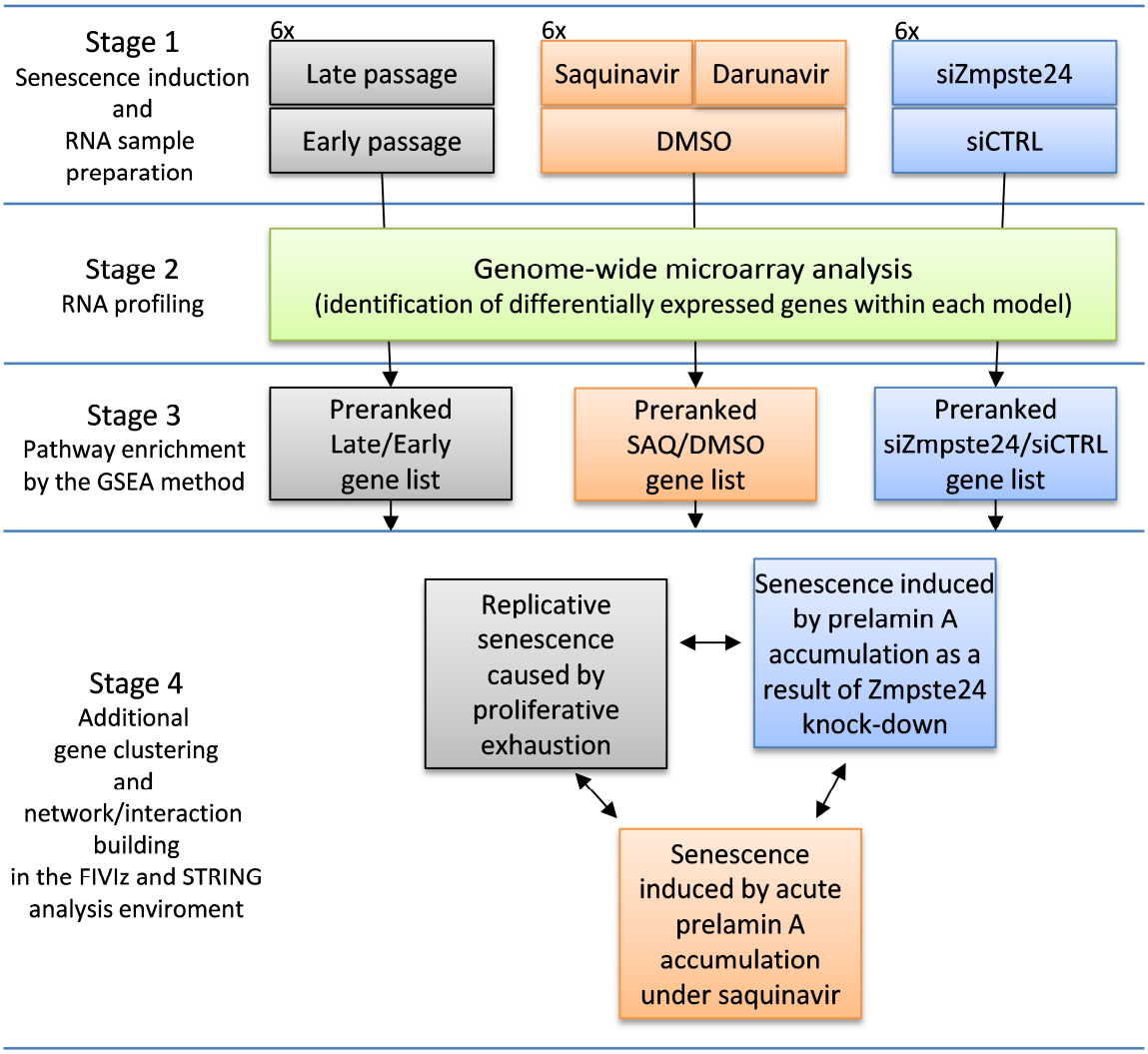

Figure 4.1. Flow chart representing transcriptome analysis of the ageing models.

In Stage 1, 6 biological replicates were prepared for each condition, followed by microarray analysis of the RNA profiles in Stage 2. In Stage 3 differentially expressed genes (at $P < 0.1$) within each model were ordered according to their Log_2 Fold change and analysed by the GSEA method. The SAQ/DMSO preranked list excluded genes that showed the same directionality of expression changes in the darunavir-treated cells. Further analysis of enriched pathways, together with additional gene clustering and interaction investigation was performed at the Stage 4 by exploring FIVIz and STRING resources, which helped to gain an insight into relationship between tested ageing models.

Dye-specific effects on the microarray hybridisation were eliminated by including dye-swaps within each comparison. Depending on the analyses performed, the statistical significance of the data presented was at $P < 0.05$ or $P < 0.1$, as indicated.

Of note, in the siZmpste24/siCTRL model most likely a mixed population of cells transfected and untransfected with Zmpste24 siRNA would be present. Presumably the experimental approach would benefit from including fluorescent siRNA in the transfection step, followed by cell sorting to obtain a homogenous population of transfected cells. This step, however, has not been incorporated in this study and the potential implications for the results are explained in the Discussion section of this Chapter.

4.2.1.1 Summary of gene expression in the models analysed

The number of genes upregulated above a 1.2 fold change ratio or downregulated below a 0.8 fold change ratio in each pairwise comparison separately at $P < 0.05$ or $P < 0.1$ are presented in Table 4.1. The biggest number of genes differentially expressed was observed in the late to early passage comparison, with over 65% being downregulated in senescent cells at a significance level of $P < 0.05$. The saquinavir to vehicle control (DMSO) comparison showed a much lower number of genes differentially expressed, with over 69% being upregulated at $P < 0.05$. Conversely, the darunavir to vehicle control (DMSO) comparison, at $P < 0.05$, caused a substantial decrease in gene expression (over 89% of gene hits). A comparable number of genes being up- or downregulated was observed in the siZmpste24 to siCTRL comparison.

Table 4.1. Summary of gene expression in four pairwise microarray analyses. Genes showing fold change ratio of above 1.2 or below 0.8 were considered as upregulated or downregulated, respectively.

Comparison	P < 0.05			P < 0.1		
	upregulated	**downregulated**	**total**	**upregulated**	**downregulated**	**total**
Late/Early	633	1194	1827	1129	1719	2848
SAQ/DMSO	263	115	378	633	252	885
DAR/DMSO	64	553	617	240	1326	1566
siZmpste24/siCTRL	365	446	811	660	701	1361

Despite a relatively high number of genes being differentially expressed within each comparison, there was only a modest overlap between ageing models. In Figure 4.2, Venn diagrams represent the number of genes differentially expressed and how many overlap between the three comparisons: Late/Early, SAQ/DMSO and siZmpste24/siRNA. Genes that demonstrated a similar pattern of expression after

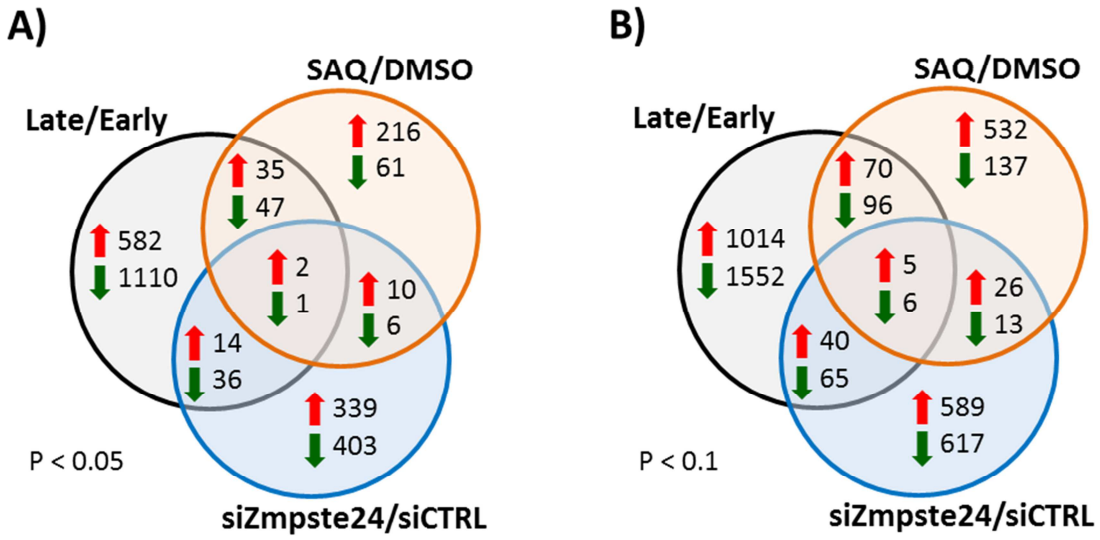

Figure 4.2. Summary of gene expression in the microarrays analysis.

Venn diagrams representing the number of genes differentially expressed and how many overlap between the three conditions at two significance levels of P < 0.05 (**A**) and P < 0.1 (**B**). Genes showing fold change ratio of above 1.2 or below 0.8 were considered as upregulated or downregulated, respectively. SAQ/DMSO comparison excludes genes that overlapped with DAR/DMSO at a given P cut off.

treatment with saquinavir or darunavir were excluded from the analysis because the changes observed would most likely result from the HIV-PI effect on enzymes other than Zmpste24, and therefore would not relate to acute prelamin A accumulation. In the three models, at $P < 0.05$, only two genes were consistently upregulated (ME1 and OPN3) and one consistently downregulated (PLAT) (Figure 4.2 A). An additional three and five genes were up- or downregulated, respectively, when the P level was increased to < 0.1 (Figure 4.2 B).

4.2.1.2 Overlap of gene expression between the ageing models

Gene expression was further pairwise-compared between ageing models at $P < 0.05$. One hundred four genes showed differential expression in both the Late/Early and SAQ/DMSO datasets at $P < 0.05$, with 82% of genes (85 genes) showing the same directionality of changes in expression level (Figure 4.3 A). Whereas the remaining 19 genes showed opposite directionality in expression in these two models. siZmpste24/siCTRL shared 173 genes with the Late/Early dataset, but only 31% (53 genes) showed the same directionality (Figure 4.3 B). There was a 56 gene overlap between SAQ/DMSO and siZmpste24/siCTRL, with 34% (19 genes) having expression altered in the same direction (Figure 4.3 C).

Twenty three genes were identified when datasets were compared for the three ageing models together at $P < 0.05$, without selecting towards the same directionality of gene expression changes. This increased to 61 genes when the statistical significance was relaxed to $P < 0.1$ (Figure 4.4). This clustering again showed the best overlap in the Late/Early and SAQ/DMSO datasets, with only a small subset of genes similarly expressed in the siZmpste24/siCTRL dataset.

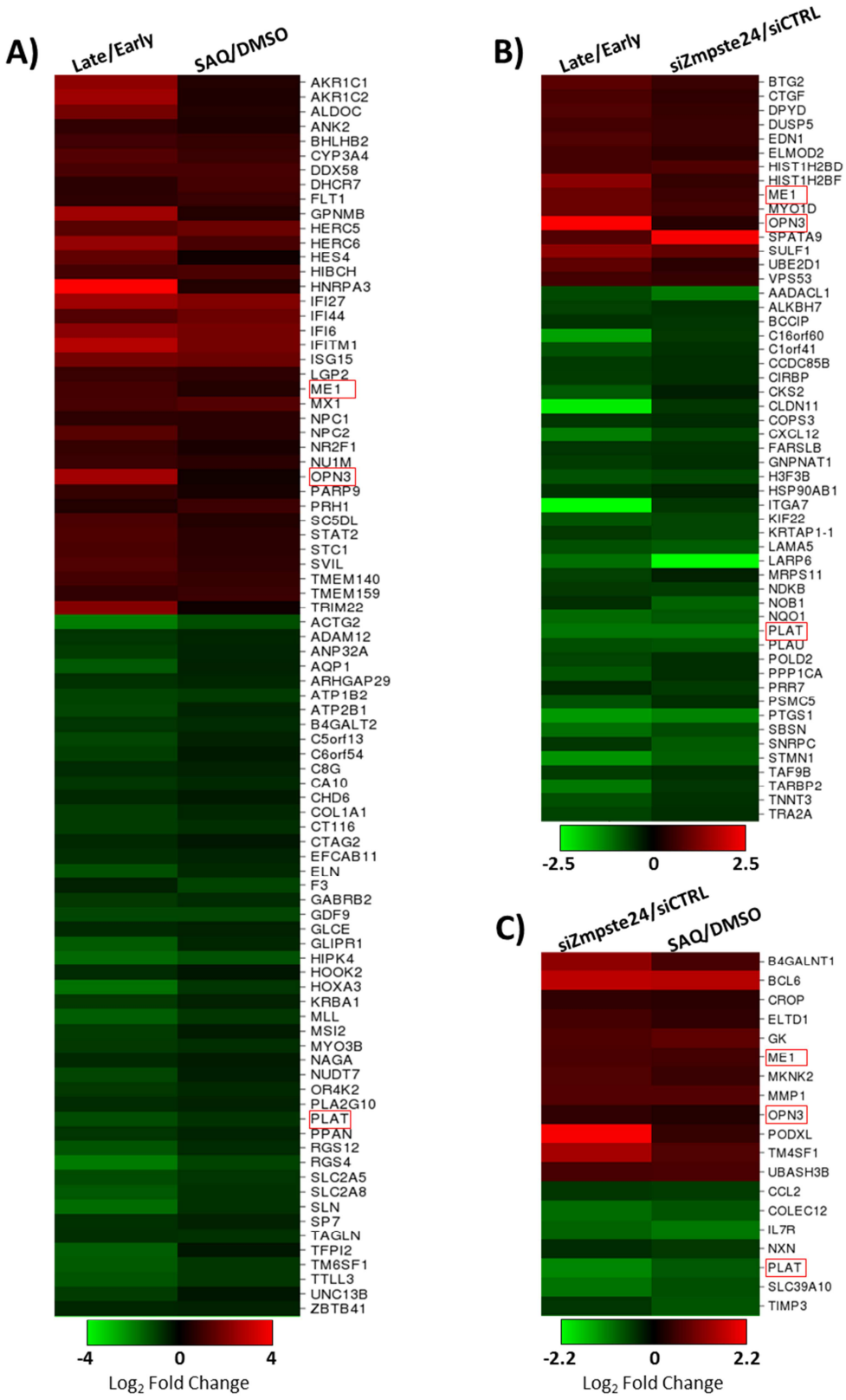

Figure 4.3. Genes that overlap in pairwise comparison between ageing models and show the same directionality of expression changes.

(A) Overlap between the Late/Early and SAQ/DMSO. **(B)** Overlap between the Late/Early and siZmpste24/siCTRL. **(C)** Overlap between the siZmpste24/siCTRL and SAQ/DMSO. $P < 0.05$ cut off was applied and fold change below 0.8 or above 1.2 for downregulated and upregulated genes respectively (here transformed into Log_2 scale). Red rectangles highlight the three genes overlapping between the three ageing models at $P < 0.05$. SAQ/DMSO dataset excludes genes that overlap and show the same directionality with the DAR/DMSO dataset at $P < 0.05$ significance level.

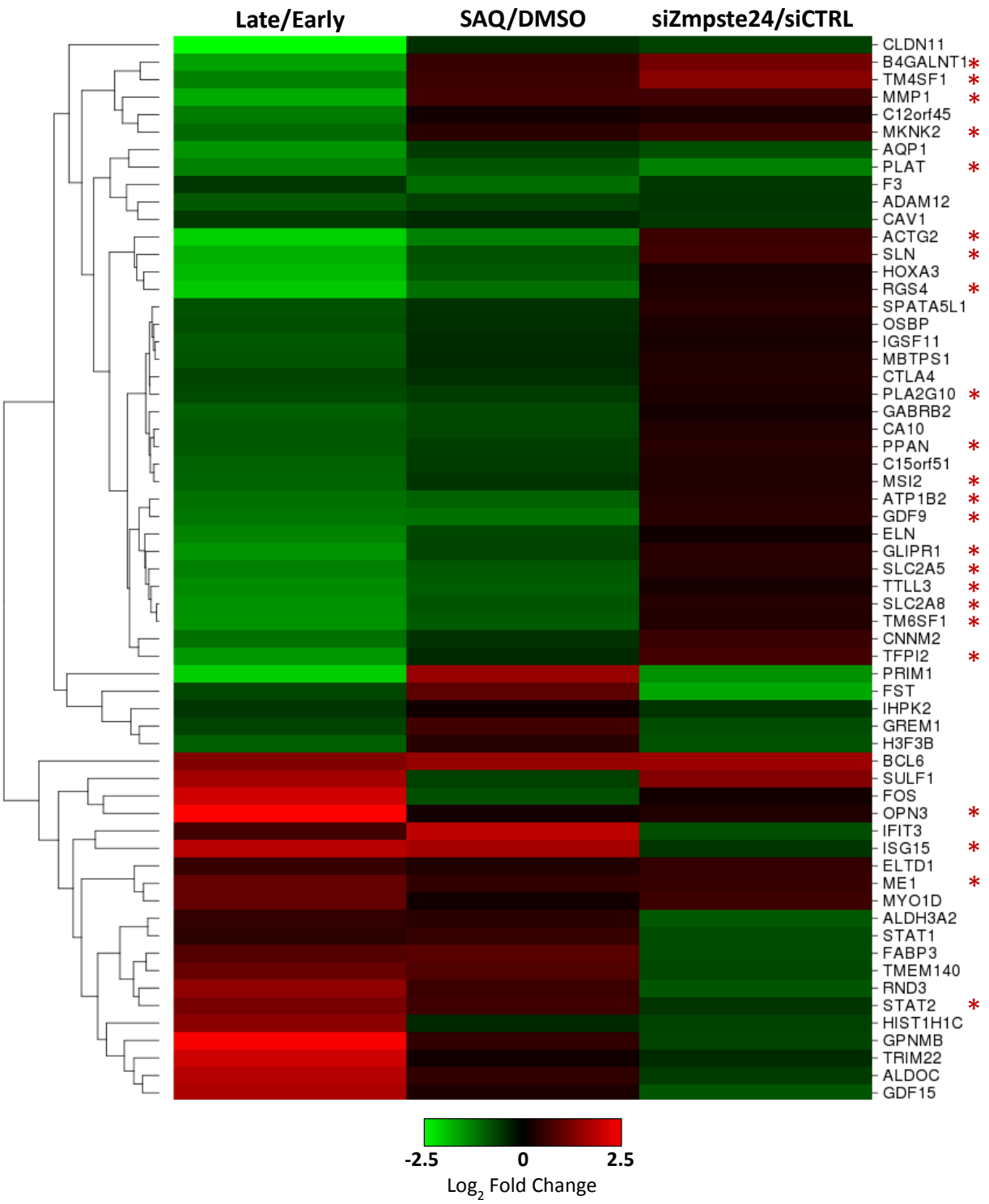

Figure 4.4. Genes differentially expressed and overlapping in the three ageing models.

Rows were clustered using CIMminer tool and the Euclidean distance is depicted on the left. P < 0.1 cut off was applied without fold change filter. Red asterisks highlight the 23 genes overlapping between the three ageing models at P < 0.05. SAQ/DMSO data set excludes genes that overlap and show the same directionality with DAR/DMSO dataset at P < 0.1.

4.2.1.3 Darunavir as a double control for saquinavir experiments

The DAR/DMSO microarray analysis was used to account for the effects of HIV-PI on gene expression unrelated to prelamin A accumulation. When compared to the SAQ/DMSO microarray data it showed a very different expression pattern, with only a small subset of genes overlapping. It identified only 2 genes (10% of the subset) with the same directionality of expression change at P < 0.05 (Figure 4.5 A, C). Relaxing the statistical significance to P < 0.1 resulted in identification of 13 genes similarly either up- or downregulated (Figure 4.5 B). This still only accounted for a 10% fraction of overlapping genes. The remaining 90% (110 genes), showed expression changes in opposite directions, suggesting that darunavir has off-target effects of its own, unrelated to saquinavir response.

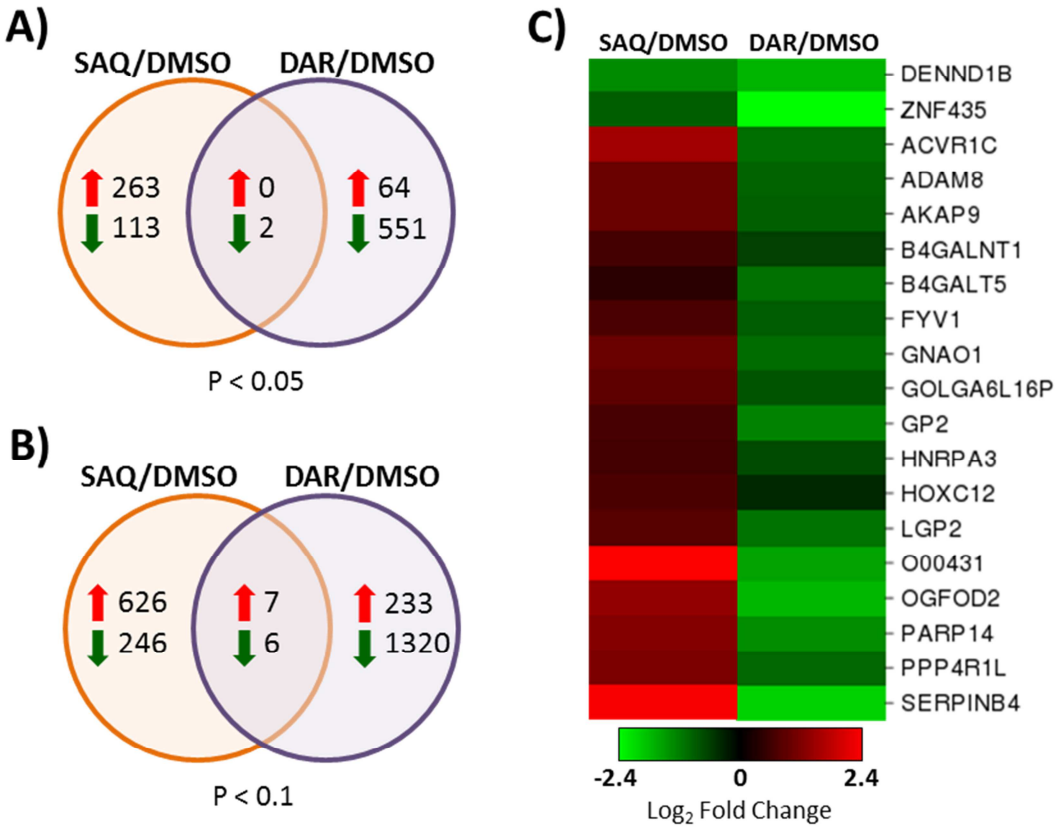

Figure 4.5. Overlap between the SAQ/DMSO and DAR/DMSO datasets.

Venn diagrams showing number of differentially expressed genes and the overlap between the two comparisons at P < 0.05 **(A)** or P < 0.1 **(B)**. **(C)** Heat map for differentially expressed genes at P < 0.05.

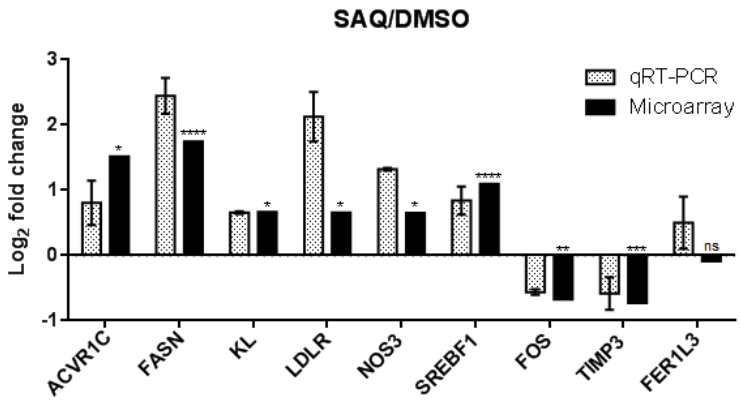

Figure 4.6. Validation of microarray results.

An example showing qRT-PCR validation for selected genes identified in microarray screen for the SAQ/DMSO dataset. Error bars indicate standard deviation. Asterisks above microarray bars represent P value as follows: * P < 0.05; ** P < 0.01; *** P < 0.001; **** P < 0.0001; ns, P not significant.

4.2.1.4 qRT-PCR validation of microarray data

Microarray data was validated by qRT-PCR. Random genes that showed overexpression, underexpression, or no significant change were selected, and qRT-PCR was performed, further confirming the directionality of changes and the quality of the microarray analysis (Figure 4.6).

4.2.2 The Gene Set Enrichment Analysis (GSEA) of microarray data

The Gene Set Enrichment Analysis (GSEA) method was employed to determine the biological significance of the observed changes in gene expression in the ageing models. The GSEA method allows for interpretation of microarray data at the level of gene sets corresponding to known pathways, networks, biological processes, etc. (Subramanian et al., 2005), rather than focusing on individual genes showing the highest fold change in transcript level. This therefore offers a broad overview of the

biology behind the observed changes in gene expression. The GSEA method works with continuous expression data represented as a ranked list of genes, and searches for enrichment of gene sets at the top or bottom, within the overexpressed or underexpressed populations, respectively.

A ranked gene list was prepared separately for each aging model by applying a $P < 0.1$ cut off, transforming fold change ratio into $\log_2$ value, and ordering the genes from the highest $\log_2$ fold ratio to the lowest. The SAQ/DMSO preranked list genes that showed similar directionality of expression changes to the DAR/DMSO dataset were excluded from the list. This approach produced three preranked lists: Late/Early (2899 genes), SAQ/DMSO (978 genes), and siZmpste24/siCTRL (1464 genes). They were analysed using the GSEAPreranked tool in reference to the Molecular Signature Database v5.0 (MSigDB), which contains a collection of annotated gene sets for use with GSEA software. Three collections from MSigDB were used in particular: hallmark gene sets, C2 curated gene sets, and the C5 collection. Hallmark gene sets are coherently expressed signatures derived by aggregating many MSigDB gene sets to represent well-defined biological states or processes. C2 curated gene sets are derived from online pathway databases, publications in PubMed, and knowledge of domain experts, including Reactome and Kyoto Encyclopedia of Genes and Genomes (KEGG) annotations. The C5 collection represents genes annotated by the same Gene Ontology (GO) terms.

In the GSEA method, an enrichment score (ES) is calculated by walking down the preranked gene list and increasing a running-sum statistic when encountering a gene that is present in a gene set (from the database collections) and decreasing it when the encountered gene is absent. The ES score represents the maximum deviation from

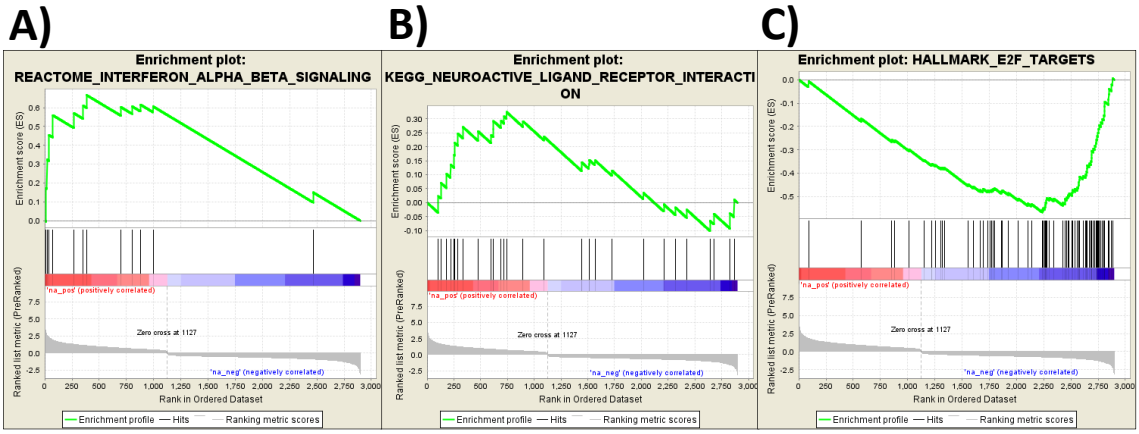

Figure 4.7. An example of GSEA plots.

Database and the gene set name are provided at the top of each plot. Enrichment profile as it walks down the preranked gene list (the Late/Early in this example) is shown as a green line in the top section. Hits from the preranked list present in the gene set are shown as vertical lines in the mid-section. At the bottom of each panel, the ranked list metric represents Log_2 fold change of expression. **A)** A representative plot showing significant enrichment of overexpressed genes (in red) within the gene set (positively correlated). **B)** A plot showing no significant enrichment, neither positive nor negative. **C)** A plot showing significant enrichment of underexpressed genes (in blue) within the indicated gene set (negatively correlated).

zero that would be produced in a random walk, and reflects the degree to which a gene set from the database collection is overrepresented at either the top or bottom of the entire preranked gene list.

In order to provide context for the calculated gene specific ES values, genes in the preranked list were permutated 1000 times, and the ES for permutated data was recalculated to generate a null distribution for the ES. The empirical, nominal P value (NOM p-val) of the observed ES was then calculated relative to this null distribution in order to estimate the statistical significance. Further adjustment for multiple hypothesis testing was achieved by calculating a normalised enrichment score (NES). This accounts for the size of gene sets from the database collections. The proportion of false positives was controlled by determining the false discovery rate (FDR q-val)

corresponding to each NES. To create a hypothesis, an FDR cut-off of 0.25 was applied in accordance with advice from the GSEA developers (Subramanian et al., 2005). This indicates that the result is likely to be valid at least three out of four times (Benjamini and Hochberg, 1995). An example of enrichment plots with description is provided in Figure 4.7.

4.2.3 Characterisation of transcriptome profile in replicative senescence

To relate our microarray results for replicative senescence to existing data reported in the literature, the Late/Early dataset was compared to recently published results for transcriptional changes in normal human dermal fibroblasts upon replicative exhaustion (Lackner et al., 2014). In this study 1248 genes showed altered expression while in our Late/Early dataset this number was equal to 1827 (at $P < 0.05$ cut off). 191 genes overlapped between these two datasets, with computed P-value for an overlap of this size (or bigger) based on the Fisher exact test equal to P = 5.9366e-34 (Figure 4.8 A). When directionality of expressional changes for the overlapping genes was compared between these two datasets, it showed a moderate positive correlation (Pearson correlation coefficient = 0.45328) (Figure 4.8 B).

Various databases can use different descriptors for a process or pathway. Thus gene sets derived from four different collections, namely KEGG, Reactome, Hallmark MSigDB, and GO were reported here. For convenience, entries in the tables listing the enriched gene sets are colour-coded. KEGG sets are highlighted in yellow, Reactome in blue, Hallmark MSigDB in magenta, and GO in green.

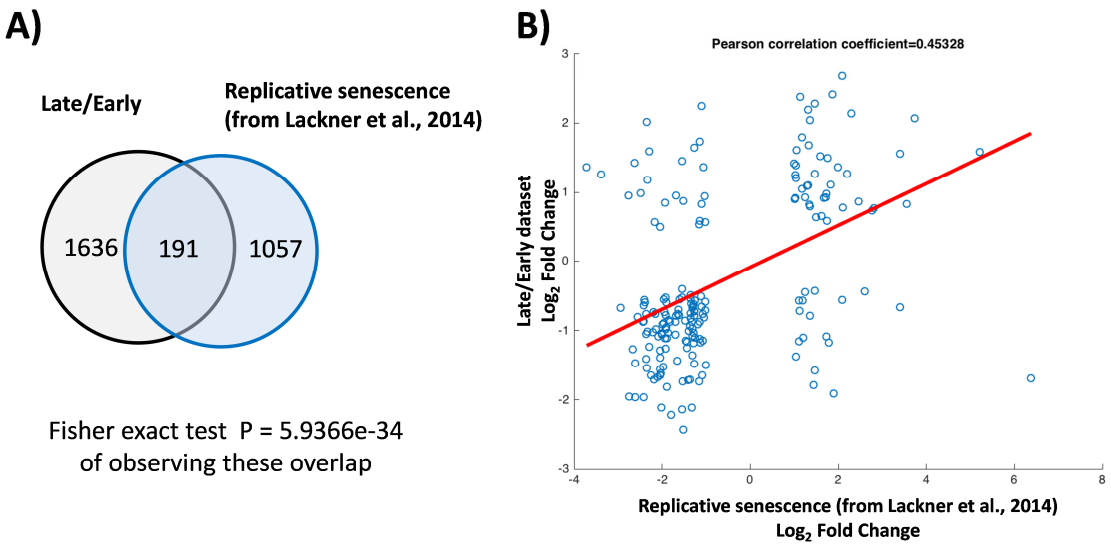

Figure 4.8. Comparison of the Late/Early dataset with published microarray results for replicative senescence.

A) Overlap between the Late/Early dataset and microarray results reported by Lackner and colleagues (Lackner et al., 2014). Fisher exact test for observing this overlap between these two sets was calculated out of 25,100 genes total represented on a microarray chip. **B)** Correlation between the overlapping genes from the two datasets. Data analysed in collaboration with Dr Margarita Schlackow.

4.2.3.1 Senescent cells suffer from decline in basic cellular processes

Upon reaching replicative senescence, HDF cells show a decline in function of many basic cellular processes (Table 4.2). As expected, and further confirmed by analysis of gene sets from different database collections, the majority of downregulated genes in replicative senescence correspond to cell proliferation. Processes like mitosis, DNA replication, RNA metabolism, translation and microtubule formation in late passage HDFs therefore were highly affected by underexpression of the components of these pathways (Figure 4.9). This indicates that senescent cells have passed the state in which compensatory feedback may maintain activity in specific pathways. For example, all 47 genes from the preranked Late/Early list which encode translation initiation factors and ribosomal proteins, and had been assigned to

the Reactome category Translation Initiation, were underexpressed in the late passage HDFs (Figure 4.10). Similarly, DNA synthesis is heavily affected in late passage HDFs (Figure 4.11). Another striking example is the clustering of Myc targets within the underexpressed gene population in late passage HDFs (Figure 4.9 B), including the myc transcript itself (0.6 fold change). The Myc protein is a transcriptional regulator with a broad range of target genes. It is predominantly involved in fundamental cellular processes like growth, proliferation, differentiation, metabolism, and cell death, but is also important in longevity (Hofmann et al., 2015; Meyer and Penn, 2008).

Table 4.2. Gene sets correlating with genes underexpressed in replicative senescence of HDFs. GSEA results showing Kyoto Encyclopedia of Genes and Genomes (KEGG), Reactome, Hallmark and Gene Ontology (GO) pathways identified. For clarity, redundant sets were removed. Size, number of genes from the preranked gene list identified in the gene set; ES, enrichment score; NES, normalised enrichment score; NOM p-val, nominal P value; FDR q-val, false discovery rate Q value.

GENE SET NAME	SIZE	ES	NES	NOM p-val	FDR q-val
KEGG_RIBOSOME	43	-0.40	-2.02	0.00	0.01
KEGG_DNA_REPLICATION	13	-0.53	-1.88	0.00	0.03
KEGG_RNA_DEGRADATION	14	-0.48	-1.73	0.02	0.08
KEGG_CELL_CYCLE	32	-0.37	-1.71	0.03	0.09
KEGG_AMINOACYL_TRNA_BIOSYNTHESIS	11	-0.48	-1.57	0.06	0.15
KEGG_VEGF_SIGNALING_PATHWAY	6	-0.62	-1.56	0.04	0.16
KEGG_SPLICEOSOME	33	-0.32	-1.54	0.03	0.18
REACTOME_DNA_REPLICATION	50	-0.47	-2.58	0.00	0.00
REACTOME_TRANSLATION	53	-0.40	-2.29	0.00	0.00
REACTOME_METABOLISM_OF_RNA	87	-0.37	-2.29	0.00	0.00
REACTOME_CELL_CYCLE	96	-0.35	-2.21	0.00	0.00
REACTOME_SRP_DEPENDENT_COTRANSLATIONAL_ PROTEIN_TARGETING_TO_MEMBRANE	47	-0.40	-2.13	0.00	0.01
REACTOME_3_UTR_MEDIATED_TRANSLATIONAL_ REGULATION	47	-0.40	-2.13	0.00	0.01
REACTOME_NONSENSE_MEDIATED_DECAY_ENHANCED_ BY_THE_EXON_JUNCTION_COMPLEX	48	-0.37	-1.95	0.00	0.02
REACTOME_REGULATION_OF_MRNA_STABILITY_BY_ PROTEINS_THAT_BIND_AU_RICH_ELEMENTS	23	-0.45	-1.90	0.01	0.03
REACTOME_METABOLISM_OF_PROTEINS	94	-0.30	-1.90	0.00	0.03

GENE SET NAME	SIZE	ES	NES	NOM p-val	FDR q-val
REACTOME_EXTRACELLULAR_MATRIX_ORGANIZATION	21	-0.45	-1.89	0.00	0.03
REACTOME_MICRORNA_MIRNA_BIOGENESIS	8	-0.62	-1.79	0.02	0.05
REACTOME_CELL_CELL_COMMUNICATION	8	-0.60	-1.74	0.02	0.08
REACTOME_RECRUITMENT_OF_MITOTIC_CENTROSOME_ PROTEINS_AND_COMPLEXES	9	-0.55	-1.69	0.03	0.10
REACTOME_CELL_JUNCTION_ORGANIZATION	5	-0.68	-1.64	0.02	0.12
REACTOME_REGULATION_OF_ORNITHINE_ DECARBOXYLASE_ODC	14	-0.45	-1.64	0.03	0.12
REACTOME_SCFSKP2_MEDIATED_DEGRADATION_ OF_P27_P21	14	-0.45	-1.60	0.03	0.14
REACTOME_KINESINS	7	-0.58	-1.58	0.05	0.15
REACTOME_ER_PHAGOSOME_PATHWAY	13	-0.45	-1.56	0.05	0.16
REACTOME_AMINO_ACID_SYNTHESIS_AND_ INTERCONVERSION_TRANSAMINATION	5	-0.63	-1.55	0.04	0.17
REACTOME_P53_INDEPENDENT_G1_S_DNA_DAMAGE_ CHECKPOINT	13	-0.45	-1.55	0.06	0.17
REACTOME_AUTODEGRADATION_OF_THE_E3_UBIQUITIN_ LIGASE_COP1	12	-0.45	-1.52	0.06	0.19
REACTOME_CROSS_PRESENTATION_OF_SOLUBLE_ EXOGENOUS_ANTIGENS_ENDOSOMES	12	-0.45	-1.52	0.07	0.19
REACTOME_P53_DEPENDENT_G1_DNA_DAMAGE_RESPONSE	12	-0.45	-1.52	0.08	0.19
REACTOME_PROTEIN_FOLDING	11	-0.45	-1.50	0.05	0.20
REACTOME_SIGNALING_BY_WNT	14	-0.41	-1.50	0.08	0.20
REACTOME_ACTIVATION_OF_ATR_IN_RESPONSE_TO_ REPLICATION_STRESS	11	-0.44	-1.46	0.07	0.22
REACTOME_COLLAGEN_FORMATION	13	-0.42	-1.43	0.11	0.24
HALLMARK_E2F_TARGETS	80	-0.57	-3.48	0.00	0.00
HALLMARK_G2M_CHECKPOINT	61	-0.57	-3.18	0.00	0.00
HALLMARK_MYC_TARGETS_V1	84	-0.46	-2.90	0.00	0.00
HALLMARK_EPITHELIAL_MESENCHYMAL_TRANSITION	64	-0.34	-1.99	0.00	0.01
HALLMARK_MITOTIC_SPINDLE	34	-0.35	-1.67	0.02	0.08
HALLMARK_UNFOLDED_PROTEIN_RESPONSE	28	-0.34	-1.54	0.06	0.13
HALLMARK_DNA_REPAIR	30	-0.29	-1.40	0.10	0.22
HALLMARK_APICAL_JUNCTION	27	-0.30	-1.35	0.12	0.25
GO_STRUCTURAL_CONSTITUENT_OF_RIBOSOME	39	-0.40	-2.01	0.00	0.11
GO_MITOTIC_CELL_CYCLE	34	-0.38	-1.87	0.01	0.17
GO_DNA_DEPENDENT_DNA_REPLICATION	7	-0.68	-1.88	0.01	0.18
GO_REGULATION_OF_MITOSIS	10	-0.61	-1.89	0.01	0.19
GO_REGULATION_OF_G_PROTEIN_COUPLED_RECEPTOR_ PROTEIN_SIGNALING_PATHWAY	5	-0.78	-1.92	0.00	0.19
GO_SPINDLE_ORGANIZATION_AND_BIOGENESIS	5	-0.72	-1.74	0.02	0.24
GO_MICROTUBULE_BASED_PROCESS	16	-0.47	-1.78	0.01	0.25
GO_DNA_METABOLIC_PROCESS	44	-0.32	-1.71	0.01	0.25

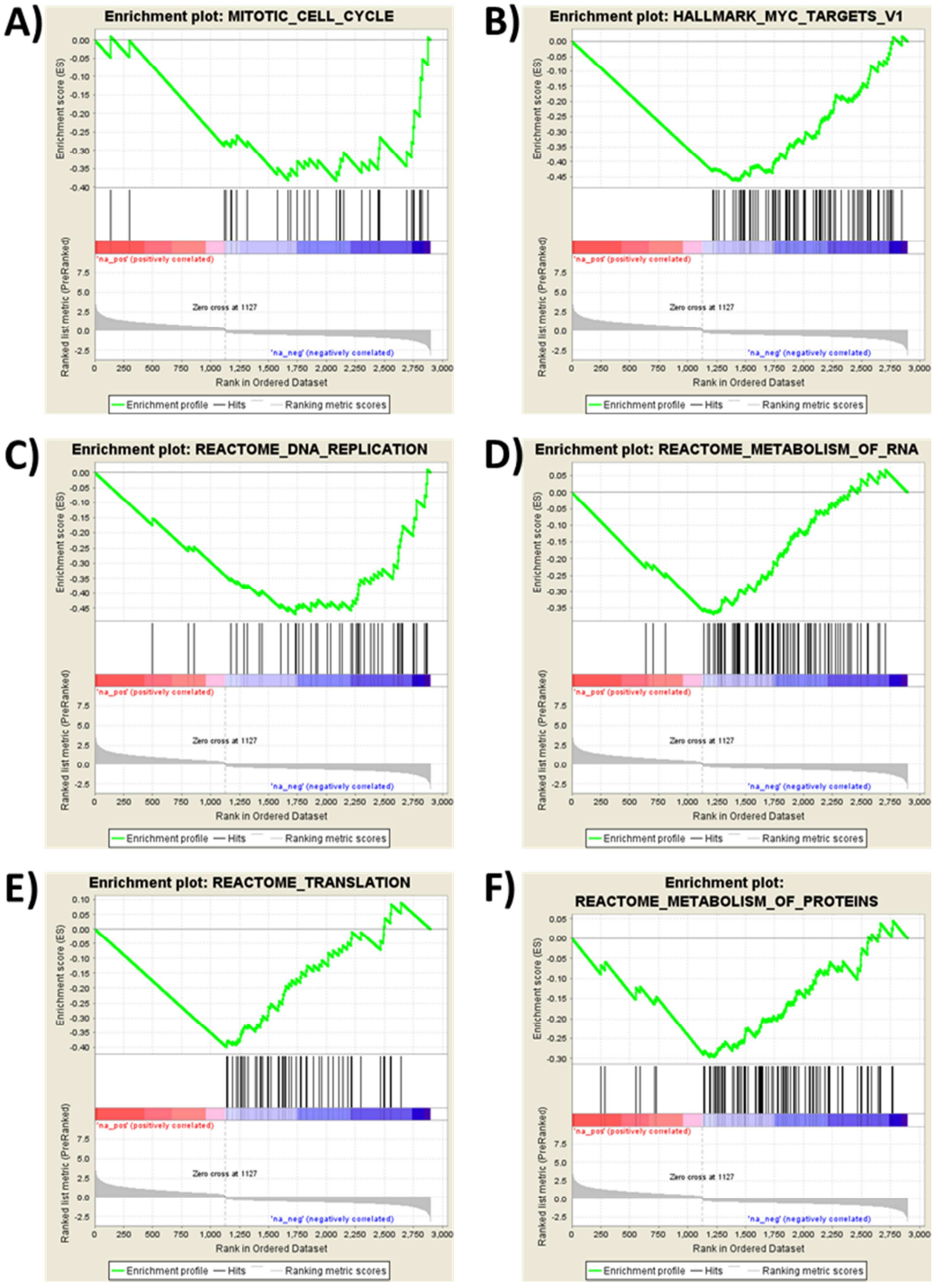

Figure 4.9. Examples of enrichment plots for selected gene sets enriched in underexpressed genes in replicative senescence.

List of hits for each gene set is available as an electronic file.

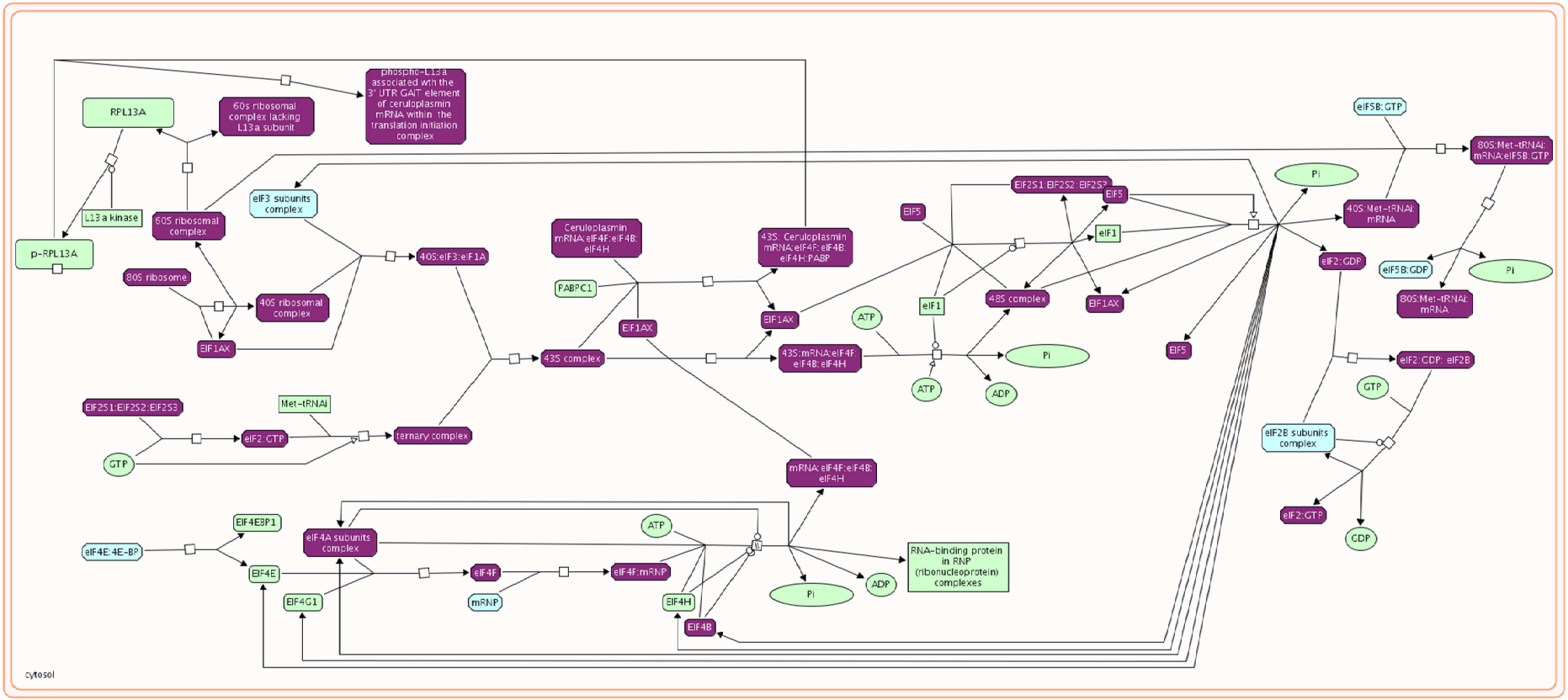

Figure 4.10. Reactome diagram representing Translation initiation.

Nodes and genes in purple indicate hits from the microarray analysis for the Late/Early comparison. 47 genes were assigned to Translation initiation category in the Reactome database (5 elongation initiation factors and 42 ribosomal proteins), each of them showing underexpression in late passage HDFs.

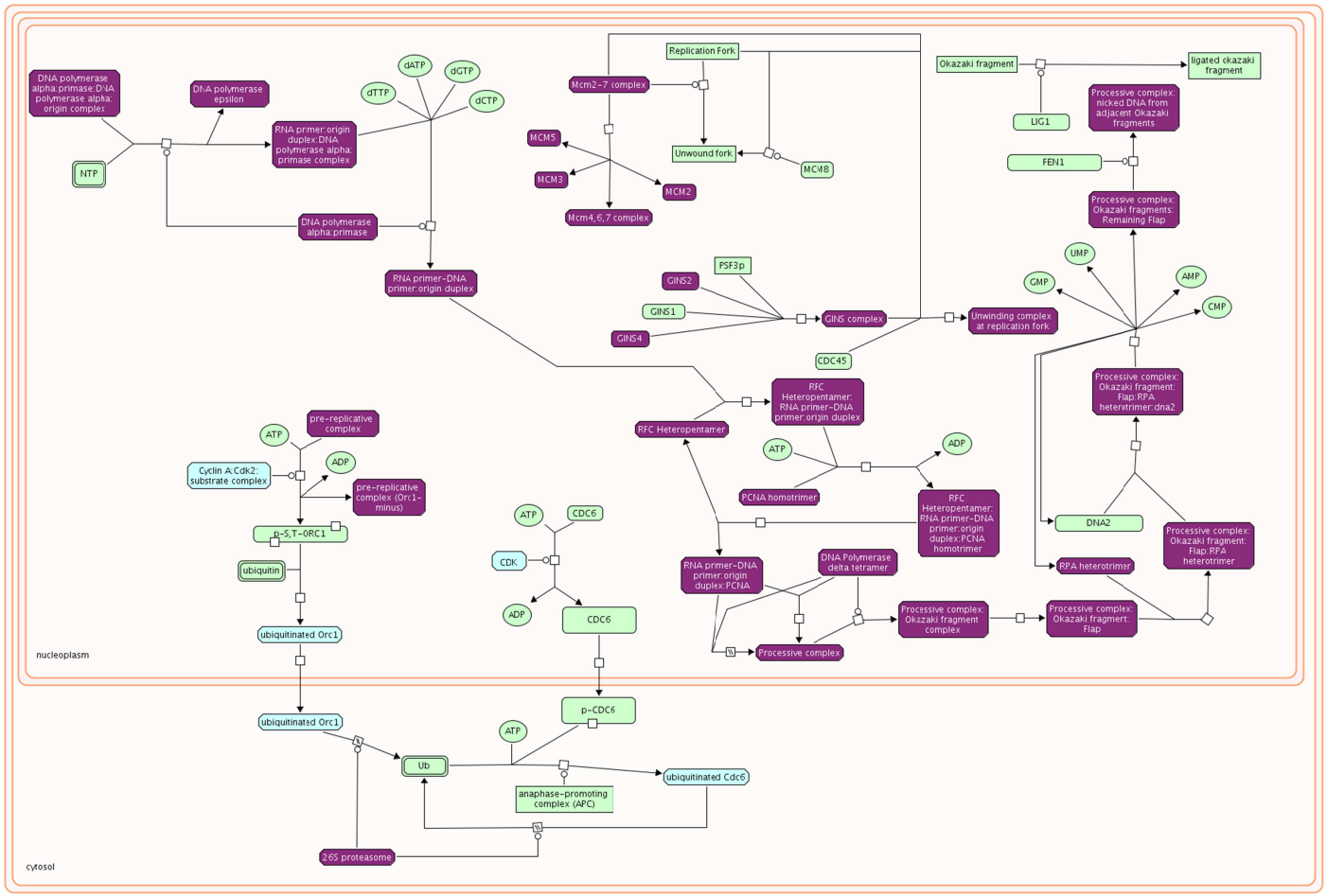

Figure 4.11 Reactome diagram representing Synthesis of DNA.

Nodes and genes in purple indicate hits from the microarray analysis for the Late/Early comparison. 27 genes were assigned to Synthesis of DNA category in the Reactome database of which 25 showed underexpression in late passage HDFs. They included 6 MCM complex components, 2 GINS complex subunits, PCNA, primase, polymerase delta subunit, and other DNA replication factors.

Furthermore, senescent cells show a decline in DNA repair and response to DNA damage. This is suggested by the enrichment of downregulated genes with pathways like Hallmark DNA Repair, Reactome P53 Dependent G1 DNA Damage Response or Reactome Activation of ATR in Response to Replication Stress. This may indicate exhaustion of the cell's capacity to cope with stress caused by DNA damage, and has been suggested as the main cause of senescence.

4.2.3.2 Late passage cells remodel extracellular matrix

Senescent cells remain metabolically active and remodel the extracellular matrix (ECM) through a range of secreted proteins (Cristofalo and Pignolo, 1996). The GSEA method identified a number of differentially expressed genes from the Late/Early dataset that were represented in the gene sets related to the ECM. There was the indication that the genes responsible for ECM organisation were affected, including a number of MMPs and TIMPs demonstrating differential expression (Figure 4.12 A, B). Among the most affected processes related to the ECM was collagen formation.

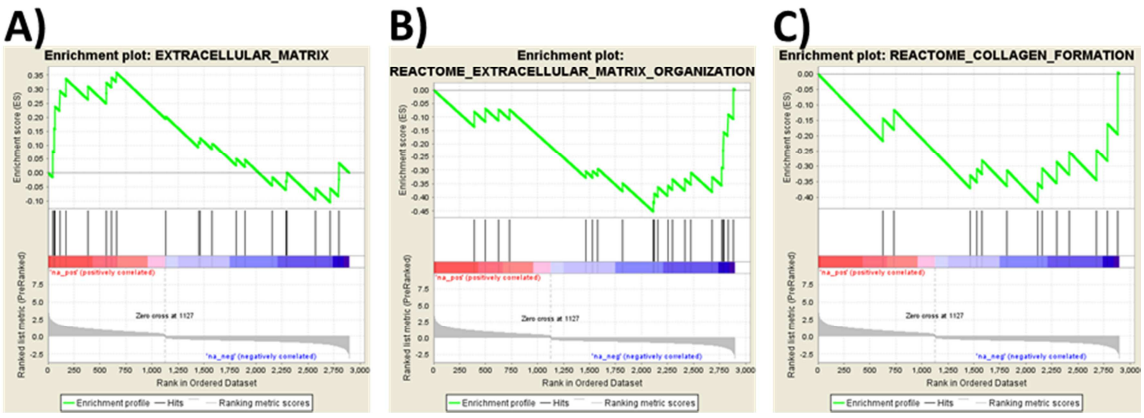

Figure 4.12. Enrichment plots for gene sets corresponding to extracellular matrix.

A) GO Extracellular Matrix gene set with 22 genes from the Late/Early preranked list belonging to this category showing differential expression, but no clear enrichment at either end of the list (FDR q-value = 0.43; NOM p- value = 0.14). **B)** and **C)** Reactome gene sets (Extracellular Matrix Organisation and Collagen Formation) with significant enrichment of the downregulated genes (see Table 4.2).

Multiple genes encoding collagens (COL1A1, COL4A1, COL4A2, COL4A3, COL5A1, COL6A1, COL6A2, COL13A1) and collagen-modifying enzymes (PCOLCE2, P4HB, PPIB) were underexpressed (fold ratio ranging from 0.2-0.7) (Figure 4.12 C). This suggests that there is continued overall production of the ECM by senescent cells, however, its composition is distinct.

4.2.3.3 Senescent cells show chronic inflammation symptoms

The GSEA of expressional changes in HDFs upon reaching replicative senescence revealed that the cells at this stage become potent producers of various cytokines and chemokines. When gene sets from the various database collections were analysed, an enrichment of overexpressed genes in late passage HDFs was observed for multiple pathways. These genes related to the immune response, cytokine signalling, and interferon activity, often with the lowest FDR q-values observed for such gene sets (Table 4.3, Figure 4.13 A, B). These are changes observed in fibroblasts, not immune competent cells, suggesting a massive shift in the expression profile and function.

Table 4.3. Gene sets correlating with genes overexpressed in HDFs reaching replicative senescence. GSEA results showing Kyoto Encyclopedia of Genes and Genomes (KEGG), Reactome, Hallmark, and Gene Ontology (GO) pathways identified. For clarity, redundant sets were removed. Size, number of genes from the preranked gene list identified in the gene set; ES, enrichment score; NES, normalised enrichment score; NOM p-val, nominal P value; FDR q-val, false discovery rate Q value.

GENE SET NAME	SIZE	ES	NES	NOM p-val	FDR q-val
KEGG_STEROID_HORMONE_BIOSYNTHESIS	7	0.86	2.22	0.00	0.02
KEGG_METABOLISM_OF_XENOBIOTICS_BY_CYTOCHROME_P450	11	0.70	2.11	0.00	0.05
KEGG_CYTOKINE_CYTOKINE_RECEPTOR_INTERACTION	23	0.55	2.06	0.00	0.06
KEGG_PYRUVATE_METABOLISM	5	0.83	1.90	0.00	0.11
KEGG_B_CELL_RECEPTOR_SIGNALING_PATHWAY	7	0.72	1.85	0.01	0.13
KEGG_LYSOSOME	21	0.49	1.84	0.02	0.13

KEGG_JAK_STAT_SIGNALING_PATHWAY	16	0.52	1.79	0.02	0.16
KEGG_PROPANOATE_METABOLISM	5	0.75	1.73	0.01	0.20
KEGG_TRYPTOPHAN_METABOLISM	5	0.74	1.69	0.02	0.23
KEGG_GLYCOLYSIS_GLUCONEOGENESIS	8	0.61	1.65	0.05	0.25
REACTOME_INTERFERON_ALPHA_BETA_SIGNALING	12	0.67	2.05	0.01	0.07
REACTOME_CYTOKINE_SIGNALING_IN_IMMUNE_SYSTEM	45	0.44	1.97	0.00	0.09
REACTOME_INTERFERON_SIGNALING	29	0.47	1.92	0.00	0.10
REACTOME_INNATE_IMMUNE_SYSTEM	38	0.43	1.87	0.00	0.12
REACTOME_CLASS_A1_RHODOPSIN_LIKE_RECEPTORS	28	0.47	1.85	0.00	0.13
REACTOME_GPCR_LIGAND_BINDING	37	0.42	1.82	0.01	0.14
REACTOME_CGMP_EFFECTS	6	0.66	1.68	0.03	0.23
REACTOME_VOLTAGE_GATED_POTASSIUM_CHANNELS	7	0.65	1.66	0.04	0.25
REACTOME_GLYCOSPHINGOLIPID_METABOLISM	5	0.73	1.65	0.04	0.25
HALLMARK_INTERFERON_ALPHA_RESPONSE	22	0.63	2.34	0.00	0.00
HALLMARK_INTERFERON_GAMMA_RESPONSE	36	0.53	2.25	0.00	0.00
HALLMARK_KRAS_SIGNALING_DN	19	0.54	1.96	0.00	0.03
HALLMARK_ESTROGEN_RESPONSE_EARLY	34	0.43	1.78	0.01	0.09
HALLMARK_KRAS_SIGNALING_UP	37	0.37	1.58	0.04	0.23
GO_DEFENSE_RESPONSE	24	0.58	2.24	0.00	0.02
GO_LIPID_METABOLIC_PROCESS	48	0.49	2.19	0.00	0.03
GO_ CELLULAR_LIPID_METABOLIC_PROCESS	34	0.51	2.16	0.00	0.03
GO_INFLAMMATORY_RESPONSE	16	0.64	2.25	0.00	0.04
GO_EXTRACELLULAR_SPACE	42	0.47	2.09	0.00	0.05
GO_STEROID_METABOLIC_PROCESS	8	0.76	2.05	0.00	0.06
GO_CYTOKINE_ACTIVITY	9	0.70	1.96	0.00	0.09
GO_CELL_CELL_SIGNALING	54	0.40	1.88	0.00	0.14
GO_TISSUE_REMODELING	7	0.71	1.85	0.00	0.14
GO_SUBSTRATE_SPECIFIC_TRANSPORTER_ACTIVITY	59	0.39	1.86	0.00	0.15
GO_RESPONSE_TO_WOUNDING	24	0.49	1.86	0.00	0.15
GO_RESPONSE_TO_EXTERNAL_STIMULUS	42	0.42	1.88	0.00	0.15
GO_G_PROTEIN_SIGNALING_COUPLED_TO_CYCLIC_NUCLEOTIDE_SECOND_MESSENGER	13	0.57	1.82	0.01	0.16
GO_POSITIVE_REGULATION_OF_TRANSFERASE_ACTIVITY	11	0.60	1.79	0.02	0.18
GO_SUBSTRATE_SPECIFIC_CHANNEL_ACTIVITY	19	0.49	1.77	0.02	0.19
GO_SECOND_MESSENGER_MEDIATED_SIGNALING	18	0.50	1.74	0.01	0.19
GO_OXIDOREDUCTASE_ACTIVITY	48	0.37	1.69	0.01	0.23
GO_REGULATION_OF_MULTICELLULAR_ORGANISMAL_PROCESS	27	0.42	1.68	0.02	0.24
GO_CYCLIC_NUCLEOTIDE_MEDIATED_SIGNALING	14	0.53	1.67	0.03	0.25

A)

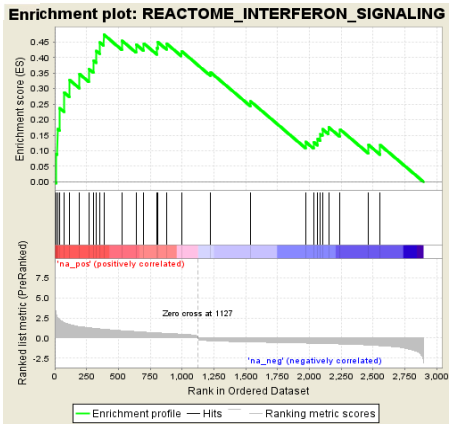

Reactome_Interferon_Signaling		
Gene Name	Log2 Fold Change	Running ES
IFITM1	2.94	0.09
IFI27	2.57	0.17
IFI6	2.28	0.24
ISG15	1.94	0.29
IFNG	1.71	0.33
HERC5	1.43	0.35
STAT2	1.29	0.36
GBP7	1.23	0.39
DDX58	1.19	0.42
MX1	1.15	0.45
OASL	1.11	0.47
ICAM1	0.93	0.45
NUPL2	0.81	0.44
IFIT3	0.75	0.45
IFI35	0.65	0.43
NUP133	0.65	0.45
OAS2	0.59	0.44
STAT1	0.50	0.42
KPNA2	-0.35	0.35
KPNB1	-0.48	0.26
UBE2N	-0.63	0.13
NUP37	-0.65	0.13
RAE1	-0.67	0.14
CD44	-0.67	0.15
NUP205	-0.68	0.17
EIF4E2	-0.70	0.18
AAAS	-0.75	0.17
SOCS3	-0.87	0.12
EIF4A1	-0.96	0.12

B)

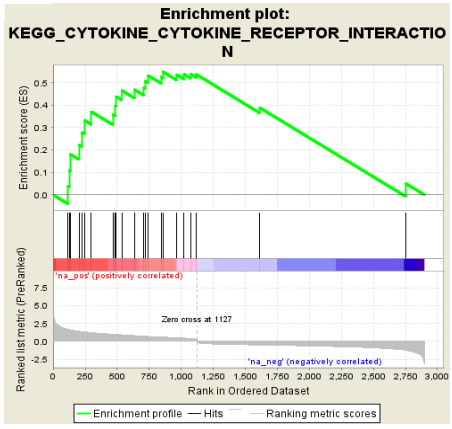

KEGG_Cytokine_Receptor_Interaction		
Gene Name	Log2 Fold Change	Running ES
IFNG	1.71	0.04
CXCL14	1.65	0.11
IL28RA	1.61	0.18
CXCL2	1.41	0.22
CXCR4	1.37	0.28
IL1RAP	1.35	0.33
TGFB3	1.24	0.37
TNFRSF21	1.00	0.36
IL6	0.98	0.40
VEGFB	0.96	0.44
TNFSF18	0.92	0.47
IL1R2	0.82	0.47
FLT1	0.74	0.48
GHR	0.73	0.51
PRLR	0.70	0.53
BMP2	0.62	0.53
FASLG	0.61	0.55
TNFRSF10B	0.52	0.54
CSF1	0.47	0.54
OSMR	0.40	0.54
ACVR1	0.29	0.54
GDF5	-0.51	0.39
CXCL12	-1.27	0.05

Figure 4.13. Examples of enrichment plots for immune response-related gene sets.

A) Reactome Interferon Signaling pathway with a table showing genes detected in the Late/Early preranked gene list. **B)** KEGG Cytokine Receptor Interaction with corresponding table showing genes from the Late/Early preranked list detected in that gene set. Core enrichment (the subset of genes that contributes most to the enrichment result) of the ES score is highlighted in green.

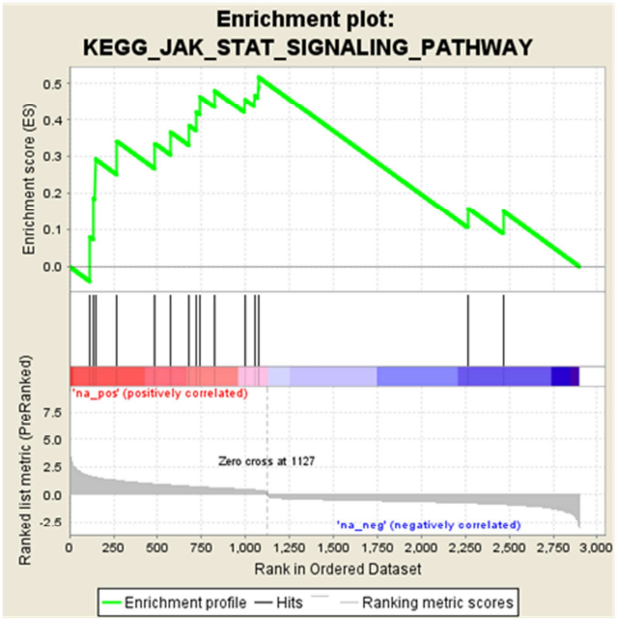

Gene Name	Log2 Fold Change	Running ES
IFNG	1.71	0.08
IL28RA	1.61	0.19
CCND2	1.58	0.29
STAT2	1.29	0.34
IL6	0.98	0.34
CISH	0.88	0.37
JAK3	0.77	0.38
GHR	0.73	0.42
PRLR	0.70	0.46
SOS1	0.64	0.48
STAT1	0.50	0.46
PIAS4	0.44	0.47
STAM2	0.41	0.49
OSMR	0.40	0.52
MYC	-0.76	0.16
SOCS3	-0.87	0.15

Figure 4.14. JAK/STAT signalling pathway enrichment analysis.

Left panel shows enrichment plot, while the table on the right lists hits from the preranked gene list present in the KEGG JAK/STAT Signaling Pathway gene set. Core enrichment of the ES score is highlighted in green.

Interestingly, the Janus Kinase/Signal Transducers and Activators of Transcription (JAK/STAT) pathway was also enriched among the upregulated genes in the late passage HDFs (Table 4.3, KEGG JAK STAT Signaling Pathway). The JAK/STAT is the main signal transduction pathway for a broad range of cytokines and growth factors which translates extracellular signals into the transcriptional activation of a wide spectrum of genes involved in homeostasis and immunity (Rawlings et al., 2004). Key components of JAK/STAT signalling such as JAK3, STAT1 and STAT2 showed overexpression in late passage cells (over 1.4 fold change), while, for example, SOCS3, a negative regulator of JAK/STAT pathway, was downregulated (Figure 4.14).

4.2.3.4 Late passage HDFs alter their lipid metabolic processes

Changes in lipid metabolism in senescence and ageing have been noted with profound alterations in fatty acid composition. This is particularly observed in cellular

membranes, which in turn can affect both the structure and function of organelles (Ford, 2010; Gey and Seeger, 2013; Maeda et al., 2009). The GSEA of differential gene expression in late passage HDFs showed a significant enrichment in gene set GO Lipid Metabolic Process, correlating with upregulated genes (Figure 4.15). An organelle playing a key role in lipid metabolism, other than the mitochondria, is the peroxisome. They house enzymatic pathways for the β-oxidation of acyl-CoAs, as well as for cholesterol and isoprenoid metabolism, and bile-acid synthesis. Peroxisomes are also regulators of cellular redox balance, and are able to synthesise and degrade reactive oxygen species (Giordano and Terlecky, 2012). Interestingly, when analysed by the GSEA method, the GO Oxidoreductase Activity gene set showed positive correlation with genes overexpressed in replicative senescence in HDFs. Furthermore, a number of genes linked to peroxisomes were upregulated in late passage HDFs. For example, PEX11A, a gene belonging to the PEX11 family of membrane elongation factors, which are responsible for the maintenance and proliferation of peroxisomes (Li and Gould, 2002), demonstrated over a 1.5 fold increase in expression. PEX11A can drive an increase in peroxisome abundance by responding to outside stimuli and interactions with other peroxisomal proteins. Furthermore, the intracellular level of free fatty acids and coenzyme A can be regulated by several acyl-CoA thioesterase enzymes (ACOTs) (Hunt et al., 2006). ACOT4, a peroxisomal enzyme catalysing hydrolysis of acyl-CoAs to the free fatty acid and coenzyme A, showed over a 2.5 fold increase in expression. This further implies a role of peroxisomes in lipid metabolism in senescent cells. Another peroxisomal enzyme, trypsin domain containing 1 (TYSND1), was also overexpressed by 1.5 fold in the microarray analysis of the replicative senescence in HDFs. TYSND1 has been shown to promote peroxisomal β-oxidation of lipids by its role in processing

and assembly of peroxisomal enzymes into a supramolecular complex that is responsible for this process (Kurochkin et al., 2007).

Ageing cells have disrupted cholesterol homeostasis resulting from dysfunctional cholesterol efflux and the deterioration of physiological functions (Berrougui and Khalil, 2009). Although the GSEA did not show enrichment in any pathway specifically naming cholesterol, when gene hits identified in sets corresponding to lipid

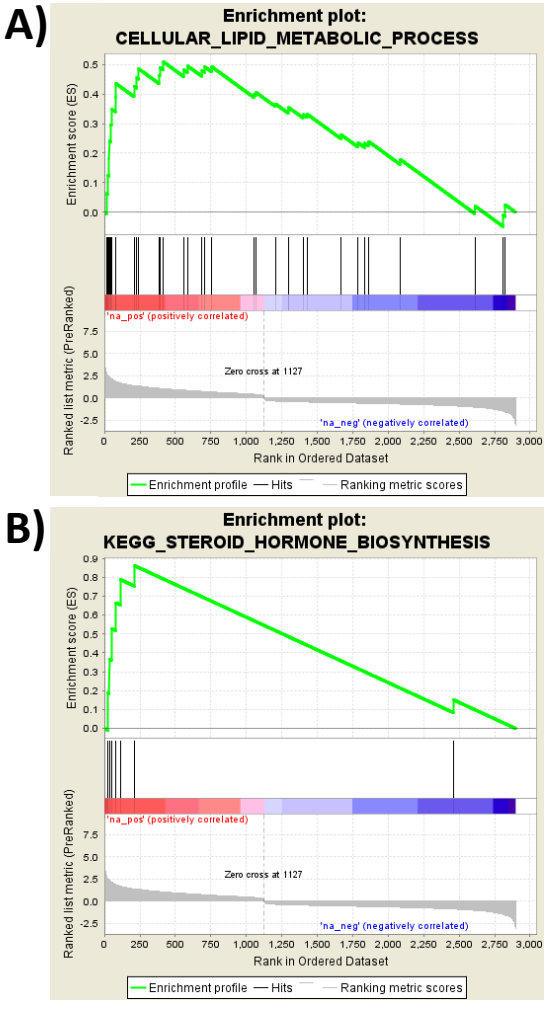

GO_Cellular_Lipid_Metabolic_Process		
Gene Name	Log2 Fold Change	Running ES
RARRES2	2.73	0.06
AKR1C2	2.55	0.13
PTGES	2.34	0.18
AKR1C1	2.34	0.24
APOC2	2.24	0.30
AKR1C3	2.16	0.35
AKR1C4	1.90	0.39
SCARB1	1.90	0.44
NPC2	1.40	0.43
PSAP	1.37	0.45
ACOT4	1.35	0.48
SMPD3	1.11	0.46
ASAH1	1.10	0.49
PPARA	1.08	0.51
ANG	0.90	0.48
DHRS3	0.87	0.49
CPT1B	0.76	0.48
NPC1	0.74	0.49
DHCR7	0.69	0.49
BDH2	0.44	0.40
RDH11	0.42	0.41
PDSS1	-0.33	0.37
SMG1	-0.39	0.34
SOAT1	-0.39	0.35
MIF	-0.43	0.33
CYP4F3	-0.45	0.33
YWHAH	-0.53	0.26
PLA2G2E	-0.56	0.24
DGAT1	-0.58	0.23
DPM1	-0.59	0.24
SPHK1	-0.67	0.18
BRCA1	-1.02	0.02
B4GALNT1	-1.50	-0.01
PTGS1	-1.57	0.03

Figure 4.15. Examples of enrichment plots related to lipometabolism.

A) GO Cellular Lipid Metabolic Process, with corresponding genes listed in the table on the right. **B)** KEGG Steroid Hormone Biosynthesis.

metabolism were combined and reanalysed in ReactomeFIViz application (via Cytoscape platform), cholesterol biosynthesis was among the top identified specific pathways. A number of genes, like MVD, CYP3A4, S5DL and DHCR7 are directly involved in cholesterol synthesis from mevalonate, and showed upregulation in replicative senescence.

Overexpression of enzymes involved in cholesterol biosynthesis was accompanied by an increased abundance of transcripts encoding cholesterol transporters. Both, NPC1 and NPC2, were overexpressed by 1.6 and 2.6 fold, respectively. The NPC proteins act in concert, catalysing cholesterol egress from the multivesicular environment of the late endosome or lysosome to the cytosol, and increasing the metabolically active pool of sterol. One of the main pathways for cholesterol efflux from a cell is via scavenger receptor class B type 1 (SCRAB1) (Thuahnai et al., 2001). SCRAB1 also demonstrated a 3.7 fold overexpression in the microarray screen. The other regulatory pathway for cellular cholesterol exchange occurs through ABCA1 transporters. In the microarray data for replicative senescence ABCA1 did not, however, demonstrate differential expression. Interestingly, SCRAB1 also regulates the selective uptake of lipoproteins. A number of apolipoprotein precursors (LPA, APOC2, APOD) were upregulated by at least 2.9 fold in senescent HDFs. Moreover, VLDR, a receptor for very low density lipoprotein, composed of triglycerides, cholesterol, and apolipoproteins, was also upregulated by 2 fold. These are changes associated with increased extracellular uptake. Since the same defined media were used consistently for early and late passage cells, it is therefore unlikely that the observed changes arose from medium composition. Thus they represent a response to intracellular signalling occurring in response to senescence.

Many of the transcriptional changes related to lipid metabolism, and to cholesterol synthesis in particular, can be linked to the coordinated action of PPARs (Peroxisome Proliferator-Activated Receptors) and SREBP (Sterol Regulatory Element Binding Protein). PPARA indeed demonstrated over a 2 fold increase in expression in late passage HDFs. This is in concordance with the seemingly higher activity of peroxisome related processes. However, RXRA, the binding partner of PPARA, required for heterodimerisation and transactivational activity, demonstrated underexpression by a 0.6 fold change, which could suggest activation of an inhibitory feedback loop.

Cholesterol is not only a component of cell membranes but also a precursor of all steroid hormones. It is therefore not surprising to see gene sets related to steroids significantly correlating with overexpressed genes in the GSEA (KEGG Steroid Hormone Biosynthesis, GO Steroid Metabolic Process). Four prominent identifiers in these sets were genes encoding aldo-keto reductase family 1 members (AKR1C1, AKR1C2, AKR1C3, AKR1C4). They demonstrated over a 3.7 fold expression increase when compared to young HDFs (Figure 4.15 B). They are involved in the synthesis of active androgens, oestrogens or progestins, but are also able to eliminate these hormones in a whole-cell context. Additionally, they contribute to the synthesis of bile acids (Penning et al., 2000). Another gene identified in this set is CYP3A4, overexpressed by 2.6 fold. It encodes cytochrome P450 3A4 protein, which is involved in the oxidation of a variety of substrates, including steroids and fatty acids. It has also been demonstrated that CYP3A4 can hydroxylate cholesterol to 4β-hydroxycholesterol which in turn is able to activate the nuclear receptor LXRα. LXRα is a very important

transcription factor involved in regulation of lipid metabolism and cholesterol homeostasis (Bodin et al., 2001; Janowski et al., 1996).

The GSEA method identified REACTOME Glycosphingolipid Metabolism pathway as correlating with overexpressed genes in replicative senescence. Increased levels of ceramide and elevated sphingomyelinase activity have been observed both in cellular senescence and in the organismal ageing process (Lightle et al., 2000; Venable et al., 2006). Sphingosine and ceramide are second messenger mediators that respond to stress and inflammation and can lead to cell cycle arrest or apoptosis (Futerman and Hannun, 2004). In late passage HDFs, an expression increase of 2.1 fold for the gene encoding neutral sphingomyelinase (SMPD3) was observed. This enzyme is responsible for the hydrolysis of sphingomyelin to form ceramide and phosphocholine. Furthermore, expression of lysosomal acidic ceramidase ASAH1 was also increased by 2.1 fold. ASAH1 enzyme hydrolyses ceramides to sphingosine. Moreover, PSAP encoding prosaposin, a highly conserved, non-enzymatic glycoprotein assisting in lysosomal degradation of sphingolipids by SMPD3, among others, was upregulated by almost a 2.6 fold change. Interestingly, prosaposin was also shown to protect primary astrocytes against oxidative stress via the equally important G-protein-coupled receptors, GPR37 and GPR37L1. These receptors, highly expressed in nervous system, upon PSAP binding, internalise and activate ERK phosphorylation signalling, promoting cell survival (Meyer et al., 2013). The microarray data showed upregulation of GPR37 (1.55 fold change) while GPR37L1 was downregulated (0.7 fold change) in late passage HDFs, possibly suggesting a differential feedback regulation of these receptors in replicative senescence.

4.2.3.5 Late passage HDFs showed enrichment in lysosome related genes

Cells undergoing replicative senescence have been shown to elevate lysosomal activity (Brunk et al., 1973; Robbins et al., 1970), presumably as a response to intracellular accumulation of damaged macromolecules with age. Furthermore, senescence associated β-galactosidase activity has been attributed to increased lysosomal activity (Kurz et al., 2000; Lee et al., 2006). The GSEA of transcriptional changes in late passage HDFs also identified the enrichment of genes belonging to KEGG Lysosome pathway. Altered expression of a number of lysosomal hydrolases (proteases, glycosidases, lipases, ceramidases) as well as overexpression of major (LAMP2) and minor components (NPC1, NPC2, MCOLN1, SLC17A5, CLN5, CTNS) of the lysosomal membrane was observed (Figure 4.16).

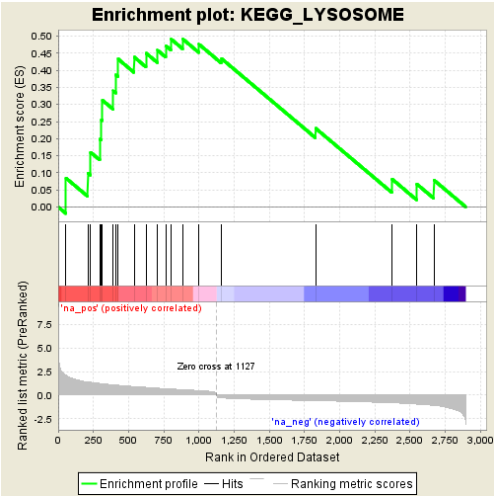

Figure 4.16. Expression of lysosome related genes in the late passage HDFs.

Top panel shows enrichment plot, while the table on the right lists hits from the preranked gene list present in the KEGG Lysosome pathway gene set. Core enrichment of the ES score is highlighted in green.

KEGG_Lysosome		
Gene Name	Log2 Fold Change	Running ES
CTSK	2.11	0.08
NPC2	1.40	0.10
PSAP	1.37	0.16
MCOLN1	1.25	0.20
TPP1	1.23	0.26
CTSD	1.21	0.31
ASAH1	1.10	0.34
LAMP2	1.08	0.39
SLC17A5	1.05	0.43
MANBA	0.92	0.44
GAA	0.83	0.45
NPC1	0.74	0.46
CLN5	0.68	0.47
FUCA1	0.65	0.49
CTNS	0.59	0.49
CTSO	0.50	0.48
CTSB	-0.28	0.43
NAGA	-0.57	0.23
ATP6V0A2	-0.81	0.08
CTSC	-0.95	0.07
LIPA	-1.09	0.08

4.2.4 Characterisation of transcriptome profile in cells acutely accumulating prelamin A as a result of saquinavir treatment

Global changes in gene expression after acute prelamin A accumulation upon saquinavir treatment (the SAQ/DMSO dataset) were compared with results obtained for replicative senescence in HDFs (the Late/Early dataset). 104 genes overlapped between these two datasets, with computed P-value for an overlap of this size or bigger based on the Fisher exact test equal to P = 2.6196e-58 (Figure 4.17 A). Pearson correlation coefficient equal to 0.49 was calculated for the overlap and suggests moderate positive correlation of observed expressional changes for the overlapping genes (Figure 4.17 B).

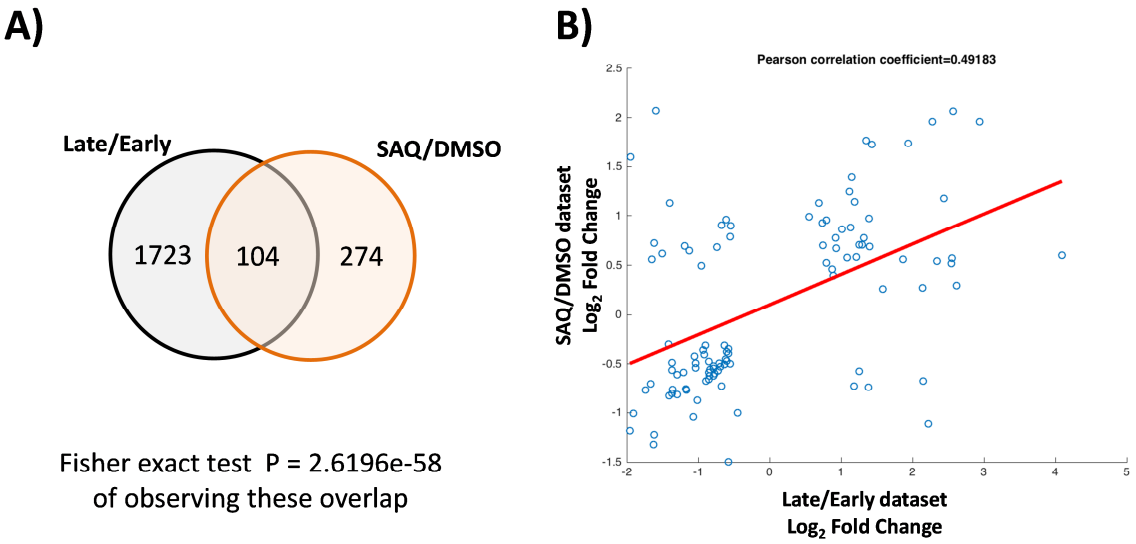

Figure 4.17. Comparison of the SAQ/DMSO and Late/Early datasets.

A) Venn diagram showing overlap between the SAQ/DMSO and Late/Early datasets. Fisher exact test for observing this overlap between these two sets was calculated out of 25,100 genes total represented on a microarray chip. **B)** Correlation between the overlapping genes from the two datasets. Data analysed in collaboration with Dr Margarita Schlackow.

4.2.4.1 Acute prelamin A accumulation induces expression of immune response genes

Analysis of gene expression by the GSEA method after prelamin A accumulation from the SAQ/DMSO comparison produced significant correlation of overexpressed genes with the immune response (Table 4.4). A number of gene sets from various databases particularly pointing towards the immune system and interferon signalling were enriched (Figure 4.18).

Interferons, in addition to their antiviral activity, also display immunoregulatory functions, and have been shown to play a role in the regulation of both replicative and stress-induced senescence (Kim et al., 2009; Moiseeva et al., 2006; Novakova et al., 2010; Yu et al., 2015). Genes identified in gene sets relating to the immune system

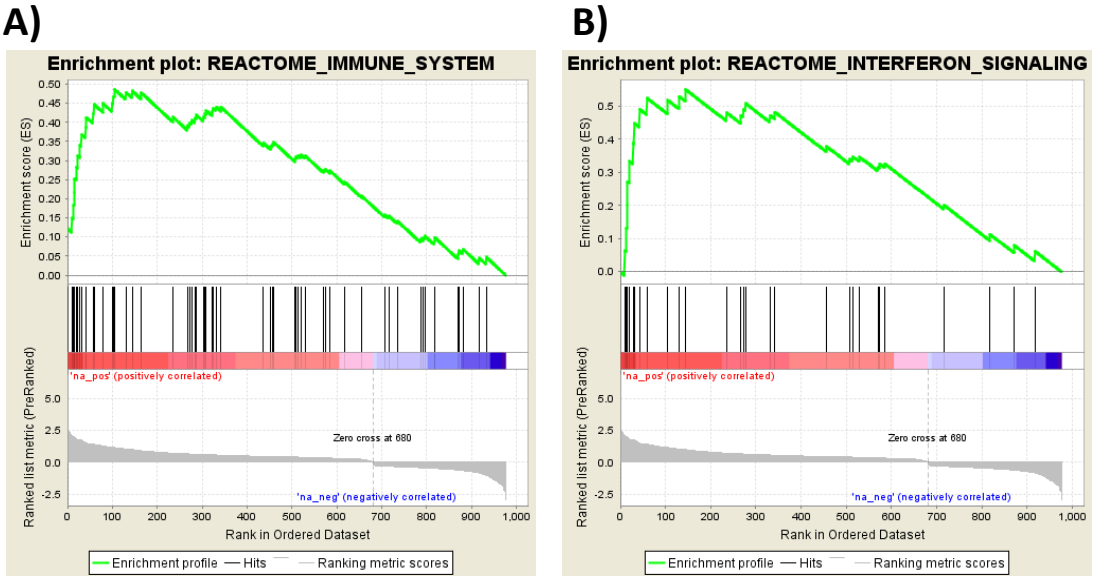

Figure 4.18. Examples of enrichment plots corresponding to immune response.

A) Reactome Immune System with 60 genes identified in the set, represented as vertical lines below the x axis of the enrichment plot. **B)** Reactome Interferon signalling with corresponding 29 genes identified in the set, represented as vertical lines below the x axis of the enrichment plot.

were combined and reanalysed in the ReactomeFIViz application, which again indicated both type I and II interferon signalling. Interestingly, RIG-I/MDA5 mediated induction of IFN-alpha/beta was also enriched. Key players in this pathway were overexpressed in cells accumulating prelamin A upon saquinavir inhibition of Zmpste24 (Figure 4.19). RIG-I is primarily responsible for the recognition of viral RNA in the infected cell and triggers the immune response by type I interferon induction (Yoneyama et al., 2004). It has also been suggested, however that it plays a role in the induction of inflammation and cytokine production in senescence (Liu et al., 2011).

Table 4.4. Gene sets correlating with genes overexpressed in HDFs exposed to saquinavir and acutely accumulating prelamin A. GSEA results showing Kyoto Encyclopedia of Genes and Genomes (KEGG), Reactome, Hallmark, and Gene Ontology (GO) pathways identified. For clarity, redundant sets were removed. Size, number of genes from the preranked gene list identified in the gene set; ES, enrichment score; NES, normalised enrichment score; NOM p-val, nominal p value; FDR q-val, false discovery rate q value.

GENE SET NAME	SIZE	ES	NES	NOM p-val	FDR q-val
KEGG_STEROID_BIOSYNTHESIS	6	0.80	1.82	0.00	0.06
KEGG_PPAR_SIGNALING_PATHWAY	10	0.62	1.68	0.03	0.17
KEGG_TERPENOID_BACKBONE_BIOSYNTHESIS	5	0.77	1.67	0.00	0.18
KEGG_CHEMOKINE_SIGNALING_PATHWAY	8	0.64	1.57	0.04	0.31
KEGG_BIOSYNTHESIS_OF_UNSATURATED_FATTY_ACIDS	5	0.70	1.52	0.04	0.38
REACTOME_INTERFERON_ALPHA_BETA_SIGNALING	19	0.67	2.16	0.00	0.01
REACTOME_IMMUNE_SYSTEM	60	0.49	2.01	0.00	0.01
REACTOME_INTERFERON_SIGNALING	29	0.55	1.99	0.00	0.02
REACTOME_CHOLESTEROL_BIOSYNTHESIS	10	0.72	1.92	0.01	0.03
REACTOME_METABOLISM_OF_LIPIDS_AND_ LIPOPROTEINS	43	0.48	1.89	0.00	0.03
REACTOME_CYTOKINE_SIGNALING_IN_IMMUNE_ SYSTEM	33	0.52	1.89	0.00	0.04
HALLMARK_CHOLESTEROL_HOMEOSTASIS	20	0.63	2.07	0.00	0.01
HALLMARK_mTORC1_SIGNALING	27	0.51	1.81	0.01	0.05
HALLMARK_PEROXISOME	7	0.74	1.76	0.01	0.06
HALLMARK_INTERFERON_ALPHA_RESPONSE	32	0.51	1.83	0.01	0.06
HALLMARK_ADIPOGENESIS	14	0.58	1.73	0.02	0.06
HALLMARK_INTERFERON_GAMMA_RESPONSE	41	0.43	1.67	0.02	0.09
HALLMARK_BILE_ACID_METABOLISM	10	0.59	1.60	0.04	0.11
HALLMARK_FATTY_ACID_METABOLISM	11	0.58	1.60	0.03	0.12

GO_LIPID_BIOSYNTHETIC_PROCESS	8	0.80	2.02	0.00	0.05
GO_NEGATIVE_REGULATION_OF_CATALYTIC_ACTIVITY	6	0.78	1.79	0.00	0.20
GO_REGULATION_OF_PROGRAMMED_CELL_DEATH	18	0.57	1.82	0.01	0.21
GO_BIOSYNTHETIC_PROCESS	27	0.48	1.67	0.02	0.24
GO_IMMUNE_RESPONSE	12	0.59	1.67	0.03	0.27
GO_STEROID_METABOLIC_PROCESS	6	0.73	1.67	0.02	0.29
GO_ANTI_APOPTOSIS	5	0.79	1.69	0.01	0.32
GO_LIPID_METABOLIC_PROCESS	28	0.45	1.56	0.04	0.38

The RIG-I/MDA5 signalling is initiated by the action of three key RIG-I-like receptors, RIG-I (DDX58), MDA5 (IFIH1) and LGP2 (DHX58). In the microarray data for HDFs acutely accumulating prelamin A were upregulated in each by a 2.2, 1.85 and 1.7 fold change, respectively (Figure 4.19). The signal from activated RIG-I-like receptor is transduced by binding to the mitochondria antiviral signalling protein IPS1 (MAVS), which demonstrated overexpression by 1.5 fold in saquinavir treated cells. Downstream signalling occurs via action of IKK-related kinases, TBK1 and IKBKE, which phosphorylate interferon regulatory factors IRF3 and IRF7 (overexpressed by 1.35 fold). This then leads to the transcriptional activation of interferons α and β. Also, a number of auxiliary proteins that contribute to the RIG-I signalling pathway showed overexpression. TRIM25, which mediates ubiquitination of DDX58, and is crucial for activation of the receptor, was upregulated by 1.5 fold. ISG15, modulating the DDX58 activation, stabilisation of IRF3, and mediating interferon γ induction, was upregulated by 3.3 fold. ZBP1, involved in the recruitment of TBK1 and IRF3 to its C-terminal region, followed by activation of type I interferon and NF-kB transcription factors, was upregulated by 1.3 fold. MAPK14 (p38) is a protein kinase involved in multiple cellular processes in response to proinflammatory stimuli. It is also implicated in the transcription of IL6 via phosphorylation of histone H3 and increasing the accessibility of NF-κB transcription factor. MAPK14 (p38) was overexpressed by 2.2 fold. The

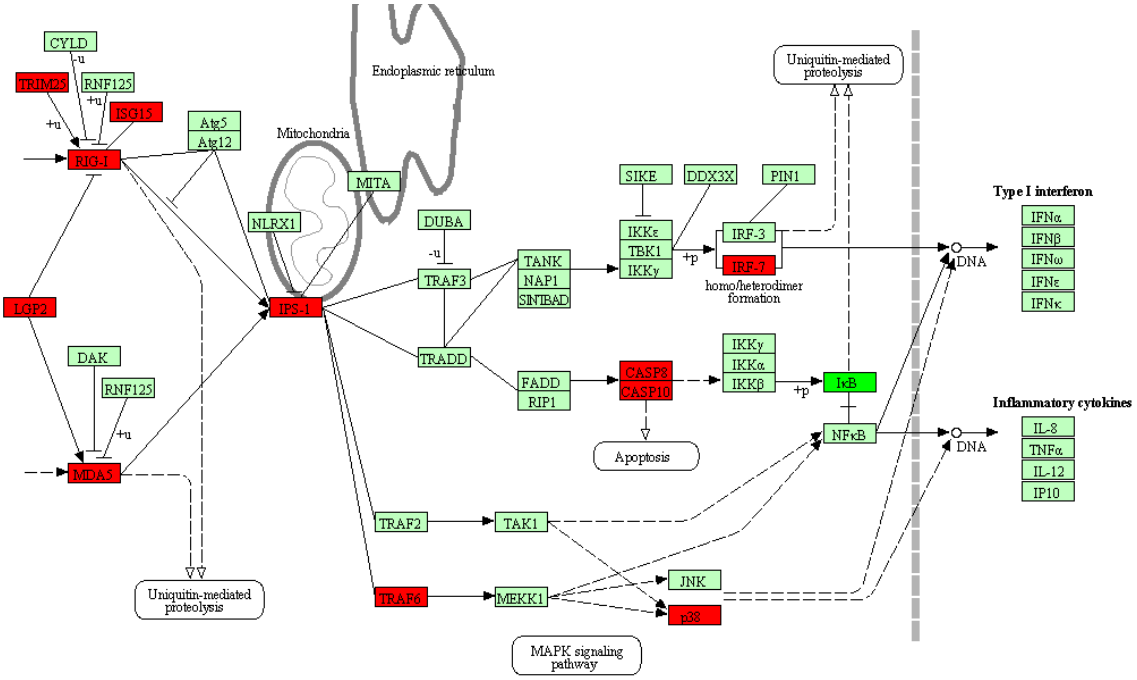

Figure 4.19. Diagram representing KEGG RIG-I-like receptor signalling pathway.

Genes identified as being overexpressed upon prelamin A accumulation in saquinavir treated HDFs are highlighted in red, while the underexpressed IκB (NFKBIB) is highlighted in bright green (schematic derived from KEGG website).

MAPK14 activator, TRAF6, was upregulated by 1.5 fold. While NFKBIB (IκB) that has been shown to complex with NF-κB and inhibit its transcriptional activity by trapping it in the cytoplasm, was underexpressed by a 0.8 fold change. This is consistent with increased cytokine production.

4.2.4.2 Lipid metabolism is altered after acute prelamin A accumulation

Acute prelamin A accumulation upon saquinavir treatment leads to significant changes in metabolism of lipids and lipoproteins (Table 4.4). The GSEA identified a number of gene sets from various data bases that correspond to lipometabolism and correlate with genes overexpressed in saquinavir treated cells (Figure 4.20).

Transcriptome analysis suggests that acute prelamin A accumulation leads to increased fatty acid biosynthesis. Genes like fatty acid synthase (FASN), a key enzyme responsible for long-chain fatty acid formation from acetyl CoA, malonyl-Coa, and

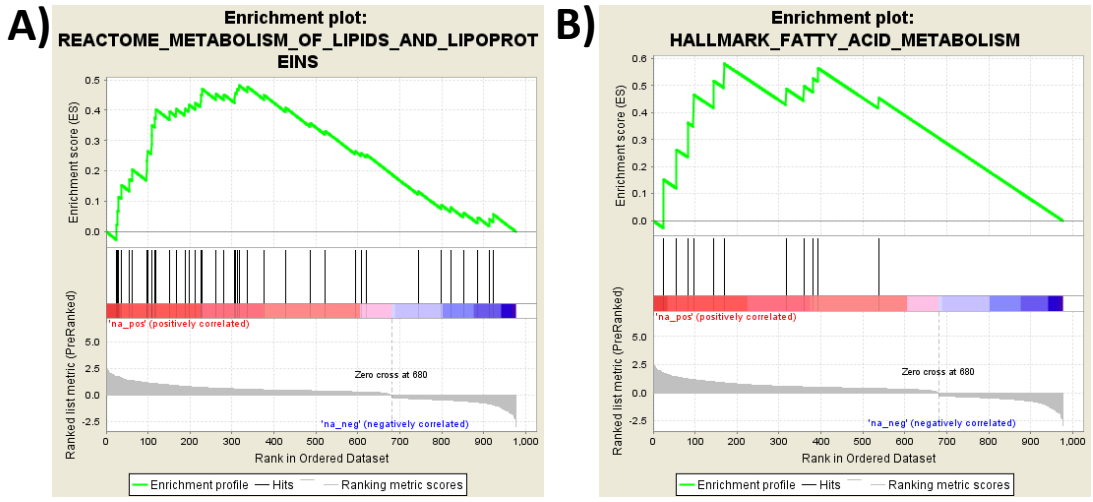

Figure 4.20. Examples of enrichment plots for the GSEA of the SAQ/DMSO preranked gene list.

A) Reactome Metabolism of Lipids and Lipoproteins with 43 genes identified as hits. **B)** Hallmark Fatty Acid Metabolism with 11 genes identified in this gene set.

NADPH, was overexpressed by 3.3 fold in saquinavir treated HDFs. Also, HSD17B12, whose product is involved in catalysing long chain fatty acid elongation, was upregulated by a 1.6 fold change. Furthermore, ME1 encoding malic enzyme 1, which generates NADPH required for fatty acid biosynthesis was upregulated by 1.5 fold. Interestingly, acyl-CoA thioesterases ACOT1 and ACOT7, which catalyse the hydrolysis of acyl-CoAs to free fatty acids and coenzyme A, were also moderately overexpressed by a 1.2 and 1.3 fold change, respectively. One of the enriched gene sets in the GSEA was KEGG Biosynthesis of Unsaturated Fatty Acids. It contained genes like FADS2 (upregulated by 3.3 fold) and SCD (upregulated by 3.6 fold) whose products can introduce double bonds between carbons in the fatty acyl chains. Conversely, ELOVL7, encoding fatty acid elongase which participates in the key step in synthesis of saturated and polyunsaturated very long chain fatty acids (with over 22 carbons in the aliphatic tail) was underexpressed by a 0.6 fold change.

Increased fatty acids availability is consistent with activation of the PPAR signalling pathway, which upon acute prelamin A accumulation, had also been

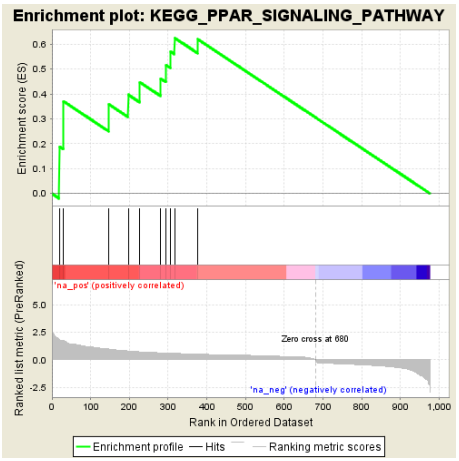

Gene Name	Log_2 Fold Change	Running ES
SCD	1.87	0.19
FADS2	1.73	0.37
FABP3	0.97	0.36
GK	0.80	0.40
MMP1	0.72	0.45
ACSL3	0.62	0.46
DBI	0.61	0.52
CPT1B	0.59	0.57
ME1	0.58	0.62
PPARG	0.50	0.62

Figure 4.21. Expression of genes related to PPAR signalling pathway in cells accumulating prelamin A.

Left panel shows enrichment plot, while the table on the right lists hits from the preranked SAQ/DMSO gene list present in the KEGG PPAR signaling pathway gene set. Core enrichment of the ES score is highlighted in green.

identified by the GSEA as being enriched with overexpressed genes (Figure 4.21). PPARG, encoding a potent transcriptional activator, showed overexpression by 1.4 fold. A number of its target genes were also upregulated. In addition to ME1, SCD, and FADS2 (mentioned above), FABP3 was also upregulated by 2 fold. FABP3 encodes a fatty acid-binding protein that is thought to play a role in the uptake of long-chain fatty acids which further stimulates PPARG activity (Desvergne and Wahli, 1999).

Increased lipid synthesis could explain the higher rates of fatty acid oxidation. This conclusion may be based on the upregulated expression levels of enzymes involved in β-oxidation, like CPT1B (overexpressed by 1.5 fold), ACSL3 (overexpressed by 1.5 fold) or ACAT2 (overexpressed by 1.8 fold). CPT1B, regulated by PPARG, encodes a protein belonging to carnitine/choline acetyltransferase family which is essential for the transport of long-chain fatty acyl-CoA to mitochondria for oxidation. It is believed to be the rate controlling enzyme in this process (Rinaldo et al., 2002).

The GSEA of the transcriptional changes upon acute prelamin A accumulation showed that cholesterol homeostasis is also strongly affected, with the indication of

increased cholesterol biosynthesis (Figure 4.22). Expression of HMGCR, HMG-CoA reductase that catalyses synthesis of mevalonic acid and is the rate limiting step in cholesterol biosynthesis, was increased by 1.6 fold. Furthermore, expression of IDI1, FDPS2, and MVD, which is involved in the terpenoid backbone synthesis, was also upregulated in cells accumulating prelamin A. Similarly, other genes encoding enzymes from the cholesterol biosynthesis pathway showed overexpression. DHCR24, responsible for the final reduction of desmosterol to cholesterol, was upregulated by 2.6 fold when compared to its expression level in DMSO treated cells. Also a number of genes involved in sterol transport and regulation of intracellular cholesterol levels were upregulated. For example STARD4, encoding StAR-Related Lipid Transfer (START) Domain Containing protein which may participate in cholesterol binding and lipid transport, was upregulated by 1.2 fold. Furthermore, transmembrane protein 97-coding gene TMEM97, whose product is a conserved protein engaged in controlling cellular cholesterol levels, was overexpressed by 1.5 fold.

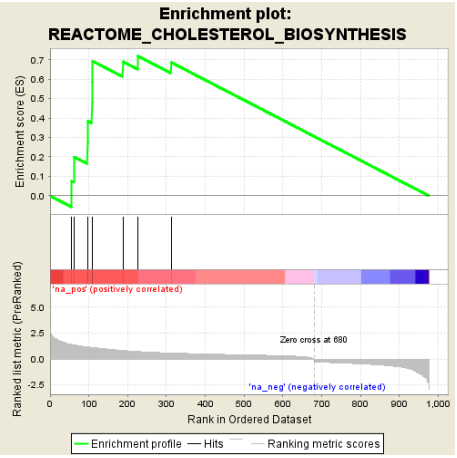

Gene Name	Log_s Fold Change	Running ES
DHCR24	1.41	0.07
FDFT1	1.38	0.20
IDI1	1.16	0.27
FDPS	1.16	0.38
LSS	1.13	0.48
DHCR7	1.13	0.59
SQLE	1.13	0.69
MVD	0.81	0.69
HMGCR	0.72	0.72
SC5DL	0.58	0.69

Figure 4.22. Expression of genes related to cholesterol biosynthesis in cells acutely accumulating prelamin A.

Left panel shows enrichment plot, while the table on the right lists hits from the preranked SAQ/DMSO gene list present in the Reactome Cholesterol Biosynthesis gene set. Core enrichment of the ES score is highlighted in green.

Expression of genes mediating cholesterol biosynthesis is mainly regulated by SREBPs, and indeed, SREBF1 (also known as SREBP1) showed overexpression by 2.1 fold. This may account for the increased expression of genes in this pathway, as well as changes in lipometabolism in general, because SREBP can regulate expression of fatty acid synthase (FASN). FASN was also strongly upregulated. Interestingly, INSIG1 showed overexpression in saquinavir treated cells (by 2 fold). Product of this gene can negatively regulate the activity of SREBP by mediating retention of SREBP in its inactive form in a complex with SCAP in the endoplasmic reticulum. Furthermore, INSIG1 can also mediate degradation of HMGCoA reductase (HMGCR), thus limiting mevalonic acid synthesis, a first committed step in cholesterol biosynthesis. Overexpression of INSIG1 could indicate activation of a negative control loop in response to increased cholesterol levels.

Differential expression of genes involved in cholesterol biosynthesis was the main contributor to the enrichment of pathways related to steroid metabolism in the GSEA method. However, genes like HSD3B7 (upregulated by 3.3 fold) or AKR1C1 and AKR1C2 (both upregulated by 1.4 fold) involved in the biosynthesis of hormonal steroids from cholesterol, were also identified. They have also been shown to be involved in bile acid synthesis. Bile acids are the end products of cholesterol catabolism, but are also recognised as signalling molecules contributing to energy homeostasis (Chiang, 2013).

Cells accumulating prelamin A upon saquinavir treatment moderately upregulated (1.2 to 1.3 fold change) a several genes involved in the detoxification of reactive oxygen species. They included peroxiredoxin (PRDX5), peroxisomal catalase

(CAT), disulfide isomerases (P4HB), and heme oxygenase (HMOX1) possibly indicating increased oxidative stress.

Activation of SREBP and the increased expression of its targets could be further linked to the mTORC1 signalling pathway. The mTORC1 signalling pathway was identified in the GSEA as being enriched in genes overexpressed after acute prelamin A accumulation (Hallmark mTORC1 Signaling). mTORC1 integrates inputs from growth factors, oxygen, energy status, stress, and nutrients. As a response to these inputs, it regulates cellular processes like growth, proliferation, and metabolism. It has been shown to regulate SREBP activity at multiple levels (Bakan and Laplante, 2012), and also play a role in longevity.

4.2.4.3 *The GSEA of underexpressed genes in saquinavir treated cells*

The preranked SAQ/DMSO list of genes differentially expressed in cells acutely accumulating prelamin A after saquinavir treatment included 978 entries. Only 297 genes, however, demonstrated underexpression. They did not show enrichment of any gene set when analysed by the GSEA method with a cut off of $q < 0.25$ for false discovery rate. Thus, the criteria limits were relaxed, and nominal p-value cut off of 0.1 was applied. Gene sets showing correlation with downregulated genes from the SAQ/DMSO preranked list are shown in Table 4.5.

Table 4.5. Gene sets correlating with genes underexpressed in HDFs exposed to saquinavir and acutely accumulating prelamin A. GSEA results showing Kyoto Encyclopedia of Genes and Genomes (KEGG), Reactome, Hallmark, and Gene Ontology (GO) pathways identified. For clarity, redundant sets were removed. Note: no gene set was identified at 0.25 FDR q-value cut off, hence the sets listed in the table were selected based on the nominal p-value < 0.1. Size, number of genes from the preranked gene list identified in the gene set; ES, enrichment score; NES, normalised enrichment score; NOM p-val, nominal p value; FDR q-val, false discovery rate q value.

NAME	SIZE	ES	NES	NOM p-val	FDR q-val
KEGG_VASCULAR_SMOOTH_MUSCLE_CONTRACTION	9	-0.53	-1.60	0.05	0.68
REACTOME_SMOOTH_MUSCLE_CONTRACTION	5	-0.69	-1.69	0.02	0.56
REACTOME_TRANSCRIPTION	7	-0.64	-1.74	0.02	0.52
REACTOME_TRANSPORT_OF_GLUCOSE_AND_OTHER_SUGARS_BILE_SALTS_AND_ORGANIC_ACIDS_METAL_IONS_AND_AMINE_COMPOUNDS	6	-0.58	-1.48	0.08	0.66
GO_TRANSMEMBRANE_TRANSPORTER_ACTIVITY	22	-0.37	-1.59	0.02	0.63
GO_SYSTEM_DEVELOPMENT	40	-0.30	-1.48	0.03	0.51
GO_ION_TRANSPORT	11	-0.48	-1.56	0.05	0.66
GO_TRANSPORT	45	-0.26	-1.30	0.09	0.60
GO_CELL_JUNCTION	8	-0.50	-1.45	0.09	0.52
GO_GTPASE_REGULATOR_ACTIVITY	7	-0.52	-1.44	0.10	0.50

Vascular smooth muscle contraction was one of the highest scoring gene sets, with genes like MYL9 (myosin light chain), TPM1 (tropomyosin), ACTA2 (actin alpha) and ACTG2 (actin gamma) demonstrating downregulation. Originally, products of these genes were shown to be involved in the contractile system of smooth muscles, but they are also components of the cytoskeleton in other cell types, playing a role in cell adhesion to the extracellular matrix and to each other. LASP1, which plays a role in the regulation of dynamic actin-related cytoskeletal activities, was also downregulated. Interestingly, cardiovascular problems are common in HGPS patients (Olive et al., 2010), and prelamin A has been demonstrated to accumulate in vascular smooth muscles in the normal ageing process (Ragnauth et al., 2010).

Transcription also appears to be moderately affected by acute prelamin A accumulation, with downregulation of genes like GTF2E2 (General Transcription Factor TFIIE-beta) or NFIB (Nuclear Factor I/B). TFIIE, in concert with TFIIH, is essential for

promoter clearance by RNA polymerase. NFIB has been shown to repress transcription of p21, a cycling kinase inhibitor activated in senescence, by interaction with the p21 proximal promoter (Ouellet et al., 2006). Several other genes encoding proteins responsible for maintaining chromosomes and needed for DNA replication, like HIST1H2B clusters or PCNA, were also identified as being underexpressed. PCNA is also important for DNA repair via the DNA damage response (DDR). A few other genes involved in DNA repair, like FANCM or XRCC1, also showed underexpression after prelamin A accumulation. This could suggest that DNA repair mechanisms are impaired in these cells.

Downregulation was identified in several genes encoding proteins responsible for cell junction formation. Examples include: CLDN11 and WNK4, which are involved in forming tight junctions, or GJB2, which is involved in gap junction formation. Furthermore ZYX, encoding adhesion plaque protein was also downregulated by a 0.8 fold change in expression. Products of these genes can also contribute to ion transport. The GO Transport category appeared to correlate with underexpressed genes. It encompasses a number of genes, however, both up and downregulated in cells accumulating prelamin A (Figure 4.23).

An interesting group is constituted by genes encoding proteins with GTPase regulatory activity. It consists of a few Regulators of G-protein Signaling (RGS4, RGS12 and RGS20), among others. They play a role in the inhibition of signal transduction through G proteins by driving them into their inactive GDP-bound state. All were underexpressed upon acute prelamin A accumulation by over 0.65 fold change. ARHGAP29, responsible for conversion of Rho-type GTPases into an inactive

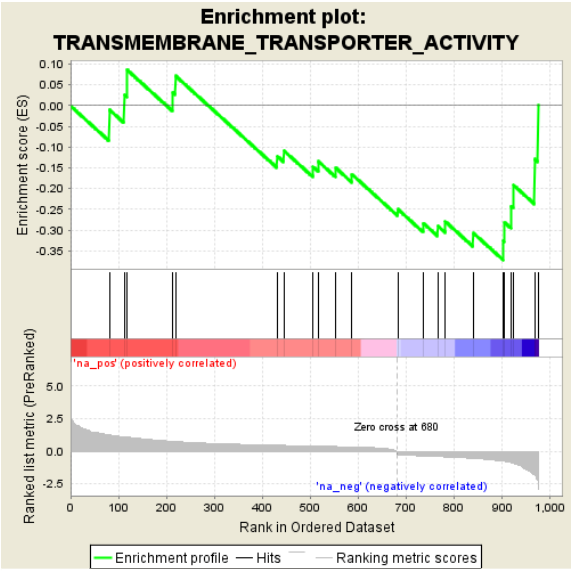

Figure 4.23. Expression of Transmembrane transporter activity related genes in the saquinavir treated HDFs.

Top panel shows enrichment plot, while the table on the right lists hits from the preranked gene list present in the GO Transmembrane transporter activity gene set. Core enrichment of the ES score is highlighted in green.

Gene Name	Log_2 Fold Change	Running ES
KCNA2	1.25	-0.01
CACNA1G	1.12	0.03
CLCNKB	1.09	0.09
SLCO1B3	0.75	0.03
SLC1A1	0.74	0.07
ATP6V1B2	0.46	-0.12
ATP4A	0.45	-0.11
SLC1A4	0.40	-0.15
SLC7A11	0.39	-0.13
AQP6	0.36	-0.15
STEAP1	0.31	-0.17
COX10	-0.25	-0.25
KCNMB1	-0.35	-0.28
ATP2A2	-0.40	-0.29
LASP1	-0.43	-0.28
ATP2B1	-0.54	-0.31
SLC2A8	-0.76	-0.33
SLC2A5	-0.77	-0.28
ATP1B2	-0.87	-0.24
SLC7A9	-0.92	-0.19
SCN7A	-1.80	-0.13
NMUR2	-2.28	0.00

GDP-bound form was also downregulated by 0.67 fold change. Conversely, RGS3 showed overexpression by almost 2 fold.

4.2.5 Characterisation of transcriptome profile of cells with Zmpste24 knock-down

The preranked siZmspte24/siCTRL gene list included 1464 entries of genes differentially expressed upon Zmpste24 knock-down, with an almost equal number of genes being over- and underexpressed. Zmpste24 mRNA itself was lowered by a 0.09 fold change (-3.4 Log_2 fold change) at $P < 0.09E^{-10}$ in knocked-down cells. However, the GSEA method did not identify any gene sets that would correlate with either down- or upregulated genes at the FDR cut off of $Q < 0.25$. The criteria was

therefore relaxed, and nominal P value cut off < 0.1 was applied. Identified gene sets are listed in Table 4.6 and Table 4.7 for overexpressed and underexpressed genes, respectively. It should be noted though that FDR for many sets reported for this analysis was equal to 1.

Table 4.6. Gene sets correlating with genes overexpressed after Zmpste24 siRNA knock-down in HDFs. GSEA results showing Kyoto Encyclopedia of Genes and Genomes (KEGG), and Gene Ontology (GO) pathways identified. No enrichment in Reactome or Hallmark pathways was found. For clarity, redundant sets were removed. Size, number of genes from the preranked gene list identified in the gene set; ES, enrichment score; NES, normalised enrichment score; NOM p-val, nominal p value; FDR q-val, false discovery rate q value.

GENE SET NAME	SIZE	ES	NES	NOM p-val	FDR q-val
KEGG_VEGF_SIGNALING_PATHWAY	7	0.61	1.60	0.05	1
GO_PROTEIN_SERINE_THREONINE_KINASE_ACTIVITY	17	0.45	1.60	0.05	1
GO_CYTOSKELETON	24	0.36	1.45	0.07	1

4.2.5.1 Cellular processes correlating with overexpressed genes in Zmpste24 knock-down model

Cytoskeleton was one of the categories correlating with overexpressed genes in the Zmpste24 knock-down model, with the majority of differentially expressed genes related to the actin cytoskeleton (Figure 4.24). Indeed, several genes encoding proteins either interacting or modulating the actin cytoskeleton were overexpressed. These included, for example: actin gamma (ACTG1), tropomyosins (TRPM1, 2 and 4) involved in stabilizing cytoskeleton actin filaments, VASP participating in actin filament elongation and cytoskeleton rearrangement, FLNB playing a role in linking actin filament to membrane glycoproteins, or ABRA encoding actin-binding Rho activating

protein. Also a few genes encoding microtubule associated proteins, like centrin (CETN3) or MAP1B, showed overexpression.

Another enriched category was KEGG VEGF Signaling (Figure 4.25). The genes identified in this set have a broad activity and are involved in a diverse array of cellular events, including cell proliferation and cytoskeleton reorganisation. Interestingly, overexpression of PPP3CB, which encodes calcium dependent protein phosphatase, can be linked to upregulation of PTGS2. PTGS2 encodes inducible prostaglandin-endoperoxide synthase (cyclooxygenase 2) which is the key enzyme (together with PTGS1) in prostaglandin biosynthesis. Prostaglandin biosynthesis can contribute to inflammation, a phenotype linked to senescence. Furthermore, overexpressed MAPK1 may stimulate phospholipase PLA2G10 (also overexpressed). This in turn, can lead to the liberation of arachidonic acid from the membrane and provide an essential substrate for PTGS2-mediated oxidation leading to prostaglandin synthesis.

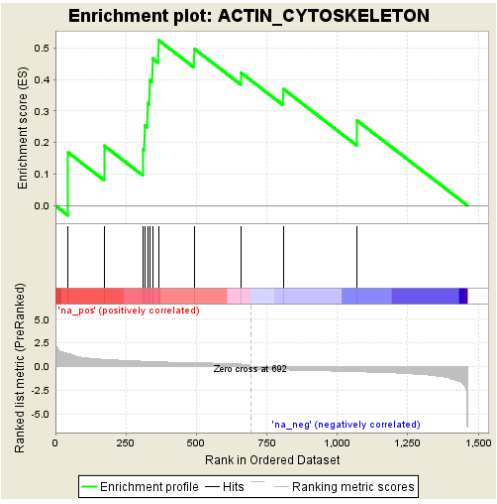

Gene Name	Log_2 Fold Change	Running ES
TPM4	1.38	0.17
ABRA	0.75	0.19
PKD2	0.56	0.18
FLNB	0.55	0.25
TPM1	0.54	0.33
TNNI3	0.53	0.40
VASP	0.52	0.47
MYO18B	0.50	0.53
FYB	0.41	0.50
TPM2	0.26	0.42
MYH10	-0.35	0.37
BIN1	-0.55	0.27

Figure 4.24. Expression of genes related to GO Actin cytoskeleton category in cells accumulating prelamin A as a result of Zmpste24 knock-down.

Left panel shows enrichment plot, while the table on the right lists hits from the preranked siZmpste24/siCTRL gene list present in the GO Actin Cytoskeleton gene set. Core enrichment of the ES score is highlighted in green.

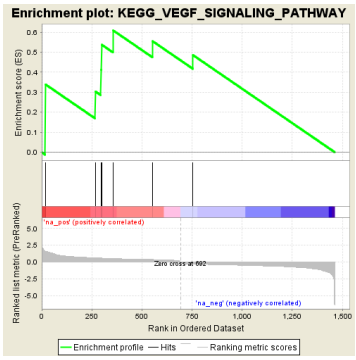

Gene Name	Log_2 Fold Change	Running ES
PTGS2	1.61	0.34
PPP3CB	0.62	0.30
KRAS	0.58	0.41
RAC1	0.58	0.54
MAPK1	0.50	0.61
PLA2G10	0.37	0.56
PRKCA	-0.31	0.49

Figure 4.25. Expression of genes related to VEGF signalling pathway in cells accumulating prelamin A as a result of Zmpste24 knock-down.

Left panel shows enrichment plot, while the table on the right lists hits from the preranked siZmpste24/siCTRL gene list present in the KEGG VEGF signaling pathway gene set. Core enrichment of the ES score is highlighted in green.

4.2.5.2 Cellular processes correlating with underexpressed genes in Zmpste24 knock-down model

Cells with Zmpste24 knock-down exhibited reduced expression of several growth factors as well as underexpression of positive regulators of cell proliferation. Furthermore, microarray analysis of gene expression changes in these cells suggested impairment in the translation process, with several factors of translational machinery downregulated. These included translation factors (EEF1A1, ETF1), ribosomal proteins (RPL22, MRPS24), and cofactors binding to poly-A tails and mediating translation and mRNA metabolism (PABPC4, PAIP1). Interestingly, ERN2 kinase, which can mediate translational repression in response to ER stress was upregulated by 1.7.

Table 4.7. Gene sets correlating with genes underexpressed after Zmpste24 siRNA knock-down in HDFs. GSEA results showing Kyoto Encyclopedia of Genes and Genomes (KEGG), Reactome, and Gene Ontology (GO) pathways identified. No enrichment in Hallmark pathways was found at P < 0.1 cut off. For clarity, redundant sets were removed. Size, number of genes from the preranked gene list identified in the gene set; ES, enrichment score; NES, normalised enrichment score; NOM p-val, nominal p value; FDR q-val, false discovery rate q value.

GENE SET NAME	SIZE	ES	NES	NOM p-val	FDR q-val
KEGG_LYSOSOME	11	-0.46	-1.38	0.10	0.93
REACTOME_TRANSPORT_OF_INORGANIC_CATIONS_ ANIONS_AND_AMINO_ACIDS_OLIGOPEPTIDES	5	-0.72	-1.64	0.04	1.00
REACTOME_INTERFERON_GAMMA_SIGNALING	5	-0.67	-1.57	0.04	1.00
REACTOME_INTEGRIN_CELL_SURFACE_INTERACTIONS	6	-0.62	-1.53	0.05	0.92
REACTOME_POST_TRANSLATIONAL_PROTEIN_MODIFICATION	16	-0.44	-1.49	0.07	0.93
REACTOME_MEMBRANE_TRAFFICKING	6	-0.59	-1.44	0.08	0.96
GO_METALLOPEPTIDASE_ACTIVITY	5	-0.79	-1.79	0.01	1.00
GO_KINASE_BINDING	6	-0.71	-1.78	0.01	0.84
GO_CYTOKINE_ACTIVITY	11	-0.56	-1.69	0.02	0.63
GO_RECEPTOR_BINDING	41	-0.38	-1.62	0.02	0.90
GO_RECEPTOR_ACTIVITY	35	-0.38	-1.58	0.03	0.96
GO_ACTIVE_TRANSMEMBRANE_TRANSPORTER_ACTIVITY	11	-0.57	-1.71	0.03	0.82
GO_CELL_CELL_SIGNALING	32	-0.42	-1.73	0.03	0.82
GO_TRANSLATION	14	-0.53	-1.70	0.03	0.75
GO_PROTEOLYSIS	23	-0.42	-1.59	0.05	0.98
GO_GROWTH_FACTOR_ACTIVITY	9	-0.55	-1.56	0.07	0.93
GO_REGULATION_OF_CELL_PROLIFERATION	28	-0.38	-1.53	0.07	0.93
GO_REGULATION_OF_CELLULAR_COMPONENT_ORGANIZATION_ AND_BIOGENESIS	12	-0.47	-1.46	0.10	0.94
GO_NUCLEAR_ENVELOPE_ENDOPLASMIC_RETICULUM_NETWORK	7	-0.58	-1.48	0.10	0.94
GO_DNA_REPLICATION	7	-0.54	-1.42	0.11	0.95

Conversely, translation initiation factor EIF4A2 and ribosomal protein RPL39 showed overexpression. A number of genes encoding enzymes responsible for posttranslational modification, especially linked to asparagine N-linked glycosylation, were also underexpressed.

Proteolysis was also identified by the GSEA as a process correlating with underexpressed genes in Zmpste24 knock-down (Figure 4.26). A number of metallopeptidases like MME, MMP2, CPZ or ADAM10 showed underexpression,

whereas MMP1 and MMP23 were overexpressed. A similar situation was observed in a few ubiquitin-conjugating enzymes, with some being upregulated and others downregulated. Lowered expression of genes encoding proteolytic enzymes was accompanied by a decline in lysosomal cathepsin-coding genes, as well as a reduced expression of minor lysosomal membrane proteins.

Transmembrane transport appeared to be affected by lowered expression of several members of solute carrier families (SLC1A1, SLC3A2, SLC7A11, SLC7A5, SLC8A1), as well as membrane trafficking regulators like ADP-ribosylation factor 1 (ARF1), adaptor-related protein complex subunits (AP1M1, AP3B1), synataxin 4 (STX4), coatomer protein complex (COPB2) and clathrin (CLTB). These all assist in protein

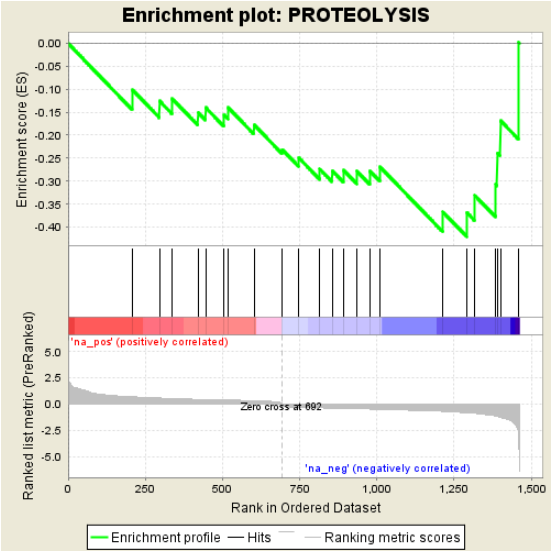

Figure 4.26. Expression of genes related to GO Proteolysis category in cells accumulating prelamin A as a result of Zmpste24 knock-down.

Top panel shows enrichment plot, while the table on the right lists hits from the preranked siZmpste24/siCTRL gene list present in the GO Proteolysis gene set. Core enrichment of the ES score is highlighted in green.

Gene Name	Log_2 Fold Change	Running ES
MMP1	0.70	-0.10
CASP3	0.58	-0.13
UBE3A	0.53	-0.12
MMP7	0.45	-0.15
UBE2D1	0.44	-0.14
UBE2G1	0.40	-0.16
MBTPS1	0.39	-0.14
MMP23B	0.33	-0.18
TIMP1	-0.14	-0.23
CTSB	-0.30	-0.25
RCE1	-0.36	-0.27
CTSO	-0.39	-0.28
RNF11	-0.41	-0.28
PSMC5	-0.44	-0.28
SYVN1	-0.47	-0.28
UBE2B	-0.50	-0.27
CPZ	-0.69	-0.37
PLAU	-0.84	-0.37
MME	-0.88	-0.33
MMP2	-1.14	-0.31
PLAT	-1.16	-0.24
ADAM10	-1.24	-0.17
ZMPSTE24	-3.42	0.00

trafficking between different compartments.

Interestingly, in contrast to other two ageing models, interferon signalling was identified to correlate with underexpressed genes in Zmpste24 knock-down cells. Genes playing a major role in interferon signal transduction, like STAT1, STAT2, ISG15 and IFIT3, were underexpressed. Furthermore, a number of cytokines also showed lower expression in siZmpste24 knock-down cells (Figure 4.27).

In Reactom FIVis software (Cytoskape platform), extracellular matrix organisation was identified as being the most significantly affected, with elastic fibre formation potentially impaired. This was judged by the underexpression of several key players in that process (GDF5, FBLN1, FBLN2, MFAB2, MFAB3 and LTBP3). Conversely, a few other genes, like elastin (ELN), TGFB1 or LTBP1, whose products are involved in this process, showed moderate overexpression.

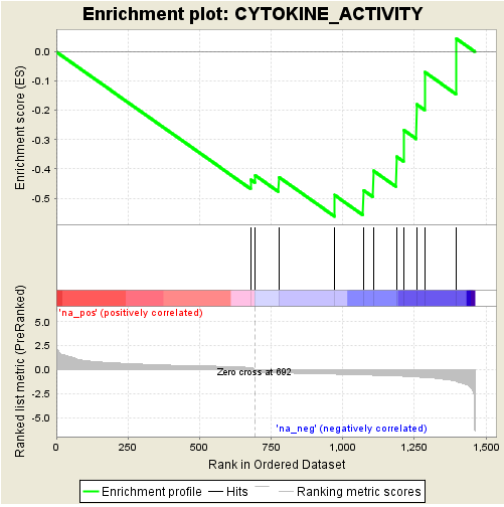

Gene Name	Log_2 Fold Change	Running ES
CCL13	0.20	-0.44
CXCL9	-0.16	-0.42
CDK5	-0.33	-0.43
CCL2	-0.47	-0.49
CSF1	-0.55	-0.47
GLMN	-0.58	-0.41
CXCL12	-0.67	-0.36
CCL7	-0.69	-0.27
GDF15	-0.76	-0.18
IL1RN	-0.83	-0.07
TNFRSF11B	-1.22	0.04

Figure 4.27. Expression of cytokine-coding genes in cells accumulating prelamin A as a result of Zmpste24 knock-down.

Left panel shows enrichment plot, while the table on the right lists hits from the preranked siZmpste24/siCTRL gene list present in the GO cytokine activity gene set. Core enrichment of the ES score is highlighted in green.

4.2.6 Similarities in transcriptional changes between ageing models

The GSEA method produced a number of gene sets from four databases (KEGG, Reactome, Hallmark, and Gene Ontology) enriched with differentially expressed genes for each ageing model. A nominal P value cut off of 0.1 was applied and gene sets overlapping between the models were identified. Not a single gene set overlapped all three studied ageing models. Replicative senescence and senescence induced by acute prelamin A after saquinavir treatment however, resulted in a number of gene sets being enriched with overexpressed genes in these two types of senescence (Table 4.8).

Table 4.8. Gene sets enriched in overexpressed genes in the ageing models. Gene sets enriched at FDR q value below 0.25 are highlighted in red.

GENE SET NAME	Late/Early			Saquinavir/DMSO		
	SIZE	NOM p-val	FDR q-val	SIZE	NOM p-val	FDR q-val
HALLMARK_BILE_ACID_METABOLISM	14	0.10	0.34	10	0.04	0.11
HALLMARK_INTERFERON_ALPHA_RESPONSE	22	0.00	0.00	32	0.01	0.06
HALLMARK_INTERFERON_GAMMA_RESPONSE	36	0.00	0.00	41	0.02	0.09
REACTOME_CLASS_A1_RHODOPSIN_LIKE_ RECEPTORS	28	0.00	0.13	9	0.08	0.43
REACTOME_CYTOKINE_SIGNALING_IN_IMMUNE_ SYSTEM	45	0.00	0.09	33	0.00	0.04
REACTOME_INNATE_IMMUNE_SYSTEM	38	0.00	0.12	24	0.01	0.12
REACTOME_INTERFERON_ALPHA_BETA_SIGNALING	12	0.01	0.07	19	0.00	0.01
REACTOME_INTERFERON_SIGNALING	29	0.00	0.10	29	0.00	0.02
REACTOME_METABOLISM_OF_LIPIDS_AND_ LIPOPROTEINS	55	0.07	0.38	43	0.00	0.03
GO_LIPID_METABOLIC_PROCESS	48	0.00	0.03	28	0.04	0.38
GO_CELLULAR_LIPID_METABOLIC_PROCESS	34	0.00	0.04	18	0.07	0.36
GO_STEROID_METABOLIC_PROCESS	8	0.00	0.06	6	0.02	0.29
GO_CHEMICAL_HOMEOSTASIS	33	0.05	0.28	9	0.05	0.37
GO_ION_HOMEOSTASIS	26	0.10	0.37	7	0.06	0.37
GO_DEFENSE_RESPONSE	24	0.00	0.02	13	0.09	0.36
GO_IMMUNE_RESPONSE	28	0.06	0.33	12	0.03	0.27
GO_INFLAMMATORY_RESPONSE	16	0.00	0.04	9	0.05	0.40
GO_CELL_SURFACE_RECEPTOR_LINKED_SIGNAL_ TRANSDUCTION	86	0.02	0.28	39	0.10	0.38
GO_RECEPTOR_BINDING	49	0.04	0.28	23	0.10	0.39
GO_REGULATION_OF_BIOLOGICAL_QUALITY	68	0.03	0.28	21	0.09	0.37
GO_RESPONSE_TO_WOUNDING	24	0.00	0.15	12	0.08	0.38

Moreover, six gene sets showed enrichment at the false discovery rate below 0.25. They all corresponded to the immune system, in particular cytokine signalling and interferon response, both α/β and γ. The second theme, strongly repeated in the enriched gene sets, corresponded to lipid metabolic processes. Signal transduction via cell surface receptors, especially with G-protein coupled receptors, was another shared feature of replicative and prelamin A-induced senescence.

At P < 0.1 cut off, only two gene sets correlating with underexpressed genes overlapped between replicative senescence and senescence induced by acute prelamin A accumulation upon saquinavir treatment. Increasing the nominal P value cut off to 0.2 enlarged the number of gene sets shared between the ageing models, however, no gene set was identified as common for all three ageing models at these selection criteria (Table 4.9).

Table 4.9. Gene sets enriched in underexpressed genes in the ageing models. Nominal p value < 0.2 cut off.

GENE SET NAME	Late/Early			Saquinavir/DMSO		
	SIZE	NOM p-val	FDR q-val	SIZE	NOM p-val	FDR q-val
HALLMARK_EPITHELIAL_MESENCHYMAL_TRANSITION	64	0.00	0.01	29	0.04	0.64
HALLMARK_MYC_TARGETS_V1	84	0.00	0.00	6	0.19	0.82
GO_REGULATION_OF_G_PROTEIN_COUPLED_RECEPTOR_PROTEIN_SIGNALING_PATHWAY	5	0.00	0.19	5	0.09	0.48
GO_DNA_BINDING	87	0.04	0.49	27	0.18	0.63
GENE SET NAME	Late/Early			siZmpste24/siCTRL		
	SIZE	NOM p-val	FDR q-val	SIZE	NOM p-val	FDR q-val
KEGG_GLUTATHIONE_METABOLISM	9	0.17	0.38	6	0.19	0.97
REACTOME_G1_S_TRANSITION	32	0.00	0.00	5	0.18	0.98
REACTOME_SYNTHESIS_OF_DNA	28	0.00	0.00	5	0.17	0.96
REACTOME_TCA_CYCLE_AND_RESPIRATORY_ELECTRON_TRANSPORT	21	0.12	0.32	13	0.15	0.95
GO_DNA_REPLICATION	16	0.02	0.25	7	0.11	0.95
GENE SET NAME	Saquinavir/DMSO			siZmpste24/siCTRL		
	SIZE	NOM p-val	FDR q-val	SIZE	NOM p-val	FDR q-val
GO_CELL_CELL_SIGNALING	25	0.16	0.59	32	0.03	0.82

4.2.6.1 Inflammation

Both replicative and saquinavir induced senescence showed strong signs of inflammation as judged by the overexpression of various cytokines. Reactome Cytokine Signaling in Immune System gene set was significantly enriched in overexpressed genes in both models, with 45 and 33 genes identified in the Late/Early and SAQ/DMSO comparisons, respectively (Table 4.10). This gene set encompassed all of the genes identified by the GSEA in Reactome Interferon Signalling gene set (reported in Table 4.8), pointing toward interferon pathway activation, presumably mediated through RIG-I. Fourteen genes identified in the Reactome Cytokine Signaling in Immune System overlapped between the Late/Early and SAQ/DMSO datasets, with 13 genes showing the same directionality of expressional changes and comparable fold change (Pearson correlation coefficient = 0.69) (Figure 4.28 A). Moreover, the interferon responsive genes such as IFI27, IFITM1, IFI1 or ISG15 were the top scoring hits in both replicative and saquinavir induced senescence. Only one overlapping cytokine, SOCS3 which negatively regulates cytokine signalling through the JAK/STAT pathway, showed underexpression in both sets (Figure 4.28 B). Of note, in replicative senescence a number of genes associated with cytokine signalling showed underexpression, while that was not the case in cells acutely accumulating prelamin A upon saquinavir treatment. This could suggest expressional changes that are prelamin A-independent.

All overlapping cytokines have been shown to mediate interferon induced response, with STAT1 and STAT2 as the core nodes in downstream signal transduction. Indeed, interferon type I (α/β) and type II (γ) responses were also identified as a

Table 4.10. List of genes assigned to Reactome Cytokine Signalling in Immune System. Genes differentially expressed upon saquinavir treatment (SAQ/DMSO dataset) and replicative senescence (Late/Early dataset). Gene names highlighted in orange overlapped between the two sets.

Reactome Cytokine Signalling in Immune System			
SAQ/DMSO		**Late/Early**	
Gene	Log_2 Fold change ratio	Gene	Log_2 Fold change ratio
IFI27	2.07	IFITM1	2.94
IFIT3	1.98	IFI27	2.57
IFI6	1.96	IFI6	2.28
IFITM1	1.96	ISG15	1.94
IFIT2	1.82	IFNG	1.71
ISG15	1.74	HERC5	1.43
HERC5	1.73	IL1RAP	1.35
IFIT1	1.50	STAT2	1.29
IRAK1	1.41	GBP7	1.23
MX1	1.39	DDX58	1.19
DDX58	1.14	MX1	1.15
NUP43	1.04	CASP1	1.14
UBE2L6	0.98	OASL	1.11
STAT2	0.70	IL6	0.98
EIF2AK2	0.65	ICAM1	0.93
STAT1	0.64	CISH	0.88
TRIM25	0.62	IL1R2	0.82
IL6	0.62	NUPL2	0.81
TRAF6	0.61	GAB2	0.80
IRF4	0.56	JAK3	0.77
ADAR	0.55	IFIT3	0.75
IRF7	0.44	GHR	0.73
B2M	0.40	PRLR	0.70
USP18	0.39	IFI35	0.65
IFI35	0.38	NUP133	0.65
ISG20	0.34	SOS1	0.64
SP100	0.33	OAS2	0.59
OAS3	0.32	STAT1	0.50
SOCS3	-0.33	KPNA2	-0.35
FLNB	-0.50	RBX1	-0.36
VCAM1	-0.62	KPNB1	-0.48
OASL	-0.83	YWHAB	-0.52
IL7R	-1.03	RIPK2	-0.60
		TAB3	-0.60
		UBE2N	-0.63
		HRAS	-0.63
		NUP37	-0.65
		RAE1	-0.67
		CD44	-0.67
		NUP205	-0.68
		EIF4E2	-0.70
		AAAS	-0.75
		SOCS3	-0.87
		CHUK	-0.93
		EIF4A1	-0.96

common feature between replicative and prelamin A induced senescence. In late passage HDFs, interferon γ showed upregulation, at least at the transcript level. Furthermore, components of the RIG-I pathway leading to type I interferon induction were overexpressed in both models. There appears to be a stronger activation of RIG-I pathway in saquinavir treated cells than that in aged HDFs. Nevertheless, RIG-I pathway activation appears to occur in both. In cells acutely accumulating prelamin A as an effect of saquinavir treatment, not only DDX58 (encoding RIG-I receptor) showed overexpression, but also other key downstream effectors and mediators (like IFIH1 (MAD-5) or MAVS (IPS-1)). In replicative senescence, only DDX58 was overexpressed, however, it was accompanied by overexpression of other regulatory proteins involved in this signalling pathway, like ISG15 or IFIT3. IFIT3 may stimulate MAVS-mediated activation of TBK1, which in turn phosphorylates IRF3, promoting IRF3 translocation to the nucleus and transcription of type I interferons. Interestingly, IFIT3 also exhibits antiproliferative characteristics, by its ability to activate cell cycle inhibitors (including p21). ISG15, by its action, can also protect IRF3 from degradation and, in its secreted form, can act as an IFNγ-inducing cytokine. Moreover, it can contribute to translation inhibition via its interaction with translation initiation factor EIF4E2.

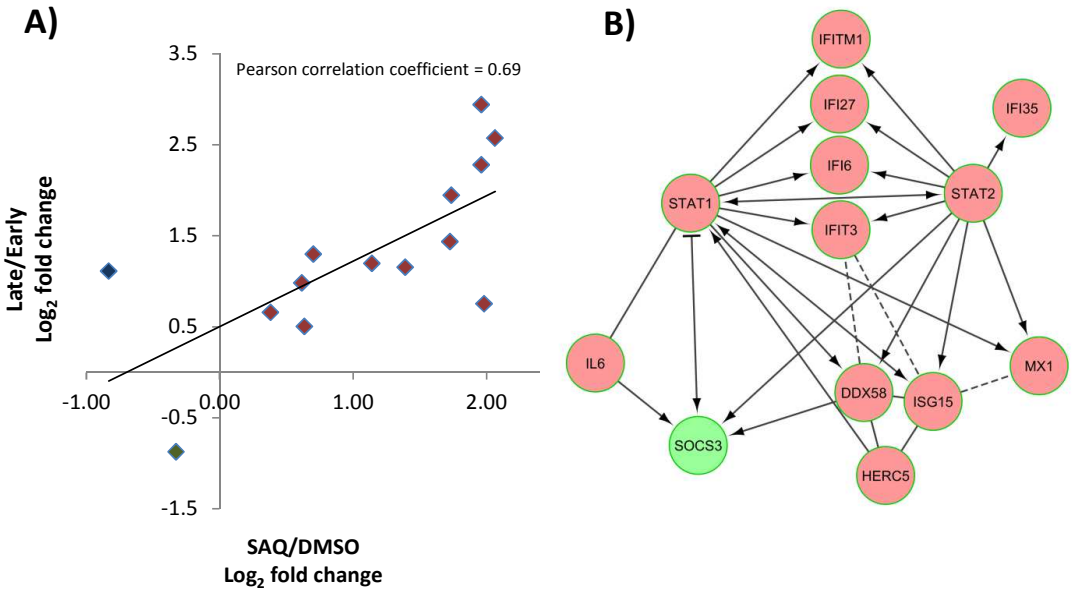

Figure 4.28. Cytokines differentially expressed in both replicative senescence and prelamin A-induced senescence after saquinavir treatment.

A) Plot showing positive correlation between overlapping cytokines, differentially expressed in both replicative senescence (Late/Early) and saquinavir induced senescence (SAQ/DMSO). **B)** Interaction map of cytokines shown in the plot in A (except for OASL). Pink nodes indicate overexpressed genes, while green represents underexpressed. Schematic prepared in Reactome FIViz application.

Interestingly though, what appears to be an overexpression of a set of key mediators of inflammation in replicative senescence and senescence induced via acute prelamin A accumulation upon saquinavir treatment, is absent or even regulated in an opposite direction in cells with siZmpste24 knock-down. Both STAT1 and STAT2 were underexpressed in knock-down cells, conversely, STAT3 (aka Acute-Phase Response Factor) showed overexpression by 1.5 fold. Furthermore, RAC1 which is a STAT3 activator in response to cytokine binding, like IL6 (Faruqi et al., 2001), was also overexpressed by 1.5 fold. This may suggest a differential regulation depending on the type and severity of the stress stimuli, or cross regulation between heterogeneous cell populations in the siRNA experiment.

4.2.6.2 Lipid metabolism

The GSEA of transcriptional changes in the ageing models identified lipid metabolism as a reoccurring theme in the identified gene sets correlating at least with replicative and saquinavir induced senescence. Based on the transcript analysis, replicative senescence appeared to correlate with overexpression of genes encoding enzymes involved in lipid oxidation, with peroxisomal enzymes being prominently represented. The rate of mitochondrial oxidation however, also appeared increased, as judged by the overexpression of CPT1B gene. This gene encodes carnitine palmitoyltransferase 1, which is responsible for the transport of long-chain fatty acyl-CoAs into the mitochondria and is considered the rate-limiting step (Rinaldo et al., 2002). This gene also showed overexpression in cells treated with saquinavir, suggesting that acute prelamin A accumulation can contribute to enhanced lipid oxidation. Furthermore, the cells accumulating prelamin A as an effect of saquinavir treatment showed induction of free fatty acid biosynthesis, particularly unsaturated fatty acids. This should also contribute to increased levels of free fatty acids.

Saquinavir treated cells showed overexpression of genes SREBF1 (encoding sterol regulatory element-binding protein 1; SREBP1) and PPARG (encoding peroxisome proliferator-activated receptor γ). This is consistent with the observed activation of other genes involved in lipid biosynthesis and particularly in cholesterol homeostasis. This may somehow be an unexpected result, since prelamin A can interact with SREBPs and sequester this transcription factor, which in turn would lead to reduced expression of SREBP-responsive genes, including PPARG transcription factor (Hübner et al., 2006; Lloyd et al., 2002). However, based on the microarray results, many genes involved in lipometabolism (including SREBF1 gene) showed

overexpression upon acute prelamin A accumulation in response to saquinavir treatment. Therefore, it would suggest that even if the sequestration occurred, the cell could compensate by increasing SREBP1 expression and presumably prelamin A ability to bind SREBP1 would saturate, leaving the remaining free pool of SREBP1 available for transcriptional activation of target genes.

In replicative senescence overexpression of peroxisome proliferator-activated receptor α (PPARA) rather than PPARG was observed. Increased expression of genes encoding enzymes from the cholesterol biosynthetic pathway (MVD, CYP3A4, S5DL and DHCR7) would also direct towards SREBP activition in replicative senescence. Interestingly though, in both replicative and saquinavir induced senescence, activation of negative regulatory loops of sterol biosynthesis seemed to be triggered. In replicative senescence, INSIG2 was overexpressed by 1.5 fold, while in saquinavir treated cells, INSIG1 was overexpressed by 2.1 fold. INSIGs encode insulin induced proteins that inhibit the action of SREBPs by sequestering them at the ER in complex with SCAP (Yang et al., 2002a). This blocks the translocation of transcriptionally active SREBPs to the nucleus and inhibits transcriptional activation of the target genes.

Cells with Zmpste24 knock-down did not demonstrate such dramatic changes in lipid metabolism-related genes. Although some changes were observed. The gene MBTPS1, for example, which encodes serine protease and mediates the first step in the proteolytic cleavage of SREBPs in their activation process, showed overexpression by 1.3 fold. Also, INSIG2, a negative regulator of SREBP activity, showed underexpression. Furthermore, PPARGC1A and CARM1, both encoding coactivators of PPARG, showed upregulation (each by 1.7 fold). Interestingly, CARM1 can also act as a coactivator of NF-kappa-B during inflammatory stimulation. In addition, fatty acid

binding protein 5 (FABP5) that may mediate PPAR activation, was upregulated in cells with Zmpste24 knock-down. The FABP3 gene which had been upregulated in replicative senescence and saquinavir treated cells, showed downregulation in the siZmpste24 model. Several lipases though, like monoglyceride lipase (MGLL) or phospholipase PLA2G10 also showed overexpression. This may contribute to increased availability of free fatty acids, but the expressional changes noted here are not as strong as in the other two ageing models.

4.2.6.3 Fundamental cell processes (cell cycle progression, replication, translation)

In replicative senescence, the machinery responsible for fundamental cellular processes such as DNA replication, transcription, translation, and cell proliferation in general suffered major decline. In cells accumulating prelamin A, either via saquinavir treatment or the siRNA approach, changes in gene expression that could potentially affect these processes were less prominent. Nevertheless, a few genes, like PCNA encoding proliferating cell nuclear antigen, which acts in the leading strand synthesis during DNA replication, was underexpressed both in saquinavir treated cells and replicative senescence. Also XRCC1, whose product is involved in DNA strand-break repair, showed underexpression in both models. Furthermore, general transcription factor TFII-beta (GTF2E2) similar to replicative senescence, showed underexpression in saquinavir treated cells by 0.8 fold. Interestingly, NFIB, encoding nuclear factor I/B, a transcriptional factor that has been shown to be a key repressor of p21 (Ouellet et al., 2006), was underexpressed in both replicative and saquinavir induced senescence.

Histones play a central role in DNA replication, DNA repair and in transcription. The microarray data revealed several HIST1H2B clusters and HIST1H1C to be underexpressed in cells acutely accumulating prelamin A under saquinavir treatment. Interestingly, in replicative senescence the same clusters were upregulated, with underexpression of others (HIST1H3G, HIST1H4B, HIST1H4D, and HIST1H4G). The siZmpste24/siCTRL model represented a mixed picture of the two prior models, with HIST1H1C and HIST1H2A underexpressed, and overexpression of HIST1H2B, HIST1H3A, and HIST1H3G.

4.2.7 Genes showing the same directionality of expression changes in the three ageing models

Microarray analysis of transcriptional changes in the studied ageing models identified 6 genes showing underexpression in: replicative senescence, senescence induced by acute prelamin A accumulation after saquinavir treatment, and in cells with Zmpste24 knock-down. These genes were: A Disintegrin And Metalloproteinase Domain 12 (ADAM12), Aquaporin 1 (AQP1), tight junction protein Claudin 11 (CLDN11), Caveolin 1 (CAV1), Coagulation Factor (F3), and Tissue Plasminogen Activator (PLAT). Five genes were found to be overexpressed consistently across the three ageing models. They were: B-Cell CLL/Lymphoma 6 (BCL6), Adhesion G Protein-Coupled Receptor L4 (ELTD1 or ADGRL4), Malic Enzyme 1 (ME1), Myosin 1D (MYO1D), and Opsin 3 (OPN3). Microarray results for the expression of these genes were further confirmed by qRT-PCR (Figure 4.29).

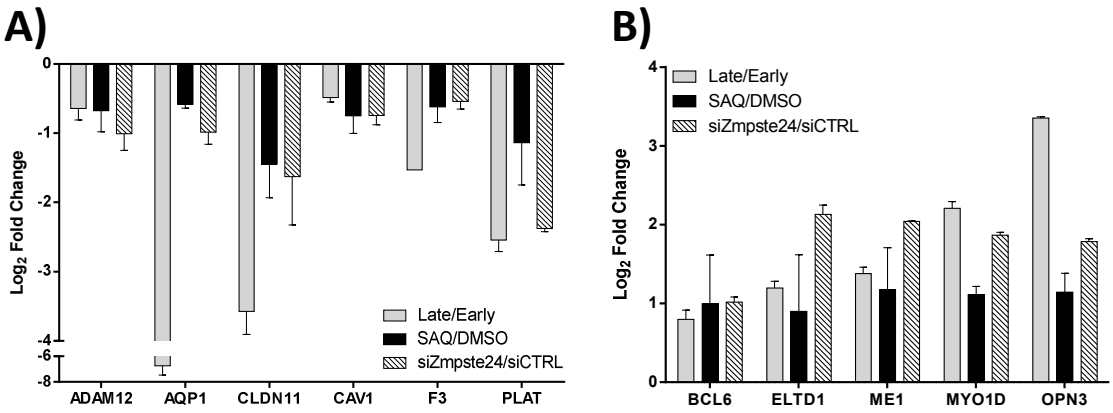

Figure 4.29. qRT-PCR validation of expression levels for selected genes.

A) 6 genes showing consistent underexpression in the ageing models. **B)** 5 genes consistently overexpressed in the three ageing models. Error bars represent SD.

4.3 DISCUSSION

The past few decades have brought more understanding of the mechanisms triggering senescence and its implication in ageing (Salama et al., 2014; Van Deursen, 2014). The emerging image is complex, with multiple effectors contributing to the senescent phenotype and engaging various, not always overlapping pathways. A huge variability of stressors, with different degrees of importance for different cell types, confers a diverse nature to senescence. Many insights into the molecular mechanisms involved in senescence were gained through transcriptional profiling, further advancing our understanding of cellular senescence in different contexts (Lackner et al., 2014; Purcell et al., 2014; Schnabl et al., 2003; Shelton et al., 1999).

This chapter characterises the transcriptional profiles from the laboratory ageing models described in Chapter 3 which included: (i) physiological cellular ageing by replicative senescence, (ii) prelamin A induced senescence after treatment with saquinavir, and (iii) prelamin A induced senescence after siRNA knock-down of

Zmpste24. An extensive, genome-wide microarray analysis of mRNA abundance in the three ageing models was performed, as well as a cross-model comparison. While analysis of the transcriptional changes in replicative senescence and prelamin A induced senescence after saquinavir treatment identified a number of statistically significant alterations in signalling pathways, they were not observed in the siRNA model, despite the large number of differentially expressed genes in this model. Moreover, cells accumulating prelamin A after siRNA knock-down of Zmpste24 displayed very little overlap with either the SAQ/DMSO or Late/Early comparisons. Cellular heterogeneity in the siZmpste24 model may be a plausible explanation for this observation. Although Zmpste24 expression was knocked-down below the population average, it remains most likely that untransfected cells were also present, due to the inefficiency of transfection. Thus the microarray read out may have been affected by the presence of a heterogeneous population. With some cells accumulating prelamin A and others not, they would be able to communicate either via signal mediators secreted into the culture medium or/and through cell-cell contact, and perhaps activate compensating cis-acting signalling. Therefore, despite identifying a substantial number of differentially expressed genes in the siZmpste24 model, no clear clustering was observed. Often differentially expressed genes implicated in the same pathway would demonstrate as much enrichment at the overexpressed end as at the underexpressed, plausibly due to a heterogeneous cellular background. This was unlike saquinavir-treated cells evenly exposed to the drug, or late passage fibroblasts, in which the entire population was at relatively the same cellular stage. Although some expressional changes could still point to certain affected pathways, like SREBP activation or cytokine signalling (STAT3, Rac1), which bear some similarities with the

other two models. Plausibly, these expressional changes may represent those cells least susceptible to compensatory signals from unaffected cells, or the most dominant, and therefore the most sensitive in response to prelamin A accumulation. However, the heterogeneity of the background indicated that the response mechanisms triggered by prelamin A accumulating cells were most likely counterbalanced by communication from untransfected neighbouring cells. A clearer picture might arise if the Zmpste24 siRNA was co-transfected with fluorescently labelled siRNA, allowing for cell sorting, and the ability to obtain a homogenous population of transfected cells. An alternative approach could be the use of shRNA or creating knock-out cells with technology like CRISPR/Cas9. This would stably abolish Zmpste24 expression across the entire cell population. Alternatively one could attempt identification of putative signals between siRNA modified cells and unaffected cells. Preliminary efforts in this direction will be described in Chapter 6, after the cytokine landscape of senescent changes has been studied. Although the siRNA model still offers some clues regarding transcriptional changes upon prelamin A accumulation, for the reasons mentioned above, this model will not be discussed here in detail.

Replicative senescence is characterised by stable cell cycle arrest, caused predominantly by telomere attrition and accumulation of macromolecular damage over an extended time. It is therefore not surprising that the microarray data of replicative senescence clearly identified a decline in fundamental cellular processes related to cell proliferation, DNA replication, transcription, and translation. This further validates the quality of the data analysis and experimental approach. Furthermore, many pathways and cellular components that were identified as

significantly enriched in differentially expressed genes are supported by existing literature. Increased lysosomal activity described in senescent cells (Cuervo and Dice, 2000; Lee et al., 2006) was reflected by the upregulation of mRNA of many lysosomal proteins. Modification of the extracellular matrix was also reported to play a role in cellular senescence (Choi et al., 2011), with profound changes in collagen expression. These changes have also been described in organismal ageing (de Magalhães et al., 2009). Our microarray screen of replicative senescence is in concordance with these studies, and points toward the same conclusions. Furthermore, increased synthesis of sphingolipids and ceramide that have been observed not only in cellular senescence (Venable et al., 2006), but also in ageing rat livers (Lightle et al., 2000), and brain tissue of senescence-accelerated mice (Kim et al., 1997) is in agreement with the overexpression of genes whose products (acid ceramidase, neutral sphingomyelinase or prosaposin) are involved in this pathway, as observed in the microarray analysis of late passage HDFs. Interestingly, acid ceramidase like protein and prosaposin were also upregulated in saquinavir treated cells, possibly indicating the triggering of ceramide signalling.

However, the most enriched pathways in differentially expressed genes, both in replicative senescence and saquinavir induced senescence, were observed in immune response and lipid metabolism. Despite a relatively low number of genes showing a statistically significant change in expression after acute prelamin A accumulation in saquinavir treated cells, the overlap with replicative senescence in these aspects was substantial.

The microarray screen revealed activation of proinflammatory cytokines in replicative senescence and in cells acutely accumulating prelamin A after saquinavir

treatment. Inflammation has been observed as a feature of senescent cells, not only in those reaching replicative exhaustion (Freund et al., 2010), but also in those where senescence was induced by other stressors (Kuilman et al., 2008; Minamino et al., 2003; Purcell et al., 2014), and in normal organismal ageing (Kriete et al., 2008). Our data suggest that acute prelamin A accumulation, at the level of the entire cell population, can trigger a similar immune response. Changes in gene expression suggest that type I and type II interferons play a key role in both replicative and prelamin A induced senescence with activation of the RIG-I-like receptor signalling pathway contributing to inflammatory cytokine production. Interferons are well recognised for their action in the immune response to viral infection, but also display characteristics of immunomodulation and cell growth regulation (Katze et al., 2002; Trinchieri, 2010). It has been shown that exposure to exogenous interferons, both type I and type II, can induce cellular senescence (Kim et al., 2009; Moiseeva et al., 2006). Moreover, patients undergoing IFNα treatment for hepatitis C were noted to exhibit a higher number of senescent cells (O'Bryan et al., 2011). Additionally, the type I interferon signature, induced by ageing in human and mouse brains, was identified and implicated in age-related cognitive decline (Baruch et al., 2014). This suggests that interferon signalling has a crucial role in not only senescence, but also in the organismal ageing process. Furthermore, interferons exhibit anti-tumorigenic activities, which supports the notion that senescence is a mechanism preventing tumour development (Fridman et al., 2006; Kulaeva et al., 2003; Li et al., 2008). DNA damage, a feature of replicative senescence, has been shown to stimulate interferon production and downstream signalling (Brzostek-Racine et al., 2011; Yu et al., 2015). Saquinavir treated cells that acutely accumulate prelamin A did not display an obvious

response to DNA damage at the transcript level. This was with the exception of a few enzymes involved in DNA repair that demonstrated underexpression. These cells, however, showed upregulation of few genes encoding enzymes involved in the detoxification of ROS; whereas ROS themselves have been shown to enhance interferon stimulation (Eguchi et al., 2011; Moiseeva et al., 2006). This could suggest that ROS contributes to the robust activation of interferon signalling in cells acutely accumulating prelamin A after saquinavir treatment. Type I interferon activation in the Late/Early and SAQ/DMSO models could be linked to RIG-I like receptor signalling. Interestingly, an antiageing hormone klotho, which also favours longevity (Kurosu et al., 2005) by increasing resistance to oxidative stress (Yamamoto et al., 2005), was shown to exhibit antinflammatory characteristics by blocking the RIG-I mediated pathway (Liu et al., 2011). It is most likely however, that other pathways contributing to the inflammation phenotype also exist, because blocking the RIG-I pathway does not completely abolish production of the inflammatory cytokines. This further highlights the complexity of the senescence process and the existence of multiple mechanisms contributing to the aged phenotype.

Second mostly affected process that showed overlap between late passage HDFs and HDFs accumulating prelamin A upon saquinavir treatment was the metabolism of lipids and lipoproteins. The relationship between lipid biosynthetic pathways and senescence gains more attention as it appears to be an important aspect of ageing (Ford, 2010; Gey and Seeger, 2013; Jiang et al., 2008; Wang et al., 2008).

Enhanced lipogenesis mediated by SREBP1 was noted in senescent cells (Kim et al., 2010). This could contribute to expanding cellular mass, particularly cell membranes, which is observed in senescence. In our data, late passage HDFs showed

changes in gene expression that could point to increased SREBP activity, especially regarding cholesterol biosynthesis. Cells accumulating prelamin A upon saquinavir treatment demonstrated even stronger signs of SREBP activation, with overexpression of the SREBF1 gene itself. The FASN gene was also upregulated, consistent with Kim *et al*. Moreover, SREBP1 was shown to play a role in cell cycle arrest (Nakakuki et al., 2007) which may support its contribution to the senescent phenotype that is characterised by a stable proliferation arrest. Moreover, mTORC signalling, which contributes to ageing (Johnson et al., 2013), can also regulate SREBP (Bakan and Laplante, 2012; Han et al., 2015). Saquinavir treated cells showed a statistically significant correlation of overexpressed genes with the mTORC1 pathway. This was mainly attributed to overexpression of genes from lipometabolic pathways.

Based on the microarray data, late passage HDFs showed elevated peroxisomal activity which could account for increased lipid oxidation. Overexpression of carnitine palmitoyltransferase 1 in both saquinavir-treated cells and old HDFs, would also support heightened mitochondrial lipid oxidation. Similar conclusions were made for oncogene-induced senescence (Quijano et al., 2012), in which enhanced lipid oxidation accounted for increased levels of long chain free fatty acids. However, it was not accompanied by *de novo* synthesis of lipids, which, based on the gene expression pattern, is most likely the case for saquinavir treated cells. Both processes, lipid oxidation and synthesis, can contribute to increased levels of free fatty acids. Therefore, in senescence, the lipid composition may be more important than the process by which it is achieved. Interestingly, in contrast to Kim and colleagues (Kim et al., 2010), Maeda and colleagues observed strong underexpression of mRNA for fatty acid synthase and Acyl-CoA desaturase in replicative senescence (Maeda et al., 2009).

Our data for replicative senescence did not show such changes, and as mentioned above, the data for cells acutely accumulating prelamin A upon saquinavir treatment showed overexpression of these genes, consistent with Kim's findings. However, both Kim and Maeda's results indicate increased cholesterol synthesis. This is in agreement with our predictions, based on the gene expression data.

PPAR signalling was also affected in our models of premature ageing. PPARα overexpression was observed in replicative senescence, whereas PPARγ in saquinavir-treated cells. Senescent cells, despite cell cycle arrest, remain metabolically active, and PPARs have been clearly delineated as the master regulators of metabolism (Desvergne and Wahli, 1999). However, in addition to their role in energy homeostasis, PPARs also display non-canonical functions, like regulation of inflammation, and response to oxidative stress (Polvani et al., 2012; Varga et al., 2011). This is consistent with their overexpression in senescent cells and the observed activation of the inflammatory response combined with clues suggesting an increased anti-oxidative response.

The links between cellular senescence and the physiological ageing process have been investigated intensively, with more reports arising in support of the pivotal role of senescence in the ageing process (Baker et al., 2011; Collado et al., 2007; Herbig et al., 2006; Jeyapalan and Sedivy, 2008; López-Otín et al., 2013). Magalhães and colleagues performed a meta-analysis on 27 available RNA profiles from aged organisms (humans, mice, and rats), and defined a signature of transcriptional changes in ageing (de Magalhães et al., 2009). They identified 17 genes consistently underexpressed with age, most coding for mitochondrial proteins and collagen. Some of these genes were also detected in our microarray screen, not only in the late

passage HDFs (e.g., COL1A1, UQCRFS1, NDUFB11), but also in saquinavir treated cells (COL1A1) and the siZmpste24 model (UQCRQ). Moreover, many overexpressed genes overlapped between their meta-analysis and our findings, particularly in replicative senescence. The highest scoring gene in their study, APOD, was also overexpressed in the late passage HDFs in our study. The general observation of overall immune response could also be extrapolated to HDFs acutely accumulating prelamin A under saquinavir treatment. These observations taken together, suggest that there are significant similarities in both replicative and prelamin A induced cellular senescence, which resemble the changes in molecular mechanisms driving organismal ageing. However, some differences between our dataset and their meta-analysis exist, particularly among the overexpressed genes. While some changes are universal for senescence and ageing, shared between tissues and species, there are most likely other mechanisms existing that differentiate replicative senescence observed *in vitro* from cells ageing in tissues. Factors like the state of differentiation, presence of multiple cell types in the tissue environment, nutritional status, and consequences of long term chronic inflammation surely contribute to execution of the senescence programme (Franceschi and Campisi, 2014; Salama et al., 2014).

Many studies have also focused on comparing the normal ageing process with progeria syndromes, such as HGPS or WS, in an attempt to evaluate if progeria truly resembles accelerated ageing (Burtner and Kennedy, 2010). A great insight into the molecular mechanisms behind HGPS came from RNA profiling studies (Csoka et al., 2004; Ly et al., 2000; Marji et al., 2010; Scaffidi and Misteli, 2008), with the suggestion that HGPS resembles the overall changes observed in normal ageing, only at an accelerated pace (Aliper et al., 2015; Wang et al., 2013b). Importantly, acute prelamin

A accumulation induced by saquinavir treatment triggered a discrete subset of gene expression changes observed in HGPS fibroblasts, particularly regarding the immunoresponse and interferon signalling (e.g. overexpression of STAT1, IFI27, TRIM22 in (Csoka et al., 2004)). Furthermore, the activation of pathways like PPAR or mTOR, which were clearly observed in saquinavir treated cells, was also enhanced in RNA profiles from HGPS patients (Aliper et al., 2015). Genomic instability, caused by impaired recruitment of DNA repair factors (RAD53 and 53BP1), was observed in HGPS cells, Restrictive Dermopathy (RD), as well as in Zmpste24 knock-out Mouse Embryonic Fibroblasts (Liu et al., 2005; Liu et al., 2008). There is a postulated role of PCNA loss at the replication fork as the underlying cause of abnormal recruitment of the DNA repair machinery to the DNA double strand break foci (Musich and Zou, 2009). Our microarray screen demonstrated underexpression of PCNA for both late passage HDFs and HDFs acutely accumulating prelamin A upon saquinavir treatment, which could support this hypothesis. However, it is necessary to insert a cautionary note. The overlap in the gene expression pattern observed in multiple experiments involving HGPS cells is moderate at best. This variability has been ascribed to donor age effects, and the consequence of variable times in culture *in vitro* (Marji et al., 2010). Thus detection of the exact set of genes in saquinavir treated cells seems rather unlikely.

It is also worth noting that microarrays represent a snapshot, an insight into a fixed time point, rather than continuous observation of the changes as they occur. Thus it is impossible to say with certainty in which direction the cellular processes are moving. Often induction of a pathway activates feedback loops that compensate or deactivate the pathway (Ferrell, 2013; Mitrophanov and Groisman, 2008). Also the

severity of the stressor and the time that is allowed for compensation will most likely affect the transcriptome profiling. Therefore it is possible that simultaneous detection of genes encoding proteins which display counteracting characteristics was observed. Furthermore, replicative senescence is a slowly developing process, over an extended period of time, during which the burden of cellular damage arises continuously, thereby allowing more time for cellular response. In saquinavir-treated cells, the adverse effect on prelamin A occurs more quickly, and within 48 hours, cells are faced with a different cellular balance. Therefore, the response is most likely distinct in some aspects, for example, in the lack of obvious deterioration of fundamental cellular processes. The response however, retains some similarities with replicative senescence, especially in rapidly modulatable signal dependent cellular functions.

Nevertheless, five genes were identified as being overexpressed and six as underexpressed consistently across the three ageing models studied. It is tempting to speculate that those might be the links that mediated the impact of prelamin A on senescence. The overexpressed genes encode proteins involved in various processes and their transcriptional regulation, if known, seems to be just as diverse. Among them was ME1, encoding cytosolic malic enzyme, which is crucial in fatty acid biosynthetic pathways (Pongratz et al., 2007). Interestingly, ME1 was reported to play a role in p53-dependent senescence, but surprisingly induced senescence when underexpressed (Jiang et al., 2013). Conversely, reduced expression of ME1 observed in FMO5 knock-out mice was shown to contribute to longevity by slowing metabolic ageing (Gonzalez Malagon et al., 2015). BCL6 encodes a transcriptional repressor, a potent oncogene that has also been proposed to play a role in senescence regulation, although without a clear consensus (Ranuncolo et al., 2008; Shvarts, 2002). ELTD1 and

OPN3 encode G-protein-coupled receptors, which makes them interesting candidates for signal transduction studies. Furthermore, OPN3 was shown to play a role in apoptosis (Jiao et al., 2012) while ELTD1 is involved in angiogenesis and cell adherence (Masiero et al., 2013). MYO1D encodes myosin, a molecular motor with ATPase activity, that plays a role in control of membrane trafficking (Huber et al., 2000), tension (Nambiar et al., 2009), and neurodevelopment (Benesh et al., 2012). Interestingly, as observed in our data, Lackner and colleagues also detected increased MYO1D expression in their transcriptome study of senescent fibroblasts (Lackner et al., 2014). The group of underexpressed genes is just as heterogeneous, and will be discussed in more detail in the next Chapter.

In summary, the unbiased genome-wide transcript analysis presented in this chapter has shown that a significant part of the common senescence programme seen by us and others during cellular aging can be replicated in young cells simply by accumulating prelamin A at the nuclear periphery. While the emerging picture is complex, some important underlying common themes were identified. It is worth noting though, that hypothesis building was based on the mRNA profiles. This does not take into account translational or post-translational pathway regulation. Moreover, microarrays are a method measuring the population average, rather than changes at a single cell-level. Therefore a functional study of the six underexpressed genes was undertaken in a more cell-centred approach. This is presented in the following chapter. Activation of the inflammatory response will also be studied in more detail in Chapter 6.

CHAPTER 5

5 Exploration of links between underexpressed candidates from microarray screen and senescence

5.1 INTRODUCTION

The microarray analysis of mRNA profiles from the studied laboratory models of ageing identified six genes as significantly underexpressed in senescent cells across the models. These were: A Disintegrin And Metalloproteinase Domain 12 (ADAM12), Aquaporin 1 (AQP1), tight junction protein Claudin 11 (CLDN11), Caveolin 1 (CAV1), Coagulation Factor (F3), and Tissue Plasminogen Activator (PLAT). Although transcriptome profiling offers a great insight into the potential alteration in cellular signalling, changes in mRNA levels are not always reflected in protein activity, because of existence of multiple regulatory mechanisms operating posttranscriptionally. Moreover, a microarray screen measures the population average rather than changes observed in a single cell. Therefore, in the next step, a fluorescence-activated cell sorting (FACS) assay that multiplexes several markers of senescence was set up, leaving an additional channel for a modifying agent to be measured. In this study, the modifying agents were the six identified proteins, tagged with GFP and overexpressed from CMV promoter in the studied cellular models of senescence. Since they showed underexpression in senescent cells consistently across the models, it was hypothesised that if they play an intermediate signalling role in execution of senescence programme, their overexpression could halt or reverse a senescence phenotype. This was examined by analysis of expression of senescence markers in the transfected cells

expressing GFP-tagged protein candidates. Flow cytometry was employed to distinguish transfected cells from non-transfected and to gather data for a large cell population, allowing for simultaneous measurement of selected marker levels on a cell-by-cell basis. Senescence markers chosen for this study were: interleukin 6 (IL6), β-galactosidase (GLB1), and $p16^{INK4a}$ as they are widely accepted senescence markers (Muñoz-Espín and Serrano, 2014) and their expression is elevated in prelamin A-induced senescence as well as in replicative senescence in HDFs (as shown in Chapter 3).

Products of the underexpressed genes appear to be involved in a variety of cellular functions. Interestingly, some have been previously linked to senescence and/or ageing. Additionally, some have been associated with tumourigenesis. A brief characterisation of the underexpressed genes identified in the microarrays screen is presented below.

5.1.1 Tissue plasminogen activator

The PLAT gene encodes tissue plasminogen activator (tPA). It is a secreted serine protease responsible for the conversion of proenzyme plasminogen to plasmin. Plasmin subsequently leads to dissolution of fibrin clots in the vasculature (Collen and Lijnen, 1991). The activity of tPA is closely regulated by its specific inhibitor, plasminogen activator inhibitor 1 (PAI1, encoded by SERPINE1) (Suzuki et al., 2009; Urano et al., 1991). Due to the role of plasminogen activators in fibrinolysis, their impaired activity is often a cause of age-associated degenerative diseases such as atherosclerosis and hypertension (Danø et al., 1985; Oliver et al., 2005; Ridderstråle et al., 2006). Underlying atherosclerotic lesions in combination with a thrombotic

obstruction of the main blood vessels may lead to acute ischemic events like myocardial infarction and stroke. This process largely depends on the reduced activity of tPA and increased thrombus formation (Collen and Lijnen, 1991; Flores et al., 2014; Gong et al., 2012). Moreover, there is a growing body of evidence that vascular senescence itself contributes to atherosclerosis, a feature of human ageing (Minamino and Komuro, 2007). Recently, tPA was demonstrated to negatively regulate doxorubicin-induced senescence in breast cancer cells (Elzi et al., 2012). In these cells, the senescent phenotype was prompted by increased extracellular levels of insulin-like growth factor binding protein 3 (IGFBP3), a common SASP factor. IGFBP3 inhibited insulin-like growth factor (IGF) signalling by binding to IGF. This inhibition resulted in suppression of AKT, and ultimately led to senescence mediated by both p53 and RB tumour suppressors. tPA-mediated proteolysis of IGFBP3, however, abated its senescence-inducing activity. Whereas inhibition of tPA by PAI1 abolished IGFBP3 proteolysis allowing for the onset of senescence.

Interestingly, tPA overexpression has been observed in glioma-initiating cells (GIC) (Yamashita et al., 2015). GICs are a type of cancer stem cells that initiate central nervous system tumours. These cells demonstrate higher levels of tPA, which *in vitro*, promotes GIC proliferation, migration, and invasion. *In vivo* this contributes to GIC tumour growth, thus tPA appears to be a glioma-promoting factor when overexpressed. Given that senescence is a mechanism preventing tumourigenesis and at least some tumour types have elevated tPA, it is interesting to note that our microarray screen of expressional changes in senescent cells identified tPA as underexpressed. Yamashita and colleagues identified miR340 as a regulator of tPA mRNA level in GICs. Their data demonstrates that miR340 is depleted in GICs resulting

in an increased level of tPA protein. Interestingly, miR340-overexpression in GICs decreased the tPA level and also induced senescence in these cells.

5.1.2 ADAM12

Similar to tPA, a disintegrin and metalloprotease 12 (Adam12) has also been shown to interact with IGFBP3 and mediate its proteolysis (Shi et al., 2000). Alternative splicing of the Adam12 transcript results in two variants, a short secreted form Adam12S and a long membrane-bound Adam12L (Loechel et al., 1998). In addition to IGFBP3, Adam12S exhibits proteolytic activity against a SASP factor IGFBP5 (Loechel et al., 2000). Transcriptionally, Adam12 appears to be regulated by a negative regulatory element (NRE) present at the 5'-UTR region of Adam12 gene (Ray et al., 2011). The NRE acquires a Z-DNA conformation that is recognised by hZα ADAR1 protein and forms a repressive complex upon binding. Interestingly, ADAR1 showed upregulation in saquinavir treated cells in our microarray screen. Post-transcriptionally, Adam12 mRNA may be negatively regulated by microRNA miR-29 (Li et al., 2011). Expression of miR-29 micro RNA family has been demonstrated to increase with ageing, and such dependence was also observed in the mouse model of Hutchinson–Gilford progeria syndrome (Ugalde et al., 2011b). This further suggests a possible link between Adam12 and senescence, especially in the context of prelamin A accumulation. Moreover, increased Adam12 expression has been correlated with the progression and prognosis of many diseases including primary brain tumours, lung adenocarcinoma, bladder cancer, and breast cancer (Nyren-Erickson et al., 2013; Roy et al., 2004).

5.1.3 Tissue factor

Tissue factor (TF), encoded by the F3 gene, is a cell surface glycoprotein that is the primary initiator of the blood coagulation cascade. TF binds factor VIIa, leading to activation of factor IX and factor X, and ultimately to fibrin formation (Mackman, 2004). Although TF is mainly expressed by endothelial cells, its activity was also confirmed in fibroblasts and cancer cells (Kothari et al., 2013). Other than its well-defined role in thrombogenesis, TF has also been implicated in carcinogenesis (Garnier et al., 2010; Kasthuri et al., 2009; Van Den Berg et al., 2012). TF upregulation has been linked with aggressive malignancies (Contrino et al., 1996) and increased tumour growth (Rak et al., 2006; Ruf, 2007). In agreement, the selective knock-down of TF in mouse colorectal cancer cells led to reduced tumour growth (Yu et al., 2005).

Expression of TF is tightly regulated and its surface activity is absent in the quiescent endothelium (Stähli et al., 2006). It has also been shown that senescent endothelial cells lose their ability to induce TF due to heterochromatin-associated silencing of the TF promoter region (Kurz et al., 2014). This was proposed to be an additional anti-tumorigenic mechanism of the senescence programme. The increased incidence of thrombo-embolism and atherothrombosis observed in the elderly could be linked to loss of tPA expression and reduced fibrinolysis. Underexpression of TF should have the opposite effect and lead to less thrombus formation. Consistent with that, it appears that bleeding events are more frequent with age (Lakatta and Levy, 2003). However, altered TF expression has not been described in human ageing.

5.1.4 Caveolin 1

Caveolins are the structural proteins of caveolae, small cholesterol and sphingolipid-enriched clathrin-free invaginations in the plasma membrane measuring 50-100 nanometres in diameter (Palade, 1953; Parton and del Pozo, 2013). In vertebrates the caveolin family has three members: caveolin 1 (CAV1), caveolin 2 (CAV2), and caveolin 3 (CAV3). Their expression levels differ from tissue to tissue, with the CAV1 being the most abundant and found in most cell types, particularly in differentiated cells (Rothberg et al., 1992). Although caveolins localise predominantly to the plasma membrane, they are also present in the Golgi, the ER, vesicles, and in cytosol (Williams and Lisanti, 2004). They are not only structural components of the caveolae, but also function as an important signal transduction regulator. Caveolins are able to anchor other proteins in caveolae and either inhibit or enhance the signalling capacity of their interacting proteins. They are also involved in vesicular transport, cholesterol homeostasis, calcium signalling, t-tubule formation, and mechanosensing (Hardin and Vallejo, 2006; Minetti et al., 2002; Pelkmans and Helenius, 2002; Sinha, 2011; Williams and Lisanti, 2004).

Although upregulation of CAV1 has been shown to mediate oxidative stress-induced senescence by p53-p21 pathway activation (Volonte et al., 2015; Zou et al., 2011), other studies have demonstrated that oxidants lead to CAV1 degradation and reduced expression (Hsieh et al., 2013; Mougeolle et al., 2015). The discrepancy regarding the impact of oxidative stress on the CAV1 protein level could be context-dependent. Nevertheless, CAV1 is known to inhibit specific activity of several oxidative enzymes, like endothelial nitric oxide synthase (eNOS) and NADPH Oxidase (NOX)

(Patel and Insel, 2009), implying its role in oxidative-regulating pathways. Moreover, oxidative damage is often associated with tissue deterioration in ageing.

Studies in senescent fibroblasts also remain contradictory. Some studies showed loss of caveolae without the depletion of CAV1 expression (Wheaton et al., 2001), while other studies showed overexpression of CAV1 in replicative senescence and increased number of caveolae structures (Park et al., 2000). Several reports, however, have demonstrated decreased expression of caveolins and their association with caveolae with age (Kawabe et al., 2001; Ratajczak et al., 2003; Sarati et al., 2013). This may contribute to age-associated pathologies like cardiovascular diseases (Fridolfsson and Patel, 2013) or neurodegeneration (Head et al., 2010). As an example, CAV1 knock-out mice show signs of premature neuronal ageing and develop pathologies characteristic to Alzheimer's Disease (Jasmin et al., 2007; Trushina et al., 2006).

5.1.5 Aquaporin 1

Aquaporin 1 (AQP1) was the first identified member of the aquaporin family (Agre et al., 1993). These proteins form transmembrane channels with a specific bidirectional water permeability and are essential for maintaining cell water-ion balance (Borgnia et al., 1999). The aquaporins are widely expressed in a variety of tissues and cells (Mobasheri and Marples, 2004), although they are most abundant in membranes with underlying physiological function in water absorption and secretion. This is observed in the proximal convoluted tubules, descending thin limbs of the loop of Henle (Denker et al., 1988) and renal vasa recta (Pallone et al., 1997). AQP1 has been proposed to participate in a number of pathologies, such as renal injury (Sonoda

et al., 2009), spinal cord injury (Nesic et al., 2008), brain edema (Tran et al., 2010), and rheumatoid arthritis (Trujillo et al., 2004).

Interestingly, a few transcriptome profile studies have shown decrease in AQP1 expression in senescent cells. For example, human umbilical vein endothelial cells (HUVECs), senesced either by proliferative exhaustion or by irradiation, showed more than two-fold underexpression of AQP1 (Kim et al., 2014; Mun et al., 2009). Moreover, age-dependent decrease in AQP1 expression has been shown to underlie degenerative aging of the intervertebral disc (Taş et al., 2012; Wang and Zhu, 2011), with the suggestion that AQP1 may play an important role in the interaction between cells and the extracellular matrix proteins. Interestingly, in a mouse model of early physiological ageing, a silicic acid-induced delay of vascular senescence correlated with increase of AQP1 expression (Buffoli et al., 2013).

In addition, decline in expression of several other members of the aquaporin family were shown to correlate with ageing in different tissues. For example, aquaporin 3 (AQP3) was demonstrated to decrease in skin biopsies of the elderly. This was also observed in normal aged human epidermal keratinocytes and skin fibroblasts (Li et al., 2010). Loss of AQP3 in the skin is presumably contributing to age-related development of excessive skin dryness, termed xerosis. Overexpression of AQP3 in keratinocytes appears to protect from UVA-induced oxidative stress (Xie et al., 2013). AQP3 and aquaporin 2 are downregulated in ageing kidneys (Combet et al., 2008; Preisser et al., 2000). Changes of aquaporin 4 expression in the cochlea and inferior colliculus appear to influence age-related hearing loss (Christensen et al., 2009), and salivary gland function during aging is accompanied by a decrease in aquaporin 8 mRNA level (Hiratsuka et al., 2002).

5.1.6 Claudin 11

Claudins (CLDNs) are integral membrane proteins involved in the formation of the tight junction seal in tissues (Hewitt et al., 2006; Van Itallie and Anderson, 2013). Tight junctions maintain a physical barrier preventing the free passage of water and solutes through the paracellular space. They also play a critical role in cell polarity and signal transduction. In the human genome, 27 members of the CLDN family have been identified (Mineta et al., 2011). They demonstrate a varied expression pattern in different tissues, with CLDN3, 4, 5, 7, 12 and CLDN11 being more widely expressed (Hewitt et al., 2006).

Although CLDN11 has been mainly associated with myelin sheets in central nervous system and regulation of oligodendrocyte proliferation and migration (Gow et al., 1999; Morita et al., 1999), there is a growing body of evidence suggesting a role for CLDN11 in tumourigenesis. The pattern of expression of CLDN11 appears to depend on the tumour type (Gao et al., 2014; Hensley et al., 2014; Lin et al., 2013; Walesch et al., 2015; Yang et al., 2015). Interestingly, it has been shown that the transition of normal quiescent fibroblasts into cancer-associated fibroblasts (CAFs) is accompanied by a TGFβ-dependent increase in CLDN11 expression (Karagiannis et al., 2014). This appears to be a context-dependent behaviour, but highlights the importance of CLDN11 in this carcinogenesis. Tight junction formation strengthens the contractile ability of CAFs and may play a role in increased interstitial pressure, thus delaying delivery of chemotherapeutic drugs to malignant tissues (Heldin et al., 2004).

Claudin 11 has not been investigated specifically with regard to its role in senescence. However, in concordance with our results, CLDN11 has been reported as an underexpressed gene in diploid human fibroblasts upon replicative senescence, but

not in quiescent cells (Lackner et al., 2014). In addition, expression of CLDN5 has been shown to decrease in senescent HUVECs *in vitro*. This led to disruption of tight junctions in senescent cells and, in turn, to loss of the integrity of the endothelial barrier (Krouwer et al., 2012), suggesting a role of claudins in the senescence process.

5.2 RESULTS

Fluorescence-activated cell sorting (FACS) was employed to simultaneously analyse the expression of several senescence markers in a cell population. The advantage of this approach is its ability to quickly measure protein levels on a cell-by-cell basis within a population of thousands of cells, thereby offering greater statistical power of the observed phenotype. Moreover, FACS allows for gaining insights into networks and their components while accounting for cross-component concentration.

5.2.1 Dynamics of senescence marker expression within a cell population

Chapter Three showed that at the population level, a significant increase can be observed in expression of several senescence markers, like $p16^{INK4a}$, IL6, and β-galactosidase in response to prelamin A accumulation after saquinavir treatment. Replicative senescence is accompanied by similar changes. Expression analysis of aforementioned markers on a cell-by-cell basis by FACS showed that higher expression of prelamin A correlates with higher levels of other senescence markers (Figure 5.1). As shown in the example of early to late passage HDF comparison, three subpopulations were selected based on the level of prelamin A expression (low, intermediate and high prelamin A-expressing cells). The levels of IL6, β-galactosidase

(GLB1), and p16^{INK4a} were calculated for each subpopulation and compared between early and late passage cells. It showed that even within an early passage cell population, there is a fraction of prelamin A expressing cells, accompanied by elevated GLB1 expression. Although IL6 and p16^{INK4a} expression also positively correlated with prelamin A in early passage cells, they remained significantly lower than in late passage cells.

Expression of senescence markers to prelamin A level in a dose-response

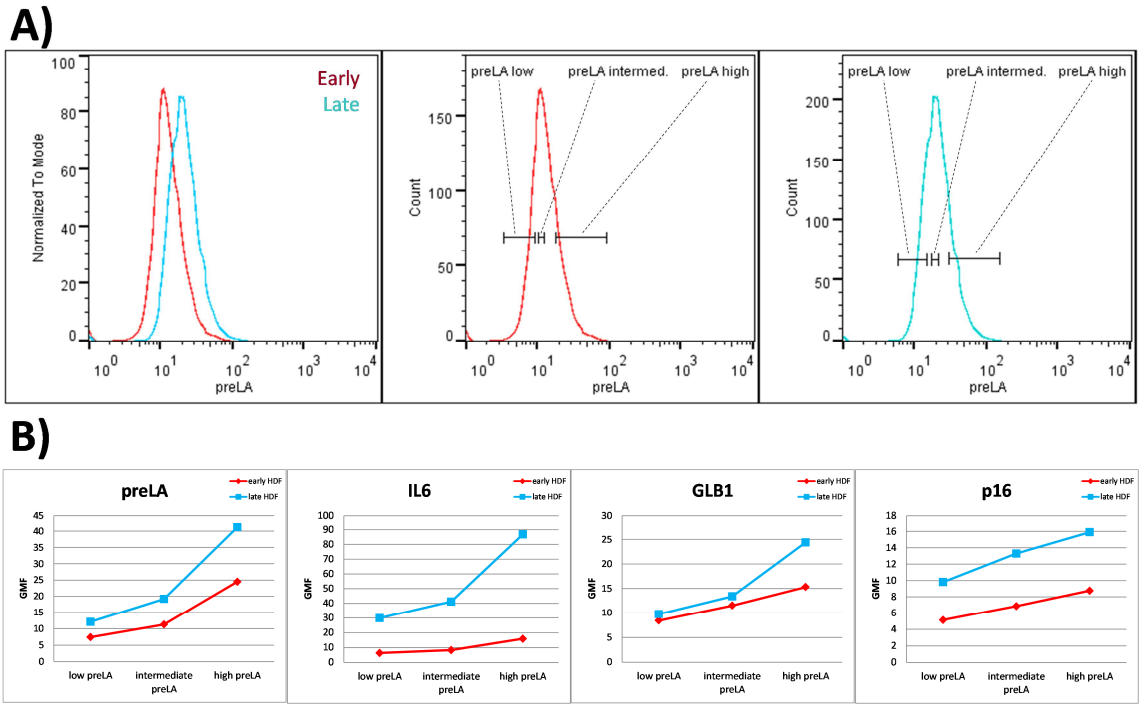

Figure 5.1. Expression of senescence markers in cell subpopulations within early and late passage HDFs.

A) Top panel shows histograms from FACS analysis of prelamin A expression in early passage HDFs (passage below 22) and late passage HDFs (passage over 40). Three subpopulations within early and late passage group were gated, each consisting of 20% of the total cell number, based on the prelamin A expression. They were: cells expressing low level of prelamin A, cells expressing intermediate level of prelamin A, and cells expressing the highest prelamin A level. **B)** Expression level of senescence markers in the subpopulations depicted in panel A, represented as geometric mean fluorescence (GMF) intensity for early and late passage HDFs. Total cell number 5000.

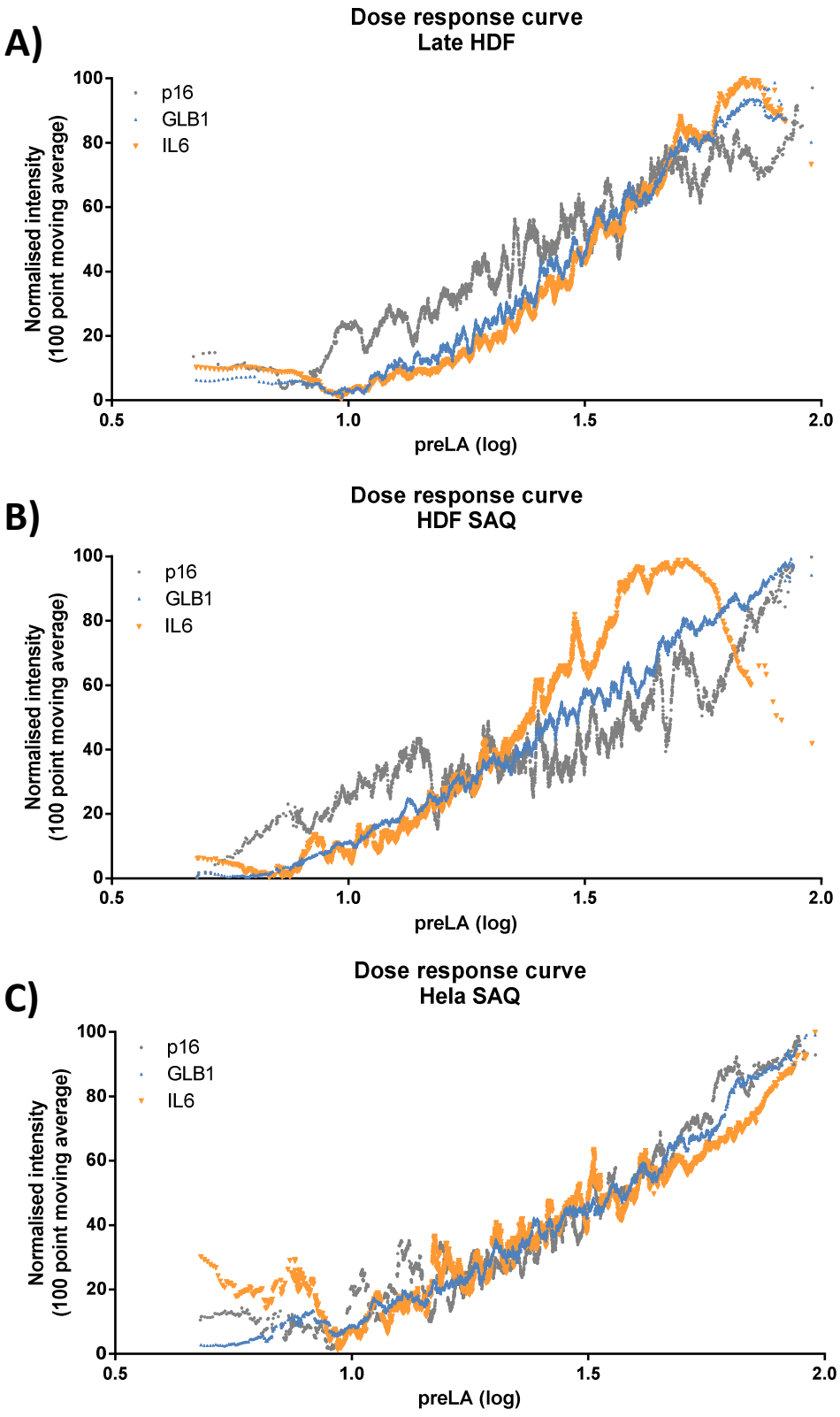

Figure 5.2. Expression of senescence markers in response to increasing prelamin A level.

A) Late passage HDF. **B)** Early passage HDF after 48 hours of saquinavir treatment. **C)** HeLa cells after 48 hours of saquinavir treatment. X axis represents prelamin A expression level, transformed into logarithmic scale. Y axis represents normalised intensity of senescence markers after applying 100 point moving average. Each data point represents a measurement for a single cell. Total cell number 5000. p16, $p16^{INK4a}$; GLB1, β-galactosidase; IL6, interleukin 6.

manner was calculated for HDFs senesced by either replicative exhaustion or saquinavir treatment. Response in HeLa cells to prelamin A accumulation was also measured. Five thousand cells were ranked by the level of expression of prelamin A. The corresponding staining intensities for senescence markers were plotted as dependent response variables. A 100 point moving average was applied to the senescence marker expression level and the range was normalised. Although there were slight differences between senescence and cell types, it appears that the relation between prelamin A and other senescence marker levels is linear (Figure 5.2). Higher prelamin A accumulation in a cell corresponded to an increase in expression of other senescence markers. Although in HDFs, either saquinavir-treated or aged by replicative exhaustion, the cell cycle regulating $p16^{INK4a}$ changes are earlier with low dose prelamin A. This does not seem to be the case for HeLa cells.

5.2.2 Expression of GFP-tagged proteins

Six genes were identified in the microarray screen as being underexpressed in the three cellular models of ageing when cells were senesced. Therefore, these genes were tagged with GFP and overexpressed in senescent cells in order to determine if such an approach could halt or reverse the senescent phenotype.

Plasmid encoding GFP-tagged tPA was obtained from Dr Suzuki (Hamamatsu University School of Medicine, Japan) (Suzuki et al., 2009), while construct encoding GFP-tagged Adam12L (long splice variant) was kindly provided by Dr Wewer (University of Copenhagen, Denmark) (Hougaard et al., 2000). Unfortunately, attempts to clone Adam12S (short isoform) were unsuccessful. AQP1, CLDN11, F3, and two CAV1 isoforms (CAV1α and CAV1β) were tagged with GFP attached to the N terminus.

Cells transfected with plasmids encoding GFP-tagged proteins demonstrated increase in the mRNA level of the corresponding gene, as well as expressed GFP-tagged proteins. Examples of HDFs overexpressing these proteins are shown in Figure 5.3. Although GFP is widely used for tagging it may interfere with proper folding of the target protein. tPA-GFP and Adam12L-GFP have previously been tested functionally (Hougaard et al., 2000; Suzuki et al., 2009). CAV1α and CAV1β were also shown to

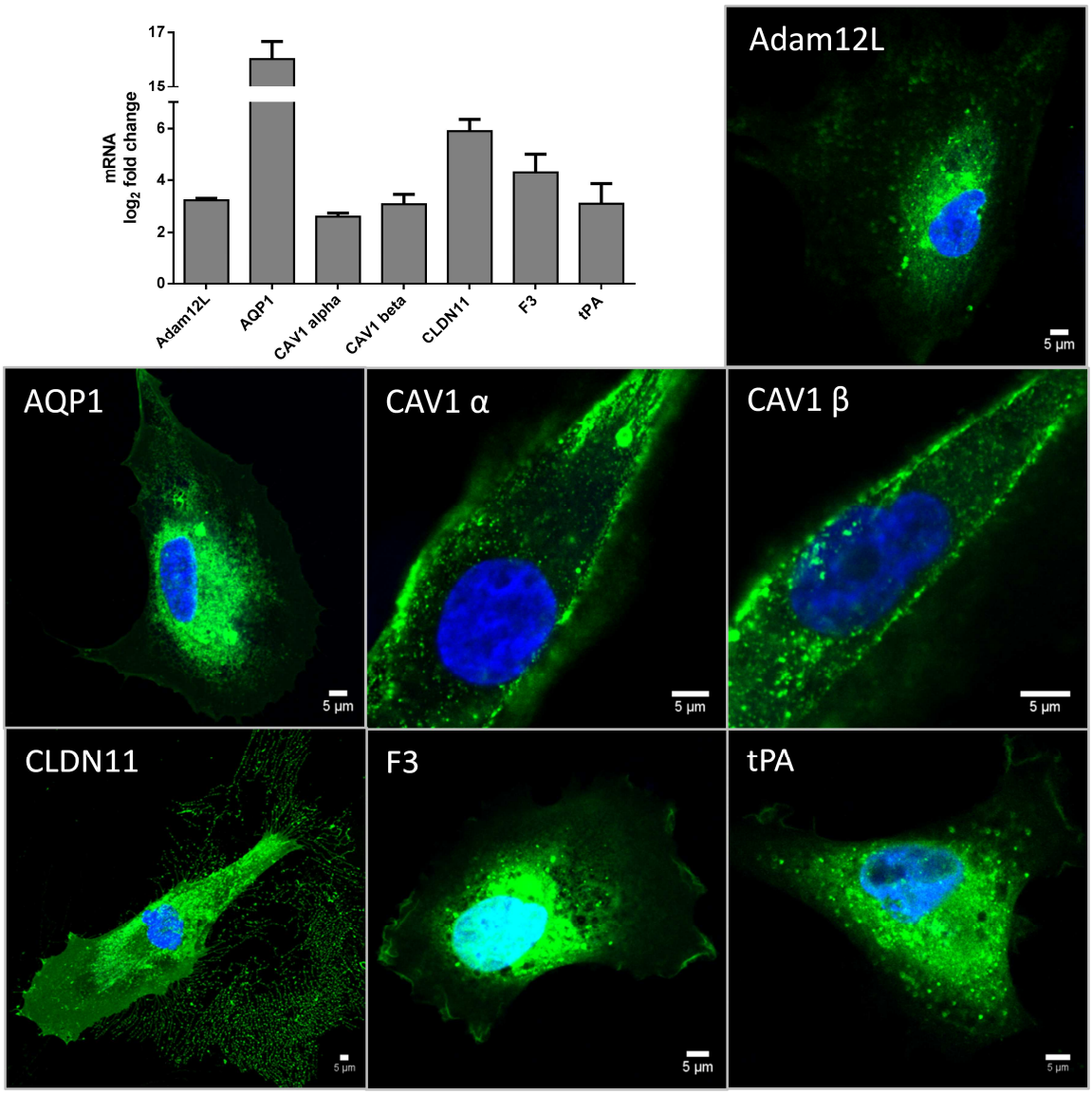

Figure 5.3. Overexpression of GFP-tagged candidate proteins.

Graph represents mRNA fold change for corresponding genes over untransfected HDF control. Microscopy images of HDFs expressing GFP-tagged proteins (depicted in the corners). In green GFP. In blue DAPI.

function normally when GFP-tagged (Scherer et al., 1995). The other three proteins (AQP, CLDN11 and F3) demonstrated expected subcellular localisation when examined by microscopy imaging, suggesting that they are folded correctly, despite the attached GFP tag. As an example, higher magnification images of CLDN11 (Figure 5.4), a tight junction protein, showed that the GFP-tagged protein was delivered to the cellular membrane and localised mainly to the sites of cell to cell contact.

5.2.2.1 Acute overexpression can contribute to senescence

Transfection efficiency may differ from cell to cell and transfected cells normally display a range of expression of the plasmid-encoded proteins. Investigation of cells transfected with GFP-tagged proteins by FACS allowed for a better understanding of the impact of overexpression on the senescence markers. Figure 5.5 shows an example of such an analysis for two proteins, GFP-CLDN11 and tPA-GFP.

HeLa cells were initially used for transfection because they yield better transfection efficiency, while still responding to prelamin A accumulation under saquinavir treatment by senescing. This was shown by their increased expression of

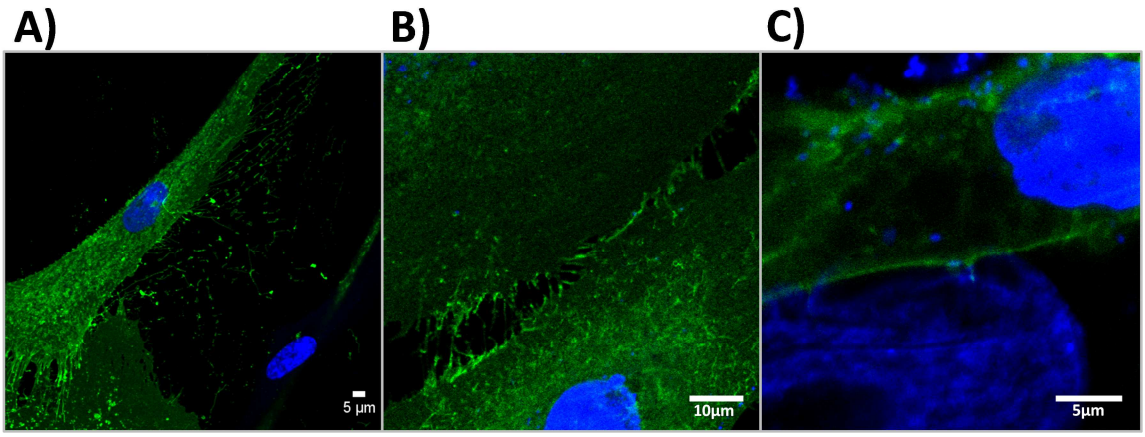

Figure 5.4. Subcellular localisation of GFP-CLDN11.

A) CLDN11 is a tight junction protein and localises to the cellular membrane, especially to the sites of a cell-cell contact **(B)**, also between transfected and untransfected cells **(C)**.

senescence markers and induction of cell-cycle arrest in Chapter 3. After transfection, cells were cultured for 48 hours to allow for expression of the plasmid-encoded GFP-tagged proteins. This was followed by another 48 hours of saquinavir treatment to induce prelamin A accumulation and the senescent phenotype. Cells were then harvested and prepared for FACS analysis of immunolabelled senescence markers $p16^{INK4a}$, IL6, and β-galactosidase (GLB1). Dose response curves to increasing GFP signal was calculated as described in the previous section for a population of 5000 transfected cells. To determine the cut-off for GFP signal and to distinguish transfected cells (real GFP signal) from non-transfected (background autofluorescence), each FACS analysis always included a non-transfected cell control. The dose-response to expression of GFP-tagged proteins showed that acute overexpression can actually contribute to the senescent phenotype, rather than prevent it (Figure 5.5). After reaching certain expression level, which varied between GFP-tagged proteins, cells began to show increasing expression of senescence markers. For example, for GFP-CLDN11 expression signal (measured as GFP intensity) above Log 1.5 level began to correlate with increasing expression of tested senescence markers, including prelamin A. For tPA-GFP expression the response started earlier, at the Log 1.2 GFP intensity level. Presumably, exogenous expression of proteins may put additional strain on cell homeostasis and trigger a stress response in cells when the overexpression exceeds a certain threshold. Plausibly, this could lead to potentiation of the senescence programme, for example by leading to the endoplasmic reticulum stress and an unfolded protein response (Sharpless and Sherr, 2015). All the tested GFP-tagged proteins, when acutely expressed, led to increase in expression of $p16^{INK4a}$,

IL6, and GLB1. Interestingly, increasing expression of tPA-GFP (Figure 5.5 B) and GFP-F3 correlated with a decrease in prelamin A in HeLa cells treated with saquinavir.

Based on these dose-response curves, a threshold for cut off was determined

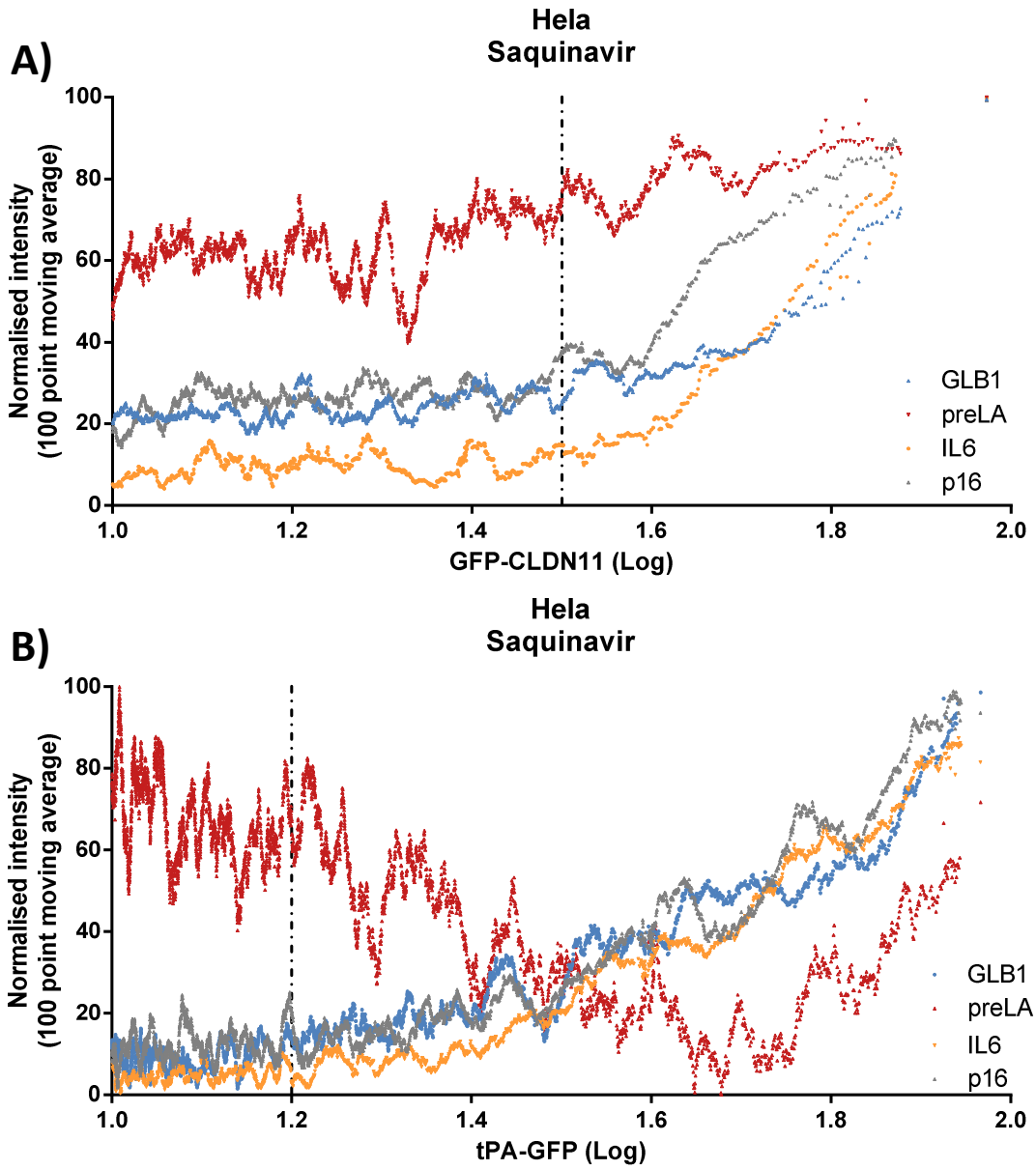

Figure 5.5. Expression of senescence markers in response to increasing level of GFP-tagged proteins.

HeLa cells were transfected with GFP-tagged CLDN11 **(A)** or tPA **(B).** 48 hours post-transfection, cells were treated with saquinavir for another 48 hours, harvested and analyses by FACS. X axis represents GFP-tagged protein expression level, transformed into logarithmic scale. Y axis represents normalised intensity of senescence markers after applying 100 point moving average. Each data point represents a measurement for a single cell. Total cell number 5000. p16, $p16^{INK4a}$; GLB1, β-galactosidase; IL6, interleukin 6; preLA, prelamin A. Vertical line indicates applied cut-off threshold for subsequent analysis.

separately for expression of each GFP-tagged candidate protein (in the examples of GFP-CLDN11 and tPA-GFP it is indicated as a vertical line in the plots in Figure 5.5). For further analysis, only cells expressing moderated levels of GFP-tagged protein were selected. This level was chosen so not to cause additional stress to the cells as monitored by expression of senescence markers.

5.2.3 Effects of overexpression of GFP-tagged candidates on senescence marker levels

After determination of the cut-off threshold for the expression level of the studied GFP-tagged proteins, as explained in the previous section, expression of the senescence markers was analysed in the selected subpopulations as described below. Cell transfection with plasmid DNA was never 100% efficient, and substantial number of cells remained GFP negative, showing GFP fluorescence intensity at the same range as untransfected control cells (Figure 5.6 A). FACS analysis permitted distinction between these two subpopulations within the same sample.

HeLa cells were transfected with plasmids encoding the GFP-tagged candidate proteins and induced to accumulate prelamin A with saquinavir. Untransfected cells were always included in the analysis for determination of background fluorescence for the GFP channel. Then, in the transfected cell sample, a subpopulation of untransfected cells was selected. A second subpopulation was selected based on the dose-response curves (described in the previous section), and gated around the moderate expression level of GFP-tagged proteins. These two subpopulations had matching numbers of cells. The expression level of senescence markers was measured for the entire subpopulation and calculated as a geometric mean fluorescence

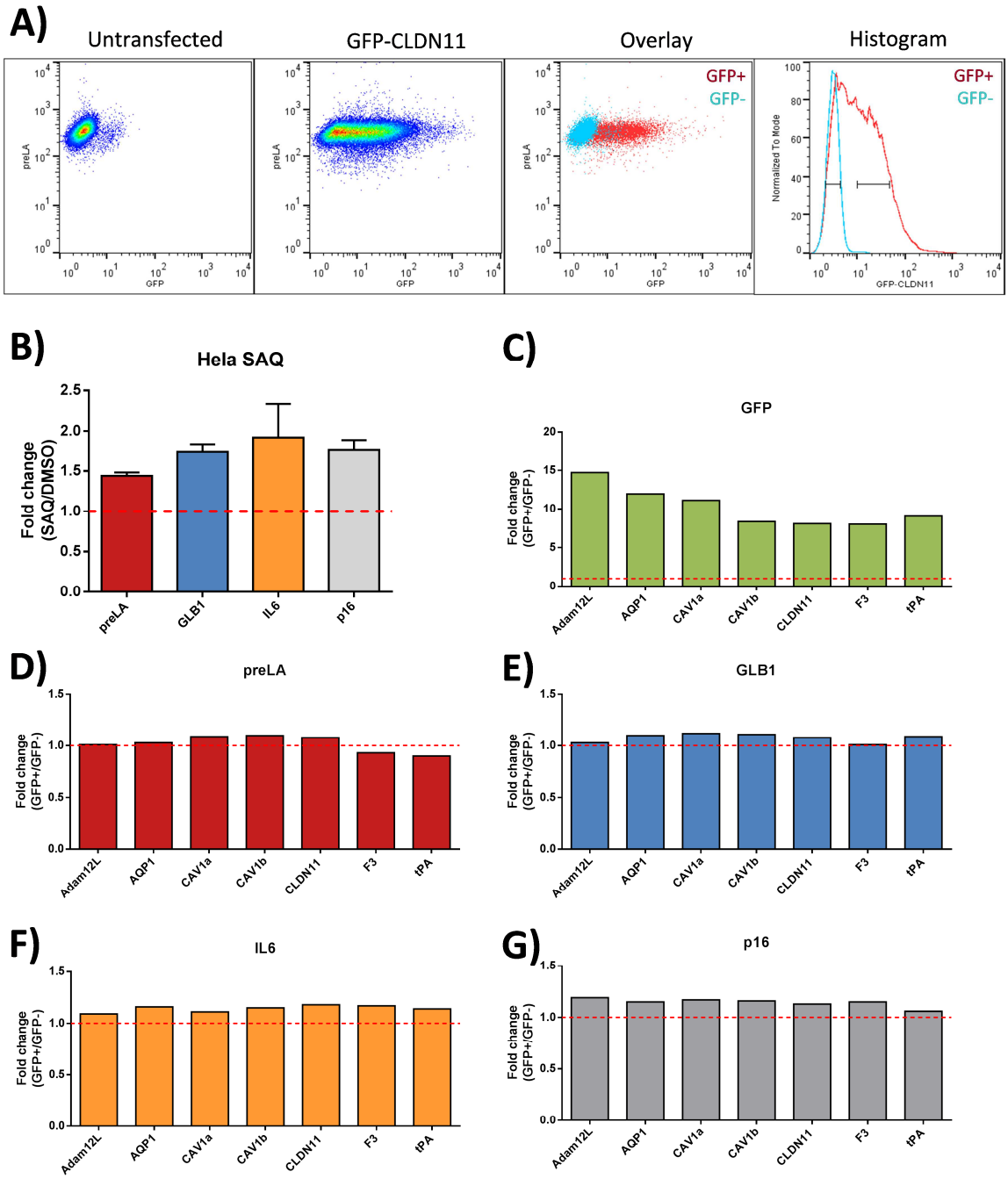

Figure 5.6. Effect of the expression of GFP-tagged candidate proteins on the levels of senescence markers in HeLa cells treated with saquiavir.

A) An example of dot plots from FACS analysis representing population of: untransfected cells, cells expressing GFP-CLDN11 and overlay of the two dot plots. Last diagram in panel (A) represents the overlay dot plot as a histogram, with indication of gates used for selecting GFP negative and GFP positive cell subpopulation within the transfected cell sample. **B)** Fold change of the GMFI measured for corresponding proteins in untransfected cells treated with either saquinavir or (SAQ) or DMSO (vehicle) control. **C) –G)** Fold change of the GMF measured for corresponding proteins (indicated above each graph) between GFP positive and GFP negative cells within a population of cells transfected with plasmid encoding GFP-tagged version of studied candidate proteins (indicated below each bar). GMFI, geometric mean fluorescence intensity; GFP, green fluorescent protein; preLA, prelamin A; GLB1, β-galactosidase.

intensity (GMFI). This approach helped to minimise the impact of potential variations in cell immunolabelling between the different samples, since the subpopulations were within the same sample. Each transfection experiment was accompanied by control samples representing untransfected cells treated with saquinavir or DMSO (vehicle), in order to validate senescence induction and the increased expression of senescence markers in saquinavir treated cells (Figure 5.6 B).

Pairwise comparison of GFP negative and GFP positive subpopulations within the sample showed that there is a substantial increase in expression of all GFP-tagged proteins (Adam12L, AQP1, CAV1α. CAV1β, CLDN11, F3, tPA), as expected (Figure 5.6 C). However, when the expression of senescence markers was analysed, no

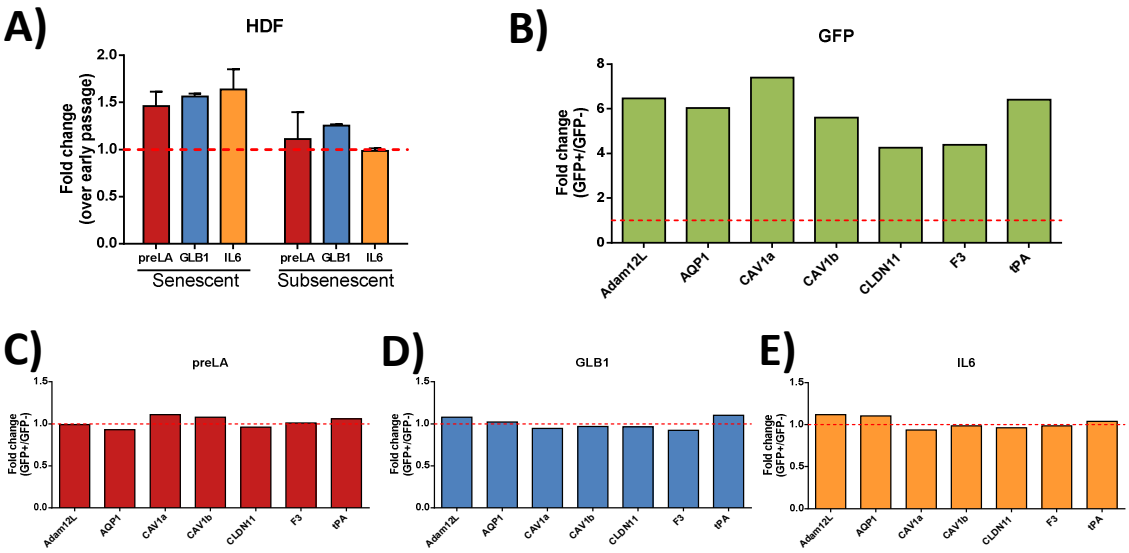

Figure 5.7. Effect of the expression of GFP-tagged candidate proteins on the levels of senescence markers in subsenescent HDFs.

A) Fold change of the GMFI measured for corresponding proteins in untransfected HDFs. Senescent cells were at passage 40 and over. Subsenescent cells were at passage 34, while early passage cells were at passage below 22. **B) –E)** Fold change of the GMF measured for corresponding proteins (indicated above each graph) between GFP positive and GFP negative cells within a population of cells transfected with plasmid encoding GFP-tagged version of studied candidate proteins (indicated below each bar). GMFI, geometric mean fluorescence intensity; HDF, human dermal fibroblast; GFP, green fluorescent protein; preLA, prelamin A; GLB1, β-galactosidase.

substantial difference was observed between the GFP positive and GFP negative subpopulations for either of the senescence markers (Figure 5.6 D-G).

A similar analysis was performed for HDFs. Plasmids encoding GFP-tagged proteins were transfected into subsenescent cells at passage 34 because senescent (late passage) HDFs are very difficult to transfect and they did not recover after electroporation. When compared to early passage cells (passage 22 and below), the untransfected cell control showed that subsenescent cells displayed only modest elevation in β-galactosidase expression, while IL6 and prelamin A remained unchanged (Figure 5.7 A). Transfected subsenescent HDFs, after allowing them to overexpress

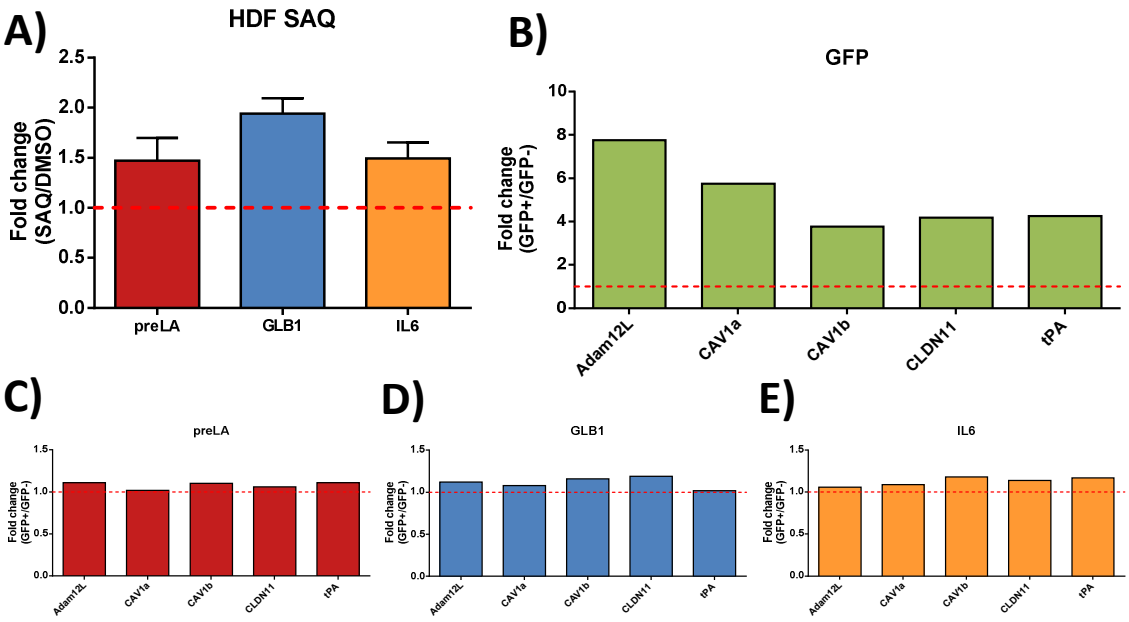

Figure 5.8. Effect of the expression of GFP-tagged candidate proteins on the levels of senescence markers in HDFs accumulating prelamin A.

A) Fold change of the GMFI measured for corresponding proteins in untransfected early passage HDFs treated with either saquinavir (SAQ) or vehicle control (DMSO). **B) –E)** Fold change of the GMF measured for corresponding proteins (indicated above each graph) between GFP positive and GFP negative cells within a population of cells transfected with plasmid encoding GFP-tagged version of studied candidate proteins (indicated below each bar). GMFI, geometric mean fluorescence intensity; HDF, human dermal fibroblast; GFP, green fluorescent protein; preLA, prelamin A; GLB1, β-galactosidase.

plasmid encoded proteins, were subject to FACS analysis, as described for HeLa cells earlier. Similar to the observations in HeLa cells, comparison between GFP positive and GFP negative HDFs showed increased expression of the studied GFP-tagged proteins. It was not however accompanied by significant alterations in expression of senescence markers (Figure 5.7 B-E).

In addition, early passage HDFs were also analysed. Cells were subject to transfection, followed by treatment with saquinavir to induce prelamin A accumulation, and FACS analysis. As expected, untransfected cells accumulating prelamin A showed increased expression of senescence markers when compared to DMSO treated cells (Figure 5.8 A). However, as with other experiments, increased expression of the GFP-tagged candidate proteins had only moderate effect on the levels of tested senescence markers (Figure 5.8 B-E).

5.3 DISCUSSION

Human dermal fibroblasts showed significant underexpression of Adam12, AQP1, CAV1, CLDN11, F3, and PLAT genes not only in replicative senescence, but also in senescence induced by prelamin A accumulation upon saquinavir treatment. Moreover, these six genes were also underexpressed in the Zmpste24 siRNA knock-down study model. Published literature implied a role for proteins encoded by these genes in senescence and the ageing process. Thus they made interesting candidates whose loss of activity might contribute to the execution of a senescence programme.

Data reported in this chapter represent an attempt to functionally evaluate the role of the six genes identified in the microarray screen as being consistently

underexpressed in senescent cells across the three studied models. Proteins encoded by these genes were GFP-tagged and overexpressed in senescent cells that, based on the microarray data, are depleted of the endogenously encoded products of the six genes. The expression level of the tagged proteins was monitored by measurement of GFP intensity. The effect of this approach on the senescence programme was studied by following expression of the downstream senescence markers $p16^{INK4a}$, β-galactosidase (GLB1), and IL6. It appears that overexpression of a single protein is insufficient to block or reverse the senescent phenotype. While moderate levels of GFP-tagged proteins had a minimal effect on the chosen senescence markers, high GFP-tagged protein expression appeared to potentiate expression of these markers. This is most likely an effect of additional strain on the ER, which can lead to accumulation of misfolded or unfolded proteins, and ultimately, the activation of unfolded protein response (Harding et al., 2002; Kaufman, 1999). This can further enhance the senescent phenotype (Campisi, 2013; Sharpless and Sherr, 2015).

Reinstated expression of GFP-tagged proteins did not prevent induction of senescence. This would suggest that their role in senescence mediation is not dominant. Other pathways that ensure the establishment of senescence most likely coexist in the studied models, and presumably more than one is triggered, both in prelamin A-induced and replicative senescence. Indeed, multiple stress signals can trigger senescence, often operating through coexisting effector pathways (Kuilman et al., 2010; Rodier and Campisi, 2011; Salama et al., 2014). In this study, only one candidate protein was overexpressed at a time. It may be necessary to simultaneously overexpress more than one candidate protein to observe reversal in expression of senescence markers. It could be achieved, for example, by tagging the studied

candidate proteins with red fluorescent protein (RFP) and co-transfecting two at a time, one GFP-tagged and the other RFP-tagged. It is also possible that simultaneous expression of more than two proteins is required. Alternatively, instead of focusing on the inhibition/reversal of the senescent phenotype, expression of the candidate genes could be knocked-down in proliferating cells to investigate if this may lead to senescence.

Although the role of the underexpressed genes in senescence regulation in the studied cellular models has not been determined yet, this research developed a powerful assay for the simultaneous analysis of senescence-associated protein expression. This offers the potential of a three way analysis to look for networks and their components while accounting for concentration and cross-response between these components. This will be a powerful tool in subsequent research.

In addition data presented here demonstrated that the level of prelamin A expression positively correlates with levels of senescence markers on a cell-by-cell basis. Prelamin A dose and induction of senescence markers appears to be a linear response, showing apparently earlier/bigger effect on $p16^{INK4a}$ tumour suppressor expression in HDFs, but not in HeLa cells. Moreover, at least to some extent, similar correlation can be observed in a sub-population of untreated early passage HDFs that are prelamin A positive. This may indicate a possible hormetic effect and raises several questions and possible scenarios. Is a low level of prelamin A a normal regulator in non-senescent cells? Is tight regulation of Zmpste24 required for normal function because it is supposed to leave a small prelamin A pool? Or perhaps this usefully varies around the cell cycle with rate of lamin A synthesis and nuclear import? The developed FACS assay may be able to answer some of these questions.

CHAPTER 6

6 Secretory phenotype in prelamin A-induced senescence

6.1 INTRODUCTION

Inflammation, under normal conditions, is a defensive mechanism that occurs in tissues in response to an insult such as injury, infection or toxin exposure (Florey, 1970; Lawrence et al., 2002; Majno, 1975). In the inflammatory process, activation of the immune system aims at neutralising the cause and effects of the insult. The ultimate goal of this process is to protect the tissue and organism from further damage. Inflammation can either be acute, leading to relatively quick neutralisation of the insult within days, or chronic, which persists over an extended period of time. Although the inflammatory process is fundamentally a protective response, when uncontrolled it may be harmful and lead to tissue damage, loss of function and resultant severe disease.

Chronic inflammation is often observed in ageing (Franceschi et al., 2007). It is characterised by an elevated level of proinflammatory factors in plasma or in the tissue environment persisting over years. The magnitude of the chronic inflammatory response is many-fold lower than that observed in acute inflammation (Nathan, 2002; Sarkar and Fisher, 2006). Many age-related diseases such as Alzheimer's disease, Parkinson's disease, atherosclerosis, diabetes, osteoarthritis and cancer are associated with chronic inflammation. Increased serum levels of proinflammatory cytokines and chemokines measured near the sites of pathology in many of these conditions have been demonstrated (Glass et al., 2010; Vasto et al., 2007). The continued presence of

pro-inflammatory mediators can further contribute to degradation of the tissue microenvironment. This occurs either through their inner proteolytic enzymatic activities, or the persistent activation of innate immune cells (Campisi, 2005; Prelog, 2006). The process of chronic inflammation in ageing, resulting from extended exposure to antigenic stresses over a lifetime and progressive activation of immune cells, has been termed “inflammageing” (Franceschi and Campisi, 2014; Vasto et al., 2009). Although increased secretion of pro-inflammatory mediators in inflammageing is often attributed to macrophages and other innate immune system cell types, these are not the only cells which produce such mediators.

Cells of non-immune origin, like fibroblasts and epithelial cells, have been shown to secrete a number of pro-inflammatory cytokines and chemokines upon senescence induction (Coppé et al., 2008; Kuilman and Peeper, 2009). It is suggested that increased frequency of senescent cells within aged tissues is a major contributor to chronic inflammation (Coppé et al., 2010a; Freund et al., 2010). This is because senescent cells remain metabolically active and secrete a vast range of cytokines, growth factors and proteases, albeit at a lower level than seen at sites of acute inflammation in the presence of recruited immune cells (Acosta et al., 2008; Bavik et al., 2006; Chang et al., 2002; Coppé et al., 2008; Kortlever et al., 2006; Kuilman et al., 2008; Liu and Hornsby, 2007; Novakova et al., 2010; Wajapeyee et al., 2008). The ongoing production of these proteins by senescent cells can further impact tissue homeostasis for as long as the senescent cells persist. The term “senescence associated secretory phenotype” (SASP) has been introduced to describe the phenomenon of secretion of a broadly defined protein set in senescence (Coppé et al., 2008), also referred to as senescence-messaging secretome (SMS) (Kuilman and

Peeper, 2009). SASP is a broad term, encompassing dozens of proteins that demonstrate association with inflammation, modulation of the extracellular matrix (ECM), and proliferation. The specific composition of SASP varies between both cell and senescence types, greatly depending on the cell context, stress type, and its duration and magnitude. Factors such as interleukins (IL6, IL8, IL1), monocyte chemotactic proteins (MCP2, MCP3), granulocyte macrophage colony-stimulating factor (GM-CSF), matrix metalloproteinases (MMPs), growth regulated oncogene α (GROα) and a number of insulin-like growth factor-binding proteins (IGFBPs) appear to be the most prominent SASP factors, observed in multiple senescence types (Freund et al., 2010; Salama et al., 2014; Young and Narita, 2009).

Considering the complexity of senescence and diversity among SASP components it is not surprising that SASP is controlled at multiple levels, from transcriptional regulation to autocrine feedback loops. A growing body of evidence indicates that the NF-κB signalling pathway is the major regulator of the SASP response (Ren et al., 2009; Salminen et al., 2012). NF-κB, the major cell regulator of both adaptive and innate immune response (Vallabhapurapu and Karin, 2009), has been shown to cooperate with the C/EBP β transcription factor in the regulation of expression of many SASP components. Examples include IL1, IL6, IL8, MIF and others (Acosta et al., 2008; Chien et al., 2011; Hardy et al., 2005; Kuilman et al., 2008; Orjalo et al., 2009). Another potent transcription regulator of SASP factors is mammalian p38 mitogen-activated protein kinase (MAPK). It has been linked to enhanced expression of SASP factors such as IL6, IL8, RANTES (CCL5), MCP1, MIP1α/β, and others through various mechanisms of NF-κB activation (Freund et al., 2011; Saccani et al., 2002; Schieven, 2009). Other than p38, the retinoic acid inducible gene 1 (RIG-1) signalling

pathway can promote NF-κB activity. This leads to increased secretion of IL6 and IL8, a process that can be blocked with the antiageing hormone Klotho (Liu et al., 2011). DNA damage, TGFβ-TAK1 pathway, ceramides, and the HMGB1 protein, all of which activate NF-κB, can also potentiate SASP (Salminen et al., 2012).

Posttranscriptional regulation adds another level to SASP control. It is achieved by affecting the stability of the mRNAs which encode SASP factors (via mRNA binding proteins) as well as through microRNA-mediated degradation (Schott and Stoecklin, 2010). Regulation of the stability and translational status of mRNA encoding SASP components offers another means of tight control over the expression of encoded proteins and allows a rapid response to stress and inflammatory signals. A number of mRNA binding proteins, including nuclear factor 90, among many others, can affect turnover and translation of mRNA encoding SASP components further contributing to senescence and the repertoire of secreted proteins (Abdelmohsen et al., 2008; Tominaga-Yamanaka et al., 2012). Several microRNAs have also been shown to regulate the onset of SASP by targeting mRNA encoding factors belonging to the NF-κB signalling pathway (Olivieri et al., 2013). Interestingly, miR-146a/b was shown to block excessive secretion of IL6 and IL8 by inhibiting IRAK1 (IL-1 receptor-associated kinase 1) expression and abolishing signal transduction via the IL1 pathway (Bhaumik et al., 2009). Abated IL1 signalling lowered IL6 and IL8 expression in response to oversecretion of these interleukins. Such observations only underscore the plasticity of the SASP and existence of multiple feed-back control loops that offer tight regulation of SASP appearance.

Recently, the mammalian target of rapamycin kinase (mTOR) pathway has also been shown to modulate SASP by affecting translation of SASP regulators (Herranz et

al., 2015; Laberge et al., 2015). As a sensor of nutrient and growth signals, high mTOR kinase activity can promote cell proliferation and limit lifespan, whereas inhibited mTOR signalling favours longevity (Harrison et al., 2009; Kapahi et al., 2010; Stanfel et al., 2009). Laberge and colleagues demonstrated that inhibition of mTOR by rapamycin led to suppressed translation of membrane-bound IL1α. This in turn abated the transcriptional activity of NF-κB, the main regulator of the SASP (Laberge et al., 2015). mTOR signalling has also been shown to regulate SASP through MAPKAPK2 kinase translation (Herranz et al., 2015). In oncogene-induced senescence, the MAPKAPK2 kinase inhibits ZFP36L1 through phosphorylation. The ZFP36L1 is an mRNA-binding protein involved in ARE (AU-rich element)-mediated decay of many SASP factors. As a result, upon senescence induction and phosphorylation of ZFP36L1, SASP appears. Whereas inhibition of mTOR downregulates MAPKAPK2 translation; ZFP36L1 remains active and supresses SASP by the decay of mRNA encoding SASP components.

The existence of multiple mechanisms as well as positive and negative feedback loops that regulate SASP most likely contribute to SASP plasticity and context-dependence. SASP has clearly beneficial roles, because it reinforces senescence growth arrest to reduce the risk of oncogenic transformation in an autocrine manner (Acosta et al., 2008; Kuilman et al., 2008; Wajapeyee et al., 2008; Yang et al., 2006). Through a variety of secreted cytokines, SASP may also potentiate activation of the immune system to clear senescent cells and promote tissue repair (Kang et al., 2011; Krizhanovsky et al., 2008; Xue et al., 2007). Conversely, the pleiotropic effect of SASP may be deleterious in ageing tissues when control pathways are disregulated or less effective. The persistent inflammation creates an environment which could potentially promote cancerogenesis (Ben-Neriah and Karin, 2011). Some SASP factors have been

shown to induce the epithelial-mesenchymal transition that could contribute to tumour invasiveness and metastasis (Coppé et al., 2008; Coppé et al., 2006; Ren et al., 2009). SASP factors can also exhibit their activity in a paracrine manner, inducing senescence in surrounding cells (Acosta et al., 2013), in a process termed "bystander senescence" (Nelson et al., 2012). Expansion of such a senescent footprint in tissues, from a few senescent cells to broader surroundings, could potentially help to ensure that the entire pre-neoplastic lesion is cleared by the immune system. Conversely however, the trans-effect of senescent cells on neighbouring non-senescent cells could pose a risk of a larger cell loss within the tissue fraction, resulting in a much greater impact on homeostasis (Tchkonia et al., 2013). Considering the complexity of SASP and potentially opposing effects of its action, more studies are required to better understand this phenomenon, its composition in response to different cellular stresses, and potential outcomes.

The microarray data described in Chapter 4 strongly suggested activation of immune response in aged HDFs and the differential expression of many SASP components in the studied laboratory models of ageing. Analysis of the transcriptome implied that prelamin A-induced senescence upon saquinavir treatment shares many similarities with replicative senescence, especially in regard to a pro-inflammatory response. To my knowledge, there are no comprehensive studies of SASP in prelamin A accumulating cells. In this chapter, secretion of over 30 SASP components was analysed, both in replicative senescence and in prelamin A-induced senescence. Moreover, secretion of SASP factors was also studied in cells undergoing apoptosis in order to further characterise its relation to senescence. Consistent with the microarray experiments, HDFs were used as a model cell line, while SASP analysis of

conditioned cell culture medium was performed using Luminex bead-based immunoassay. Subsequent ELISA testing validated observations from the multiplex immunoassay.

6.2 RESULTS

6.2.1 Multiplex analysis of senescence associated secretory phenotype

The ageing process of an organism is accompanied by chronic inflammation with the continued presence of proinflammatory proteins at elevated levels, both in the tissue microenvironment as well as circulating in blood plasma. These levels, however, are many-fold lower than those observed in acute inflammation (Franceschi et al., 2007; Sarkar and Fisher, 2006). Senescent cells have been shown to secrete a broad range of cytokines, chemokines, growth factors, and proteases that jointly have been termed the senescence associated secretory phenotype (SASP) (Freund et al., 2010; Salama et al., 2014; Young and Narita, 2009).

In order to study the SASP of HDFs acutely accumulating prelamin A and how this compares to replicative senescence, a multiplex immunoassay based on the Luminex platform was employed (Lin et al., 2015; Tighe et al., 2013). Cells were cultured without growth medium change for five days to maximise medium enrichment in secreted proteins. The supernatant was then harvested and analysed by the Luminex bead-based multianalyte assay. This assay utilises a mixture of colour-coded beads. Each bead has a unique amount of two dyes, red and infrared (IR), both excited by the 635 nm laser. Therefore the beads can be identified by a 2 parameter definition. One determines the amount of red dye, and the other the

intensity coming from the IR dye. In the assay for this study, 34 types of beads representing a unique combination of the two dyes were used (one bead type per each analyte). Beads were pre-coated with analyte-specific antibodies that recognised the targets present in the conditioned cell culture supernatant. In the next step, biotinylated detection antibodies, specific to the analytes of interest, were added to form an antibody-antigen sandwich. It was followed by the addition of phycoerythrin-conjugated streptavidin with subsequent detection reading on a dual-laser flow-based instrument. One laser detected the two channels of bead colour to identify the secreted protein that was being analysed. Simultaneous scanning with the second laser measured the magnitude of the phycoerythrin-derived signal, which was in direct proportion to the amount of analyte bound. A minimum of 50 beads of each type were quantified per sample. To allow for cross-sample comparison, the concentration of detected proteins secreted into the culture medium was normalised to the cell number from each sample tested. This number had been predetermined at the time of medium harvest.

6.2.1.1 *Selection of analytes for SASP investigation*

A panel of 34 analytes for SASP determination via Luminex bead-based assay was composed. It included a range of proteins that have been previously identified as SASP components in various types of senescence or have demonstrated a correlation with ageing (Table 6.1). The selection contained not only cytokines and chemokines commonly accepted as hallmarks of SASP, but also a number of growth factors, extracellular matrix remodelling proteins, components of the apoptosis-signalling pathway, and proteins demonstrating differential expression based on the microarray

analysis described in Chapter 4. While the list could have been more comprehensive with the inclusion of other proteins, the bead-based immunoassay is limited by the available analytes, bead-compatibility, and analysis conditions required for each analyte (e.g., buffer compatibility, detection range, etc.). As a result of these limitations, the analytes selected for this study were chosen to represent the broadest possible spectrum of SASP components. The selection included factors that are broadly acknowledged in SASP, some that demonstrate differential secretion dependent on the senescence type, and others that have yet to be characterised in the context of SASP.

Table 6.1. List of analytes selected for the multiplex immunoassay.

Analyte	Reason for selection	Reference
Autotaxin (ENPP-2) (Extracellular Lysophospholipase D)	Phospholipase generating lysophosphatidic acid (LPA) that stimulates cell motility and tumourigenesis	(Umezu-Goto et al., 2002)
EGF (Epidermal Growth Factor)	Secreted in replicative senescence	(Coppé et al., 2008)
ENA78 (CXCL5) (Neutrophil-Activating Protein 78)	Moderately increased secretion in oncogene- and DNA damage-induced senescence but unchanged in replicative senescence	(Coppé et al., 2008)
FAS (Cell Surface Death Receptor)	Secreted in replicative, but not in oncogene-induced senescence; mediates apoptosis in senescent tumour cells	(Coppé et al., 2008; Crescenzi et al., 2011)
FAS ligand (TNFSF6)	Upregulated in apoptotic and senescent tumour cells; cooperates with FAS	(Crescenzi et al., 2011; Nihal et al., 2014)
FGF (basic) (Fibroblast Growth Factor 2)	Secreted in multiple types of senescence (replicative, oncogene-induced, DNA damage-induced) by several cell types (including fibroblasts)	(Coppé et al., 2008)
G-CSF (Granulocyte Colony-Stimulating Factor)	Secreted in oncogene-induced senescence but not in replicative senescence	(Coppé et al., 2008)
GDF15 (Growth Differentiation Factor 15)	Secreted in oncogene-induced senescence and in paracrine mediated senescence; activated via TGFβ signalling	(Acosta et al., 2013)

Analyte	Reason for selection	Reference
GM-CSF (Granulocyte Macrophage-Colony Stimulating Factor)	Highly increased secretion in multiple types of senescence (replicative, oncogene-induced, DNA damage-induced) by several cell types (including fibroblasts)	(Acosta et al., 2008; Coppé et al., 2008)
GROα (CXCL1) (Neutrophil-Activating Protein 3)	Highly increased secretion in multiple types of senescence (replicative, oncogene-induced, DNA damage-induced) by several cell types (including fibroblasts)	(Acosta et al., 2008; Bavik et al., 2006; Coppé et al., 2008)
ICAM1 (Intercellular Adhesion Molecule 1)	Moderately increased secretion in multiple types of senescence (replicative, oncogene-induced, DNA damage-induced) by several cell types (including fibroblasts)	(Coppé et al., 2008; Rodier et al., 2009)
IGFBP1 (Insulin Growth Factor Binding Protein 1)	Secreted in replicative and DNA damage-induced senescence by fibroblasts	(Coppé et al., 2008)
IGFBP3 (Insulin Growth Factor Binding Protein 3)	Regulator of stress-induced senescence in cooperation with PLAT; secreted in replicative and DNA-damage induced senescence	(Bavik et al., 2006; Elzi et al., 2012; Rodier et al., 2009)
IL17α (Interleukin 17α)	Proinflammatory cytokine, associated with chronic inflammatory diseases; involved in regulation of IL6 expression	(Ruddy et al., 2004; Shen et al., 2015)
IL1α (Interleukin 1α)	Highly increased secretion in oncogene-induced and DNA damage-induced senescence, but not replicative; important for NF-κB activation and SASP regulation	(Acosta et al., 2008; Coppé et al., 2008; Liu and Hornsby, 2007)
IL1β (Interleukin 1α)	Moderately increased secretion in multiple types of senescence (replicative, oncogene-induced, DNA damage-induced) by several cell types (including fibroblasts)	(Coppé et al., 2008; Liu and Hornsby, 2007)
IL6 (Interleukin 6)	Highly increased secretion in multiple types of senescence (replicative, oncogene-induced, DNA damage-induced) by several cell types (including fibroblasts); a commonly accepted hallmark of senescence	(Acosta et al., 2008; Coppé et al., 2008; Rodier et al., 2009)
IL8 (CXCL8) (Interleukin 8)	Highly increased secretion in multiple types of senescence (replicative, oncogene-induced, DNA damage-induced) by several cell types (including fibroblasts)	(Acosta et al., 2008; Bavik et al., 2006; Coppé et al., 2008; Rodier et al., 2009)
MCP1 (CCL2) (Monocyte Chemotactic Protein 1)	Highly increased secretion in multiple types of senescence (replicative, oncogene-induced, DNA damage-induced) by several cell types (including fibroblasts); also elevated in ageing and senescent tumour cells	(Acosta et al., 2008; Coppé et al., 2008; Iannello et al., 2013; Liu and Hornsby, 2007; Rodier et al., 2009; Seidler et al., 2010)
MCP3 (CCL7) (Monocyte Chemotactic Protein 3)	Attracts macrophages during inflammation and metastasis; member of senescence associated gene signature; differentially expressed in aged cells	(Coppé et al., 2008; Coppola et al., 2014; Metcalf et al., 2015)
MIF (Macrophage Migration Inhibitory Factor)	Moderately increased secretion in multiple types of senescence (replicative, oncogene-induced, DNA damage-induced) by several cell types (including fibroblasts)	(Coppé et al., 2008)

Analyte	Reason for selection	Reference
MIP1α (CCL3) (Macrophage Inflammatory Protein 1α)	Highly increased secretion in multiple types of senescence (replicative, oncogene-induced, DNA damage-induced) by several cell types (including fibroblasts)	(Coppé et al., 2008)
MIP1β (CCL4) (Macrophage Inflammatory Protein 1β)	Inflammatory chemokine showing increased expression with ageing	(Cheng et al., 2015; Chiu et al., 2006; Seidler et al., 2010)
MIP3α (CCL20) (Macrophage Inflammatory Protein 3α)	Moderately increased secretion in multiple types of senescence (replicative, oncogene-induced, DNA damage-induced) by several cell types (including fibroblasts)	(Coppé et al., 2008; Rodier et al., 2009)
MMP1 (Matrix Metalloproteinase 1)	Highly increased secretion in multiple types of senescence (replicative, oncogene-induced, DNA damage-induced) by several cell types (including fibroblasts)	(Coppé et al., 2008; Liu and Hornsby, 2007)
MMP2 (Matrix Metalloproteinase 2)	Secreted in replicative and DNA damage-induced senescence in fibroblasts	(Bavik et al., 2006)
MMP3 (Matrix Metalloproteinase 3)	Highly increased secretion in multiple types of senescence (replicative, oncogene-induced, DNA damage-induced) by several cell types (including fibroblasts)	(Coppé et al., 2008; Liu and Hornsby, 2007; Parrinello et al., 2005)
PAI1 (SERPIN E1) (Plasminogen Activator Inhibitor 1)	Regulator of PLAT and IGFBP3 in mediating stress-induced senescence; also secreted in replicative senescence	(Elzi et al., 2012; Kortlever et al., 2006; West et al., 1996)
PCSK9 (Proprotein Convertase Subtilisin/ Kexin Type 9	Plays a role in cholesterol and fatty acid metabolism; elevated in aged individuals; correlates with plasma levels of LDL-cholesterol;	(Kosenko et al., 2013; Lakoski et al., 2009)
RANTES (CCL5)	Moderately increased secretion in DNA damage-induced senescence in fibroblasts	(Liu and Hornsby, 2007)
TNFα (Tumour Necrosis Factor α)	Senescence inducer in cancer cells; elevated in aged organisms	(Braumuller et al., 2013; Chen et al., 2013)
TRAIL R2 (TNFRSF10B) (Tumour Necrosis Factor Receptor Superfamily, Member 10b)	NF-κB activator; upregulated with age; regulator of apoptosis	(Edwards et al., 2007; Wu et al., 1997)
VCAM1 (Vascular Cell Adhesion Molecule 1)	Cell adhesion and signalling molecule; secreted in replicative senescence	(Yepuri et al., 2012)
VEGF (Vascular Endothelial Growth Factor)	Secreted in oncogene- and DNA damage-induced senescence, but not in replicative senescence	(Coppé et al., 2008)

6.2.1.2 Protein secretion by HDFs upon various stimuli

Five conditions were tested to assess the secretory phenotype of HDFs:

1. HDFs senesced by replicative exhaustion (passage 40-42) in comparison with early passage cells (up to passage 22)
2. Early passage HDFs senesced by acute prelamin A accumulation upon saquinavir treatment in comparison with passage-matched cells exposed to DMSO (vehicle control).
3. Passage-matched HDFs treated with darunavir to compare with saquinavir-treated cells in order to account for off-target effects of the HIV-PI.
4. Early passage HDFs with Zmpste24 siRNA knock-down in comparison with cells transfected with control siRNA.
5. Early passage HDFs treated with camptothecin to account for the secretory phenotype in response to apoptosis.

Saquinavir and darunavir treatments, with their corresponding DMSO controls, were performed for 48 hours prior to the five day period of culture medium conditioning, with continuous drug presence in the medium. SiRNA knock-down was also performed 48 hours prior to the initiation of medium conditioning. SiRNA transfection was not repeated during the experiment because it requires multiple medium changes.

Camptothecin (CPT) is a well-recognised inducer of apoptosis that acts through inhibition of topoisomerase I (Tomicic and Kaina, 2013). Apoptosis and senescence can both be evoked by broadly defined cellular stress and each has a protective role against the unrestricted proliferation of damaged cells. Despite the fact that they

represent two distinct effector programmes, there are overlapping signalling pathways in both processes (Childs et al., 2014). Thus CPT-treated cells were also included in the secretome profiling analysis. The addition of CPT led to cell death within five days of cell culture. At the beginning of the experiment, 150 000 cells were seeded. This roughly corresponded to the cell number at the end time point for the other four conditions. It should be noted that the concentration of analytes for CPT-treated samples was normalised to 150 000 cells, representing the cell count at the start point of the experiment. The large scale cell death observed indicates that some detected analytes may have been intracellular and released on apoptosis rather than actively secreted by the cells as a part of a phenotypic programme. *In vivo*, unlike the macrophage-free culture environment, these proteins might not be observed because apoptotic cells are ingested intact before their contents are released (Erwig and Henson, 2007).

The data for analysis of protein secretion by HDFs exposed to the above described stimuli is presented in Table 6.2. The values represent the average concentration of specific analytes per thousand cells from three biological replicates. Of the 34 analytes tested, seven were below the detection threshold (EGF, G-CSF, GM-CSF, IL1α, IL1β, IL17, TNFα) while the PAI-1 secretion level was above the threshold, beyond estimation of concentration.

Table 6.2. Secretion of SASP components by HDFs in response to various stimuli. Values represent the average of three biological replicates and show concentration in [pg/1000 cells]. Numbers highlighted in red were obtained by extrapolation beyond the minimum or maximum data points on the standard curve. OOR, out of range beyond extrapolation, < below detection threshold, > above maximum quantifiable level. Early, HDFs at passage below 22; Late, HDF at passage above 40; DAR, darunavir treated early passage HDFs; SAQ, saquinavir treated early passage HDFs; siCTRL, early passage HDFs transfected with control siRNA; siZmpste24, early passage HDFs transfected with Zmpste24 siRNA; CPT, early passage HDFs treated with camptothecin.

Analyte	Early	Late	DMSO	DAR	SAQ	siCTRL	siZmpste24	CPT
Autotaxin	12.63	OOR <	14.98	15.01	28.21	20.52	26.32	11.05
EGF	OOR <	OOR <	OOR <	OOR <	OOR <	OOR <	OOR <	OOR <
ENA78	0.49	0.69	0.38	0.35	0.43	0.57	0.76	0.84
FAS	0.68	1.48	0.49	0.46	0.72	1.36	1.96	3.11
FAS ligand	0.05	0.11	0.22	0.21	3.80	0.08	0.10	0.04
FGF (basic)	0.05	0.13	0.03	0.03	0.06	0.06	0.06	1.40
G-CSF	OOR <	OOR <	OOR <	OOR <	OOR <	OOR <	OOR <	OOR <
GDF15	0.10	0.70	0.67	0.48	0.50	0.92	0.55	65.26
GM-CSF	OOR <	OOR <	OOR <	OOR <	OOR <	OOR <	OOR <	OOR <
GROα	0.62	0.64	0.54	0.47	0.85	0.60	0.55	2.23
ICAM1	OOR <	OOR <	OOR <	OOR <	OOR <	OOR <	OOR <	29.18
IGFBP1	0.24	0.65	0.23	0.22	0.34	0.46	0.46	0.37
IGFBP3	84.72	837.34	41.05	41.89	50.35	141.26	131.40	117.84
IL1α	OOR <	OOR <	OOR <	OOR <	OOR <	OOR <	OOR <	OOR <
IL1β	OOR <	OOR <	OOR <	OOR <	OOR <	OOR <	OOR <	OOR <
IL6	1.36	3.57	0.83	0.89	2.43	1.66	1.97	3.52
IL17α	OOR <	OOR <	OOR <	OOR <	OOR <	OOR <	OOR <	OOR <
IL8	1.07	0.63	1.28	1.10	0.51	1.21	1.56	3.88
MCP1	3.87	2.61	4.32	3.94	5.61	11.09	13.82	9.09
MCP3	OOR <	OOR <	0.16	0.15	0.26	0.25	0.29	0.22
MIF	4.53	17.16	5.21	3.65	8.91	10.20	12.18	202.55
MIP1α	0.03	0.14	0.13	0.12	0.70	0.17	0.12	0.22
MIP1β	0.37	1.08	0.19	0.17	0.43	0.44	0.51	0.38
MIP3α	0.09	0.20	0.06	0.06	0.19	0.14	0.14	0.13
MMP1	43.75	32.64	93.69	174.50	194.23	161.37	218.10	147.25
MMP2	41.74	128.54	20.55	19.32	51.25	47.77	53.64	43.73
MMP3	108.34	205.89	57.24	53.97	97.12	150.13	180.35	87.25
PAI1	OOR >	OOR >	OOR >	OOR >	OOR >	OOR >	OOR >	OOR >
PCSK9	1.50	4.45	1.04	1.04	3.73	1.93	2.20	2.62
RANTES	0.04	0.12	0.24	0.23	3.87	0.10	0.12	0.05
TNFα	OOR <	OOR <	OOR <	OOR <	OOR <	OOR <	OOR <	OOR <
TRAIL R2	0.29	0.83	0.16	0.14	0.37	0.37	0.41	0.97
VCAM1	4.78	11.37	2.95	2.69	4.68	6.00	7.36	5.99
VEGF	OOR <	OOR <	OOR <	OOR <	OOR <	OOR <	OOR <	0.34

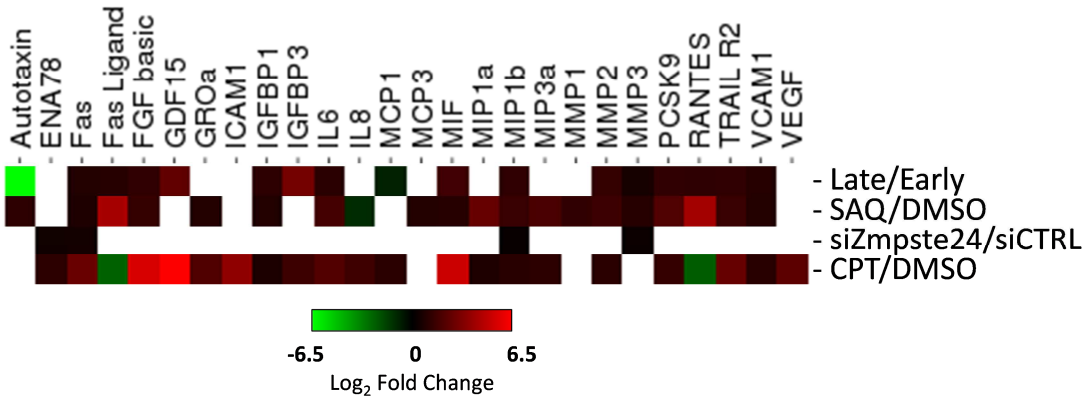

Figure 6.1. Secretion of SASP components.
Description as for **Table** 6.3.

Table 6.3. Secretion of SASP components. Log_2 fold changes are reported in the table for pairwise comparisons showing statistical significance at $P < 0.05$. * indicates analysis for values extrapolated beyond the minimum or maximum data points of the corresponding standard curves. Red colour highlights increased secretion while green indicates decreased. Late, late passage HDFs (over passage 40); Early, early passage HDFs (below passage 22); SAQ, saquinavir; DMSO, vehicle control; CPT, camptothecin; siZmpste24, Zmpste24 siRNA knock-down; siCTRL, control siRNA.

Analyte	Late/Early	SAQ/DMSO	siZmpste24/siCTRL	CPT/DMSO
Autotaxin	-6.61	0.91	-	-
ENA78	-	-	0.41	1.12
Fas	1.13	0.55	0.53	2.66
Fas Ligand	1.21	4.11	-	-2.57
FGF (basic)*	1.53	1.16	-	5.61
GDF15*	2.81	-	-	6.60
GROα	-	0.65	-	2.04
ICAM1*	-	-	-	3.75
IGFBP1	1.44	0.57	-	0.68
IGFBP3	3.30	-	-	1.52
IL6	1.39	1.55	-	2.08
IL8	-	-1.33	-	1.60
MCP1	-0.57	-	-	1.07
MCP3	-	0.66	-	-
MIF	1.92	0.77	-	5.28
MIP1α*	-	2.43	-	0.73
MIP1β	1.56	1.21	0.20	1.04
MIP3α	-	1.70	-	1.13
MMP1*	-	1.05	-	-
MMP2	1.62	1.32	-	1.09
MMP3*	0.93	0.76	0.26	-
PCSK9*	1.57	1.84	-	1.33
RANTES	1.49	4.02	-	-2.39
TRAIL R2	1.54	1.25	-	2.63
VCAM1*	1.25	0.67	-	1.02
VEGF*	-	-	-	2.41

6.2.1.3 Changes in secretory phenotype between test conditions

Pairwise comparison of the secretory phenotype in HDFs was performed as described in paragraph 6.2.1.2. The fold change was calculated for each of the secreted protein levels over their corresponding controls. The statistical significance of the observed changes was assessed by performing an unpaired two-tailed t-test for each comparison. Only those values with $P < 0.05$ are reported in Table 6.3 with the corresponding heat map shown in Figure 6.1. Darunavir-treated cells demonstrated no statistically significant difference in secretory phenotype when compared to DMSO control cells; therefore this comparison was excluded from the table and the figure. The table reports fold changes in secreted protein levels for 26 analytes, 13 of which overlapped between replicative senescence and prelamin A-induced senescence upon saquinavir treatment. Of those, only three (FAS, MIP1β and MMP3) were further shared with the Zmpste24 knock-out model. Interestingly, camptothecin, which triggers the apoptosis pathway, also appeared to be a potent inducer of expression of those proteins that are considered to be associated with senescence.

6.2.1.4 Validation of the multiplex immunoassay by ELISA

Luminex bead-based assay allowed for multiplexing of over 30 analytes simultaneously in the same sample. A number of proteins which were expected to be found in this analysis were not detected, despite their reported roles in SASP. GM-CSF and IL1α (Acosta et al., 2013; Coppé et al., 2008; Orjalo et al., 2009) were among these. Considering the fact that in multiplex immunoassay detection sensitivity may be compromised, an ELISA test for selected single analytes was performed. The presence of GM-CSF, IL1α and TNFα in conditioned medium was tested. Despite the fact that

ELISA kits offered a significant increase in sensitivity (GM-CSF ELISA sensitivity of 3 pg/ml as opposed to 90 pg/ml in Luminex multiplex assay; IL1α ELISA sensitivity of 1 pg/ml as opposed to 9 pg/ml in Luminex multiplex assay; TNFα ELISA sensitivity of 8 pg/ml as opposed to 25 pg/ml in Luminex multiplex assay) none of these proteins were detected in the conditioned medium.

6.2.2 IL6 is secreted by aged HDFs but not IL8

Interleukin-6 and IL8 are widely recognised as hallmarks of SASP. While both late passage HDFs and saquinavir-treated cells demonstrated elevated secretion of IL6 as detected by the Luminex immunoassay, the secretion of IL8 was unchanged or decreased upon acute prelamin A accumulation after saquinavir treatment. Individual ELISA tests were employed to validate these results because it is a more sensitive technique. IL6 ELISA confirmed that saquinavir treatment and replicative exhaustion leads to increased IL6 secretion (Figure 6.2 A). Furthermore, ELISA also revealed that Zmpste24 knock-down results in similar elevated IL6 levels in the culture medium. The identification of IL6 as a statistically significant hit, despite its absence in the Luminex immunoassay analysis, was likely related to the higher sensitivity of ELISA and lower standard deviation between biological replicates. ELISA also offered more sensitive detection of IL8 (Figure 6.2 B). It revealed that IL8 was downregulated not only in saquinavir treated cells, but also in late passage cells. Zmpste24 knock-down, however, slightly increased IL8 secretion. Due to the unexpected nature of this observation, particularly regarding decreased IL8 secretion in replicative senescence, ELISA tests were performed for at least 10 biological replicates. These were prepared

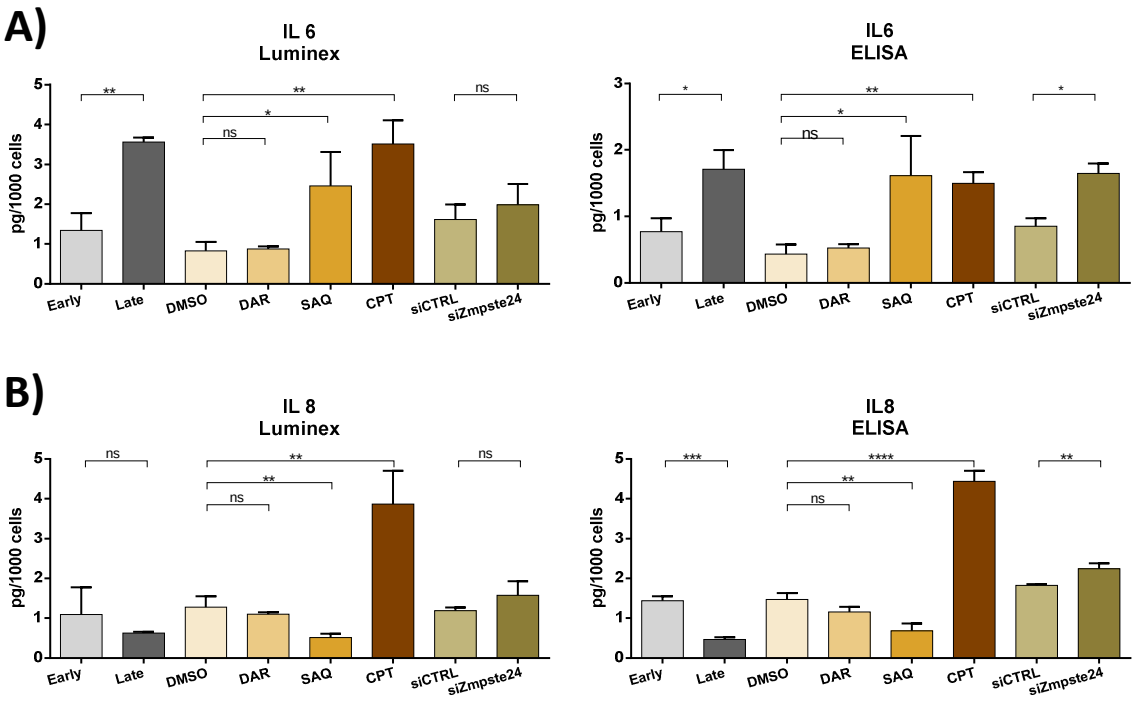

Figure 6.2. Detection of (A) IL6 and (B) IL8 in conditioned medium.

Validation of results from the Luminex immunoassay (left panels) by ELISA test (right panels). Late, late passage HDFs (over passage 40); Early, early passage HDFs (below passage 22); SAQ, saquinavir; DMSO, vehicle control; CPT, camptothecin; siZmpste24, Zmpste24 siRNA knock-down; siCTRL, control siRNA. Error bars represent SD; * $P < 0.05$; ** $P < 0.01$; *** $P < 0.001$; **** $P < 0.0001$; ns, P not significant.

separately from different HDF batches, and consistently displayed the same pattern of secretion. CPT appeared to be a potent inducer of both IL6 and IL8 secretion.

6.2.3 Cell culture conditions can impact secretory phenotype

The absence of some key components of SASP (e.g. IL1α, GM-CSF) and the unexpected pattern of IL8 secretion prompted us to further examine the effect of cell culture conditions on secreted factors. The experiment investigating SASP was designed to ensure enrichment of the culture medium in secreted proteins, without affecting cell viability. Keeping cells in culture for five days without medium change allowed for improved enrichment in secreted proteins as shown in MMP3 detection

by ELISA (Figure 6.3 A). Early or late passage cells were cultured for five days, counted (demonstrating a viability of approximately 95%), and the MMP3 level determined. In comparison, passage-matched cells were seeded at the density corresponding to the cell number determined at the end of five day experiment, and allowed to condition medium for 24 hours. Comparison between the five day and one day experiments demonstrated increased secretion of MMP3 by late passage cells in both; however the enrichment after five days was significantly higher. It is also worth noting that MMP3 is normally secreted at high concentrations. This is not the case with other proteins selected for multiplexing. Therefore, medium conditioning for one day would most likely be insufficient.

Medium was also conditioned for 12 days to determine if it would improve detection of analytes that had not been detected in the Luminex multiplex immunoassay. It was observed that a longer period of medium conditioning resulted in detection of GM-CSF secretion. This was noted only in early passage cells (Figure 6.3 B). The longer period of medium conditioning was also found to affect the secretion pattern for IL8 (Figure 6.3 C). However, as a result of the extended cell culture

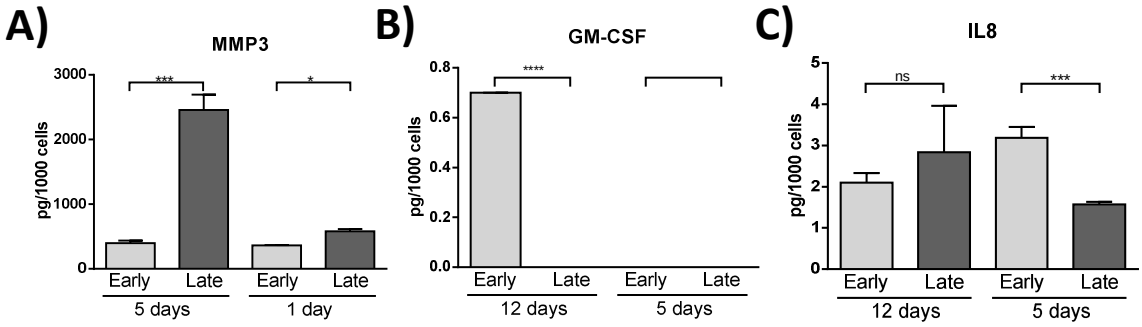

Figure 6.3. Effects of cell culture conditions on the secretory phenotype.

Detection of secreted MMP3 (**A**), GM-CSF (**B**), and (**C**) IL8 by ELISA tests. Late, late passage HDFs (over passage 40); Early, early passage HDFs (below passage 20). Error bars represent SD; * $P < 0.05$; *** $P < 0.001$; **** $P < 0.0001$; ns, P not significant.

duration, HDFs demonstrated clear signs of cell death, with viability below 75%. It is therefore likely that the secretory phenotype observed in the 12 day cell culture was a result of poor cell culture conditions, leading to necrosis and leakage of intracellular protein pools.

6.2.4 FAS and MMP3 display increased secretion in the three ageing models

Three analytes, Fas, MIP1β and MMP3, demonstrated increased secretion in replicative senescence and in cells accumulating prelamin A (either as a result of saquinavir treatment or siRNA knock-down of Zmpste24) in the multiplex assay. The secretion level of MMP3, however, was determined based on the extrapolation from standard curve beyond the maximum data mark. Therefore, to further validate the Luminex immunoassay results, secretion of MMP3 and Fas were analysed by the ELISA tests. Results from the ELISA confirmed the secretion patterns observed in the Luminex immunoassay (Figure 6.4), reaffirming the validity of the conclusions.

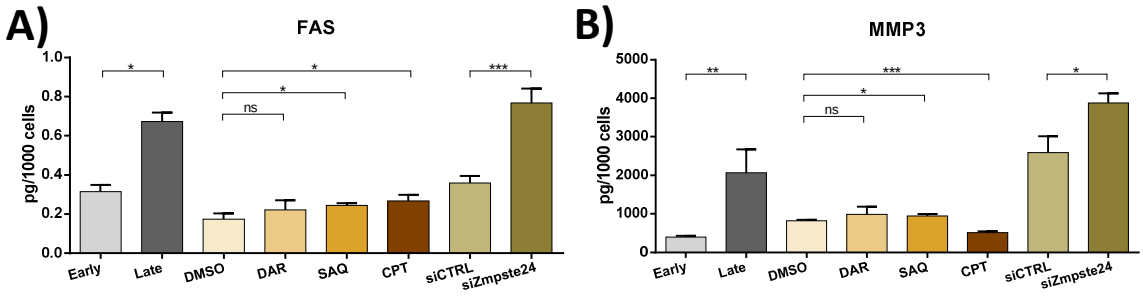

Figure 6.4. Detection of FAS (A) and MMP3 (B) in conditioned medium by ELISA test.

Validation of the Luminex immunoassay results by ELISA test. Late, late passage HDFs (over passage 40); Early, early passage HDFs (below passage 22); SAQ, saquinavir; DMSO, vehicle control; CPT, camptothecin; siZmpste24, Zmpste24 siRNA knock-down; siCTRL, control siRNA. Error bars represent SD; * $P < 0.05$; ** $P < 0.01$; *** $P < 0.001$; ns, P not significant.

6.2.5 PLAT and PAI-1 secretion in senescence

PLAT and PAI-1 have been shown to cooperate in senescence regulation (Comi et al., 1995; Elzi et al., 2012; Kortlever et al., 2006). PAI-1 has been reported as an overexpressed protein in senescent cells that counteracted PLAT anti-senescence activity. Our microarray data demonstrated underexpression of both PAI-1 and PLAT in the late passage HDFs. The Luminex immunoassay did not determine the level of PAI-1 secretion in either condition tested. ELISA was therefore employed for the quantification of PAI-1 protein level in conditioned medium. Confirming the microarray data, it revealed a lower level of secreted protein by late passage HDFs (Figure 6.5 A). Cells accumulating prelamin A (either saquinavir treated or with Zmpste24 knock-down) did not demonstrate differential secretion of this protein. Camptothecin treatment appeared to reduce the secretion of PAI-1, to a lower extent that in replicative senescence though.

Expression of PLAT mRNA was decreased in the three ageing models as revealed by microarray analysis. When PLAT protein secretion was measured by ELISA, it exhibited lowered levels in late passage HDFs and in cells with Zmpste24 knock-down, but not in saquinavir-treated cells.

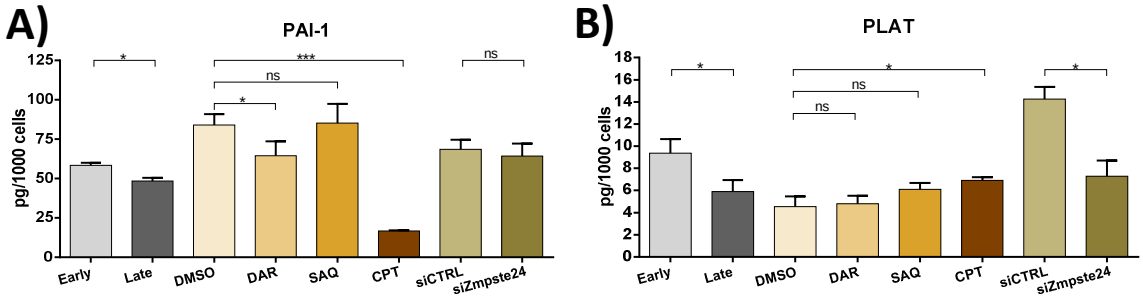

Figure 6.5. Detection of PAI-1 (A) and PLAT (B) in conditioned medium by ELISA test.

Late, late passage HDFs (over passage 40); Early, early passage HDFs (below passage 22); SAQ, saquinavir; DMSO, vehicle control; CPT, camptothecin; siZmpste24, Zmpste24 siRNA knock-down; siCTRL, control siRNA. Error bars represent SD; * P < 0.05; ** P < 0.01; *** P < 0.001; ns, P not significant.

6.2.6 Expression of mRNA and changes in secretory phenotype

Changes in the level of secreted protein often correspond to changes in mRNA expression (Acosta et al., 2008; Kuilman et al., 2008; Wajapeyee et al., 2008), however this is not always observed (Coppé et al., 2008). Data acquired during this project also revealed that changes of mRNA expression examined by microarrays (Chapter 4) and qRT-PCR were not always proportional to the changes in secretion of corresponding proteins. Some secreted analytes demonstrated the same directionality of changes in both mRNA and protein level. For example, IGFBP3 mRNA was overexpressed only in late passage HDFs (Figure 6.6 A), and only these cells exhibited increased secretion of the protein. PAI-1 mRNA was underexpressed in the late passage cells (Figure 6.6 B)

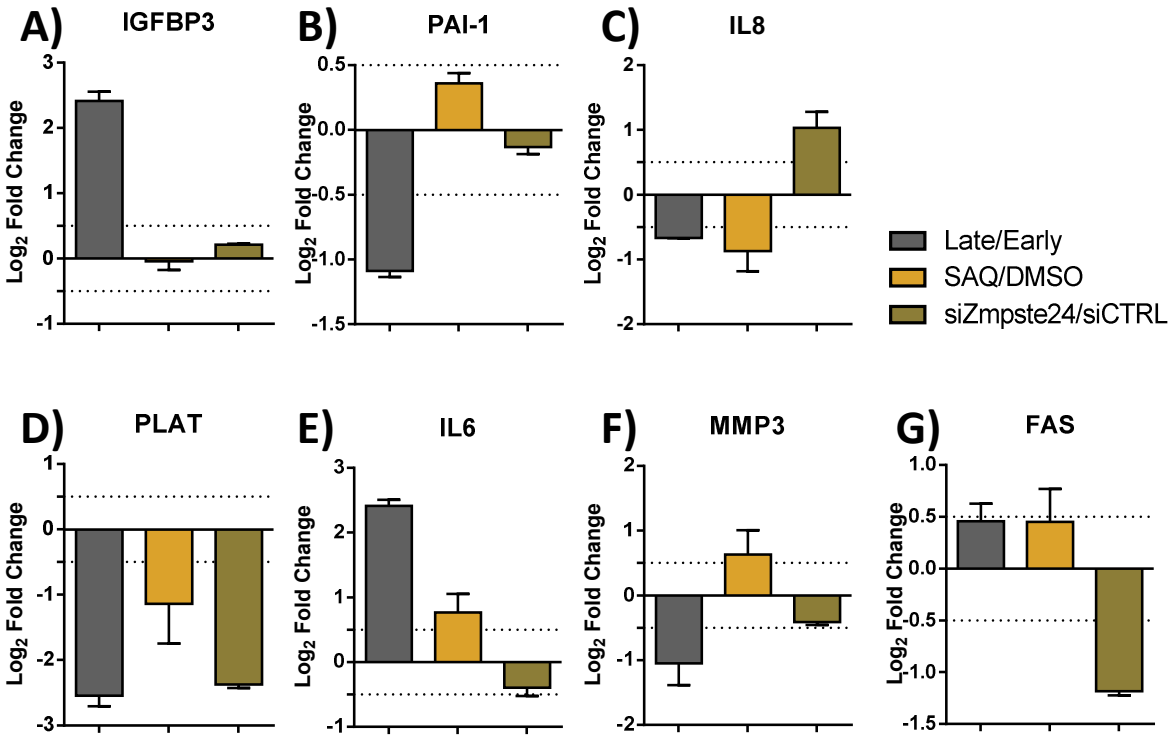

Figure 6.6. mRNA expression changes measured by qRT-PCR.

A) IGFBP3. **B)** PAI-1. **C)** IL8. **D)** PLAT. **E)** IL6. **F)** MMP3. **G)** FAS. Dashed lines (at -/+ 0.5 Log_2 Fold Change) denote the cut off level below which the expression was considered as not significant. Late, late passage HDFs (over passage 40); Early, early passage HDFs (below passage 22); SAQ, saquinavir; DMSO, vehicle control; siZmpste24, Zmpste24 siRNA knock-down; siCTRL, control siRNA. Error bars represent SD.

and was recapitulated by the drop in protein secretion only in the cells senesced by replicative exhaustion. Similarly, changes in IL8 mRNA expression (Figure 6.6 C) corresponded with the observed protein secretion pattern.

The same directionality of changes, both at the mRNA level and at the level of secreted protein, was also true for a number of other analytes. There were, however, examples of analytes which displayed a significant change at the mRNA level that was absent when the corresponding secreted protein was analysed. As an example, this was observed with PLAT in saquinavir treated cells (Figure 6.6 D). Conversely, IL6 mRNA did not demonstrate differential expression upon Zmpste24 knock-down (Figure 6.6 E), despite increased secretion of this interleukin. FAS and MMP3 mRNA were underexpressed in Zmpste24 knock-down and replicative senescence, respectively, (Figure 6.6 F, G), while the level of secreted proteins was increased in these models. These observations underscore the importance of post-transcriptional and post-translational mechanisms in regulation of protein secretion.

6.3 DISCUSSION

Senescent cells, despite undergoing stable proliferative arrest, remain metabolically active and are able to influence their surroundings for as long as they persist. One of the hallmarks of senescence is the onset of SASP, secretion of a range of cytokines, chemokines, growth factors and ECM remodelling proteins. SASP may display both anti- and pro-tumorgenic activities and contribute to tissue repair and the ageing process (Ovadya and Krizhanovsky, 2014; Rodier and Campisi, 2011). In this Chapter we demonstrate that acute prelamin A accumulation upon saquinavir

treatment induces SASP. The composition of SASP in this setting bears strikingly high similarity to the secretory phenotype observed in HDFs senesced by replicative exhaustion. The secretion of 35 SASP factors was analysed, by both Luminex bead-based immunoassay and subsequent ELISA testing. These analyses demonstrate that at least 13 analytes showed consistently increased secretion in senescence induced by both replicative exhaustion and acute prelamin A accumulation upon saquinavir treatment. Among them were: FAS ligand, FGF (basic), IGFBP1, MIF, MMP2, PCSK9, RANTES, TRAIL R2 and VCAM1. These are proteins that have been previously demonstrated to be upregulated in senescence and ageing (Acosta et al., 2008; Bavik et al., 2006; Cheng et al., 2015; Coppé et al., 2008; Lakoski et al., 2009; Liu and Hornsby, 2007; Nihal et al., 2014; Yepuri et al., 2012). Our observations suggest that, at least to some extent, the induction of senescence by acute prelamin A accumulation leads to a similar overproduction of pro-inflammatory mediators observed in other types of senescence. Furthermore, the reported increased presence of prelamin A and/or progerin in cells during organismal ageing (Ragnauth et al., 2010; Scaffidi and Misteli, 2006) may therefore be one of the contributors to inflammageing (Franceschi and Campisi, 2014).

Similar to our microarray data (Chapter 4), analysis of SASP revealed that cells with Zmpste24 knock-out did not alter their secretory phenotype drastically and showed little overlap with physiological and pharmacological models. Again, it is presumably an effect of having a mixed cell population due to differences in siRNA transfection efficiency, with some cells accumulating prelamin A and others not. Although it has been reported that senescent cells can propagate senescence to their neighbours via the paracrine effect of SASP (Acosta et al., 2013; Hubackova et al.,

2012; Nelson et al., 2012), it seems to depend largely on the severity of the senescence-inducing insult and the duration of the exposure to senescent neighbour cells. It is possible that prelamin A is not significant enough of a factor to promote quick spreading of senescence to the neighbours of prelamin A-accumulating cells. However, as observed in the siZmpste24 model, increased concentration of a few key components of SASP (like IL6 and IL8) in conditioned medium, could indicate that such a process had been initiated, although at a slower pace. Further studies will be required to answer this question.

Interleukin 6 demonstrated elevated secretion in the three laboratory models of ageing. This is in concordance with the postulated role for IL6 as a central regulator of the inflammatory network observed in senescence (Kuilman et al., 2008; Ren et al., 2009) and in aged individuals (Álvarez-Rodríguez et al., 2012; Lin et al., 2014; Pilling et al., 2015; Sansoni et al., 2008). Surprisingly, IL8, whose expression can be stimulated by IL6, showed reduced secretion in both replicative senescence and prelamin A-induced senescence upon saquinavir treatment. Interleukin 8 has often been reported as a hallmark of SASP (Freund et al., 2010). More recent data, however, has demonstrated that IL8 can actually supress senescence (Shen et al., 2013). It appears that the IL8 receptor CXCR2 plays a more important role in senescence reinforcement by mediating the signalling pathway leading to NF-κB stimulation (Acosta et al., 2008). CXCR2 is a ligand to GROα and ENA-78, among others. Although CXCR2 protein levels were not studied in our experiments, the gene that encodes this protein demonstrated overexpression in late passage HDFs (microarray data). Moreover, GROα secretion was increased by saquinavir treatment, while ENA-78 was elevated in the siZmpste24 model. Despite the variation in the mediators engaged, it is possible

that the outcome is still similar in the three studied laboratory models of ageing. They appear to converge at CXCR2-mediated signalling leading to senescence-associated chronic inflammation.

Expression of IL6 is known to be stimulated by IL1 signalling, leading to NF-κB activation (Kimura et al., 1998; Naugler and Karin, 2008). In oncogene-induced senescence, IL1α is highly secreted and can potentiate SASP through both NF-κB and C/EBPβ transcription factors, as well as in a paracrine manner (Acosta et al., 2013; Kuilman et al., 2008). In replicative senescence, however, both IL1α and IL1β are secreted at much lower levels, if at all (Coppé et al., 2008). In fact, IL1α acts primarily as an intracellular or cell-surface bound protein, rarely being secreted (Apte et al., 2006). It has been shown that cell-surface bound IL1α is the form primarily responsible for the regulation of SASP onset via NF-κB and C/EBPβ transcriptional activation (Orjalo et al., 2009). This therefore may explain the absence of IL1 in conditioned medium in our settings. The microarray data (Chapter 4), however, suggests that the IL1 signalling pathway may still be activated. At a protein level, IL1 binds to its cell-surface receptor (IL1R). The signal is subsequently transduced by IRAKs (IL1 receptor activated kinases), leading to NF-κB activation and resultant expression of its target genes, including many SASP components (Janssens and Beyaert, 2003; Loiarro et al., 2005). The microarray results showed overexpression of IL1R in late passage HDFs, and IRAK1 upregulation in prelamin A-induced senescence, at least upon saquinavir treatment. These observations suggest that IL1 signalling may contribute to the observed secretory phenotype, also in prelamin A-induced senescence. Additional functional studies will be required to validate this assumption though. Testing for surface-bound IL1α, especially in the context of prelamin A

accumulation in the heterogeneous siZmpste24 population, would be of particular interest. It would allow for comparison of cell-autonomous IL1α signalling to the severity of prelamin A accumulation.

Other SASP components, such as G-CSF, GM-CSF, IL17 or TNFα were not detected in our immunoassay under normal study conditions, even in cellular replicative senescence. These findings, however, were not unanticipated given the plasticity of SASP and its dependence on cell-context and severity of senescence-inducing stimuli. In fact, it has been previously noted that even hallmark components of SASP, like IL6, can be absent (Quijano et al., 2012). Furthermore, the entire repertoire of secreted proteins in senescence-associated inflammatory response can show no overlap with SASP identities (Bondar and Medzhitov, 2013; Pribluda et al., 2013). While seemingly distinct, they can still belong to the same functional categories and display common features. This may suggest that in the senescence process, whether it is induced by genomic instability, oncogene activation, ROS, or prelamin A, etc., the outcome identified as chronic inflammation is more important than the actual mediators leading to it. To complicate the picture further, some senescence models show no SASP at all (Coppé et al., 2011), which highlights the diversity within the process. Our results for IL8 and GM-CSF secretion in prolonged cell cultures, in turn affecting cell viability, also emphasize the importance of appropriate study design. This degree of caution is necessary to ensure that the observed changes in secretory phenotype are the result of senescence, rather than cell death or suboptimal culture conditions. It has been noted before that cell culture conditions can strongly affect SASP composition or even completely diminish its onset in a cell type-dependent manner. For example, mouse fibroblasts initiate SASP only under a

physiological oxygen level (Coppé et al., 2010b), while human fibroblasts do not demonstrate such dependence (Coppé et al., 2008).

Similarities between mRNA and protein levels for some analytes were observed, while for others there was a discrepancy between protein and transcript changes. It has been noted before (Coppé et al., 2008; Metcalf et al., 2015) and may suggest different kinetics in expression of some factors. Furthermore, as discussed in the introduction, SASP is controlled at multiple levels (Abdelmohsen et al., 2008; Salminen et al., 2012; Schott and Stoecklin, 2010). Even after translation, the SASP components still need to be trafficked to the cell membrane and secreted, offering another level of control. Therefore, while mRNA analysis can offer a great insight and reveal some clues about regulation of SASP, further examination at the protein level is truly needed to validate proposed hypothesis.

Human Dermal Fibroblasts treated with camptothecin inducing apoptosis, released a number of pro-inflammatory factors that overlapped with SASP observed in senesced cells. Apoptosis is generally viewed as a process of cell clearance that prevents inflammation (Erwig and Henson, 2007). In some circumstances, however, it may have the opposite effect. When the clearance of apoptotic cells by phagocytes is delayed (or is impossible, for example in a cell culture flask) the cells eventually lyse and undergo secondary necrosis, releasing pro-inflammatory cytokines (Rock and Kono, 2008; Silva et al., 2008). Our study demonstrates that senescence and apoptosis eventually aim at activation of immune system via similar secreted factors. This is despite the fact that they are two distinct responses of a cell to an insult (Childs et al., 2014). Interestingly, FAS protein, a prototypical death receptor (Itoh et al., 1991; Nagata, 1997), showed increased secretion in the three studied laboratory models of

ageing. While membrane-bound FAS mediates apoptosis, the secreted soluble variant has opposing effects by inhibiting death receptor signalling (Cheng et al., 1994). FAS has not only been identified previously as a SASP component in replicative senescence (Coppé et al., 2008), but has also been shown to mediate premature senescence in cancer cells (Crescenzi et al., 2011). Furthermore, senescent cells generally show increased resistance to apoptosis (Salminen et al., 2011a) and increased secretion of soluble FAS potentially could contribute to this phenomenon. Moreover, elderly people have elevated plasma levels of soluble FAS (Pinti et al., 2004). This correlates with increased prelamin A accumulation in aged individuals (Lattanzi et al., 2014). It is therefore possible that prelamin A may play an important role in regulation of soluble FAS expression during ageing.

Senescent cells also appear to contribute to organismal ageing by affecting tissue homeostasis (Campisi, 2013; Van Deursen, 2014), not only by causing chronic inflammation, but also by secreting ECM-remodelling factors that can degrade the tissue microenvironment. Our results showed increased secretion of several matrix metalloproteinases (MMPs) by senesced cells. This is concordant with previous reports for various types of senescence (Coppé et al., 2010b; Coppé et al., 2008). Interestingly, MMP3 was upregulated in the three studied laboratory models of ageing, but was not observed in camptothecin-treated cells. Balanced ECM composition is crucial for tissue structure and function, and MMP3 over-secretion by senescent cells may lead to disruption of tissue homeostasis (Parrinello et al., 2005). This often correlates with ageing and age-related diseases (Jing and Jiang, 2015).

We closely investigated secretion of another protease, tissue-type plasminogen activator (PLAT), together with its inhibitor PAI-1. Both have been previously

implicated in the regulation of senescence (Kortlever et al., 2006; West et al., 1996). Our microarray data showed underexpression of PLAT in the three laboratory models of senescence, and PAI-1 in replicative senescence. PLAT has been shown to prevent senescence induction by proteolytic inactivation of IGFBP3 (Elzi et al., 2012), which when uncleaved, stimulates the senescent phenotype. In fact, many IGFBP proteins are known to be involved in induction and/or regulation of senescence (Fridman and Tainsky, 2008; Grillari et al., 2000; Rombouts et al., 2014; Severino et al., 2013). Our analysis of the secretory phenotype showed increased secretion of IGFBP1 and IGFBP3 by senescent cells. Conversely, PLAT secretion was reduced by late passage cells and in the siZmpste24 model. This is in concordance with the model in which PLAT prevents senescence by cleavage of IGFBP proteins. There was no observed change in PLAT secretion by saquinavir-treated cells though. PAI-1 showed lower secretion in late passage HDFs, which may indicate that cells lacking PLAT do not require further inhibition of plasminogen activator by PAI-1. Observed variability in the PAI-1-PLAT-IGFBP axis could be an effect of changing dynamics of the cellular response to the severity of the senescence-inducing stressor.

In summary, here we characterise the repertoire of secreted proteins in prelamin A-induced senescence. It is the first such a broad investigation of SASP under this condition. The secretory phenotype induced by prelamin A resembles that observed in replicative senescence, perhaps with a specific subgroup (consisting of IL6, FAS, MMP, and MIP1β) being the signature of SASP initiated by prelamin A accumulation.

CHAPTER 7

7 Nucleoplasmic Reticulum Formation

7.1 INTRODUCTION

The nuclear envelope (NE) is a unique structure forming a physical barrier between the nuclear environment and the cytoplasm. It is comprised of two phospholipid bilayers, the inner nuclear membrane (INM) and outer nuclear membrane (ONM), with an intervening luminal space between them called the perinuclear space (PNS). The NE is underlain by a lamin-rich proteinaceous meshwork (Prunuske and Ullman, 2006). It is well established that the structure of the nucleus is more complicated than just a membrane-bound sphere containing chromatin, pierced by nuclear pore complexes (NPC). The NE contains a complex network of penetrating and branching invaginations, collectively referred to as the nucleoplasmic reticulum (NR) (Fricker et al., 1997a; Fricker et al., 1997b). The NR is a widespread feature of many cells and tissues, both under normal cellular conditions (Fricker et al., 1997b; Langevin et al., 2010; Storch et al., 2007) and in pathological states (Bussolati et al., 2008; Malhas and Vaux, 2014). These NR structures are classified into two types: type I invaginations involve only the INM with PNS core, and type II involve invagination of both the INM and ONM with cytoplasmic core (Malhas et al., 2011). The NR structure can be more complex though, with type I invaginations branching off type II, both as membrane sheets and as tubules. These complex invaginations may traverse the nucleus, forming cross-nuclear channels. In addition, these traversing channels cannot be resolved during interphase without a membrane scission event.

The exact function of the NR remains incompletely understood. It appears to play a role in the structural support of the nucleus and in communication between the cytoplasm and nucleoplasm because it increases the interface between these two environments. Moreover, there is a growing body of evidence implicating the NR in calcium signalling in sub-nuclear regions, contributing to gene expression and cell growth (Chamero et al., 2008; Collado-Hilly et al., 2010; Nalaskowski et al., 2011), lipid metabolism (Gehrig et al., 2009), and nuclear import-export. It is also suggested that the presence of NPC proteins and structures that resemble NPC at both type I and II NR invaginations may impact chromatin organisation (Goulbourne et al., 2011).

It has been shown that nuclear morphology is affected and NR complexity increases upon prelamin A accumulation in interphase nuclei (Goulbourne et al., 2011). Similar changes have also been observed in Hutchinson-Gilford progeria syndrome (HGPS) cells and in physiological ageing (McClintock et al., 2006; Roblek et al., 2010; Scaffidi and Misteli, 2006). This is most likely due to the incorporation of lamin A variants harbouring a persistently farnesylated tail. NR channels also colocalise with the lamina intermediate filaments and the ER lumen marker calreticulin. The exact mechanisms and components essential for formation of the NR are not fully characterised. There are an increasing number of reports, however, that further elucidate the process. NR development seems to depend on the enzyme choline-phosphate cytidylyltransferase A (CCTα). It is the rate limiting enzyme in phosphatidylcholine synthesis, and is crucial for membrane biosynthesis (Cornell and Ridgway, 2015; Gehrig et al., 2008; Gehrig and Ridgway, 2011; Lagace and Ridgway, 2005). CCTα is also believed to introduce positive membrane curvature by its insertion

into the INM. This causes infolding of the INM, and may further support tubulation of the NR.

There are a number of proteins that interact with the phospholipid bilayer and exhibit the ability to cause or stabilise curved membrane domains. Reticulons are among them. They are regulators of membrane curvature, involved in the formation of tubular membrane structures, and are primarily associated with the ER (Hu et al., 2008; Oertle and Schwab, 2003; Voeltz et al., 2006). The C-terminal domain of these integral membrane proteins is composed of two long transmembrane regions. These can form a wedge shape which displaces phospholipids between the leaflets of the lipid bilayer and induces the membrane to bend. Moreover, reticulons can generate arc-shaped scaffolds by an oligomerisation process further contributing not only to induction, but also to the maintenance of high membrane curvature (Shibata et al., 2010). Therefore, reticulons influence the balance between the ER sheet and ER tubule proliferation, favouring conversion of sheets into tubules.

The NR appears in many cell types with multiple pathways contributing to its formation. It also occurs as a physiologic cellular response to external stimuli. It has long been recognized that a structurally advanced NR, referred to as the nucleolar channel system (NCS) is a hallmark of the postovulation endometrium (Kittur et al., 2007; Terzakis, 1965). Its transient presence manifests in human endometrial cells during a three to four day period during the midluteal, receptive phase of the menstrual cycle (Guffanti et al., 2008). The NCS structure forms multilamellar and tubular membrane cisternae within the nucleus that are derived from the INM (Isaac et al., 2001; Kittur et al., 2007). These cisternae exhibit the presence of NPC proteins and a subset of NE-specific components (Guffanti et al., 2008). The proposed

significance of this apparent complex NR is that it is formed in preparation for blastocyst attachment and implantation to the endometrium. This hypothesis is supported by several reports demonstrating the absence or delayed development of NCS in cases of unexplained primary infertility (Dockery et al., 1996; Kohorn et al., 1972), further supported by observations that contraceptives interfere with NCS formation (Feria-Velasco et al., 1972; Wynn, 1967). It has been demonstrated that the formation of NCS can be elicited by the action of oestrogen and progesterone at the time of ovulation (Nejat et al., 2014; Pryse-Davies et al., 1979). Whilst NCS is a unique tubular structure, its development from the INM suggests that it may originate as an NR invagination which, in response to hormones, gains further complexity, possibly representing an advanced NR.

This chapter investigates the formation of the NR in several cellular backgrounds. First, formation dynamics of new NR tubules was investigated in the pathological context of abnormal protein processing observed in ageing. The complexity of NR in normal Human Dermal Fibroblasts in response to prelamin A accumulation and replicative senescence was assessed. The effect of farnesyl transferase inhibition on NR formation in progeroid HGPS cells was also studied. Second, the physiological context of cell response to oestrogen and its effect on NR proliferation was tested in an endometrial cell line. Moreover, the dependence of NR channel formation on Reticulon 4 (NOGO) is demonstrated in several cell models, both pathologic and physiologic. Finally, identification of the requirements for new components, both protein and lipid, incorporated directly into a forming invagination is determined.

7.2 RESULTS

7.2.1 Aged fibroblasts develop extensive NR

Human dermal fibroblasts were aged by proliferative exhaustion and the NR complexity was evaluated by counting NR invaginations in the nuclei. The NR channels were visualised by immunolabelling with anti-lamin B1 antibody and appeared as lamin-B-positive foci within the nucleus in images acquired on a confocal microscope. Initially, Z-stack images of the whole nucleus were taken and the number of tubular structures upon 3D reconstruction was compared to the number of lamin-B-positive foci from a single midsection of the nucleus. This did not reveal significant differences in the total number of identified NR tubules (data not shown). Images of the midsections were therefore used for subsequent quantification of the total number of NR channels per nucleus. The same brightest lamin B foci counted as NR channels appeared in more than one focal plane indicating that these foci represented tubular structures, rather than insoluble intranuclear lamin B blocks. Additionally, each test condition was accompanied by a relevant control in which NR was assessed in the same manner. Therefore any potential miscalculation of the NR channel number would affect both conditions equally. It should be noted, that this approach to NR assessment discriminates against more subtle NR tubules that are too short to appear in the midsections of the nucleus.

When the number of NR tubules was compared between early passage HDFs (up to passage 22) with senescent late passage HDFs (passage 40 and over) a significant increase in the number of NR foci was observed, with over a 2 fold rise in the mean number of invaginations in senescent cells (Figure 7.1 A). Analysis of NR in fibroblasts

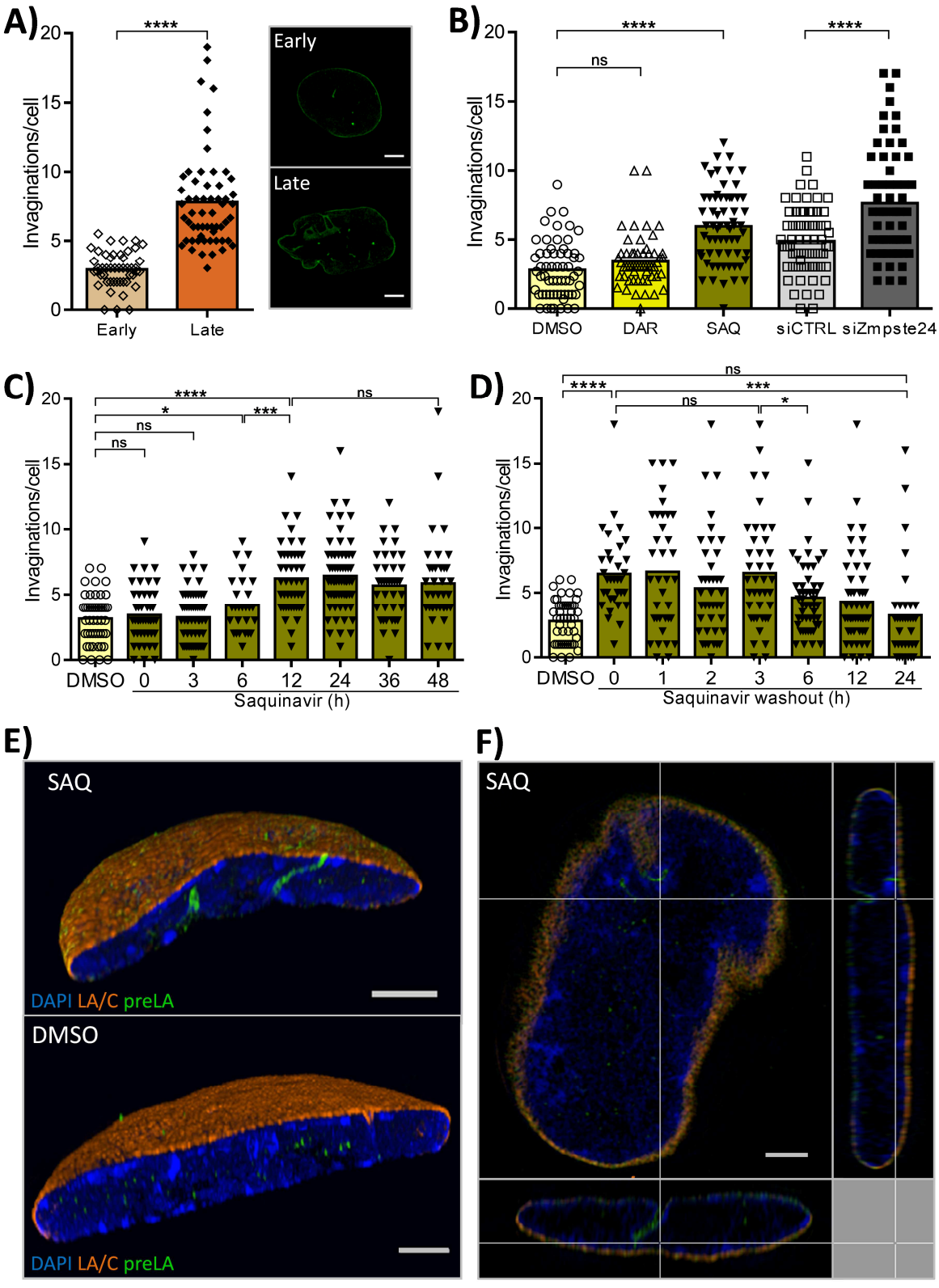

Figure 7.1. Nucleoplasmic Reticulum formation in aged Human Dermal Fibroblasts.

A) Mean frequency of NR tubules in early and late (senescent) passage HDFs with examples of confocal images used for quantification of NR foci identified as bright Lamin B foci within the nucleus; scale bar 5 µm; n=4, 30 nuclei each. **B)** Mean frequency of NR tubules in cells accumulating prelamin A under saquinavir treatment (SAQ) and Zmpste24 siRNA knock-down (siZmpste24) with corresponding controls: DMSO (vehicle), DAR (darunavir), and control siRNA (siCTRL); n=4, 30 nuclei each. **C)** Mean frequency of NR channels in saquinavir (SAQ) treatment time course (48 hour duration) and **D)** disassembly of NR upon drug washout; DMSO, vehicle control; n=2, 50 nuclei. * P < 0.05; *** P < 0.001; **** P < 0.0001; ns, P not significant. **E)** Super resolution microscopy of early passage HDFs treated with saquinavir (SAQ) or DMSO control, with corresponding cross-section of the saquinavir-treated cell in **(F)**; LA/C, lamin A/C in orange; preLA, prelamin A in green; DNA labelled with DAPI in blue; scale bar 2 µm.

senesced by acute prelamin A accumulation demonstrated a similar dependence. Matched early passage HDFs upon 48 hours of saquinavir treatment demonstrated nearly a 2-fold increase in the mean NR tubule number, while DMSO- or darunavir-treated cells remained unaffected. Furthermore, specific Zmpste24 knock-down with siRNA, which was confirmed by simultaneous immunolabelling with anti-prelamin A antibody, revealed the same pattern. This highlights the impact of prelamin A as a significant inducer of NR formation in early passage cells (Figure 7.1 B).

Next, the dynamics of the NR formation in fibroblasts exposed to saquinavir was assessed. During the first 12 hours of saquinavir treatment, the number of NR invaginations gradually increased. There was no significant increase in NR invaginations observed beyond the 12 hour time-point (Figure 7.1 C). HDFs under these culture conditions required approximately 48 hours for cell division. In concordance with previous literature (Goulbourne et al., 2011), this suggests that the NR formed in these cells presumably does not depend on mitosis. This is likely because significant rise in the NR channel number was already observed within 6 hours of exposure to saquinavir, which is a time not long enough for these cells to complete the cell cycle.

The NR formation, stimulated by prelamin A accumulation appears to be a reversible process (Figure 7.1 D). When early passage HDFs cultured for 48 hours in the presence of saquinavir, allowing for acute prelamin A accumulation and induced formation of an extensive NR, were switched back to growth medium in the absence of the drug, it resulted in resolution of the NR structures. Upon saquinavir withdrawal, rapid processing of prelamin A occurs within the first three hours, as shown in Chapter 3. This correlates with a statistically significant drop in the NR invagination

number observed between three and six hours (Figure 7.1 D). This was followed by further disassembly of the NR, before reaching the base level at 24 hour time point. This observation suggests that NR disassembly may also be mitosis-independent, since the cells would require another 24 hours to complete the cell cycle. Additional experiments will be required to further characterize this hypothesis though. For example, NR disassembly could be studied in cells under proliferation arrest (e.g., induced by hydroxyurea). Alternatively, pre-mitotic cells could be identified from post-mitotic cells by BrdU incorporation to assess cell-cycle progression (Gratzner, 1982).

Given that prelamin A accumulation conduces NR formation, in the next step super resolution microscopy was employed to investigate the distribution of prelamin A within the nuclear envelope following 48 hours of saquinavir treatment. This analysis revealed that prelamin A is highly enriched at the invagination sites (Figure 7.1 E, F). It suggests that the NR is the preferred deposition site after nuclear import of newly synthesised prelamin A copies, which supports the role of prelamin A as a contributor to newly formed NR channels.

7.2.2 Reticulons are essential in the formation of the NR in the pathological cell model

NR is a highly curved, membranous structure, continuous with the nuclear envelope and endoplasmic reticulum (ER). It was therefore investigated if reticulons could be involved in formation of the NR since they are regulators of membrane curvature and are associated with ER tubulation (Hu et al., 2008; Voeltz et al., 2006).

NOGO (Reticulon 4) was selected for further investigation, based on unpublished data from the Vaux Lab. First, siRNA knock-down of NOGO was conducted in HeLa

cells. They were chosen because they offer a good model for high transfection efficiency. A range of siRNA concentrations were tested for transfection, with 20 nM siRNA selected for subsequent experiments, as it exhibited significant knock-down of the protein (Figure 7.2 A). HeLa cells transfected with NOGO siRNA were treated with

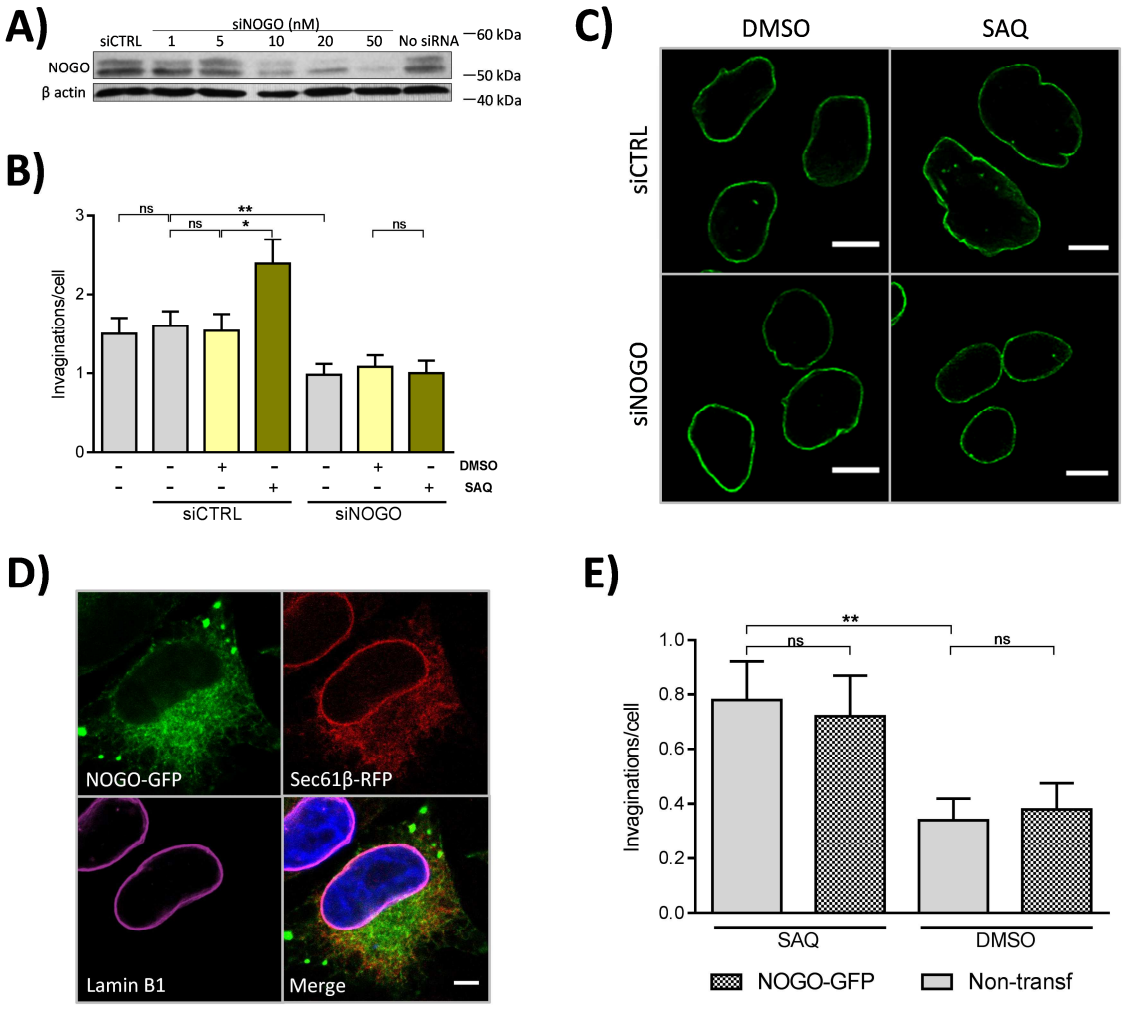

Figure 7.2. Role of NOGO in the NR formation in cell accumulating prelamin A.

A) Western blot showing NOGO knock-down with siRNA in HeLa cells. **B)** Mean number of NR channels in HeLa cells increases when control cells (siCTRL) are cultured in the presence of saquinavir (SAQ), while NOGO knock-down (siNOGO) not only removes the effect of prelamin A accumulation on the NR proliferation, but further lowers the basal frequency of NR below the level observed in control cells. **C)** Examples of confocal images used for quantification of NR channels in HeLa cells showing anti-lamin B immunolabelling; scale bar, 5 µm; of note, image contrast was adjusted for printing purposes. **D)** Overexpression of GFP-tagged NOGO in HeLa cells showing mostly ER localisation; in addition ER marker Sec61β tagged with RFP, and lamin B1 are also shown; scale bar 5 µm. **E)** whereas saquinavir (SAQ) induces significant increase of NR frequency when compared to DMSO control, overexpression of NOGO has no effect on the mean number of NR invaginations, neither in drug-treated nor DMSO-treated cells. Error bars, SEM; * $P < 0.05$; ** $P < 0.01$; **** $P < 0.0001$; ns, P not significant.

saquinavir for 48 hours in order to induce prelamin A accumulation and to allow for the formation of new NR tubules. In cells transfected with control siRNA, prelamin A accumulation significantly increased the mean number of invaginations. This is in concordance with the observations made for prelamin A's impact on the NR structure in HDFs. Interestingly though, NOGO knock-down not only blocked the effect of saquinavir treatment, but it also decreased the mean number of invaginations below the basal level observed in unperturbed HeLa cells (Figure 7.2 B, C). This suggests that NOGO is essential for formation and/or maintenance of NR tubules, presumably also at the physiological frequency observed in cells, without external NR-stimuli such as prelamin A accumulation.

NOGO depletion strongly affected the frequency of NR channels possibly indicating that it is a rate limiting component required during NR proliferation. Therefore, further testing was performed to determine if NOGO overexpression itself can induce the NR. HeLa cells were transfected with a plasmid encoding GFP-tagged NOGO under CMV promoter. Overexpression of NOGO-GFP was assessed by confocal microscopy. As expected, it showed primarily ER localisation, and overlapped with expression pattern of ER marker Sec61β, which had been cotransfected as a red fluorescence protein (RFP)-tagged version (Figure 7.2 D). Cells transfected with NOGO-GFP were treated with saquinavir or DMSO control for 48 hours, fixed, and the NR tubules were counted. Although prelamin A accumulation increased the mean number of NR invaginations by almost two-fold, the overexpression of NOGO did not have any significant effect in cells treated with saquinavir or DMSO control. This indicates that the endogenous NOGO level likely exceeds the requirement for this

reticulon protein in response to NR proliferation, and increasing its concentration further has no further effect.

7.2.3 Farnesylated progerin enhances NR formation, but not in NOGO absence

Prelamin A retains its modification at the CaaX motif, by which it resembles progerin, a splice variant of lamin A identified as the underlying cause of pathology in HGPS (De Sandre-Giovannoli et al., 2003; Eriksson et al., 2003). Progerin does not undergo the final proteolytic cleavage by Zmpste24; hence, similar to prelamin A, it retains the farnesylated C-terminus, a modification believed to underpin the dysmorphic nuclei observed in HGPS cells. Farnesyl transferase inhibitors (FTIs) were shown to improve the nuclear morphology of HGPS cells (Capell et al., 2005), thus the effect of FTI on formation of the NR was tested. The number of NR tubules decreased in HGPS cells over an extended time course of FTI treatment. This suggests that the

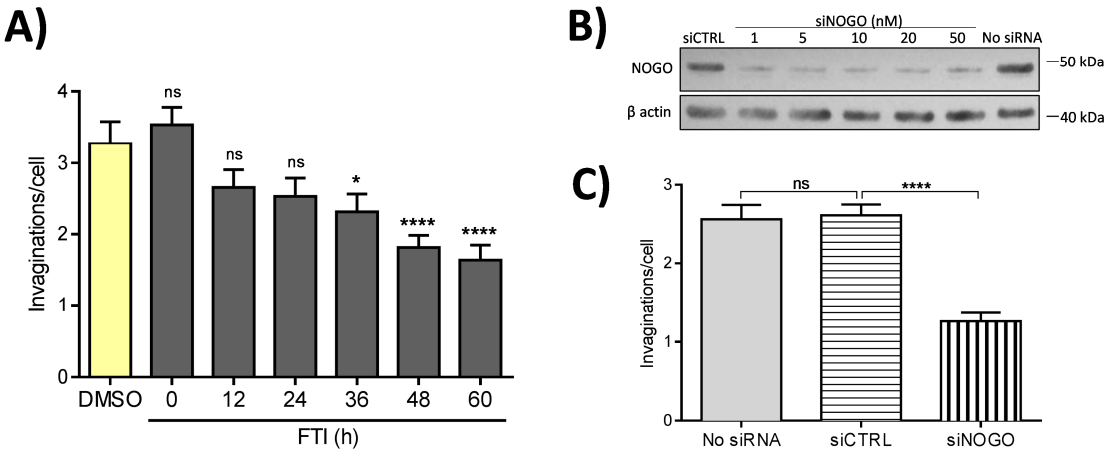

Figure 7.3. Formation of the NR in HGPS cells.

A) The NR tubule frequency is lowered in HGPS cells by treatment with farnesyl transferase inhibitors (FTI); DMSO, vehicle control. **B)** Western blot showing NOGO knock-down with siRNA in HGPS cells. **C)** NOGO knock-down in HGPS cells significantly lowers the mean number of NR invaginations. Error bars, SEM; * P < 0.05; ** P < 0.01; **** P < 0.0001; ns, P not significant.

presence of progerin with an attached farnesyl group not only affects the nuclear rim, but also has an effect on the NR and its extent (Figure 7.3 A). The dynamics of NR disassembly in HGPS cells was slow, and significant changes between FTI-treated and control cells were only observed after 36 hours. This is most likely due to the dominant effect of progerin that had already been expressed and incorporated into the lamina prior to the FTI treatment. FTI blocks farnesylation of new copies of progerin and only these would not harbour an isoprenylated tail. It is likely that cell division occurred within the 36-48 hour window, allowing for the disassembly of NR, but not re-building it to the same extent as the pool of farnesylated progerin was depleted.

Knowing that NOGO is required for NR formation in cells accumulating prelamin A, investigation of its contribution to NR formation in HGPS cells was next undertaken. SiRNA knock-down was performed to find the optimal siRNA knock-down condition for HGPS cells, selecting again a 20 nM concentration of NOGO specific siRNA for subsequent experiments (Figure 7.3 B). 48 hours post-transfection, NR tubules were counted in test cells, revealing that NOGO knock-down significantly reduced the mean number of NR invaginations in HGPS cells. This reduction was below the level observed after FTI treatment (Figure 7.3 C), which further highlights importance of NOGO in the NR formation process under pathological conditions, as observed in progeria cells.

7.2.4 NR formation in endometrial cells depends on NOGO and oestrogen

The NR channel formation was also examined in a more physiological context. It has long been recognised that human endometrial cells develop a structure called the

nucleolar channel system (NCS). It is derived from the INM and could represent a structurally advanced NR (Guffanti et al., 2008). Moreover, it has been shown that the formation of the NCS responds to the action of oestrogen and progersterone at the time of ovulation. Hence it was hypothesised that oestrogen may act to induce NR proliferation, mimicking a potential effect of oestrogen and permitting induction of the NCS during the secretory phase *in vivo.*

The Ishikawa cell line, established from an endometrial adenocarcinoma from a premenopausal patient (Nishida et al., 1985), was used as an endometrial cell model in this study. These cells display a complex NR morphology and have both oestrogen

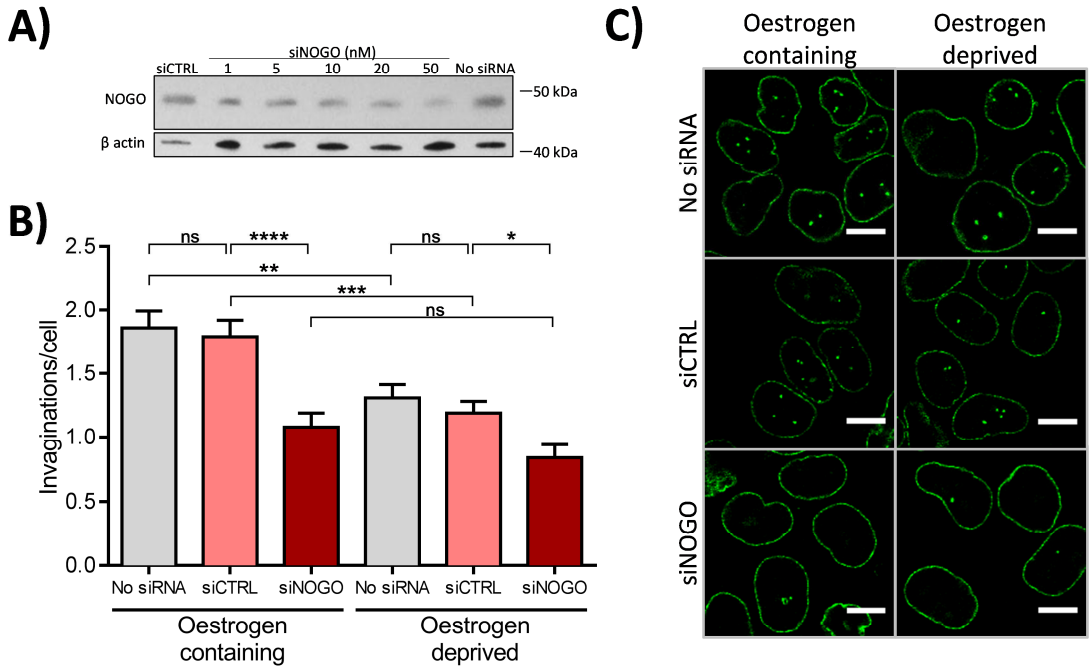

Figure 7.4. NR formation in endometrium cells depends on NOGO and oestrogen.

A) Western blot showing NOGO knock-down with siRNA in Ishikawa cells. **B)** Ishikawa cells exposed to oestrogen have higher mean frequency of NR channels than cells cultured in oestrogen-stripped medium. NOGO knock-down (siNOGO) ablates the oestrogen effect though when compared to control cells (siCTRL or No siRNA). n=2, 50 nuclei each; error bars represent SEM; * $P < 0.05$; ** $P < 0.01$; *** $P < 0.001$; **** $P < 0.0001$; ns, P not significant. **C)** Examples of confocal images used for NR tubule quantification; scale bar 5 µm.

and progesterone receptors. Dependance of NR formation in Ishikawa cells on both oestrogen and NOGO was examined. Cells were depleted of NOGO protein by performing siRNA knock-down (Figure 7.4 A) in passage-matched Ishikawa cells. These were then cultured for 48 hours, either in the presence of oestrogen or in medium that had been charcoal-stripped of the hormone. The mean number of invaginations in cells was then evaluated in the test conditions by NR visualisation with anti-lamin B1 immunolabelling and confocal microscopy (Figure 7.4 B, C), revealing that NR formation in the Ishikawa cell line depends on oestrogen. Control cells (untransfected or control siRNA-transfected) cultured in oestrogen-stripped medium displayed a significantly lower mean number of invaginations. Moreover, NOGO knock-down further reduced the number of invaginations to comparable levels in both the presence and absence of oestrogen. This indicates that NR formation in Ishikwa cells not only responds to oestrogen, but more importantly relies on NOGO.

7.2.5 NR formation requires nascent phospholipids

The regulation of NR appears to represent a dynamic process controlled by a number of pathways. Notably, the NR is known to be regulated by CCTα (Gehrig et al., 2008; Goulbourne et al., 2011), the rate limiting enzyme for *de novo* phosphatidyl choline synthesis. Phosphatidyl choline is the most abundant phospholipid in cell membranes. CCTα is believed to drive NR formation both by membrane synthesis and induction of positive membrane curvature by insertion of the enzyme into the INM (Lagace and Ridgway, 2005). Knowing that expansion of cellular membranes by CCTα-dependent synthesis of phospholipids is required for NR formation, we decided to investigate where the nascent phospholipid is incorporated into the nuclear

membrane, whether it is randomly delivered to the nuclear envelope or perhaps has preferential inclusion sites.

Mouse preadipocytes were selected as a model cell line in this study due to their efficient uptake of fatty acids (Lafontan, 2008). Furthermore, similar to other cell lines, they respond to prelamin A accumulation by formation of new NR channels. Cells were cultured in saquinavir containing medium for six hours and then fatty acyl tails of phospholipids were labelled by pulsing cells with a uniformly deuterated stearic acid D35 for an additional six hours. This was done with continued saquinavir exposure in order to maintain the prelamin A accumulation and induction of new NR tubules. Deuterated acyl chain moieties coming from the pulse labelling with stearic acid D35 were a substrate for phospholipid biosynthesis. This allowed for the identification of a nascent phospholipid population synthesised at a particular time during the pulse. Nano Secondary Ion Mass Spectrometry (NanoSIMS) in correlation with back scattered electron microscopy (BSE) imaging was used for detection of the distribution of the deuterated phospholipids. First, high resolution images of cell morphology were obtained in BSE. Corresponding regions were then analysed by nanoSIMS. In this method, a raster scanned ion beam is used to ablate a surface layer of the specimen. The released atoms are collected and subjected to secondary ion mass spectrometry. This results in an image of the spatial distribution of the analysed atoms based on their mass. In this study, the ratio of deuterium (^2H) (coming from pulse labelling with deuterated stearic acid D35) to hydrogen was measured. A higher ratio indicated a higher abundance of nascent phospholipids. The background detection during instrument set-up was determined by imaging cells pulse-labelled with non-deuterated stearic acid.

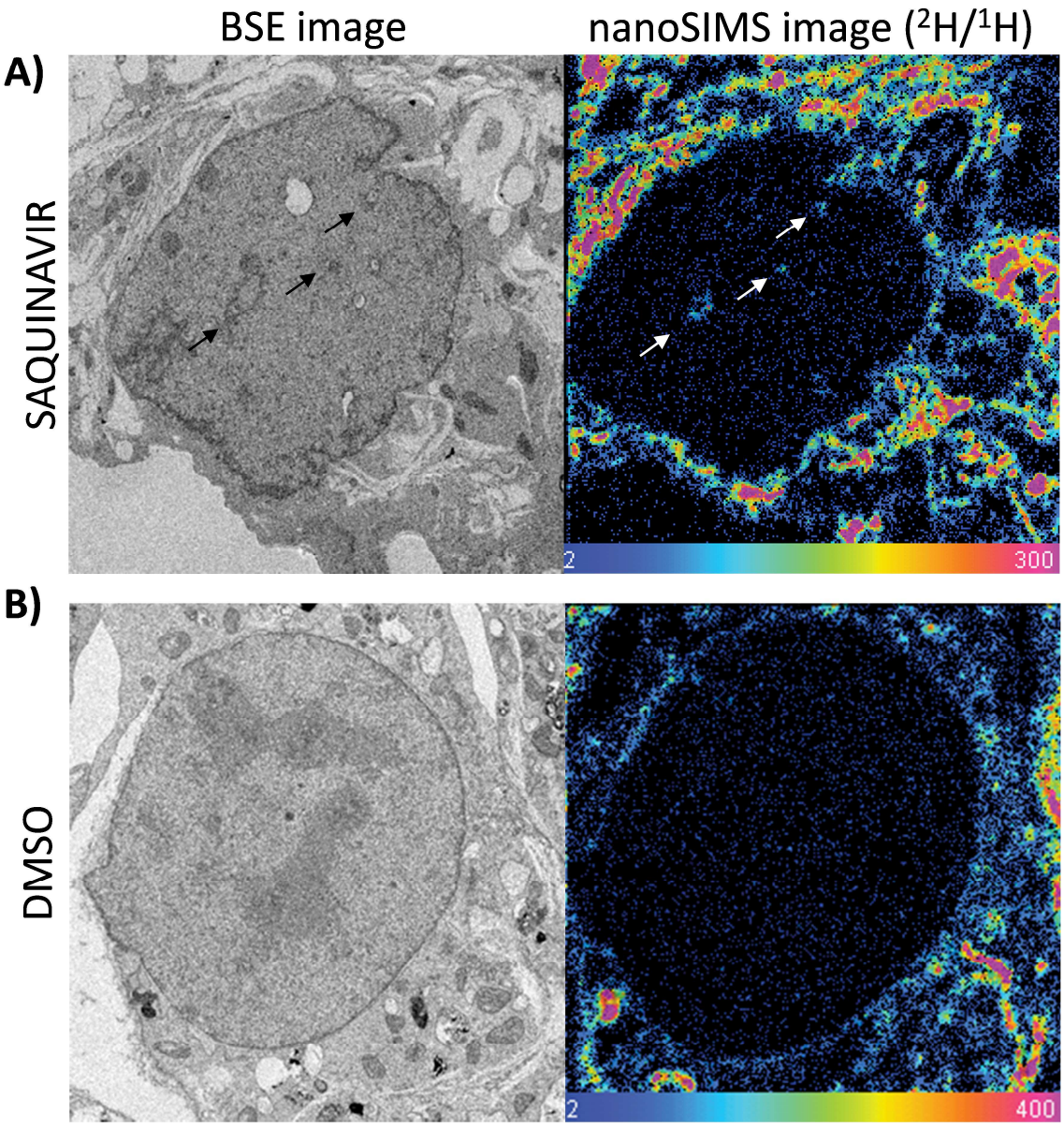

Figure 7.5. Detection of nascent phospholipids during NR formation.

A) Representative back-scattered electron (BSE) image of saquinavir-treated mouse preadipocytes with black arrows indicating NR tubules with a corresponding image from nanoSIMS showing enrichment of deuterium signal ($^{2}H/^{1}H$ ratio) indicating nascent fatty acyl species, also at the NR foci (indicated with white arrows). **B)** BSE and NanoSIMS images of a control cell treated with DMSO vehicle showing lack of NR tubules and no deuterium enrichment within the nucleus, and undistorted nuclear boundary. The very high $^{2}H/^{1}H$ ratio in both conditions at the smooth ER shows *de novo* lipid biosynthesis sites, presumably. This indicates that both saquinavir-treated and control cells are incorporating deuterated acyl moieties into lipids in the same subcellular location and to similar extent. Yet, the nuclear boundary in the control cell shows no ^{2}H enrichment, which indicates that these membranes are stable and not rapidly turning over.

As revealed by BSE imaging, mouse preadipocytes treated with saquinavir exhibited a highly distorted nuclear periphery with membranous NR structures within the nucleus. DMSO-treated control cells retained a smooth and uniform nuclear membrane without the presence of NR tubules (Figure 7.5 A, B). This is consistent with our results on other cell types. When these images were correlated with nanoSIMS analysis it showed high ratio of $^{2}H/^{1}H$ in both conditions, indicating that cells efficiently absorbed deuterated stearic acid from the growth medium. The strongest enrichment of deuterium signal was observed at the ER, which is consistent with the role of the ER as one of the main sites, other than the Golgi apparatus, of *de novo* phospholipid biosynthesis (Fagone and Jackowski, 2009). The bulk nuclear boundary in control cells displayed very modest ^{2}H enrichment indicating that these membranes were stable and not rapidly turning over. Conversely, saquinavir treated cells demonstrated a much higher ^{2}H signal around the nuclear envelope when compared to control cells. This may indicate that upon prelamin A accumulation the nuclear membrane becomes more dynamic and undergoes rearrangements requiring the incorporation of nascent phospholipids. Furthermore, NR structures observed within nuclei of saquinavir-treated cells were also accompanied by increased deuterium signal, highlighting the need for nascent phospholipids at the sites of NR invaginations.

Next, the nascent lipid distribution along the NR tubules was further analysed by 3D reconstruction. This investigation was performed by the step-wise removal of layers of the specimen surface with the ion beam and subsequent analysis of the atomic mass spectra from each consecutive tier. This analysis not only further confirmed incorporation of nascent phospholipids to the NR, but also revealed that the tip of the NR invagination deep within the nucleus is the main site of new

phospholipid incorporation during NR formation, further highlighting the need for newly imported components directly to the NR invagination sites in order to expand NR channels (Figure 7.6). Smaller foci of increased deuterium signal, however, were also observed along the NR channels.

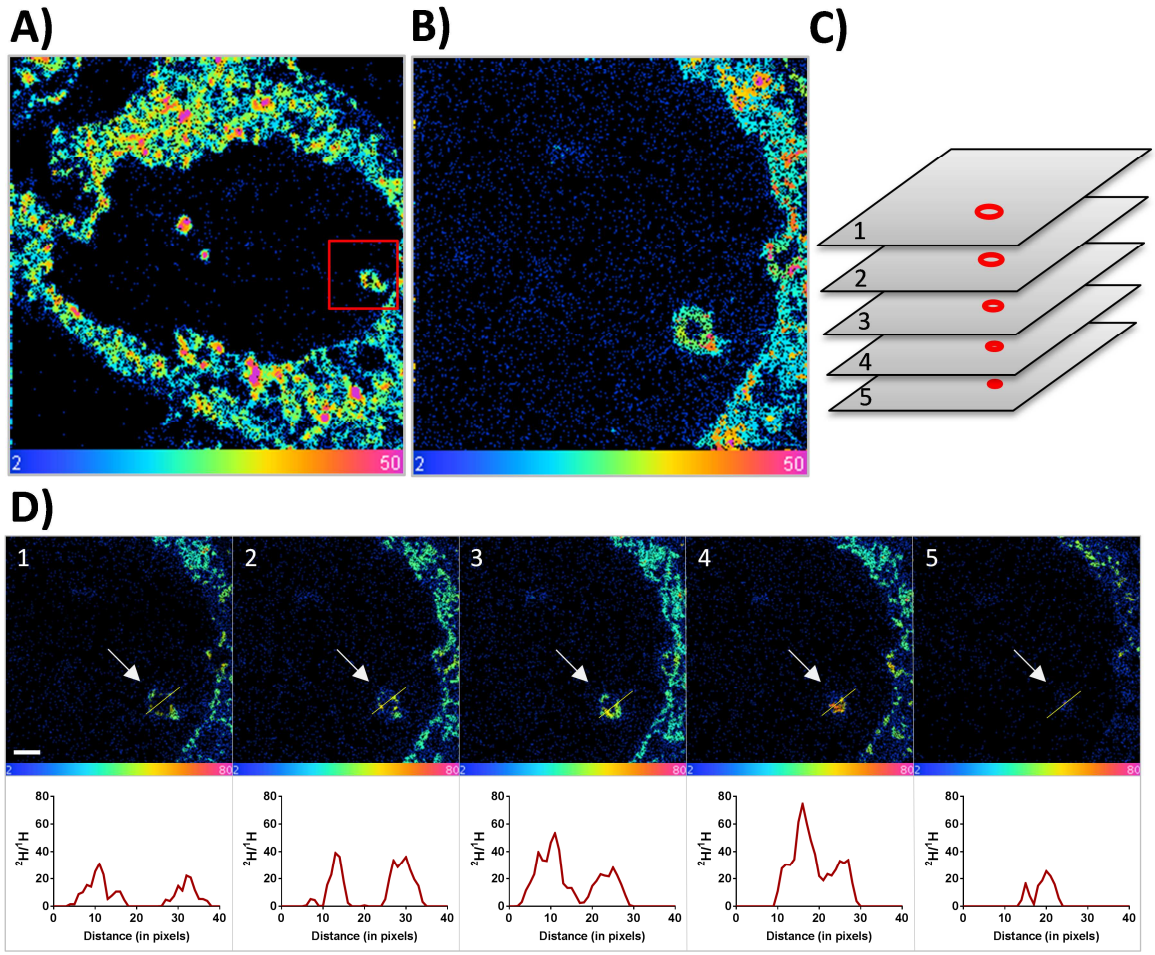

Figure 7.6. Nascent phospholipid distribution along the NR channel.

A) nanoSIMS image of nascent lipid distribution in mouse preadipocytes treated with saquinavir and pulse labelled with ^{2}H-stearate. **B)** Magnification of the region marked with a red rectangle in A. **C)** schematic representation of the orientation of subsequent nanoSIMS images shown in D. **D)** nanoSIMS images of consecutive sections measuring distribution of nascent phospholipids along the NR tubule shown in B; graph below each image represents the ^{2}H/^{1}H ratio measured along the yellow line.

7.3 DISCUSSION

The NR appears to be a dynamic structure with many pathways contributing to its formation. This chapter contributes to the current understanding of the NR formation process in three aspects. First, it presents evidence for identification of a new dominant player in the process of NR assembly, namely NOGO/Reticulon 4. It is important for NR formation not only in a pathological model of NR induction observed under prelamin A accumulation (Figure 7.8) and in HGPS cells, but also in the more physiological context of NR formation in Ishikawa cells. Second, the results presented here provide clues to oestrogen involvement in the process of NR assembly, at least in endometrial cells. Finally, the data gathered here demonstrate that NR formation requires the incorporation of new components, both protein (prelamin A) and nascent membrane phospholipids, rather than rearrangement of the already existing nuclear envelope.

The NR is a membranous organelle originating from the nuclear membrane and is continuous with the ER (Malhas et al., 2011). Induction and maintenance of a positive membrane curvature appears to be a prerequisite for development of this structure. It was therefore hypothesised that reticulons may be involved in the NR formation process since they exhibit the ability to mechanically induce bends in the phospholipid bilayer and are involved in the maintenance of membrane tubulation, as has been previously described in the ER (Shibata et al., 2010). This is the first study demonstrating that NOGO is essential for NR proliferation in a variety of cells stimulated to form NR. The presence of other promoters of NR tubule formation, whether it is pathological accumulation of prelamin A (Figure 7.8) in HeLa cells or physiological exposure to oestrogen in Ishikawa cells, seems to have no effect when

cells are depleted of NOGO protein by siRNA knock-down. This strongly indicates that Reticulon 4 is essential for the initiation process or potentially critical for stabilisation of an early invaginated state during NR formation. The data acquired for HGPS cells in which NOGO depletion reduced the extent of the NR may also suggest the role of NOGO in the maintenance of the NR. These cells normally exhibit high frequency of NR channels due to progerin harbouring an isoprenylated C-terminus. Despite the continuous presence of farnesylated progerin in HGPS cells, NOGO knock-down reduced the mean number of NR tubules. This could potentially indicate that existing invaginations retracted when the NOGO protein was depleted and was therefore unable to stabilise membrane curvature.

It would be beneficial to gather further evidence to ascertain the role of NOGO with respect to initiation and/or maintenance of NR channels. This may be examined by, for example, localised photoactivation of fluorescently-tagged NOGO and live cell imaging to observe its subcellular localisation during NR morphogenesis. Moreover, this study focused on the role of NOGO in the process of NR proliferation. Other reticulons have also been shown to play a role in the ER tubulation in concert with curvature-stabilising protein DP1 (Hu et al., 2008; Shibata et al., 2010; Voeltz et al., 2006). Investigation of their impact on formation of the NR and its maintenance could potentially represent an interesting area of new research.

Formation of the NR is a dynamic process responding to external stimuli. This was demonstrated by the formation of a more extensive NR in HDFs in response to prelamin A accumulation upon saquinavir treatment. Whereas, the NR was disassembled upon withdrawal of the drug pressure as a result of prompt lamin A maturation. The effect of prelamin A on the nucleus and NR morphology is highly

dominant and is attributed to the presence of the isoprenylated cysteine at the protein C-terminus. This, presumably, increases its affinity for the INM and may affect membrane curvature by exhibiting additional physical strain on the membrane (Goulbourne et al., 2011; Toth et al., 2005). Inhibition of lamin A farnesylation by using FTI, improves the dysmorphic nuclear shape by displacing prelamin A to the nuclear interior; processing of the protein to its mature form still fails, but the product is not held at the NE by a persistent hydrophobic interaction (Fong et al., 2006; Toth et al., 2005). Similar observations were made for progerin (Mallampalli et al., 2005). Our data for FTI-treated HGPS cells further extrapolated these observations to NR formation, a process that appears to be more robust in the presence of lamin A variants retaining an isoprenylated tail. Interestingly, late passage HDFs that reached replicative senescence also developed a more prominent NR than their young counterparts. More studies are reporting that prelamin A accumulates in the normal ageing process (as demonstrated in Chapter 3 as well) as a result of decreasing activity of Zmpste24 (Ragnauth et al., 2010), or the presence of progerin in healthy aged individuals due to the spontaneous activation of the cryptic splice site (McClintock et al., 2007; Olive et al., 2010; Scaffidi and Misteli, 2006). It is therefore tempting to speculate that the more extensive NR observed in senescent HDFs develops in response to trace levels of isoprenylated lamin A variants, progerin or prelamin A. Extrapolating further, the extent of the NR could potentially be used as an ageing marker. It would be of particular interest to see if the ageing of different cell types, tissues or organs demonstrate a pattern of changes in the NR structure, as has been observed in many tumour cell types, including breast, brain, bladder, kidney, ovary, and prostate (Fischer et al., 2003; Sarkar et al., 2009).

NR formation was also investigated in a more physiologic context by choosing the Ishikawa cell line as a study model (Nishida et al., 1985). These endometrial cells exhibit a complex NR structure and remain responsive to oestrogen and progesterone. Furthermore, it has been reported that endometrium *in vivo* develops a unique NCS structure which exhibits resemblance to the NR, dependent on hormone exposure (Guffanti et al., 2008; Nejat et al., 2014). The data presented here showed that oestrogen presence in the culture medium stimulates NR channel formation in Ishikawa cells. It may therefore be speculated that oestrogen may act on the endometrium *in vivo* to induce NR proliferation, in turn leading to development of the NCS. This hypothesis is further supported by the fact that NCS and R-rings (an NCS like structure) originate as type I NR invaginations (Isaac et al., 2001). Thus, oestrogen secretion during the menstrual cycle may permit formation of the NCS from NR precursors. Although the exact mechanism by which oestrogen affects NR proliferation remains speculative, it is possible that the action is mediated through phospholipid synthesis. Oestrogen appears to stimulate the catalytic activity of CCTα (Chu and Rooney, 1985a; Chu and Rooney, 1985b) which has been demonstrated to play a crucial role in formation of the NR (Goulbourne et al., 2011; Lagace and Ridgway, 2005). Further work is still needed to fully understand the role of oestrogen in NR formation, including whether or not this is a common response in all steroid-responsive cells. Although the study design ensured hormone ablation in the cell culture by using oestrogen-stripped medium, the use of oestrogen receptor antagonists, like Tamoxifen, may offer more complete inhibition of oestrogen signalling. This might offer a more direct approach in determining the extent to which oestrogen exerts its effects on NR proliferation. Furthermore, in addition to

oestrogen, progesterone has also been shown to induce NCS in endometrial cells (Nejat et al., 2014), also in the absence of ovulation (Kohorn et al., 1972). This suggests a role in mediating intranuclear morphological changes for progesterone as well. Therefore, more work is required to determine if there is synergy between the actions of these two steroid hormones in facilitating NR formation and/or its subsequent transition to a more complex NCS.

Other than the identification of signalling mediators and participation of particular components in the process of NR induction, another aspect is represented by the physical view of NR formation. Nuclear architecture is complex and may be affected both positively and negatively by various forces from within the nucleus and/or from the cytoplasm (Funkhouser et al., 2013; Lammerding et al., 2006; Mammoto and Ingber, 2010; Maniotis et al., 1997; Mazumder et al., 2010; Rowat et al., 2008). The intriguing question is what are the forces behind introducing such extensive alterations to the NE? A few scenarios are possible regarding the models of NR formation (Figure 7.7). Nuclear architecture may be defined by interactions

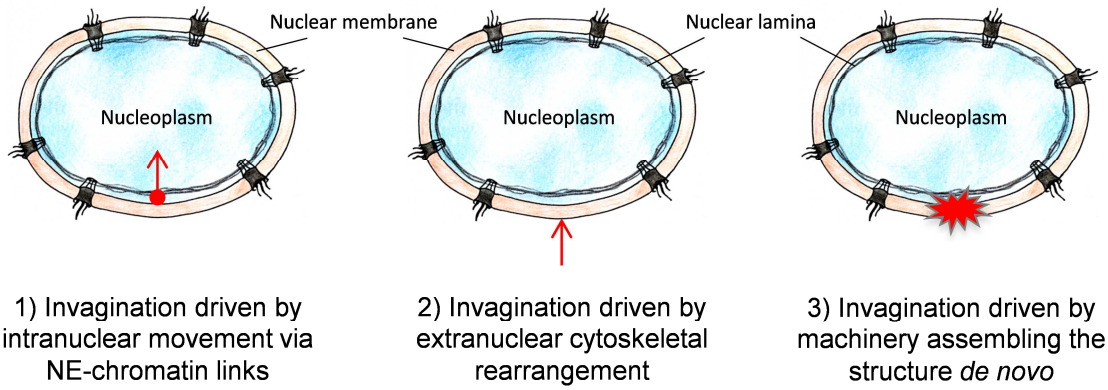

Figure 7.7. Schematic representation of possible mechanisms driving NR formation.

1) Pulling the NE by chromosome territory as indicated by red arrow. **2)** Pushing the NE by cytoskeleton as visualised by red arrow. **3)** *De novo* assembly of NR invaginations by dedicated machinery without additional forces either from within or from outside of the nucleus.

between chromatin and the NE (Mazumder et al., 2008). In addition, in an interphase nucleus, dynamic chromatin movements occur as a result of chromosome condensation (Bauer et al., 2012; Hartl et al., 2008). Thus, NR invaginations could be driven by rearrangements of chromatin tethered to the NE and pulling in the nuclear membrane. This observation was made for NR formation in polytene nuclei from *Drosophila melanogaster* salivary glands (Bozler et al., 2015). Alternatively, the pressure may come from outside of the nucleus. It is well established that the cytoskeleton can counterbalance internal forces of chromatin and the nuclear lamina, thus playing a pivotal role in stabilisation of nuclear architecture (Lammerding et al., 2006; Maniotis et al., 1997; Mazumder et al., 2008). It is possible then that the cytoskeleton exerts forces on the NE and pushes it in. In fact, it has been shown that type II NR invaginations contain microtubules and microfilaments in their core (Bol'shakova et al., 2009; Fricker et al., 1997b; Johnson et al., 2003; Malhas et al., 2011). The third scenario suggests the existence of dedicated machinery that assembles the NR structure *de novo*, rather than by rearrangement of already incorporated elements of the NE.

Our data, presented in this chapter, supports the last model, and shows that formation of the NR requires incorporation of new components directly into proliferating NR tubules (Figure 7.8). It should be noted though, that this does not preclude the other two models, and that they may co-exist. Whatever the physical strain on the NE, however, there is a need for machinery that will assemble the NR structures *de novo*. Super resolution microscopy of fibroblasts exposed to saquinavir revealed that prelamin A is enriched at the NR structures. Because it is the newly synthesised protein, it strongly suggests that forming NR displays a need for building

blocks that are delivered directly to the proliferating NR channels. Furthermore, NR proliferation requires nascent phospholipids, as shown by the nanoSIMS analysis. It has been previously demonstrated that NR formation depends on CCTα, the rate limiting enzyme in membrane phospholipid biosynthesis (Gehrig et al., 2008; Goulbourne et al., 2011). The exact origin of the membrane from which NR was

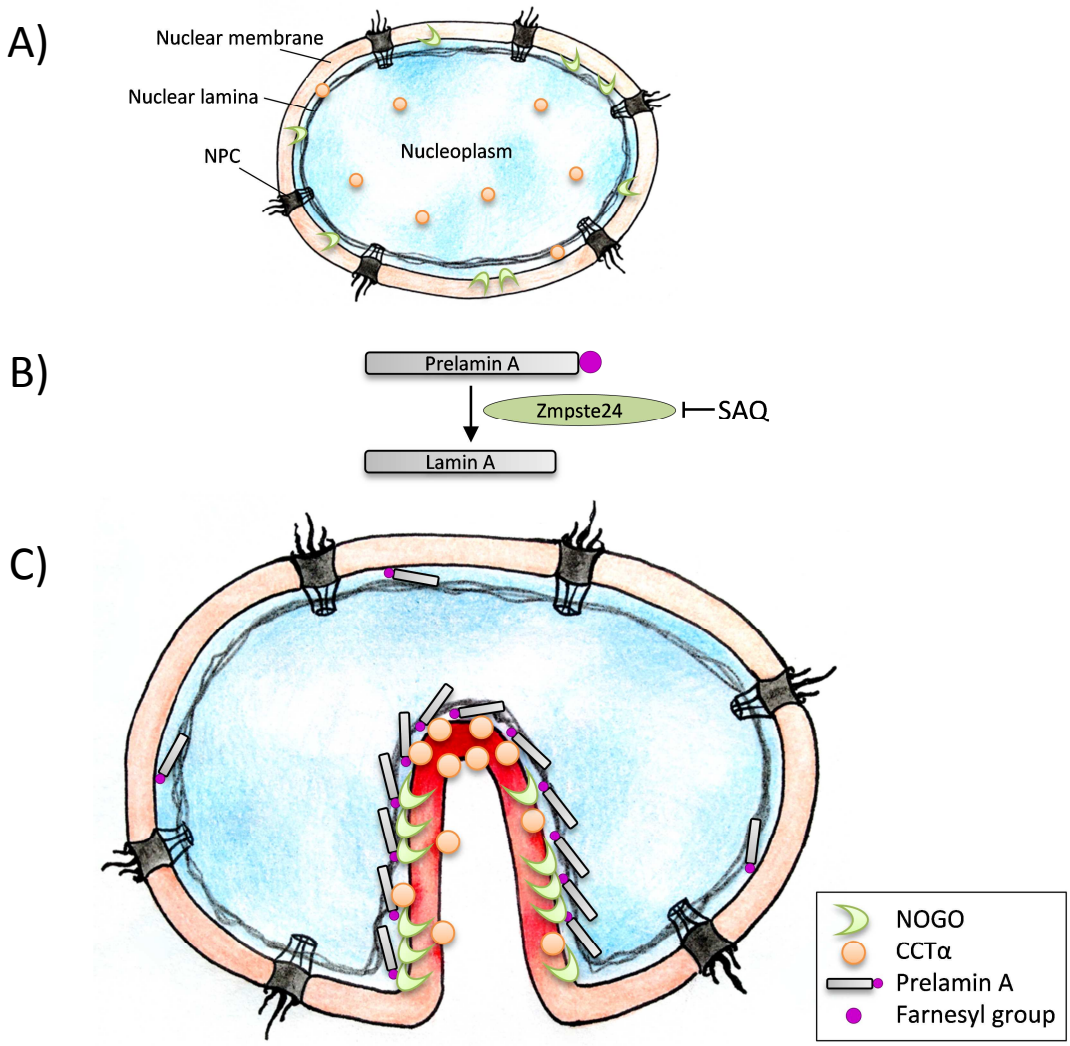

Figure 7.8. Model of NR formation induced by prelamin A accumulation.

A) uninvaginated nucleus upon **(B)** inhibition of prelamin A maturation with saquinavir (SAQ) develops NR tubules **(C)**. Farnesylated prelamin A is predominantly incorporated into the nuclear lamina at the invagination site. Forming NR channel requires NOGO for initiation and/or maintenance of the structure. *De novo* phospholipid biosynthesis by CCTα enzyme occurs on the invaginated membrane with the highest rate at the tip of the forming channel, but also with smaller synthesis foci along the channel (indicated by red colour gradient).

constituted during its proliferation was not studied, with the assumption that the NR derives directly from the components already present in the nuclear membrane. Here we show for the first time that newly synthesised phospholipids are delivered directly to the sites of NR proliferation, with the highest rate of their incorporation at the tip of the forming NR channel. Furthermore, along the channel length, small foci with higher lipid incorporation rates were also observed. This is concordant with observations that CCTα is also unevenly distributed along the NR tubules (Gehrig and Ridgway, 2011; Goulbourne et al., 2011), which may suggest that lipid synthetic machinery is focal. Moreover, such foci could mark points of NR expansion and perhaps facilitate sites of further invaginations as the NR forms branched structures. It would be interesting to see if CCTα foci colocalise with foci observed in nanoSIMS analysis.

In conclusion, the NR forms a distinct and widespread feature in nuclear organisation, therefore gaining further understanding of its form and function is an important aspect of cell biology. Intriguingly, similar to progeroid cells, senescent HDFs also displayed a more abundant NR. It would therefore be of particular interest to see if cells develop an 'ageing' phenotype when formation of the NR is absent, for example after NOGO depletion. Future experiments such as simultaneous NOGO knock-down and senescence induction with saquinavir, followed by transcriptome profiling, could aid in elucidating the existence of this relationship. It would also aid in understanding the links, if existent, between NR changes and altered gene expression.

CHAPTER 8

8 General Discussion

Advances in medicine, better healthcare, and increased understanding of the human body have helped to extend lifespan significantly. It is estimated that by 2050 the number of individuals over the age of 80 will have increased globally by three-fold (Fontana et al., 2014). This will pose a substantial financial strain on economies. Ageing, although not considered a disease itself, predisposes individuals to many chronic pathologies, like atherosclerosis and cardiovascular disease, hypertension, cancer, arthritis, osteoporosis, cataracts, type 2 diabetes, and Alzheimer's disease. The list is long, and ageing is the leading risk factor for these pathological conditions (Budovsky et al., 2006; Hekimi, 2006; Rattan, 2014). Furthermore, more than 70% of individuals over age 65 develop more than one of these age-associated chronic conditions (Hung et al., 2011). A better understanding of ageing science, both at cellular and organismal levels, is therefore crucial for the development of effective strategies and therapies to alleviate at least some of these age-related pathologies. This should also serve to reduce the cost of healthcare. Many factors contribute to ageing, making it a heterogeneous process within a population. Often chronological age does not correspond to the biological age of an individual (Belsky et al., 2015). Moreover, even within the same organism, different rates of ageing are observed in different tissues or organs (Ori et al., 2015). This is most likely a consequence of the organ's physiology and the cellular composition of the tissue.

Nowadays, cellular senescence is a widely accepted hallmark of ageing (López-Otín et al., 2013; Van Deursen, 2014). Many signalling pathways in senescence, operating at the cellular level, have been shown to contribute to the overall deterioration of an organism during the ageing process. and often underlie or are implicated in diseases of advanced age (Jeyapalan and Sedivy, 2008; Ovadya and Krizhanovsky, 2014). Indeed, studies in mouse models have shown that the clearance of senescent cells specifically, whether by genetic modifications or senolytic drugs, significantly extends a healthy lifespan (Baker et al., 2011; Zhu et al., 2015). While senescence may be less complex than ageing, it is nevertheless a multicomponent process. Diverse stress factors have been identified as the inducers of senescence. Multiple effector mechanisms have also been shown to be engaged in execution of the senescence programme and the establishment of a stable proliferative arrest.

Abnormal prelamin A maturation, resulting in slow accumulation of farnesylated lamin A splice variants, has been observed in normal ageing (Olive et al., 2010; Ragnauth et al., 2010; Scaffidi and Misteli, 2006). Whereas a more severe perturbation of prelamin A processing observed in laminopathies, such as HGPS and RD, leads to accelerated premature ageing (Pereira et al., 2008) that is accompanied by an increased abundance of senescent cells, at least in HGPS patients (Brassard et al., 2015). This suggests that farnesylated lamin A variants may contribute to the ageing process by leading to premature cellular senescence. Data in this thesis have demonstrated that acute prelamin A accumulation upon the inhibition of Zmpste24 proteinase with saquinavir induces cell proliferation arrest and the senescent phenotype.

Saquinavir is an older generation of protease inhibitors (PIs) used in highly active antiretroviral therapy (HAART) in HIV/AIDS patients. Interestingly, antiretroviral therapy in these patients appears to enhance premature ageing (Torres and Lewis, 2014). Similar to saquinavir, indinavir and nelfinavir, two currently widely used PIs, block prelamin A maturation *in vitro*, and cause prelamin A accumulation. Newer PIs, like darunavir, do not inhibit Zmpste24 as an off target effect, but are often co-administered with older generation PIs, acting as suicide inhibitors of the cytochrome system that otherwise rapidly inactivates darunavir. Although HAART itself can also cause other side-effects, it is likely that prelamin A accumulation in HIV/AIDS patients contributes to the onset of premature ageing, plausibly by the propagation of senescence.

In this thesis, the comparative study of mRNA profiles from replicative and prelamin A induced senescence revealed that there is a meaningful overlap between these two types of senescence. This is especially prominent in activation of the immune response, lipid metabolism, and cholesterol homeostasis. While similar consequences have been reported in cells senesced by replicative exhaustion, this has not been studied in the context of acute prelamin A accumulation. The unbiased genome-wide transcript analysis presented in this thesis has shown that a significant part of the common senescence programme observed in cellular ageing can be recapitulated in young cells simply by accumulating a nuclear lamin protein at the nuclear periphery. Several aspects of the transcriptional changes observed in senescent cells upon prelamin A accumulation were studied in more detail, but there is a wealth of information still awaiting further investigation. What roles do the five consistently overexpressed genes in the studied senescence models play? Can the

changes in expression of B-Cell CLL/Lymphoma 6 (BCL6), Adhesion G Protein-Coupled Receptor L4 (ADGRL4), Malic Enzyme 1 (ME1), Myosin 1D (MYO1D), and Opsin 3 (OPN3) be specifically linked to prelamin A accumulation? Transcriptome analysis could open doors to many new research areas.

Although our functional analysis of the identified underexpressed genes (A Disintegrin And Metalloproteinase Domain 12 (ADAM12), Aquaporin 1 (AQP1), tight junction protein Claudin 11 (CLDN11), Caveolin 1 (CAV1), Coagulation Factor (F3), and Tissue Plasminogen Activator (PLAT)) in senescence have yet to yield conclusive results, a useful flow cytometry-based assay has been developed for studying senescence and its mediators. Its power is not only in its ability to gather data for a large number of cells, but also because measurements are made on a cell by cell basis. Senescence has evolved regulatory redundancies, so manipulating a single component of a signalling pathway does not necessarily block triggering of the programme. The assay should however allow for testing of perturbation of multiple-components, other senescence readouts, including cell-cycle stage dependence, longer time courses, more homogenous overexpression or knock-down. Another aspect awaiting more research is how prelamin A accumulation in the studied models can regulate expression of these genes. The nuclear lamina has been shown to bind and regulate several transcription factors as well as the chromatin itself (Dechat et al., 2010; Pombo and Dillon, 2015). Transcriptional deregulation in HGPS patients has been linked to progerin accumulation and distortion of the nuclear lamina (Prokocimer et al., 2013). Interestingly, a progeroid murine model which phenocopies HGPS, demonstrated upregulation of several microRNAs, including age-associated miR-29 (Ugalde et al., 2011a). Multiple transcripts that demonstrated underexpression in both replicative

and prelamin A induced senescence have predicted miR-29 binding sites in their transcripts. These include many ECM components, as well as one of our candidates, ADAM12. Thus, investigation of prelamin A-regulated miR-29 expression could be an exciting avenue of new research.

The analysis of the senescence associated secretory phenotype (SASP) of cells acutely accumulating prelamin A presented here is the first such a broad characterisation of SASP in this type of senescence. Similar to conclusions drawn from the transcriptome analysis, acute prelamin A accumulation after saquinavir treatment upregulates the secretion of multiple inflammatory mediators as well as other SASP factors. This demonstrated substantial overlap with replicative senescence. The similarities between replicative senescence and the phenotype induced in young cell populations by prelamin A accumulation extend beyond mRNA and observed intracellular markers to known secreted markers.

Our microarray screen revealed activation of proinflammatory cytokines in replicative senescence and in cells acutely accumulating prelamin A after saquinavir treatment. This was further confirmed at the level of selected secreted cytokines. Inflammation has been observed as a feature of senescent cells in various models (Freund et al., 2010; Kuilman et al., 2008; Minamino et al., 2003; Purcell et al., 2014), but also in normal organismal ageing (Kriete et al., 2008). Our data suggest that prelamin A accumulation, at the level of the entire cell population, can induce interferon response. This occurs most likely through the activation of the RIG-I-like receptor signalling pathway, both in replicative and prelamin A induced senescence, contributing to inflammatory cytokine production. Interferons have been linked to senescence before. It has been shown that exposure to exogenous interferons, both

type I and type II, can induce cellular senescence (Kim et al., 2009; Moiseeva et al., 2006). Moreover, patients undergoing IFNα treatment for hepatitis C were noted to exhibit a higher number of senescent cells (O'Bryan et al., 2011). This suggests, together with our data, that interferon signalling could be triggered by prelamin A, and in turn contribute to senescent phenotype.

Interestingly, in the Zmpste24 knock-down model, only a small subset of SASP factors showed upregulation, including IL6, the hallmark of senescence. Based on observations from immunofluorescent microscopy, this model represents a heterogeneous population, with some cells accumulating prelamin A and others not due to the inefficiency of siRNA transfection in primary cells. Thus perhaps it may therefore represent a state more similar to that observed in tissues *in vivo*, where some cells senesce and others remain healthy. Elevated IL6 is a hallmark of senescence, whereas soluble FAS or MIP1β are less frequently reported as SASP factors. The elderly, however, demonstrate increased plasma levels of these factors (Cheng et al., 2015; Pinti et al., 2004). Thus, considering the process of prelamin A accumulation in ageing, it is plausible that prelamin A plays a vital role in the expression of FAS and MIP1β. It would also be of interest to determine if prelamin A induced SASP factors could induce senescence when added exogenously to early passage cell culture, or whether cell contact is necessary.

The integrity of the nuclear lamina is affected by the accumulation of farnesylated variants of lamin A, whether progerin or prelamin A. This leads to distorted nuclear morphology (Goldman et al., 2004; Goulbourne et al., 2011), which is also a feature observed during the normal ageing process (Scaffidi and Misteli, 2006). A particular aspect of nuclear organisation was investigated in this thesis in

more detail, namely the formation of a nucleoplasmic reticulum (NR), both in the studied ageing models and in other contexts. It was demonstrated that cells senesced by replicative exhaustion form a more extensive NR *in vitro*, in a manner similar to prelamin A accumulating cells. The NR is a common cell feature present in tissues as well (Langevin et al., 2010). Thus, it would be informative to determine if tissue biopsies from elderly individuals demonstrate a higher abundance of NR structures and if there is any tissue type specificity, perhaps correlating with tissues most prone to prelamin A accumulation. Moreover, given that NR formation is enhanced by prelamin A, and that its presence in cells from elderly individuals has been reported as elevated (Olive et al., 2010; Ragnauth et al., 2010), it is plausible that a more abundant NR could mark the tissues most susceptible to abnormal prelamin A processing. NOGO, a reticulon family member, was identified in the research presented here as a new player in the NR formation process. I demonstrate in this thesis that NOGO regulates NR formation in several cell types, under different stimuli. The reticulon family in mammals consists of four members, thus the potential involvement of other reticulons in NR formation is of particular interest. Moreover, a few studies have suggested a role for NOGO and other reticulons in the regulation of neurodegenerative diseases associated with aging, like Alzheimer's disease (He et al., 2004He et al., 2004; Murayama et al., 2006). Therefore, the function of the NR and players involved in its formation may have a far more broad impact than just on nuclear organisation. Detection, classification and quantification of the NR might provide valuable insights into this behaviour at the level of tissue biopsies.

By employing nanoSIMS technology, we show that NR formation requires *de novo* lipid biosynthesis, at least under pathological conditions when prelamin A

acutely accumulates. This is the first of its kind such a report. It also supports observation from the microarray experiment that prelamin A accumulation alters lipometabolism. It would be important to test whether such a relationship is truly prelamin A dependent and performing experiments in lamin A knock-out background would prove very informative.

The studies described in this thesis have addressed several aspects of cellular ageing and have uncovered striking similarities between replicative and prelamin A-induced senescence. Molecular, biochemical, and morphological alterations have been described in senescent cells and potential mechanisms underlying these changes have been elucidated. The role of abnormal prelamin A processing and its impact on the ageing process, including severe progeroid syndromes such as HGPS and RD, is well documented. Therefore, improved understanding of the role of prelamin A in senescence and the engaged mediator pathways will help with deciphering the general regulation of the senescence process and may pave the way for developing anti-ageing therapeutics.

References

Abdelmohsen, K., Kuwano, Y., Kim Hyeon, H., and Gorospe, M. (2008). Posttranscriptional gene regulation by RNA-binding proteins during oxidative stress: implications for cellular senescence. Biological Chemistry *389*, 243-255.

Acosta, J.C., Banito, A., Wuestefeld, T., Georgilis, A., Janich, P., Morton, J.P., Athineos, D., Kang, T.-W., Lasitschka, F., Andrulis, M.*, et al.* (2013). A complex secretory program orchestrated by the inflammasome controls paracrine senescence. Nature Cell Biology *15*, 978-990.

Acosta, J.C., O'Loghlen, A., Banito, A., Guijarro, M.V., Augert, A., Raguz, S., Fumagalli, M., Da Costa, M., Brown, C., Popov, N.*, et al.* (2008). Chemokine Signaling via the CXCR2 Receptor Reinforces Senescence. Cell *133*, 1006-1018.

Adams, M., Kelley, J., Gocayne, J., Dubnick, M., Polymeropoulos, M., Xiao, H., Merril, C., Wu, A., Olde, B., Moreno, R.*, et al.* (1991). Complementary DNA sequencing: expressed sequence tags and human genome project. Science *252*, 1651-1656.

Adams, P.D. (2009). Healing and hurting: molecular mechanisms, functions, and pathologies of cellular senescence. Molecular Cell *36*, 2-14.

Aebi, U., Cohn, J.B., Buhle, L., and Gerace, L. (1986). The nuclear lamina is a meshwork of intermediate type filaments. Nature *323*, 560-564.

Agre, P., Preston, G.M., Smith, B.L., Jin Sup, J., Raina, S., Moon, C., Guggino, W.B., and Nielsen, S. (1993). Aquaporin CHIP: The archetypal molecular water channel. American Journal of Physiology - Renal Fluid and Electrolyte Physiology *265*, F463-F476.

Ahmady, E., Deeke, S.A., Rabaa, S., Kouri, L., Kenney, L., Stewart, A.F.R., and Burgon, P.G. (2011). Identification of a novel muscle A-type lamin-interacting protein (MLIP). Journal of Biological Chemistry *286*, 19702-19713.

Alcorta, D.A., Xiong, Y., Phelps, D., Hannon, G., Beach, D., and Barrett, J.C. (1996). Involvement of the cyclin-dependent kinase inhibitor p16 (INK4a) in replicative senescence of normal human fibroblasts. Proceedings of the National Academy of Sciences *93*, 13742-13747.

Alimonti, A., Nardella, C., Chen, Z., Clohessy, J.G., Carracedo, A., Trotman, L.C., Cheng, K., Varmeh, S., Kozma, S.C., Thomas, G*., et al.* (2010). A novel type of cellular senescence that can be enhanced in mouse models and human tumor xenografts to suppress prostate tumorigenesis. The Journal of Clinical Investigation *120*, 681-693.

Aliper, A.M., Csoka, A.B., Buzdin, A., Jetka, T., Roumiantsev, S., Moskalev, A., and Zhavoronkov, A. (2015). Signaling pathway activation drift during aging: Hutchinson-Gilford Progeria Syndrome fibroblasts are comparable to normal middle-age and old-age cells. Aging (Albany NY) *7*, 26-37.

Allen, R.G., Tresini, M., Keogh, B.P., Doggett, D.L., and Cristofalo, V.J. (1999). Differences in electron transport potential, antioxidant defenses, and oxidant generation in young and senescent fetal lung fibroblasts (WI-38). Journal of Cellular Physiology *180*, 114-122.

Altieri, P., Spallarossa, P., Barisione, C., Garibaldi, S., Garuti, A., Fabbi, P., Ghigliotti, G., and Brunelli, C. (2012). Inhibition of Doxorubicin-Induced Senescence by PPARδ Activation Agonists in Cardiac Muscle Cells: Cooperation between PPARδ and Bcl6. PLoS ONE *7*, e46126.

Álvarez-Rodríguez, L., López-Hoyos, M., Muñoz-Cacho, P., and Martínez-Taboada, V.M. (2012). Aging is associated with circulating cytokine dysregulation. Cellular Immunology *273*, 124-132.

Anderson, A.S., and Loeser, R.F. (2010). Why is Osteoarthritis an Age-Related Disease? Best practice and research: Clinical Rheumatology *24*, 15-26.

Apte, R., Dotan, S., Elkabets, M., White, M., Reich, E., Carmi, Y., Song, X., Dvozkin, T., Krelin, Y., and Voronov, E. (2006). The involvement of IL-1 in tumorigenesis, tumor invasiveness, metastasis and tumor-host interactions. Cancer and Metastasis Reviews *25*, 387-408.

Bader, G.D., Cary, M.P., and Sander, C. (2006). Pathguide: a Pathway Resource List. Nucleic Acids Research *34*, D504-D506.

Bakan, I., and Laplante, M. (2012). Connecting mTORC1 signaling to SREBP-1 activation. Current Opinion in Lipidology *23*, 226-234.

Baker, D.J., Perez-Terzic, C., Jin, F., Pitel, K., Niederländer, N.J., Jeganathan, K., Yamada, S., Reyes, S., Rowe, L., Hiddinga, H.J*., et al.* (2008). Opposing roles for p16(Ink4a) and p19(Arf) in senescence and ageing caused by BubR1 insufficiency. Nature Cell Biology *10*, 825-836.

Baker, D.J., Wijshake, T., Tchkonia, T., LeBrasseur, N.K., Childs, B.G., van de Sluis, B., Kirkland, J.L., and van Deursen, J.M. (2011). Clearance of p16Ink4a-positive senescent cells delays ageing-associated disorders. Nature *479*, 232-236.

Bakkenist, C.J., and Kastan, M.B. (2003). DNA damage activates ATM through intermolecular autophosphorylation and dimer dissociation. Nature *421*, 499-506.

Bandyopadhyay, D., Okan, N.A., Bales, E., Nascimento, L., Cole, P.A., and Medrano, E.E. (2002). Down-regulation of p300/CBP histone acetyltransferase

activates a senescence checkpoint in human melanocytes. Cancer Research *62*, 6231-6239.

Barascu, A., Le Chalony, C., Pennarun, G., Genet, D., Imam, N., Lopez, B., and Bertrand, P. (2012). Oxidative stress induces an ATM-independent senescence pathway through p38 MAPK-mediated lamin B1 accumulation. EMBO J *31*, 1080-1094.

Barrowman, J., and Michaelis, S. (2009). ZMPSTE24, an integral membrane zinc metalloprotease with a connection to progeroid disorders. Biological Chemistry *390*, 761-773.

Bartkova, J., Horejsi, Z., Koed, K., Kramer, A., Tort, F., Zieger, K., Guldberg, P., Sehested, M., Nesland, J.M., Lukas, C*., et al.* (2005). DNA damage response as a candidate anti-cancer barrier in early human tumorigenesis. Nature *434*, 864-870.

Bartkova, J., Rezaei, N., Liontos, M., Karakaidos, P., Kletsas, D., Issaeva, N., Vassiliou, L.V.F., Kolettas, E., Niforou, K., Zoumpourlis, V.C*., et al.* (2006). Oncogene-induced senescence is part of the tumorigenesis barrier imposed by DNA damage checkpoints. Nature *444*, 633-637.

Baruch, K., Deczkowska, A., David, E., Castellano, J.M., Miller, O., Kertser, A., Berkutzki, T., Barnett-Itzhaki, Z., Bezalel, D., Wyss-Coray, T*., et al.* (2014). Aging-induced type I interferon response at the choroid plexus negatively affects brain function. Science *346*, 89-93.

Bates, S., Phillips, A.C., Clark, P.A., Stott, F., Peters, G., Ludwig, R.L., and Vousden, K.H. (1998). p14ARF links the tumour suppressors RB and p53. Nature *395*, 124-125.

Bauer, C.R., Hartl, T.A., and Bosco, G. (2012). Condensin II promotes the formation of chromosome territories by inducing axial compaction of polyploid interphase chromosomes. PLoS Genetics *8*, e1002873.

Bavik, C., Coleman, I., Dean, J.P., Knudsen, B., Plymate, S., and Nelson, P.S. (2006). The gene expression program of prostate fibroblast senescence modulates neoplastic epithelial cell proliferation through paracrine mechanisms. Cancer Research *66*, 794-802.

Beauséjour, C.M., Krtolica, A., Galimi, F., Narita, M., Lowe, S.W., Yaswen, P., and Campisi, J. (2003). Reversal of human cellular senescence: roles of the p53 and p16 pathways. The EMBO Journal *22*, 4212-4222.

Beck, L.A., Hosick, T.J., and Sinensky, M. (1990). Isoprenylation is required for the processing of the lamin A precursor. J Cell Biol *110*, 1489-1499.

Belsky, D.W., Caspi, A., Houts, R., Cohen, H.J., Corcoran, D.L., Danese, A., Harrington, H., Israel, S., Levine, M.E., Schaefer, J.D*., et al.* (2015). Quantification of biological aging in young adults. Proceedings of the National Academy of Sciences *112*, E4104-E4110.

Ben-Harush, K. (2009). The supramolecular organization of the C. elegans nuclear lamin filament. J Mol Biol *386*, 1392-1402.

Ben-Neriah, Y., and Karin, M. (2011). Inflammation meets cancer, with NF-κB as the matchmaker. Nature Immunology *12*, 715-723.

Ben-Porath, I., and Weinberg, R.A. (2005). The signals and pathways activating cellular senescence. The International Journal of Biochemistry & Cell Biology *37*, 961-976.

Benesh, A.E., Fleming, J.T., Chiang, C., Carter, B.D., and Tyska, M.J. (2012). Expression and localization of myosin-1d in the developing nervous system. Brain Research *1440*, 9-22.

Benjamini, Y., and Hochberg, Y. (1995). Controlling the False Discovery Rate - a Practical and Powerful Approach to Multiple Testing. Journal of the Royal Statistical Society Series B-Methodological *57*, 289 - 300.

Berrougui, H., and Khalil, A. (2009). Age-Associated Decrease of High-Density Lipoprotein-Mediated Reverse Cholesterol Transport Activity. Rejuvenation Research *12*, 117-126.

Bhat, R., Crowe, E.P., Bitto, A., Moh, M., Katsetos, C.D., Garcia, F.U., Johnson, F.B., Trojanowski, J.Q., Sell, C., and Torres, C. (2012). Astrocyte senescence as a component of Alzheimer's Disease. PLoS ONE *7*, e45069.

Bhaumik, D., Scott, G.K., Schokrpur, S., Patil, C.K., Orjalo, A.V., Rodier, F., Lithgow, G.J., and Campisi, J. (2009). MicroRNAs miR-146a/b negatively modulate the senescence-associated inflammatory mediators IL-6 and IL-8. AGING *1*, 402-411.

Bione, S. (1994). Identification of a novel X-linked gene responsible for Emery-Dreifuss muscular dystrophy. Nature Genet *8*, 323-327.

Bitto, A., Sell, C., Crowe, E., Lorenzini, A., Malaguti, M., Hrelia, S., and Torres, C. (2010). Stress-induced senescence in human and rodent astrocytes. Experimental Cell Research *316*, 2961-2968.

Bodin, K., Bretillon, L., Aden, Y., Bertilsson, L., Broomé, U., Einarsson, C., and Diczfalusy, U. (2001). Antiepileptic Drugs Increase Plasma Levels of 4β-Hydroxycholesterolin Humans: EVIDENCE FOR INVOLVEMENT OF CYTOCHROME P450 3A4. Journal of Biological Chemistry *276*, 38685-38689.

Bodnar, A.G., Ouellette, M., Frolkis, M., Holt, S.E., Chiu, C.-P., Morin, G.B., Harley, C.B., Shay, J.W., Lichtsteiner, S., and Wright, W.E. (1998). Extension of Life-Span by Introduction of Telomerase into Normal Human Cells. Science *279*, 349-352.

Bol'shakova, A.V., Petukhova, O.A., Pinaev, G.P., and Magnusson, K.E. (2009). Comparative analysis of subcellular fractionation methods for revealing α-actinin 1 and α-actinin 4 in A431 cells. Cell and Tissue Biology *3*, 188-197.

Bond, J.A., Haughton, M.F., Rowson, J.M., Smith, P.J., Gire, V., Wynford-Thomas, D., and Wyllie, F.S. (1999). Control of Replicative Life Span in Human Cells: Barriers to Clonal Expansion Intermediate Between M1 Senescence and M2 Crisis. Molecular and Cellular Biology *19*, 3103-3114.

Bondar, T., and Medzhitov, R. (2013). The Origins of Tumor-Promoting Inflammation. Cancer Cell *24*, 143-144.

Bonne, G. (1999). Mutations in the gene encoding lamin A/C cause autosomal dominant Emery-Dreifuss muscular dystrophy. Nature Genet *21*, 285-288.

Borgnia, M., Nielsen, S., Engel, A., and Agre, P. (1999). Cellular and molecular biology of the aquaporin water channels. Annual Review of Biochemistry *68*, 425-458.

Bozler, J., Nguyen, H.Q., Rogers, G.C., and Bosco, G. (2015). Condensins exert force on chromatin-nuclear envelope tethers to mediate nucleoplasmic reticulum formation in Drosophila melanogaster. G3: Genes|Genomes|Genetics *5*, 341-352.

Bracken, A.P., Kleine-Kohlbrecher, D., Dietrich, N., Pasini, D., Gargiulo, G., Beekman, C., Theilgaard-Mönch, K., Minucci, S., Porse, B.T., Marine, J.-C*., et al.* (2007). The Polycomb group proteins bind throughout the INK4A-ARF locus and are disassociated in senescent cells. Genes & Development *21*, 525-530.

Braig, M., Lee, S., Loddenkemper, C., Rudolph, C., Peters, A.H.F.M., Schlegelberger, B., Stein, H., Dorken, B., Jenuwein, T., and Schmitt, C.A. (2005). Oncogene-induced senescence as an initial barrier in lymphoma development. Nature *436*, 660-665.

Braig, M., and Schmitt, C. (2006). Oncogene-induced senescence: putting the brakes on tumor development. Cancer Res *66*, 2881-2884.

Brassard, J.A., Fekete, N., Garnier, A., and Hoesli, C.A. (2015). Hutchinson–Gilford progeria syndrome as a model for vascular aging. Biogerontology, [Epub ahead of print].

Braumuller, H., Wieder, T., Brenner, E., Aszmann, S., Hahn, M., Alkhaled, M., Schilbach, K., Essmann, F., Kneilling, M., Griessinger, C*., et al.* (2013). T-helper-1-cell cytokines drive cancer into senescence. Nature *494*, 361-365.

Brenner, A.J., Stampfer, M.R., and Aldaz, C.M. (1998). Increased p16 expression with first senescence arrest in human mammary epithelial cells and extended growth capacity with p16 inactivation. Oncogene *17*, 199-205.

Brown, J.P., Wei, W., and Sedivy, J.M. (1997). Bypass of Senescence After Disruption of p21CIP1/WAF1 Gene in Normal Diploid Human Fibroblasts. Science *277*, 831-834.

Brunk, U., Ericsson, J.L.E., Pontén, J., and Westermark, B. (1973). Residual bodies and “aging” in cultured human glia cells: Effect of entrance into phase III and prolonged periods of confluence. Experimental Cell Research *79*, 1-14.

Brzostek-Racine, S., Gordon, C., Van Scoy, S., and Reich, N.C. (2011). The DNA Damage Response Induces IFN. The Journal of Immunology *187*, 5336-5345.

Budovsky, A., Muradian, K.K., and Fraifeld, V.E. (2006). From disease-oriented to aging/longevity-oriented studies. Rejuvenation Research *9*, 207-210.

Buffoli, B., Foglio, E., Borsani, E., Exley, C., Rezzani, R., and Rodella, L.F. (2013). Silicic acid in drinking water prevents age-related alterations in the endothelium-dependent vascular relaxation modulating eNOS and AQP1 expression in experimental mice: An immunohistochemical study. Acta Histochemica *115*, 418-424.

Burke, B., and Stewart, C.L. (2013). The nuclear lamins: Flexibility in function. Nature Reviews Molecular Cell Biology *14*, 13-24.

Burtner, C.R., and Kennedy, B.K. (2010). Progeria syndromes and ageing: what is the connection? Nat Rev Mol Cell Biol *11*, 567-578.

Burton, D.A., and Krizhanovsky, V. (2014). Physiological and pathological consequences of cellular senescence. Cell Mol Life Sci *71*, 4373-4386.

Bussolati, G., Marchiò, C., Gaetano, L., Lupo, R., and Sapino, A. (2008). Pleomorphism of the nuclear envelope in breast cancer: a new approach to an old problem. Journal of Cellular and Molecular Medicine *12*, 209-218.

Butin-Israeli, V., Adam, S.A., Goldman, A.E., and Goldman, R.D. (2012). Nuclear lamin functions and disease. Trends in Genetics *28*, 464-471.

Campisi, J. (2005). Senescent cells, tumor suppression, and organismal aging: good citizens, bad neighbors. Cell *120*, 513-522.

Campisi, J. (2013). Aging, Cellular Senescence, and Cancer. Annual review of physiology *75*, 685-705.

Campisi, J., Andersen, J., Kapahi, P., and Melov, S. (2011). Cellular senescence: a link between cancer and age-related degenerative disease? Seminars in cancer biology *21*, 354-359.

Campisi, J., and d'Adda di Fagagna, F. (2007). Cellular senescence: when bad things happen to good cells. Nature Reviews Molecular Cell Biology *8*, 729-740.

Candelario, J., Borrego, S., Reddy, S., and Comai, L. (2011). Accumulation of distinct prelamin A variants in human diploid fibroblasts differentially affects cell homeostasis. Experimental Cell Research *317*, 319-329.

Cao, K., Blair, C.D., Faddah, D.A., Kieckhaefer, J.E., Olive, M., Erdos, M.R., Nabel, E.G., and Collins, F.S. (2011). Progerin and telomere dysfunction collaborate to trigger cellular senescence in normal human fibroblasts. The Journal of Clinical Investigation *121*, 2833-2844.

Capell, B.C., and Collins, F.S. (2006). Human laminopathies: nuclei gone genetically awry. Nat Rev Genet *7*, 940-952.

Capell, B.C., Erdos, M.R., Madigan, J.P., Fiordalisi, J.J., Varga, R., Conneely, K.N., Gordon, L.B., Der, C.J., Cox, A.D., and Collins, F.S. (2005). Inhibiting farnesylation of progerin prevents the characteristic nuclear blebbing of Hutchinson-Gilford progeria syndrome. Proceedings of the National Academy of Sciences of the United States of America *102*, 12879-12884.

Carboni, N., Politano, L., Floris, M., Mateddu, A., Solla, E., Olla, S., Maggi, L., Maioli, M.A., Piras, R., Cocco, E.*, et al.* (2013). Overlapping syndromes in laminopathies: A meta-analysis of the reported literature. Acta Myologica *32*, 7-17.

Caux, F., Dubosclard, E., Lascols, O., Buendia, B., Chazouillères, O., Cohen, A., Courvalin, J.C., Laroche, L., Capeau, J., Vigouroux, C.*, et al.* (2003). A new clinical condition linked to a novel mutation in lamins A and C with generalized lipoatrophy, insulin-resistant diabetes, disseminated leukomelanodermic papules, liver steatosis, and cardiomyopathy. Journal of Clinical Endocrinology and Metabolism *88*, 1006-1013.

Chamero, P., Manjarres, I.M., García-Verdugo, J.M., Villalobos, C., Alonso, M.T., and García-Sancho, J. (2008). Nuclear calcium signaling by inositol trisphosphate in GH3 pituitary cells. Cell Calcium *43*, 205-214.

Chandler, H., and Peters, G. (2013). Stressing the cell cycle in senescence and aging. Current Opinion in Cell Biology *25*, 765-771.

Chandra, T., Kirschner, K., Thuret, J.-Y., Pope, B.D., Ryba, T., Newman, S., Ahmed, K., Samarajiwa, S.A., Salama, R., Carroll, T.*, et al.* (2012). Independence of Repressive Histone Marks and Chromatin Compaction during Senescent Heterochromatic Layer Formation. Molecular Cell *47*, 203-214.

Chang, B.-D., Swift, M.E., Shen, M., Fang, J., Broude, E.V., and Roninson, I.B. (2002). Molecular determinants of terminal growth arrest induced in tumor cells by a chemotherapeutic agent. Proceedings of the National Academy of Sciences of the United States of America *99*, 389-394.

Chen, J. (2011). Hematopoietic stem cell development, aging and functional failure. International Journal of Hematology *94*, 3-10.

Chen, L., Lee, L., Kudlow, B.A., Dos Santos, H.G., Sletvold, O., Shafeghati, Y., Botha, E.G., Garg, A., Hanson, N.B., Martin, G.M.*, et al.* (2003). LMNA mutations in atypical Werner's syndrome. Lancet *362*, 440-445.

Chen, Q., Fischer, A., Reagan, J.D., Yan, L.J., and Ames, B.N. (1995). Oxidative DNA damage and senescence of human diploid fibroblast cells. Proceedings of the National Academy of Sciences of the United States of America *92*, 4337-4341.

Chen, Q., Liu, K., Robinson, A.R., Clauson, C.L., Blair, H.C., Robbins, P.D., Niedernhofer, L.J., and Ouyang, H. (2013). DNA damage drives accelerated bone aging

via an NF-κB–dependent mechanism. Journal of Bone and Mineral Research *28*, 1214-1228.

Chen, Q.M., Liu, J., and Merrett, J.B. (2000). Apoptosis or senescence-like growth arrest: influence of cell-cycle position, p53, p21 and bax in H2O2 response of normal human fibroblasts. Biochemical Journal *347*, 543-551.

Chen, Z., Trotman, L.C., Shaffer, D., Lin, H.K., Dotan, Z.A., Niki, M., Koutcher, J.A., Scher, H.I., Ludwig, T., Gerald, W.*, et al.* (2005). Crucial role of p53-dependent cellular senescence in suppression of Pten-deficient tumorigenesis. Nature *436*, 725-730.

Cheng, J., Zhou, T., Liu, C., Shapiro, J., Brauer, M., Kiefer, M., Barr, P., and Mountz, J. (1994). Protection from Fas-mediated apoptosis by a soluble form of the Fas molecule. Science *263*, 1759-1762.

Cheng, N.-L., Chen, X., Kim, J., Shi, A.H., Nguyen, C., Wersto, R., and Weng, N.-P. (2015). MicroRNA-125b modulates inflammatory chemokine CCL4 expression in immune cells and its reduction causes CCL4 increase with age. Aging Cell *14*, 200-208.

Chiang, J.Y.L. (2013). Bile Acid Metabolism and Signaling. Comprehensive Physiology *3*, 1191-1212.

Chicas, A., Wang, X., Zhang, C., McCurrach, M., Zhao, Z., Mert, O., Dickins, R.A., Narita, M., Zhang, M., and Lowe, S.W. (2010). Dissecting the Unique Role of the Retinoblastoma Tumor Suppressor during Cellular Senescence. Cancer Cell *17*, 376-387.

Chien, Y., Scuoppo, C., Wang, X., Fang, X., Balgley, B., Bolden, J.E., Premsrirut, P., Luo, W., Chicas, A., Lee, C.S.*, et al.* (2011). Control of the senescence-associated secretory phenotype by NF-κB promotes senescence and enhances chemosensitivity. Genes & Development *25*, 2125-2136.

Childs, B.G., Baker, D.J., Kirkland, J.L., Campisi, J., and van Deursen, J.M. (2014). Senescence and apoptosis: dueling or complementary cell fates? EMBO reports *15*, 1139-1153.

Chinta, S.J., Lieu, C.A., DeMaria, M., Laberge, R.M., Campisi, J., and Andersen, J.K. (2013). Environmental stress, ageing and glial cell senescence: a novel mechanistic link to Parkinson's disease? Journal of Internal Medicine *273*, 429-436.

Chiu, W.K., Fann, M., and Weng, N.-p. (2006). Generation and Growth of CD28(null)CD8(+) Memory T Cells Mediated by IL-15 and Its Induced Cytokines. Journal of immunology (Baltimore, Md : 1950) *177*, 7802-7810.

Choi, H.R., Cho, K.A., Kang, H.T., Lee, J.B., Kaeberlein, M., Suh, Y., Chung, I.K., and Park, S.C. (2011). Restoration of senescent human diploid fibroblasts by modulation of the extracellular matrix. Aging Cell *10*, 148-157.

Chomczynski, P., and Sacchi, N. (1987). Single-step method of RNA isolation by acid guanidinium thiocyanate-phenol-chloroform extraction. Analytical Biochemistry *162*, 156-159.

Christensen, N., D'Souza, M., Zhu, X., and Frisina, R.D. (2009). Age-related hearing loss: Aquaporin 4 gene expression changes in the mouse cochlea and auditory midbrain. Brain Research *1253*, 27-34.

Chu, A.J., and Rooney, S.A. (1985a). Estrogen stimulation of surfactant synthesis. Pediatric pulmonology *1*, S110-114.

Chu, A.J., and Rooney, S.A. (1985b). Stimulation of cholinephosphate cytidylyltransferase activity by estrogen in fetal rabbit lung is mediated by phospholipids. Biochimica et Biophysica Acta (BBA) - Lipids and Lipid Metabolism *834*, 346-356.

Chung, H.Y., Cesari, M., Anton, S., Marzetti, E., Giovannini, S., Seo, A.Y., Carter, C., Yu, B.P., and Leeuwenburgh, C. (2009). Molecular Inflammation: Underpinnings of Aging and Age-related Diseases. Ageing Research Reviews *8*, 18-30.

Coffinier, C., Hudon, S.E., Farber, E.A., Chang, S.Y., Hrycyna, C.A., Young, S.G., and Fong, L.G. (2007). HIV protease inhibitors block the zinc metalloproteinase ZMPSTE24 and lead to an accumulation of prelamin A in cells. Proceedings of the National Academy of Sciences *104*, 13432-13437.

Coffinier, C., Hudon, S.E., Lee, R., Farber, E.A., Nobumori, C., Miner, J.H., Andres, D.A., Spielmann, H.P., Hrycyna, C.A., Fong, L.G.*, et al.* (2008). A Potent HIV Protease Inhibitor, Darunavir, Does Not Inhibit ZMPSTE24 or Lead to an Accumulation of Farnesyl-prelamin A in Cells. Journal of Biological Chemistry *283*, 9797-9804.

Collado-Hilly, M., Shirvani, H., Jaillard, D., and Mauger, J.-P. (2010). Differential redistribution of Ca2+-handling proteins during polarisation of MDCK cells: Effects on Ca2+ signalling. Cell Calcium *48*, 215-224.

Collado, M., Blasco, M.A., and Serrano, M. (2007). Cellular senescence in cancer and aging. Cell *130*, 223-233.

Collado, M., Gil, J., Efeyan, A., Guerra, C., Schuhmacher, A.J., Barradas, M., Benguría, A., Zaballos, A., Flores, J.M., Barbacid, M.*, et al.* (2005). Tumour biology: senescence in premalignant tumours. Nature *436*, 642.

Collado, M., and Serrano, M. (2010). Senescence in tumours: evidence from mice and humans. Nature Reviews Cancer *10*, 51-57.

Collen, D., and Lijnen, H. (1991). Basic and clinical aspects of fibrinolysis and thrombolysis. Blood *78*, 3114-3124.

Collins, C.J., and Sedivy, J.M. (2003). Involvement of the INK4a/Arf gene locus in senescence. Aging Cell *2*, 145-150.

Combet, S., Gouraud, S., Gobin, R., Berthonaud, V., Geelen, G., Corman, B., and Verbavatz, J.M. (2008). Aquaporin-2 downregulation in kidney medulla of aging rats is posttranscriptional and is abolished by water deprivation. American Journal of Physiology - Renal Physiology *294*, F1408-F1414.

Comi, P., Chiaramonte, R., and Maier, J.A.M. (1995). Senescence-dependent regulation of type 1 plasminogen activator inhibitor in human vascular endothelial cells. Experimental Cell Research *219*, 304-308.

Contrino, J., Hair, G., Kreutzer, D.L., and Rickles, F.R. (1996). In situ detection of tissue factor in vascular endothelial cells: Correlation with the malignant phenotype of human breast disease. Nature Medicine *2*, 209-215.

Coppé, J.-P., Desprez, P.-Y., Krtolica, A., and Campisi, J. (2010a). The Senescence-Associated Secretory Phenotype: The Dark Side of Tumor Suppression. Annual Review of Pathology: Mechanisms of Disease *5*, 99-118.

Coppé, J.-P., Patil, C.K., Rodier, F., Krtolica, A., Beauséjour, C.M., Parrinello, S., Hodgson, J.G., Chin, K., Desprez, P.-Y., and Campisi, J. (2010b). A Human-Like Senescence-Associated Secretory Phenotype Is Conserved in Mouse Cells Dependent on Physiological Oxygen. PLoS ONE *5*, e9188.

Coppé, J.-P., Patil, C.K., Rodier, F., Sun, Y., Muñoz, D.P., Goldstein, J., Nelson, P.S., Desprez, P.-Y., and Campisi, J. (2008). Senescence-Associated Secretory Phenotypes reveal cell-nonautonomous functions of oncogenic RAS and the p53 tumor suppressor. PLoS Biol *6*, e301.

Coppé, J.-P., Rodier, F., Patil, C.K., Freund, A., Desprez, P.-Y., and Campisi, J. (2011). Tumor Suppressor and Aging Biomarker p16INK4a Induces Cellular Senescence without the Associated Inflammatory Secretory Phenotype. Journal of Biological Chemistry *286*, 36396-36403.

Coppé, J., Kauser, K., Campisi, J., and Beausejour, C. (2006). Secretion of vascular endothelial growth factor by primary human fibroblasts at senescence. Journal of Biological Chemistry *281*, 29568-29574.

Coppedè, F., and Migliore, L. (2010). DNA repair in premature aging disorders and neurodegeneration. Current Aging Science *3*, 3-19.

Coppola, D., Balducci, L., Chen, D.-T., Loboda, A., Nebozhyn, M., Staller, A., Fulp, W.J., Dalton, W., Yeatman, T., and Brem, S. (2014). Senescence-associated-gene signature identifies genes linked to age, prognosis, and progression of human gliomas. Journal of Geriatric Oncology *5*, 389-399.

Cornell, R.B., and Ridgway, N.D. (2015). CTP:phosphocholine cytidylyltransferase: Function, regulation, and structure of an amphitropic enzyme required for membrane biogenesis. Progress in Lipid Research *59*, 147-171.

Corrigan, D.P. (2005). Prelamin A endoproteolytic processing in vitro by recombinant Zmpste24. Biochem J *387*, 129-138.

Courtois-Cox, S., Genther Williams, S.M., Reczek, E.E., Johnson, B.W., McGillicuddy, L.T., Johannessen, C.M., Hollstein, P., MacCollin, M., and Cichowski, K. (2006). A negative feedback signaling network underlies oncogene-induced senescence. Cancer Cell *10*, 459-472.

Creixell, P., Jüri Reimand, Syed Haider, Guanming Wu, Tatsuhiro Shibata, Miguel Vazquez, Ville Mustonen, Abel Gonzalez-Perez, John Pearson, Chris Sander*, et al.* (2015). Pathway and network analysis of cancer genomes. Nat Meth *12*, 615-621.

Crescenzi, E., Pacifico, F., Lavorgna, A., De Palma, R., D'Aiuto, E., Palumbo, G., Formisano, S., and Leonardi, A. (2011). NF-κB-dependent cytokine secretion controls Fas expression on chemotherapy-induced premature senescent tumor cells. Oncogene *30*, 2707-2717.

Crisp, M., and Burke, B. (2008). The nuclear envelope as an integrator of nuclear and cytoplasmic architecture. FEBS Letters *582*, 2023-2032.

Cristofalo, V.J., and Pignolo, R.J. (1996). Molecular markers of senescence in fibroblast-like cultures. Experimental Gerontology *31*, 111-123.

Crosetto, N., Bienko, M., and van Oudenaarden, A. (2015). Spatially resolved transcriptomics and beyond. Nat Rev Genet *16*, 57-66.

Csoka, A.B., English, S.B., Simkevich, C.P., Ginzinger, D.G., Butte, A.J., Schatten, G.P., Rothman, F.G., and Sedivy, J.M. (2004). Genome-scale expression profiling of Hutchinson–Gilford progeria syndrome reveals widespread transcriptional misregulation leading to mesodermal/mesenchymal defects and accelerated atherosclerosis. Aging Cell *3*, 235-243.

Cuervo, A.M., and Dice, J.F. (2000). When lysosomes get old. Experimental Gerontology *35*, 119-131.

Czabotar, P.E., Lessene, G., Strasser, A., and Adams, J.M. (2014). Control of apoptosis by the BCL-2 protein family: Implications for physiology and therapy. Nature Reviews Molecular Cell Biology *15*, 49-63.

d'Adda di Fagagna, F. (2003). A DNA damage checkpoint response in telomere-initiated senescence. Nature *426*, 194-198.

d'Adda di Fagagna, F. (2008). Living on a break: cellular senescence as a DNA-damage response. Nat Rev Cancer *8*, 512-522.

Danø, K., Andreasen, P.A., Grøndahl-Hansen, J., Kristensen, P., Nielsen, L.S., and Skriver, L. (1985). Plasminogen activators, tissue degradation, and cancer. Advances in Cancer Research *44*, 139-266.

Dauer, W.T., and Worman, H.J. (2009). The nuclear envelope as a signaling node in development and disease. Dev Cell *17*, 626-638.

Davies, B.S.J., Coffinier, C., Yang, S.H., Barnes, R.H., Jung, H.J., Young, S.G., and Fong, L.G. (2011). Investigating the purpose of prelamin A processing. Nucleus *2*, 4-9.

de Las Heras, J.I., Meinke, P., Batrakou, D.G., Srsen, V., Zuleger, N., Kerr, A.R., and Schirmer, E.C. (2013). Tissue specificity in the nuclear envelope supports its functional complexity. Nucleus (Austin, Tex) *4*, 460-477.

de Magalhães, J.P., Curado, J., and Church, G.M. (2009). Meta-analysis of age-related gene expression profiles identifies common signatures of aging. Bioinformatics *25*, 875-881.

De Sandre-Giovannoli, A., Bernard, R., Cau, P., Navarro, C., Amiel, J., Boccaccio, I., Lyonnet, S., Stewart, C.L., Munnich, A., Le Merrer, M.*, et al.* (2003). Lamin A truncation in Hutchinson-Gilford progeria. Science *300*, 2055.

De Sandre-Giovannoli, A., Chaouch, M., Kozlov, S., Vallat, J.M., Tazir, M., Kassouri, N., Szepetowski, P., Hammadouche, T., Vandenberghe, A., Stewart, C.L.*, et al.* (2002). Homozygous defects in LMNA, encoding lamin A/C nuclear-envelope

proteins, cause autosomal recessive axonal neuropathy in human (Charcot-Marie-Tooth disorder type 2) and mouse. American Journal of Human Genetics *70*, 726-736.

De Vos, W.H., Houben, F., Kamps, M., Malhas, A., Verheyen, F., Cox, J., Manders, E.M.M., Verstraeten, V.L.R.M., van Steensel, M.A.M., Marcelis, C.L.M.*, et al.* (2011). Repetitive disruptions of the nuclear envelope invoke temporary loss of cellular compartmentalization in laminopathies. Human Molecular Genetics *20*, 4175-4186.

Debacq-Chainiaux, F., Borlon, C., Pascal, T., Royer, V., Eliaers, F., Ninane, N., Carrard, G., Friguet, B., de Longueville, F., Boffe, S.*, et al.* (2005). Repeated exposure of human skin fibroblasts to UVB at subcytotoxic level triggers premature senescence through the TGF-β1 signaling pathway. Journal of Cell Science *118*, 743-758.

DeBusk, F.L. (1972). The Hutchinson-Gilford progeria syndrome. Report of 4 cases and review of the literature. The Journal of Pediatrics *80*, 697-724.

Dechat, T., Adam, S.A., Taimen, P., Shimi, T., and Goldman, R.D. (2010). Nuclear lamins. Cold Spring Harb Perspect Biol *2*, a000547.

Dechat, T., Korbei, B., Vaughan, O.A., Vlcek, S., Hutchison, C.J., and Foister, R. (2000). Lamina-associated polypeptide 2α binds intranuclear A-type lamins. Journal of Cell Science *113*, 3473-3484.

Delbarre, E., Tramier, M., Coppey-Moisan, M., Gaillard, C., Courvalin, J.C., and Buendia, B. (2006). The truncated prelamin A in Hutchinson-Gilford progeria syndrome alters segregation of A-type and B-type lamin homopolymers. Human Molecular Genetics *15*, 1113-1122.

Demaria, M., Ohtani, N., Youssef, Sameh A., Rodier, F., Toussaint, W., Mitchell, James R., Laberge, R.-M., Vijg, J., Van Steeg, H., Dollé, Martijn E.T.*, et al.* (2014). An

Essential Role for Senescent Cells in Optimal Wound Healing through Secretion of PDGF-AA. Developmental Cell *31*, 722-733.

Denchi, E.L., Attwooll, C., Pasini, D., and Helin, K. (2005). Deregulated E2F Activity Induces Hyperplasia and Senescence-Like Features in the Mouse Pituitary Gland. Molecular and Cellular Biology *25*, 2660-2672.

Denker, B.M., Smith, B.L., Kuhajda, F.P., and Agre, P. (1988). Identification, purification, and partial characterization of a novel Mr 28,000 integral membrane protein from erythrocytes and renal tubules. Journal of Biological Chemistry *263*, 15634-15642.

Desvergne, B., and Wahli, W. (1999). Peroxisome Proliferator-Activated Receptors: Nuclear Control of Metabolism. Endocrine Reviews *20*, 649-688.

Dhe-Paganon, S., Werner, E.D., Chi, Y.I., and Shoelson, S.E. (2002). Structure of the globular tail of nuclear lamin. J Biol Chem *277*, 17381-17384.

Di Micco, R., Fumagalli, M., Cicalese, A., Piccinin, S., Gasparini, P., Luise, C., Schurra, C., Garre, M., Giovanni Nuciforo, P., Bensimon, A*., et al.* (2006). Oncogene-induced senescence is a DNA damage response triggered by DNA hyper-replication. Nature *444*, 638-642.

Di Micco, R., Sulli, G., Dobreva, M., Liontos, M., Botrugno, O.A., Gargiulo, G., dal Zuffo, R., Matti, V., d'Ario, G., Montani, E*., et al.* (2011). Interplay between oncogene-induced DNA damage response and heterochromatin in senescence and cancer. Nature Cell Biology *13*, 292-302.

Dickson, M.A., Tap, W.D., Keohan, M.L., D'Angelo, S.P., Gounder, M.M., Antonescu, C.R., Landa, J., Qin, L.-X., Rathbone, D.D., Condy, M.M*., et al.* (2013). Phase II Trial of the CDK4 Inhibitor PD0332991 in Patients With Advanced CDK4-Amplified

Well-Differentiated or Dedifferentiated Liposarcoma. Journal of Clinical Oncology *31*, 2024-2028.

Dimri, G.P., Lee, X., Basile, G., Acosta, M., Scott, G., Roskelley, C., Medrano, E.E., Linskens, M., Rubelj, I., and Pereira-Smith, O. (1995). A biomarker that identifies senescent human cells in culture and in aging skin in vivo. Proceedings of the National Academy of Sciences *92*, 9363-9367.

Dittmer, T.A., Sahni, N., Kubben, N., Hill, D.E., Vidal, M., Burgess, R.C., Roukos, V., and Misteli, T. (2014). Systematic identification of pathological lamin A interactors. Molecular Biology of the Cell *25*, 1493-1510.

Dockery, P., Pritchard, K., Warren, M.A., Li, T.C., and Cooke, I.D. (1996). Uterus and endometrium: Changes in nuclear morphology in the human endometrial glandular epithelium in women with unexplained infertility. Human Reproduction *11*, 2251-2256.

Dorner, D., Gotzmann, J., and Foisner, R. (2007). Nucleoplasmic lamins and their interaction partners, LAP2α, Rb, and BAF, in transcriptional regulation. FEBS Journal *274*, 1362-1373.

Dreesen, O., and Stewart, C.L. (2011). Accelerated aging syndromes, are they relevant to normal human aging? Aging *3*, 889-895.

Dyer, J.A., Kill, I.R., Pugh, G., Quinlan, R.A., Lane, E.B., and Hutchison, C.J. (1997). Cell cycle changes in A-type lamin associations detected in human dermal fibroblasts using monoclonal antibodies. Chromosome Research *5*, 383-394.

Edwards, M.G., Anderson, R.M., Yuan, M., Kendziorski, C.M., Weindruch, R., and Prolla, T.A. (2007). Gene expression profiling of aging reveals activation of a p53-mediated transcriptional program. BMC Genomics *8*, 80-93.

Efeyan, A., and Serrano, M. (2007). p53: Guardian of the genome and policeman of the oncogenes. Cell Cycle *6*, 1006-1010.

Eguchi, H., Fujiwara, N., Sakiyama, H., Yoshihara, D., and Suzuki, K. (2011). Hydrogen peroxide enhances LPS-induced nitric oxide production via the expression of interferon beta in BV-2 microglial cells. Neuroscience Letters *494*, 29-33.

Elzi, D.J., Lai, Y., Song, M., Hakala, K., Weintraub, S.T., and Shiio, Y. (2012). Plasminogen activator inhibitor 1 - insulin-like growth factor binding protein 3 cascade regulates stress-induced senescence. Proceedings of the National Academy of Sciences *109*, 12052-12057.

Emery, A.E., and Dreifuss, F.E. (1966). Unusual type of benign x-linked muscular dystrophy. Journal of Neurology Neurosurgery and Psychiatry *29*, 338-342.

Emery, A.E.H. (2000). Emery-Dreifuss muscular dystrophy - A 40 year retrospective. Neuromuscular Disorders *10*, 228-232.

Eriksson, M., Brown, W.T., Gordon, L.B., Glynn, M.W., Singer, J., Scott, L., Erdos, M.R., Robbins, C.M., Moses, T.Y., Berglund, P.*, et al.* (2003). Recurrent de novo point mutations in lamin A cause Hutchinson-Gilford progeria syndrome. Nature *423*, 293-298.

Erusalimsky, J.D., and Kurz, D.J. (2005). Cellular senescence in vivo: Its relevance in ageing and cardiovascular disease. Experimental Gerontology *40*, 634-642.

Erwig, L.P., and Henson, P.M. (2007). Clearance of apoptotic cells by phagocytes. Cell Death Differ *15*, 243-250.

Evan, G.I., and d'Adda di Fagagna, F. (2009). Cellular senescence: hot or what? Current opinion in genetics and development *19*, 25-31.

Fagone, P., and Jackowski, S. (2009). Membrane phospholipid synthesis and endoplasmic reticulum function. Journal of Lipid Research *50*, S311-S316.

Faruqi, T.R., Gomez, D., Bustelo, X.R., Bar-Sagi, D., and Reich, N.C. (2001). Rac1 mediates STAT3 activation by autocrine IL-6. Proceedings of the National Academy of Sciences *98*, 9014-9019.

Fatkin, D., Macrae, C., Sasaki, T., Wolff, M.R., Porcu, M., Frenneaux, M., Atherton, J., Vidaillet Jr, H.J., Spudich, S., De Girolami, U*., et al.* (1999). Missense mutations in the rod domain of the lamin A/C gene as causes of dilated cardiomyopathy and conduction-system disease. New England Journal of Medicine *341*, 1715-1724.

Feng, Z., Hu, W., Teresky, A.K., Hernando, E., Cordon-Cardo, C., and Levine, A.J. (2007). Declining p53 function in the aging process: A possible mechanism for the increased tumor incidence in older populations. Proceedings of the National Academy of Sciences *104*, 16633-16638.

Feria-Velasco, A., Aznar-Ramos, R., and González-Angulo, A. (1972). Ultrastructural changes found in the endometrium of women using megestrol acetate for contraception. Contraception *5*, 187-201.

Ferrell, J.E. (2013). Feedback loops and reciprocal regulation: recurring motifs in the systems biology of the cell cycle. Current Opinion in Cell Biology *25*, 676-686.

Fischer, A.H., Taysavang, P., and Jhiang, S.M. (2003). Nuclear Envelope irregularity is induced by RET/PTC during interphase. The American Journal of Pathology *163*, 1091-1100.

Fisher, D.Z., Chaudhary, N., and Blobel, G. (1986). cDNA sequencing of nuclear lamins A and C reveals primary and secondary structural homology to intermediate filament proteins. Proceedings of the National Academy of Sciences *83*, 6450-6454.

Flores, J., García-Avello, Á., Alonso, E., Ruíz, A., Navarrete, O., Álvarez, C., Lozano, C., and Arribas, I. (2014). Tissue plasminogen activator as a novel diagnostic aid in acute pulmonary embolism. Vasa *43*, 450-458.

Florey, H.W. (1970). General pathology (London, UK, Lloyd–Luke).

Foeger, N. (2006). Solubility properties and specific assembly pathways of the B-type lamin from Caenorhabditis elegans. Journal of Structural Biology *155*, 340-350.

Fong, L.G., Frost, D., Meta, M., Qiao, X., Yang, S.H., Coffinier, C., and Young, S.G. (2006). A Protein Farnesyltransferase Inhibitor Ameliorates Disease in a Mouse Model of Progeria. Science *311*, 1621-1623.

Fontana, L., Kennedy, B., Longo, V., Seals, D., and Melov, S. (2014). Medical research: treat ageing. Nature *511*, 405-407.

Ford, J.H. (2010). Saturated fatty acid metabolism is key link between cell division, cancer, and senescence in cellular and whole organism aging. Age *32*, 231-237.

Franceschi, C., and Campisi, J. (2014). Chronic Inflammation (Inflammaging) and Its Potential Contribution to Age-Associated Diseases. The Journals of Gerontology Series A: Biological Sciences and Medical Sciences *69*, S4-S9.

Franceschi, C., Capri, M., Monti, D., Giunta, S., Olivieri, F., Sevini, F., Panourgia, M.P., Invidia, L., Celani, L., Scurti, M.*, et al.* (2007). Inflammaging and anti-inflammaging: A systemic perspective on aging and longevity emerged from studies in humans. Mechanisms of Ageing and Development *128*, 92-105.

Franceschini, A., Szklarczyk, D., Frankild, S., Kuhn, M., Simonovic, M., Roth, A., Lin, J., Minguez, P., Bork, P., von Mering, C.*, et al.* (2013). STRING v9.1: protein-protein interaction networks, with increased coverage and integration. Nucleic Acids Research *41*, D808-D815.

Freund, A., Laberge, R.-M., Demaria, M., and Campisi, J. (2012). Lamin B1 loss is a senescence-associated biomarker. Molecular Biology of the Cell *23*, 2066-2075.

Freund, A., Orjalo, A.V., Desprez, P.-Y., and Campisi, J. (2010). Inflammatory networks during cellular senescence: causes and consequences. Trends in Molecular Medicine *16*, 238-246.

Freund, A., Patil, C.K., and Campisi, J. (2011). p38MAPK is a novel DNA damage response-independent regulator of the senescence-associated secretory phenotype. The EMBO Journal *30*, 1536-1548.

Fricker, M., Hollinshead, M., White, N., and Vaux, D. (1997a). The convoluted nucleus. Trends in Cell Biology *7*, 181.

Fricker, M., Hollinshead, M., White, N., and Vaux, D. (1997b). Interphase nuclei of many mammalian cell types contain deep, dynamic, tubular membrane-bound invaginations of the nuclear envelope. The Journal of Cell Biology *136*, 531-544.

Fridman, A.L., and Tainsky, M.A. (2008). Critical pathways in cellular senescence and immortalization revealed by gene expression profiling. Oncogene *27*, 10.1038/onc.2008.1213.

Fridman, A.L., Tang, L., Kulaeva, O.I., Ye, B., Li, Q., Nahhas, F., Roberts, P.C., Land, S.J., Abrams, J., and Tainsky, M.A. (2006). Expression Profiling Identifies Three Pathways Altered in Cellular Immortalization: Interferon, Cell Cycle, and Cytoskeleton.

The Journals of Gerontology Series A: Biological Sciences and Medical Sciences *61*, 879-889.

Fridolfsson, H.N., and Patel, H.H. (2013). Caveolin and caveolae in age associated cardiovascular disease. Journal of Geriatric Cardiology *10*, 66-74.

Fuchs, E., and Weber, K. (1994). Intermediate filaments: Structure, dynamics, function, and disease. Annual Review of Biochemistry *63*, 345-382.

Fuchs, Y., and Steller, H. (2011). Programmed cell death in animal development and disease. Cell *147*, 742-758.

Fumagalli, M., Rossiello, F., Clerici, M., Barozzi, S., Cittaro, D., Kaplunov, J.M., Bucci, G., Dobreva, M., Matti, V., Beausejour, C.M.*, et al.* (2012). Telomeric DNA damage is irreparable and causes persistent DNA-damage-response activation. Nature Cell Biology *14*, 355-365.

Fumagalli, M., Rossiello, F., Mondello, C., and D'Adda Di Fagagna, F. (2014). Stable cellular senescence is associated with persistent DDR activation. PLoS ONE *9*, e110969.

Funkhouser, C.M., Sknepnek, R., Shimi, T., Goldman, A.E., Goldman, R.D., and Olvera de la Cruz, M. (2013). Mechanical model of blebbing in nuclear lamin meshworks. Proceedings of the National Academy of Sciences of the United States of America *110*, 3248-3253.

Furukawa, K., and Hotta, Y. (1993). cDNA cloning of a germ cell-specific lamin B3 from mouse spermatocytes and analysis of its ectopic expression in somatic cells. EMBO J *12*, 97-106.

Furukawa, K., Inagaki, H., and Hotta, Y. (1994). Identification and cloning of an mRNA coding for a germ cell-specific A-type lamin in mice. Exp Cell Res *212*, 426-430.

Futerman, A.H., and Hannun, Y.A. (2004). The complex life of simple sphingolipids. EMBO Reports *5*, 777-782.

Galluzzi, L., Vitale, I., Abrams, J.M., Alnemri, E.S., Baehrecke, E.H., Blagosklonny, M.V., Dawson, T.M., Dawson, V.L., El-Deiry, W.S., Fulda, S*., et al.* (2012). Molecular definitions of cell death subroutines: recommendations of the Nomenclature Committee on Cell Death 2012. Cell Death Differ *19*, 107-120.

Gao, L., Van Den Hurk, K., Moerkerk, P.T.M., Goeman, J.J., Beck, S., Gruis, N.A., Van Den Oord, J.J., Winnepenninckx, V.J., Van Engeland, M., and Van Doorn, R. (2014). Promoter CpG island hypermethylation in dysplastic nevus and melanoma: CLDN11 as an epigenetic biomarker for malignancy. Journal of Investigative Dermatology *134*, 2957-2966.

Garnier, D., Milsom, C., Magnus, N., Meehan, B., Weitz, J., Yu, J., and Rak, J. (2010). Role of the tissue factor pathway in the biology of tumor initiating cells. Thrombosis Research *125 Suppl 2*, S44-50.

Gehrig, K., Cornell, R.B., and Ridgway, N.D. (2008). Expansion of the Nucleoplasmic Reticulum Requires the Coordinated Activity of Lamins and CTP:Phosphocholine Cytidylyltransferase α. Molecular Biology of the Cell *19*, 237-247.

Gehrig, K., Lagace, T.A., and Ridgway, N.D. (2009). Oxysterol activation of phosphatidylcholine synthesis involves CTP:phosphocholine cytidylyltransferase α translocation to the nuclear envelope. Biochemical Journal *418*, 209-217.

Gehrig, K., and Ridgway, N.D. (2011). CTP:phosphocholine cytidylyltransferase α (CCTα) and lamins alter nuclear membrane structure without affecting phosphatidylcholine synthesis. Biochimica et Biophysica Acta (BBA) - Molecular and Cell Biology of Lipids *1811*, 377-385.

Georgakopoulou, E.A., Tsimaratou, K., Evangelou, K., Fernandez, M.-P.J., Zoumpourlis, V., Trougakos, I.P., Kletsas, D., Bartek, J., Serrano, M., and Gorgoulis, V.G. (2013). Specific lipofuscin staining as a novel biomarker to detect replicative and stress-induced senescence. A method applicable in cryo-preserved and archival tissues. Aging (Albany NY) *5*, 37-50.

Gerace, L., and Blobel, G. (1980). The nuclear envelope lamina is reversibly depolymerized during mitosis. Cell *19*, 277-287.

Gerace, L., Blum, A., and Blobel, G. (1978). Immunocytochemical localization of the major polypeptides of the nuclear complex-lamina fraction: interphase and mitotic distribution. J Cell Biol *79*, 546-566.

Gey, C., and Seeger, K. (2013). Metabolic changes during cellular senescence investigated by proton NMR-spectroscopy. Mechanisms of Ageing and Development *134*, 130-138.

Ghosh, S., and Zhou, Z. (2014). Genetics of aging, progeria and lamin disorders. Current Opinion in Genetics and Development *26*, 41-46.

Gil, J., and Peters, G. (2006). Regulation of the INK4b-ARF-INK4a tumour suppressor locus: all for one or one for all. Nat Rev Mol Cell Biol *7*, 667-677.

Gilbert, L.A., and Hemann, M.T. (2010). DNA damage-mediated induction of a chemoresistant niche. Cell *143*, 355-366.

Giordano, C.R., and Terlecky, S.R. (2012). Peroxisomes, cell senescence, and rates of aging. Biochimica et Biophysica Acta (BBA) - Molecular Basis of Disease *1822*, 1358-1362.

Gire, V., Roux, P., Wynford-Thomas, D., Brondello, J.-M., and Dulic, V. (2004). DNA damage checkpoint kinase Chk2 triggers replicative senescence. The EMBO Journal *23*, 2554-2563.

Glass, C.K., Saijo, K., Winner, B., Marchetto, M.C., and Gage, F.H. (2010). Mechanisms Underlying Inflammation in Neurodegeneration. Cell *140*, 918-934.

Goldberg, M.W., Huttenlauch, I., Hutchison, C.J., and Stick, R. (2008). Filaments made from A- and B-type lamins differ in structure and organization. J Cell Sci *121*, 215-225.

Goldman, A.E., Moir, R.D., Montag-Lowy, M., Stewart, M., and Goldman, R.D. (1992). Pathway of incorporation of microinjected lamin A into the nuclear envelope. Journal of Cell Biology *119*, 725-735.

Goldman, R.D., Shumaker, D.K., Erdos, M.R., Eriksson, M., Goldman, A.E., Gordon, L.B., Gruenbaum, Y., Khuon, S., Mendez, M., Varga, R*., et al.* (2004). Accumulation of mutant lamin A progressive changes in nuclear architecture in Hutchinson-Gilford progeria syndrome. Proceedings of the National Academy of Sciences of the United States of America *101*, 8963-8968.

Gong, L.-L., Peng, J.-H., Han, F.-F., Zhu, J., Fang, L.-H., Wang, Y.-H., Du, G.-H., Wang, H.-Y., and Liu, L.-H. (2012). Association of tissue plasminogen activator and plasminogen activator inhibitor polymorphism with myocardial infarction: A meta-analysis. Thrombosis Research *130*, e43-e51.

González, J.M., Navarro-Puche, A., Casar, B., Crespo, P., and Andrés, V. (2008). Fast regulation of AP-1 activity through interaction of lamin A/C, ERK1/2, and c-Fos at the nuclear envelope. The Journal of Cell Biology *183*, 653-666.

Gonzalez Malagon, S.G., Melidoni, A.N., Hernandez, D., Omar, B.A., Houseman, L., Veeravalli, S., Scott, F., Varshavi, D., Everett, J., Tsuchiya, Y.*, et al.* (2015). The phenotype of a knockout mouse identifies flavin-containing monooxygenase 5 (FMO5) as a regulator of metabolic ageing. Biochemical Pharmacology *96*, 267-277.

Gonzalo, S., and Kreienkamp, R. (2015). DNA repair defects and genome instability in Hutchinson-Gilford Progeria Syndrome. Current Opinion in Cell Biology *34*, 75-83.

Gorenne, I., Kavurma, M., Scott, S., and Bennett, M. (2006). Vascular smooth muscle cell senescence in atherosclerosis. Cardiovascular Research *72*, 9-17.

Gorgoulis, V.G., and Halazonetis, T.D. (2010). Oncogene-induced senescence: the bright and dark side of the response. Current Opinion in Cell Biology *22*, 816-827.

Goulbourne, C.N., Malhas, A.N., and Vaux, D.J. (2011). The induction of a nucleoplasmic reticulum by prelamin A accumulation requires CTP:phosphocholine cytidylyltransferase-α. Journal of Cell Science *124*, 4253-4266.

Gow, A., Southwood, C.M., Li, J.S., Pariali, M., Riordan, G.P., Brodie, S.E., Danias, J., Bronstein, J.M., Kachar, B., and Lazzarini, R.A. (1999). CNS Myelin and sertoli cell tight junction strands are absent in OSP/claudin-11 null mice. Cell *99*, 649-659.

Gratzner, H.G. (1982). Monoclonal antibody to 5-bromo- and 5-iododeoxyuridine: A new reagent for detection of DNA replication. Science *218*, 474-475.

Grillari, J., Hohenwarter, O., Grabherr, R.M., and Katinger, H. (2000). Subtractive Hybridization of mRNA from early passage and senescent endothelial cells. Experimental Gerontology *35*, 187-197.

Grossman, E., Dahan, I., Stick, R., Goldberg, M.W., Gruenbaum, Y., and Medalia, O. (2012a). Filaments assembly of ectopically expressed Caenorhabditis elegans lamin within Xenopus oocytes. Journal of Structural Biology *177*, 113-118.

Grossman, E., Medalia, O., and Zwerger, M. (2012b). Functional Architecture of the Nuclear Pore Complex. Annual Review of Biophysics *41*, 557-584.

Gudise, S., Figueroa, R.A., Lindberg, R., Larsson, V., and Hallberg, E. (2011). Samp1 is functionally associated with the LINC complex and A-type lamina networks. Journal of Cell Science *124*, 2077-2085.

Guffanti, E., Kittur, N., Brodt, Z.N., Polotsky, A.J., Kuokkanen, S.M., Heller, D.S., Young, S.L., Santoro, N., and Meier, U.T. (2008). Nuclear pore complex proteins mark the implantation window in human endometrium. Journal of Cell Science *121*, 2037-2045.

Guha, M. (2013). Blockbuster dreams for Pfizer's CDK inhibitor. Nat Biotech *31*, 187.

Guney, I., Wu, S., and Sedivy, J.M. (2006). Reduced c-Myc signaling triggers telomere-independent senescence by regulating Bmi-1 and p16INK4a. Proc Natl Acad Sci USA *103*, 3645-3650.

Hahn, W.C., Dessain, S.K., Brooks, M.W., King, J.E., Elenbaas, B., Sabatini, D.M., DeCaprio, J.A., and Weinberg, R.A. (2002). Enumeration of the Simian Virus 40 Early Region Elements Necessary for Human Cell Transformation. Molecular and Cellular Biology *22*, 2111-2123.

Halazonetis, T.D., Gorgoulis, V.G., and Bartek, J. (2008). An Oncogene-Induced DNA Damage Model for Cancer Development. Science *319*, 1352-1355.

Han, J., Li, E., Chen, L., Zhang, Y., Wei, F., Liu, J., Deng, H., and Wang, Y. (2015). The CREB coactivator CRTC2 controls hepatic lipid metabolism by regulating SREBP1. Nature *524*, 243-246.

Hara, E. (1996). Regulation of p16CDKN2 expression and its implications for cell immortalization and senescence. Mol Cell Biol *16*, 859-867.

Hardin, C.D., and Vallejo, J. (2006). Caveolins in Vascular Smooth Muscle: Form Organizing Function. Cardiovascular Research *69*, 808-815.

Harding, H.P., Calfon, M., Urano, F., Novoa, I., and Ron, D. (2002). Transcriptional and translational control in the mammalian unfolded protein response. Annual review of cell and developmental biology *18*, 575-599.

Hardy, K., Mansfield, L., Mackay, A., Benvenuti, S., Ismail, S., Arora, P., O'Hare, M.J., and Jat, P.S. (2005). Transcriptional Networks and Cellular Senescence in Human Mammary Fibroblasts. Molecular Biology of the Cell *16*, 943-953.

Harley, C.B., Futcher, A.B., and Greider, C.W. (1990). Telomeres shorten during ageing of human fibroblasts. Nature *345*, 458-460.

Harrison, D.E., Strong, R., Sharp, Z.D., Nelson, J.F., Astle, C.M., Flurkey, K., Nadon, N.L., Wilkinson, J.E., Frenkel, K., Carter, C.S.*, et al.* (2009). Rapamycin fed late in life extends lifespan in genetically heterogeneous mice. Nature *460*, 392-395.

Hartl, T.A., Smith, H.F., and Bosco, G. (2008). Chromosome alignment and transvection are antagonized by condensin II. Science *322*, 1384-1387.

Hasty, P., Campisi, J., Hoeijmakers, J., van Steeg, H., and Vijg, J. (2003). Aging and genome maintenance: lessons from the mouse? Science *299*, 1355-1359.

Hayflick, L. (1965). The limited in vitro lifetime of human diploid cell strains. Experimental Cell Research *37*, 614-636.

Hayflick, L., and Moorhead, P.S. (1961). The serial cultivation of human diploid cell strains. Experimental Cell Research *25*, 585-621.

He, W., Lu, Y., Qahwash, I., Hu, X.-Y., Chang, A., and Yan, R. (2004). Reticulon family members modulate BACE1 activity and amyloid-β peptide generation. Nat Med *10*, 959-965.

Head, B.P., Peart, J.N., Panneerselvam, M., Yokoyama, T., Pearn, M.L., Niesman, I.R., Bonds, J.A., Schilling, J.M., Miyanohara, A., Headrick, J.*, et al.* (2010). Loss of caveolin-1 accelerates neurodegeneration and aging. PLoS ONE *5*, e15697.

Hegele, R.A., Cao, H., Liu, D.M., Costain, G.A., Charlton-Menys, V., Wilson Rodger, N., and Durrington, P.N. (2006). Sequencing of the reannotated LMNB2 gene reveals novel mutations in patients with acquired partial lipodystrophy. American Journal of Human Genetics *79*, 383-389.

Heitlinger, E. (1991). Expression of chicken lamin B2 in Escherichia coli: characterization of its structure, assembly, and molecular interactions. J Cell Biol *113*, 485-495.

Hekimi, S. (2006). How genetic analysis tests theories of animal aging. Nature Genetics *38*, 985-991.

Heldin, C.H., Rubin, K., Pietras, K., and Östman, A. (2004). High interstitial fluid pressure - An obstacle in cancer therapy. Nature Reviews Cancer *4*, 806-813.

Hellemans, J., Preobrazhenska, O., Willaert, A., Debeer, P., Verdonk, P.C.M., Costa, T., Janssens, K., Menten, B., Van Roy, N., Vermeulen, S.J.T.*, et al.* (2004). Loss-of-function mutations in LEMD3 result in osteopoikilosis, Buschke-Ollendorff syndrome and melorheostosis. Nature Genetics *36*, 1213-1218.

Hennekes, H., and Nigg, E.A. (1994). The role of isoprenylation in membrane attachment of nuclear lamins. A single point mutation prevents proteolytic cleavage of the lamin A precursor and confers membrane binding properties. Journal of Cell Science *107*, 1019-1029.

Hensley, P.J., Desiniotis, A., Wang, C., Stromberg, A., Chen, C.S., and Kyprianou, N. (2014). Novel pharmacologic targeting of tight junctions and focal adhesions in prostate cancer cells. PLoS ONE *9*, e86238.

Herbig, U., Ferreira, M., Condel, L., Carey, D., and Sedivy, J.M. (2006). Cellular senescence in aging primates. Science *311*, 1257.

Herbig, U., Jobling, W.A., Chen, B.P., Chen, D.J., and Sedivy, J.M. (2004). Telomere shortening triggers senescence of human cells through a pathway involving ATM, p53, and p21CIP1, but not p16INK4a. Mol Cell *14*, 501-513.

Hernandez, L., Roux, K.J., Wong, E.S.M., Mounkes, L.C., Mutalif, R., Navasankari, R., Rai, B., Cool, S., Jeong, J.-W., Wang, H*., et al.* (2010). Functional coupling between the extracellular matrix and nuclear lamina by Wnt signaling in progeria. Developmental Cell *19*, 413-425.

Herranz, N., Gallage, S., Mellone, M., Wuestefeld, T., Klotz, S., Hanley, C.J., Raguz, S., Acosta, J.C., Innes, A.J., Banito, A*., et al.* (2015). mTOR regulates MAPKAPK2 translation to control the senescence-associated secretory phenotype. Nat Cell Biol *17*, 1205-1217.

Hewitt, G., Jurk, D., Marques, F.D.M., Correia-Melo, C., Hardy, T., Gackowska, A., Anderson, R., Taschuk, M., Mann, J., and Passos, J.F. (2012). Telomeres are favoured targets of a persistent DNA damage response in ageing and stress-induced senescence. Nature Communications *3*, 708-717.

Hewitt, K.J., Agarwal, R., and Morin, P.J. (2006). The claudin gene family: Expression in normal and neoplastic tissues. BMC Cancer *6*, 186-194.

Hiratsuka, K., Kamino, Y., Nagata, T., Takahashi, Y., Asai, S., Ishikawa, K., and Abiko, Y. (2002). Microarray analysis of gene expression changes in aging in mouse submandibular gland. Journal of Dental Research *81*, 679-682.

Ho, C.Y., and Lammerding, J. (2012). Lamins at a glance. Journal of Cell Science *125*, 2087-2093.

Hoenicke, L., and Zender, L. (2012). Immune surveillance of senescent cells—biological significance in cancer- and non-cancer pathologies. Carcinogenesis *33*, 1123-1126.

Hoffmann, K., Dreger, C.K., Olins, A.L., Olins, D.E., Shultz, L.D., Lucke, B., Karl, H., Kaps, R., Müller, D., Vayá, A.*, et al.* (2002). Mutations in the gene encoding the lamin B receptor produce an altered nuclear morphology in granulocytes (Pelger-Huët anomaly). Nature Genetics *31*, 410-414.

Hofmann, Jeffrey W., Zhao, X., De Cecco, M., Peterson, Abigail L., Pagliaroli, L., Manivannan, J., Hubbard, Gene B., Ikeno, Y., Zhang, Y., Feng, B.*, et al.* (2015). Reduced Expression of MYC Increases Longevity and Enhances Healthspan. Cell *160*, 477-488.

Holtz, D., Tanaka, R.A., Hartwig, J., and McKeon, F. (1989). The CaaX motif of lamin A functions in conjunction with the nuclear localization signal to target assembly to the nuclear envelope. Cell *59*, 969-977.

Hougaard, S., Loechel, F., Xu, X., Tajima, R., Albrechtsen, R., and Wewer, U.M. (2000). Trafficking of Human ADAM 12-L: Retention in the trans-Golgi Network. Biochemical and Biophysical Research Communications *275*, 261-267.

Hsieh, S.-R., Hsu, C.-S., Lu, C.-H., Chen, W.-C., Chiu, C.-H., and Liou, Y.-M. (2013). Epigallocatechin-3-gallate-mediated cardioprotection by Akt/GSK-3β/caveolin signalling in H9c2 rat cardiomyoblasts. Journal of Biomedical Science *20*, 86-86.

Hu, J., Shibata, Y., Voss, C., Shemesh, T., Li, Z., Coughlin, M., Kozlov, M.M., Rapoport, T.A., and Prinz, W.A. (2008). Membrane Proteins of the Endoplasmic Reticulum Induce High-Curvature Tubules. Science *319*, 1247-1250.

Huang, D.W., Sherman, B.T., Tan, Q., Kir, J., Liu, D., Bryant, D., Guo, Y., Stephens, R., Baseler, M.W., Lane, H.C*., et al.* (2007). DAVID Bioinformatics Resources: expanded annotation database and novel algorithms to better extract biology from large gene lists. Nucleic Acids Research *35*, W169-W175.

Hubackova, S., Krejcikova, K., Bartek, J., and Hodny, Z. (2012). IL1- and TGFβ-Nox4 signaling, oxidative stress and DNA damage response are shared features of replicative, oncogene-induced, and drug-induced paracrine 'Bystander senescence'. Aging (Albany NY) *4*, 932-951.

Huber, L.A., Fialka, I., Paiha, K., Hunziker, W., Sacks, D.B., Bähler, M., Way, M., Gagescu, R., and Gruenberg, J. (2000). Both Calmodulin and the Unconventional Myosin Myr4 Regulate Membrane Trafficking Along the Recycling Pathway of MDCK Cells. Traffic *1*, 494-503.

Hübner, S., Eam, J.E., Hübner, A., and Jans, D.A. (2006). Laminopathy-inducing lamin A mutants can induce redistribution of lamin binding proteins into nuclear aggregates. Experimental Cell Research *312*, 171-183.

Hudon, S.E., Coffinier, C., Michaelis, S., Fong, L.G., Young, S.G., and Hrycyna, C.A. (2008). HIV-protease inhibitors block the enzymatic activity of purified Ste24p. Biochemical and Biophysical Research Communications *374*, 365-368.

Hung, W.W., Ross, J.S., Boockvar, K.S., and Siu, A.L. (2011). Recent trends in chronic disease, impairment and disability among older adults in the United States. BMC Geriatrics *11*, 47-59.

Hunt, M.C., Rautanen, A., Westin, M.A.K., Svensson, L.T., and Alexson, S.E.H. (2006). Analysis of the mouse and human acyl-CoA thioesterase (ACOT) gene clusters shows that convergent, functional evolution results in a reduced number of human peroxisomal ACOTs. The FASEB Journal *20*, 1855-1864.

Hutchison, C.J. (2012). B-type lamins and their elusive roles in metazoan cell proliferation and senescence. EMBO J *31*, 1058-1059.

Hutter, E., Renner, K., Pfister, G., Stöckl, P., Jansen-Dürr, P., and Gnaiger, E. (2004). Senescence-associated changes in respiration and oxidative phosphorylation in primary human fibroblasts. Biochemical Journal *380*, 919-928.

Iannello, A., Thompson, T.W., Ardolino, M., Lowe, S.W., and Raulet, D.H. (2013). p53-dependent chemokine production by senescent tumor cells supports NKG2D-dependent tumor elimination by natural killer cells. The Journal of Experimental Medicine *210*, 2057-2069.

Ibrahim, M.X., Sayin, V.I., Akula, M.K., Liu, M., Fong, L.G., Young, S.G., and Bergo, M.O. (2013). Targeting isoprenylcysteine methylation ameliorates disease in a mouse model of progeria. Science *340*, 1330-1333.

Isaac, C., Pollard, J.W., and Meier, U.T. (2001). Intranuclear endoplasmic reticulum induced by Nopp140 mimics the nucleolar channel system of human endometrium. Journal of Cell Science *114*, 4253-4264.

Itahana, K., Campisi, J., and Dimri, G.P. (2007). Methods to detect biomarkers of cellular senescence: The senescence-associated β-galactosidase assay. Methods in Molecular Biology *371*, 21-31.

Itoh, N., Yonehara, S., Ishii, A., Yonehara, M., Mizushima, S.-I., Sameshima, M., Hase, A., Seto, Y., and Nagata, S. (1991). The polypeptide encoded by the cDNA for human cell surface antigen Fas can mediate apoptosis. Cell *66*, 233-243.

Ivanov, A., Pawlikowski, J., Manoharan, I., van Tuyn, J., Nelson, D.M., Rai, T.S., Shah, P.P., Hewitt, G., Korolchuk, V.I., Passos, J.F.*, et al.* (2013). Lysosome-mediated processing of chromatin in senescence. The Journal of Cell Biology *202*, 129-143.

Ivorra, C. (2006). A mechanism of AP-1 suppression through interaction of c-Fos with lamin A/C. Genes Dev *20*, 307-320.

Iwasa, H., Han, J., and Ishikawa, F. (2003). Mitogen-activated protein kinase p38 defines the common senescence-signalling pathway. Genes Cells *8*, 131-144.

Jacobs, J.J., Kieboom, K., Marino, S., DePinho, R.A., and van Lohuizen, M. (1999). The oncogene and Polycomb-group gene bmi-1 regulates cell proliferation and senescence through the ink4a locus. Nature *397*, 164-168.

Jacobs, J.J.L., and de Lange, T. (2004). Significant Role for p16INK4a in p53-Independent Telomere-Directed Senescence. Current Biology *14*, 2302-2308.

Janowski, B.A., Willy, P.J., Devi, T.R., Falck, J.R., and Mangelsdorf, D.J. (1996). An oxysterol signalling pathway mediated by the nuclear receptor LXR[alpha]. Nature *383*, 728-731.

Janssens, S., and Beyaert, R. (2003). Functional Diversity and Regulation of Different Interleukin-1 Receptor-Associated Kinase (IRAK) Family Members. Molecular Cell *11*, 293-302.

Janzen, V., Forkert, R., Fleming, H.E., Saito, Y., Waring, M.T., Dombkowski, D.M., Cheng, T., DePinho, R.A., Sharpless, N.E., and Scadden, D.T. (2006). Stem-cell ageing modified by the cyclin-dependent kinase inhibitor p16INK4a. Nature *443*, 421-426.

Jasmin, J.F., Malhotra, S., Singh Dhallu, M., Mercier, I., Rosenbaum, D.M., and Lisanti, M.P. (2007). Caveolin-1 deficiency increases cerebral ischemic injury. Circulation Research *100*, 721-729.

Jeyapalan, J.C., and Sedivy, J.M. (2008). Cellular senescence and organismal aging. Mechanisms of Ageing and Development *129*, 467-474.

Jiang, N., Yan, X., Zhou, W., Zhang, Q., Chen, H., Zhang, Y., and Zhang, X. (2008). NMR-Based Metabonomic Investigations into the Metabolic Profile of the Senescence-Accelerated Mouse. Journal of Proteome Research *7*, 3678-3686.

Jiang, P., Du, W., Mancuso, A., Wellen, K.E., and Yang, X. (2013). Reciprocal regulation of p53 and malic enzymes modulates metabolism and senescence. Nature *493*, 689-693.

Jiao, J., Hong, S., Zhang, J., Ma, L., Sun, Y., Zhang, D., Shen, B., and Zhu, C. (2012). Opsin3 sensitizes hepatocellular carcinoma cells to 5-fluorouracil treatment by regulating the apoptotic pathway. Cancer Letters *320*, 96-103.

Jing, W., and Jiang, W. (2015). MicroRNA-93 regulates collagen loss by targeting MMP3 in human nucleus pulposus cells. Cell Proliferation *48*, 284-292.

Johnson, N., Krebs, M., Boudreau, R., Giorgi, G., LeGros, M., and Larabell, C. (2003). Actin-filled nuclear invaginations indicate degree of cell de-differentiation. Differentiation *71*, 414-424.

Johnson, S.C., Rabinovitch, P.S., and Kaeberlein, M. (2013). mTOR is a key modulator of ageing and age-related disease. Nature *493*, 338-345.

Joshi-Tope, G., Gillespie, M., Vastrik, I., D'Eustachio, P., Schmidt, E., de Bono, B., Jassal, B., Gopinath, G.R., Wu, G.R., Matthews, L.*, et al.* (2005). Reactome: a knowledgebase of biological pathways. Nucleic Acids Research *33*, D428-D432.

Jun, J.-I., and Lau, L.F. (2010a). Cellular senescence controls fibrosis in wound healing. Aging (Albany NY) *2*, 627-631.

Jun, J.-I., and Lau, L.F. (2010b). The matricellular protein CCN1 induces fibroblast senescence and restricts fibrosis in cutaneous wound healing. Nat Cell Biol *12*, 676-685.

Jung, H.-J., Coffinier, C., Choe, Y., Beigneux, A.P., Davies, B.S.J., Yang, S.H., Barnes, R.H., Hong, J., Sun, T., Pleasure, S.J.*, et al.* (2012). Regulation of prelamin A but not lamin C by miR-9, a brain-specific microRNA. Proceedings of the National Academy of Sciences *109*, E423-E431.

Jung, T., Bader, N., and Grune, T. (2007). Lipofuscin. Annals of the New York Academy of Sciences *1119*, 97-111.

Kang, T.-W., Yevsa, T., Woller, N., Hoenicke, L., Wuestefeld, T., Dauch, D., Hohmeyer, A., Gereke, M., Rudalska, R., Potapova, A.*, et al.* (2011). Senescence surveillance of pre-malignant hepatocytes limits liver cancer development. Nature *479*, 547-551.

Kapahi, P., Chen, D., Rogers, A.N., Katewa, S.D., Li, P.W.-L., Thomas, E.L., and Kockel, L. (2010). With TOR, Less Is More: A Key Role for the Conserved Nutrient-Sensing TOR Pathway in Aging. Cell Metabolism *11*, 453-465.

Kapinos, L.E., Schumacher, J., Mücke, N., Machaidze, G., Burkhard, P., Aebi, U., Strelkov, S.V., and Herrmann, H. (2010). Characterization of the Head-to-Tail Overlap

Complexes Formed by Human Lamin A, B1 and B2 "Half-minilamin" Dimers. Journal of Molecular Biology *396*, 719-731.

Kaplon, J., Zheng, L., Meissl, K., Chaneton, B., Selivanov, V.A., Mackay, G., van der Burg, S.H., Verdegaal, E.M.E., Cascante, M., Shlomi, T.*, et al.* (2013). A key role for mitochondrial gatekeeper pyruvate dehydrogenase in oncogene-induced senescence. Nature *498*, 109-112.

Karagiannis, G.S., Schaeffer, D.F., Cho, C.K.J., Musrap, N., Saraon, P., Batruch, I., Grin, A., Mitrovic, B., Kirsch, R., Riddell, R.H.*, et al.* (2014). Collective migration of cancer-associated fibroblasts is enhanced by overexpression of tight junction-associated proteins claudin-11 and occludin. Molecular Oncology *8*, 178-195.

Kasthuri, R.S., Taubman, M.B., and Mackman, N. (2009). Role of tissue factor in cancer. Journal of Clinical Oncology *27*, 4834-4838.

Katze, M.G., He, Y., and Gale, M. (2002). Viruses and interferon: a fight for supremacy. Nat Rev Immunol *2*, 675-687.

Kaufman, R.J. (1999). Stress signaling from the lumen of the endoplasmic reticulum: Coordination of gene transcriptional and translational controls. Genes and Development *13*, 1211-1233.

Kawabe, J.-i., Grant, B.S., Yamamoto, M., Schwencke, C., Okumura, S., and Ishikawa, Y. (2001). Changes in caveolin subtype protein expression in aging rat organs. Molecular and Cellular Endocrinology *176*, 91-95.

Kim, K.S., Kang, K.W., Seu, Y.B., Baek, S.-H., and Kim, J.-R. (2009). Interferon-γ induces cellular senescence through p53-dependent DNA damage signaling in human endothelial cells. Mechanisms of Ageing and Development *130*, 179-188.

Kim, K.S., Kim, J.E., Choi, K.J., Bae, S., and Kim, D.H. (2014). Characterization of DNA damage-induced cellular senescence by ionizing radiation in endothelial cells. International Journal of Radiation Biology *90*, 71-80.

Kim, S.S., Kang, M.S., Choi, Y.M., Suh, Y.H., and Kim, D.K. (1997). Sphingomyelinase Activity Is Enhanced in Cerebral Cortex of Senescence-Accelerated Mouse-P/10 with Advancing Age. Biochemical and Biophysical Research Communications *237*, 583-587.

Kim, W.Y., and Sharpless, N.E. (2006). The Regulation of INK4/ARF in Cancer and Aging. Cell *127*, 265-275.

Kim, Y.-M., Shin, H.-T., Seo, Y.-H., Byun, H.-O., Yoon, S.-H., Lee, I.-K., Hyun, D.-H., Chung, H.-Y., and Yoon, G. (2010). Sterol Regulatory Element-binding Protein (SREBP)-1-mediated Lipogenesis Is Involved in Cell Senescence. Journal of Biological Chemistry *285*, 29069-29077.

Kim, Y., Sharov, A.A., McDole, K., Cheng, M., Hao, H., Fan, C.-M., Gaiano, N., Ko, M.S.H., and Zheng, Y. (2011). Mouse B-type lamins are required for proper organogenesis but not by embryonic stem cells. Science *334*, 1706-1710.

Kimura, H., Inukai, Y., Takii, T., Furutani, Y., Shibata, Y., Hayashi, H., Sakurada, S., Okamoto, T., Inoue, J.I., Oomoto, Y.*, et al.* (1998). Molecular analysis of constitutive IL-1alpha gene expression in human melanoma cells: autocrine stimulation through NF-kappaB activation by endogenous IL-1alpha. Cytokine *10*, 872-879.

Kipling, D., Davis, T., Ostler, E.L., and Faragher, R.G.A. (2004). What can progeroid syndromes tell us about human aging? Science *305*, 1426-1431.

Kirkwood, T.B.L. (2008). A systematic look at an old problem. Nature *451*, 644-647.

Kitten, G.T., and Nigg, E.A. (1991). The CaaX motif is required for isoprenylation, carboxy methylation and nuclear membrane association of lamin B2. J Cell Biol *113*, 13-24.

Kittur, N., Zapantis, G., Aubuchon, M., Santoro, N., Bazett-Jones, D.P., and Meier, U.T. (2007). The Nucleolar Channel System of Human Endometrium Is Related to Endoplasmic Reticulum and R-Rings. Molecular Biology of the Cell *18*, 2296-2304.

Kochin, V., Shimi, T., Torvaldson, E., Adam, S.A., Goldman, A., Pack, C.G., Melo-Cardenas, J., Imanishi, S.Y., Goldman, R.D., and Eriksson, J.E. (2014). Interphase phosphorylation of lamin A. Journal of Cell Science *127*, 2683-2696.

Kohorn, E.I., Rice, S.I., Hemperly, S., and Gordon, M. (1972). The relation of the structure of progestational steroids to nucleolar differentiation in human endometrium. The Journal of clinical endocrinology *34*, 257-264.

Kolb, T., Maaß, K., Hergt, M., Aebi, U., and Herrmann, H. (2011). Lamin A and lamin C form homodimers and coexist in higher complex forms both in the nucleoplasmic fraction and in the lamina of cultured human cells. Nucleus *2*, 425-433.

Kong, X., Feng, D., Wang, H., Hong, F., Bertola, A., Wang, F.-S., and Gao, B. (2012). Interleukin-22 induces hepatic stellate cell senescence and restricts liver fibrosis in mice. Hepatology *56*, 1150-1159.

Korfali, N., Wilkie, G.S., Swanson, S.K., Srsen, V., de Las Heras, J., Batrakou, D.G., Malik, P., Zuleger, N., Kerr, A.R., Florens, L.*, et al.* (2012). The nuclear envelope proteome differs notably between tissues. Nucleus (Austin, Tex) *3*, 552-564.

Kortlever, R.M., Higgins, P.J., and Bernards, R. (2006). Plasminogen activator inhibitor-1 is a critical downstream target of p53 in the induction of replicative senescence. Nature Cell Biology *8*, 877-884.

Kosar, M., Bartkova, J., Hubackova, S., Hodny, Z., Lukas, J., and Bartek, J. (2011). Senescence-associated heterochromatin foci are dispensable for cellular senescence, occur in a cell type- And insult-dependent manner, and follow expression of p16ink4a. Cell Cycle *10*, 457-468.

Kosenko, T., Golder, M., Leblond, G., Weng, W., and Lagace, T.A. (2013). Low Density Lipoprotein Binds to Proprotein Convertase Subtilisin/Kexin Type-9 (PCSK9) in Human Plasma and Inhibits PCSK9-mediated Low Density Lipoprotein Receptor Degradation. Journal of Biological Chemistry *288*, 8279-8288.

Kothari, H., Pendurthi, U.R., and Rao, L.V.M. (2013). Analysis of tissue factor expression in various cell model systems: Cryptic vs. active. Journal of Thrombosis and Haemostasis *11*, 1353-1363.

Kriete, A., Mayo, K.L., Yalamanchili, N., Beggs, W., Bender, P., Kari, C., and Rodeck, U. (2008). Cell autonomous expression of inflammatory genes in biologically aged fibroblasts associated with elevated NF-kappaB activity. Immunity and Ageing *5*, 5.

Krimm, I. (2002). The Ig-like structure of the C-terminal domain of lamin A/C, mutated in muscular dystrophies, cardiomyopathy, and partial lipodystrophy. Structure *10*, 811-823.

Krishnamurthy, J., Ramsey, M.R., Ligon, K.L., Torrice, C., Koh, A., Bonner-Weir, S., and Sharpless, N.E. (2006). p16INK4a induces an age-dependent decline in islet regenerative potential. Nature *443*, 453-457.

Krishnamurthy, J., Torrice, C., Ramsey, M.R., Kovalev, G.I., Al-Regaiey, K., Su, L., and Sharpless, N.E. (2004). Ink4a/Arf expression is a biomarker of aging. Journal of Clinical Investigation *114*, 1299-1307.

Krizhanovsky, V., Yon, M., Dickins, R.A., Hearn, S., Simon, J., Miething, C., Yee, H., Zender, L., and Lowe, S.W. (2008). Senescence of Activated Stellate Cells Limits Liver Fibrosis. Cell *134*, 657-667.

Krouwer, V.J.D., Hekking, L.H.P., Langelaar-Makkinje, M., Regan-Klapisz, E., and Post, J.A. (2012). Endothelial cell senescence is associated with disrupted cell-cell junctions and increased monolayer permeability. Vascular Cell *4*, 12-22.

Krtolica, A., Parrinello, S., Lockett, S., Desprez, P., and Campisi, J. (2001). Senescent fibroblasts promote epithelial cell growth and tumorigenesis: a link between cancer and aging. Proc Natl Acad Sci USA *98*, 12072–12077.

Krüger, A., Batsios, P., Baumann, O., Luckert, E., Schwarz, H., Stick, R., Meyer, I., and Gräf, R. (2012). Characterization of NE81, the first lamin-like nucleoskeleton protein in a unicellular organism. Molecular Biology of the Cell *23*, 360-370.

Ksiazek, K., Jörres, A., and Witowski, J. (2008). Senescence Induces a Proangiogenic Switch in Human Peritoneal Mesothelial Cells. Rejuvenation Research *11*, 681-683.

Kuilman, T., Michaloglou, C., Mooi, W.J., and Peeper, D.S. (2010). The essence of senescence. Genes and Development *24*, 2463-2479.

Kuilman, T., Michaloglou, C., Vredeveld, L.C.W., Douma, S., van Doorn, R., Desmet, C.J., Aarden, L.A., Mooi, W.J., and Peeper, D.S. (2008). Oncogene-induced senescence relayed by an interleukin-dependent inflammatory network. Cell *133*, 1019-1031.

Kuilman, T., and Peeper, D.S. (2009). Senescence-messaging secretome: SMS-ing cellular stress. Nat Rev Cancer *9*, 81-94.

Kulaeva, O.I., Draghici, S., Tang, L., Kraniak, J.M., Land, S.J., and Michael, A.T. (2003). Epigenetic silencing of multiple interferon pathway genes after cellular immortalization. Oncogene *22*, 4118-4127.

Kurochkin, I.V., Mizuno, Y., Konagaya, A., Sakaki, Y., Schönbach, C., and Okazaki, Y. (2007). Novel peroxisomal protease Tysnd1 processes PTS1- and PTS2-containing enzymes involved in β-oxidation of fatty acids. *26*, 835-845.

Kurosu, H., Yamamoto, M., Clark, J.D., Pastor, J.V., Nandi, A., Gurnani, P., McGuinness, O.P., Chikuda, H., Yamaguchi, M., Kawaguchi, H*., et al.* (2005). Suppression of Aging in Mice by the Hormone Klotho. Science *309*, 1829-1833.

Kurz, D.J., Decary, S., Hong, Y., and Erusalimsky, J.D. (2000). Senescence-associated (beta)-galactosidase reflects an increase in lysosomal mass during replicative ageing of human endothelial cells. Journal of Cell Science *113*, 3613-3622.

Kurz, D.J., Payeli, S., Greutert, H., Briand Schumacher, S., Lüscher, T.F., and Tanner, F.C. (2014). Epigenetic regulation of tissue factor inducibility in endothelial cell senescence. Mechanisms of Ageing and Development *140*, 1-9.

Laberge, R.-M., Sun, Y., Orjalo, A.V., Patil, C.K., Freund, A., Zhou, L., Curran, S.C., Davalos, A.R., Wilson-Edell, K.A., Liu, S*., et al.* (2015). MTOR regulates the pro-tumorigenic senescence-associated secretory phenotype by promoting IL1A translation. Nat Cell Biol *17*, 1049-1061.

Lackner, D.H., Hayashi, M.T., Cesare, A.J., and Karlseder, J. (2014). A genomics approach identifies senescence-specific gene expression regulation. Aging Cell *13*, 946-950.

Lafontan, M. (2008). Advances in adipose tissue metabolism. International Journal of Obesity *32*, S39-S51.

Lagace, T.A., and Ridgway, N.D. (2005). The Rate-limiting Enzyme in Phosphatidylcholine Synthesis Regulates Proliferation of the Nucleoplasmic Reticulum. Molecular Biology of the Cell *16*, 1120-1130.

Lakatta, E.G., and Levy, D. (2003). Arterial and cardiac aging: Major shareholders in cardiovascular disease enterprises: Part I: Aging arteries: A "set up" for vascular disease. Circulation *107*, 139-146.

Lakoski, S.G., Lagace, T.A., Cohen, J.C., Horton, J.D., and Hobbs, H.H. (2009). Genetic and Metabolic Determinants of Plasma PCSK9 Levels. The Journal of Clinical Endocrinology and Metabolism *94*, 2537-2543.

Lammerding, J., Fong, L.G., Ji, J.Y., Reue, K., Stewart, C.L., Young, S.G., and Lee, R.T. (2006). Lamins A and C but Not Lamin B1 Regulate Nuclear Mechanics. Journal of Biological Chemistry *281*, 25768-25780.

Langevin, H.M., Storch, K.N., Snapp, R.R., Bouffard, N.A., Badger, G.J., Howe, A.K., and Taatjes, D.J. (2010). Tissue stretch induces nuclear remodeling in connective tissue fibroblasts. Histochemistry and cell biology *133*, 405-415.

LaPak, K.M., and Burd, C.E. (2014). The Molecular Balancing Act of p16INK4a in Cancer and Aging. Molecular Cancer Research *12*, 167-183.

Lattanzi, G., Ortolani, M., Columbaro, M., Prencipe, S., Mattioli, E., Lanzarini, C., Maraldi, N.M., Cenni, V., Garagnani, P., Salvioli, S*., et al.* (2014). Lamins are rapamycin targets that impact human longevity: a study in centenarians. Journal of Cell Science *127*, 147-157.

Lawrence, T., Willoughby, D.A., and Gilroy, D.W. (2002). Anti-inflammatory lipid mediators and insights into the resolution of inflammation. Nature Reviews Immunology *2*, 787-795.

Le, O., Rodier, F., Fontaine, F., Coppe, J.-P., Campisi, J., DeGregori, J., Laverdiére, C., Kokta, V., Haddad, E., and Beauséjour, C.M. (2010). Ionizing radiation-induced long-term expression of senescence markers in mice is independent of p53 and immune status. Aging Cell *9*, 398-409.

Lee, A.C., Fenster, B.E., Ito, H., Takeda, K., Bae, N.S., Hirai, T., Yu, Z.-X., Ferrans, V.J., Howard, B.H., and Finkel, T. (1999). Ras Proteins Induce Senescence by Altering the Intracellular Levels of Reactive Oxygen Species. Journal of Biological Chemistry *274*, 7936-7940.

Lee, B.Y., Han, J.A., Im, J.S., Morrone, A., Johung, K., Goodwin, E.C., Kleijer, W.J., DiMaio, D., and Hwang, E.S. (2006). Senescence-associated β-galactosidase is lysosomal β-galactosidase. Aging Cell *5*, 187-195.

Leonard, J.P., LaCasce, A.S., Smith, M.R., Noy, A., Chirieac, L.R., Rodig, S.J., Yu, J.Q., Vallabhajosula, S., Schoder, H., English, P.*, et al.* (2012). Selective CDK4/6 inhibition with tumor responses by PD0332991 in patients with mantle cell lymphoma. Blood *119*, 4597-4607.

Lettre, G., and Hengartner, M.O. (2006). Developmental apoptosis in C. elegans: a complex CEDnario. Nat Rev Mol Cell Biol *7*, 97-108.

Li, H., Solomon, E., Duhachek Muggy, S., Sun, D., and Zolkiewska, A. (2011). Metalloprotease-Disintegrin ADAM12 expression is regulated by Notch signaling via microRNA-29. Journal of Biological Chemistry *286*, 21500-21510.

Li, J., Tang, H., Hu, X., Chen, M., and Xie, H. (2010). Aquaporin-3 gene and protein expression in sun-protected human skin decreases with skin ageing. Australasian Journal of Dermatology *51*, 106-112.

Li, Q., Tang, L., Roberts, P.C., Kraniak, J.M., Fridman, A.L., Kulaeva, O.I., Tehrani, O.S., and Tainsky, M.A. (2008). Interferon Regulatory Factors IRF5 and IRF7 Inhibit Growth and Induce Senescence in Immortal Li-Fraumeni Fibroblasts. Molecular Cancer Research *6*, 770-784.

Li, X., and Gould, S.J. (2002). PEX11 promotes peroxisome division independently of peroxisome metabolism. The Journal of Cell Biology *156*, 643-651.

Liang, W.C., Mitsuhashi, H., Keduka, E., Nonaka, I., Noguchi, S., Nishino, I., and Hayashi, Y.K. (2011). TMEM43 mutations in emery-dreifuss muscular dystrophy-related myopathy. Annals of Neurology *69*, 1005-1013.

Lightle, S.A., Oakley, J.I., and Nikolova-Karakashian, M.N. (2000). Activation of sphingolipid turnover and chronic generation of ceramide and sphingosine in liver during aging. Mechanisms of Ageing and Development *120*, 111-125.

Lin, A., Salvador, A., and Carter, J.M. (2015). Multiplexed microsphere suspension array-based immunoassays. Methods in Molecular Biology *1318*, 107-118.

Lin, A.W., Barradas, M., Stone, J.C., van Aelst, L., Serrano, M., and Lowe, S.W. (1998). Premature senescence involving p53 and p16 is activated in response to constitutive MEK/MAPK mitogenic signaling. Genes & Development *12*, 3008-3019.

Lin, F., Blake, D.L., Callebaut, I., Skerjanc, I.S., Holmer, L., McBurney, M.W., Paulin-Levasseur, M., and Worman, H.J. (2000). MAN1, an inner nuclear membrane protein that shares the LEM domain with lamina-associated polypeptide 2 and emerin. Journal of Biological Chemistry *275*, 4840-4847.

Lin, F., and Worman, H.J. (1993). Structural organization of the human gene encoding nuclear lamin A and nuclear lamin C. J Biol Chem *268*, 16321-16326.

Lin, F., and Worman, H.J. (1995). Structural organization of the human gene (LMNB1) encoding nuclear lamin B1. Genomics *27*, 230-236.

Lin, H., Joehanes, R., Pilling, L.C., Dupuis, J., Lunetta, K.L., Ying, S.X., Benjamin, E.J., Hernandez, D., Singleton, A., Melzer, D.*, et al.* (2014). Whole blood gene expression and interleukin-6 levels. Genomics *104*, 490-495.

Lin, Z., Zhang, X., Liu, Z., Liu, Q., Wang, L., Lu, Y., Liu, Y., Wang, M., Yang, M., Jin, X.*, et al.* (2013). The distinct expression patterns of claudin-2, -6, and -11 between human gastric neoplasms and adjacent non-neoplastic tissues. Diagnostic pathology *8*, 1-7.

Liu, B., Wang, J., Chan, K.M., Tjia, W.M., Deng, W., Guan, X., Huang, J.-d., Li, K.M., Chau, P.Y., Chen, D.J.*, et al.* (2005). Genomic instability in laminopathy-based premature aging. Nat Med *11*, 780-785.

Liu, D., and Hornsby, P.J. (2007). Senescent human fibroblasts increase the early growth of xenograft tumors via matrix metalloproteinase secretion. Cancer Research *67*, 3117-3126.

Liu, F., Wu, S., Ren, H., and Gu, J. (2011). Klotho suppresses RIG-I-mediated senescence-associated inflammation. Nat Cell Biol *13*, 254-262.

Liu, Y., Sanoff, H.K., Cho, H., Burd, C.E., Torrice, C., Ibrahim, J.G., Thomas, N.E., and Sharpless, N.E. (2009). Expression of p16INK4a in peripheral blood T-cells is a biomarker of human aging. Aging Cell *8*, 439-448.

Liu, Y., Wang, Y., Rusinol, A.E., Sinensky, M.S., Liu, J., Shell, S.M., and Zou, Y. (2008). Involvement of Xeroderma Pigmentosum Group A (XPA) in Progeria Arising from Defective Maturation of Prelamin A. The FASEB journal : official publication of the Federation of American Societies for Experimental Biology *22*, 603-611.

Livak, K.J., and Schmittgen, T.D. (2001). Analysis of relative gene expression data using real-time quantitative PCR and the 2−ΔΔCT method. Methods *25*, 402-408.

Lloyd, D.J., Trembath, R.C., and Shackleton, S. (2002). A novel interaction between lamin A and SREBP1: implications for partial lipodystrophy and other laminopathies. Human Molecular Genetics *11*, 769-777.

Loechel, F., Fox, J.W., Murphy, G., Albrechtsen, R., and Wewer, U.M. (2000). ADAM 12-S cleaves IGFBP-3 and IGFBP-5 and is inhibited by TIMP-3. Biochemical and Biophysical Research Communications *278*, 511-515.

Loechel, F., Gilpin, B.J., Engvall, E., Albrechtsen, R., and Wewer, U.M. (1998). Human ADAM 12 (Meltrin α) is an active metalloprotease. Journal of Biological Chemistry *273*, 16993-16997.

Loiarro, M., Sette, C., Gallo, G., Ciacci, A., Fantò, N., Mastroianni, D., Carminati, P., and Ruggiero, V. (2005). Peptide-mediated Interference of TIR Domain Dimerization in MyD88 Inhibits Interleukin-1-dependent Activation of NF-κB. Journal of Biological Chemistry *280*, 15809-15814.

López-Otín, C., Blasco, M.A., Partridge, L., Serrano, M., and Kroemer, G. (2013). The hallmarks of aging. Cell *153*, 1194-1217.

Lowe, S.W., and Sherr, C.J. (2003). Tumor suppression by INK4a-ARF: progress and puzzles. Curr Opin Genet Dev *13*, 77-83.

Luderus, M.E.E. (1992). Binding of matrix attachment regions to lamin B1. Cell *70*, 949-959.

Lujambio, A., Akkari, L., Simon, J., Grace, D., Tschaharganeh, Darjus F., Bolden, Jessica E., Zhao, Z., Thapar, V., Joyce, Johanna A., Krizhanovsky, V.*, et al.* (2013). Non-Cell-Autonomous Tumor Suppression by p53. Cell *153*, 449-460.

Lutz, R.J., Trujillo, M.A., Denham, K.S., Wenger, L., and Sinensky, M. (1992). Nucleoplasmic localization of prelamin A: Implications for prenylation-dependent lamin A assembly into the nuclear lamina. Proceedings of the National Academy of Sciences of the United States of America *89*, 3000-3004.

Ly, D.H., Lockhart, D.J., Lerner, R.A., and Schultz, P.G. (2000). Mitotic Misregulation and Human Aging. Science *287*, 2486-2492.

Machiels, B.M. (1996). An alternative splicing product of the lamin A/C gene lacks exon 10. J Biol Chem *271*, 9249-9253.

Macip, S., Igarashi, M., Fang, L., Chen, A., Pan, Z.-Q., Lee, S.W., and Aaronson, S.A. (2002). Inhibition of p21-mediated ROS accumulation can rescue p21-induced senescence. The EMBO Journal *21*, 2180-2188.

Mackman, N. (2004). Role of Tissue Factor in hemostasis, thrombosis, and vascular development. Arteriosclerosis, Thrombosis, and Vascular Biology *24*, 1015-1022.

Maeda, M., Scaglia, N., and Igal, R.A. (2009). Regulation of fatty acid synthesis and Δ9-desaturation in senescence of human fibroblasts. Life Sciences *84*, 119-124.

Majno, G. (1975). The healing hand: man and wound in the ancient world (Cambridge, Massachusetts, Harvard University Press).

Malhas, A., Goulbourne, C., and Vaux, D.J. (2011). The nucleoplasmic reticulum: form and function. Trends in Cell Biology *21*, 362-373.

Malhas, A., Saunders, N.J., and Vaux, D.J. (2010). The nuclear envelope can control gene expression and cell cycle progression via miRNA regulation. Cell Cycle *9*, 531-539.

Malhas, A., and Vaux, D. (2014). Nuclear Envelope Invaginations and Cancer. In Cancer Biology and the Nuclear Envelope, E.C. Schirmer, and J.I. de las Heras, eds. (Springer New York), pp. 523-535.

Malhas, A.N., Lee, C.F., and Vaux, D.J. (2009). Lamin B1 controls oxidative stress responses via Oct-1. Journal of Cell Biology *184*, 45-55.

Mallampalli, M.P., Huyer, G., Bendale, P., Gelb, M.H., and Michaelis, S. (2005). Inhibiting farnesylation reverses the nuclear morphology defect in a HeLa cell model for Hutchinson-Gilford progeria syndrome. Proceedings of the National Academy of Sciences of the United States of America *102*, 14416-14421.

Mammoto, T., and Ingber, D.E. (2010). Mechanical control of tissue and organ development. Development *137*, 1407-1420.

Maniotis, A.J., Chen, C.S., and Ingber, D.E. (1997). Demonstration of mechanical connections between integrins, cytoskeletal filaments, and nucleoplasm that stabilize nuclear structure. Proceedings of the National Academy of Sciences of the United States of America *94*, 849-854.

Marji, J., O'Donoghue, S.I., McClintock, D., Satagopam, V.P., Schneider, R., Ratner, D., J. Worman, H., Gordon, L.B., and Djabali, K. (2010). Defective Lamin A-Rb Signaling in Hutchinson-Gilford Progeria Syndrome and Reversal by Farnesyltransferase Inhibition. PLoS ONE *5*, e11132.

Markowski, D.N., Thies, H.W., Gottlieb, A., Wenk, H., Wischnewsky, M., and Bullerdiek, J. (2013). HMGA2 expression in white adipose tissue linking cellular senescence with diabetes. Genes & Nutrition *8*, 449-456.

Martin, J.A., and Wang, Z. (2011). Next-generation transcriptome assembly. Nat Rev Genet *12*, 671-682.

Martin, N., Beach, D., and Gil, J. (2014). Ageing as developmental decay: Insights from p16INK4a. Trends in Molecular Medicine *20*, 667-674.

Masiero, M., Simões, Filipa C., Han, Hee D., Snell, C., Peterkin, T., Bridges, E., Mangala, Lingegowda S., Wu, Sherry Y.-Y., Pradeep, S., Li, D*., et al.* (2013). A Core Human Primary Tumor Angiogenesis Signature Identifies the Endothelial Orphan Receptor ELTD1 as a Key Regulator of Angiogenesis. Cancer Cell *24*, 229-241.

Maske, C.P., Hollinshead, M.S., Higbee, N.C., Bergo, M.O., Young, S.G., and Vaux, D.J. (2003). A carboxyl-terminal interaction of lamin B1 is dependent on the CAAX endoprotease Rce1 and carboxymethylation. Journal of Cell Biology *162*, 1223-1232.

Matsumoto, T., Baker, D.J., D'Uscio, L.V., Mozammel, G., Katusic, Z.S., and Van Deursen, J.M. (2007). Aging-associated vascular phenotype in mutant mice with low levels of BubR1. Stroke *38*, 1050-1056.

Mattout, A., Goldberg, M., Tzur, Y., Margalit, A., and Gruenbaum, Y. (2007). Specific and conserved sequences in D. melanogaster and C. elegans lamins and histone H2A mediate the attachment of lamins to chromosomes. J Cell Sci *120*, 77-85.

Mazumder, A., Roopa, T., Basu, A., Mahadevan, L., and Shivashankar, G.V. (2008). Dynamics of chromatin decondensation reveals the structural integrity of a mechanically prestressed nucleus. Biophysical Journal *95*, 3028-3035.

Mazumder, A., Roopa, T., Kumar, A., Iyer, K.V., Ramdas, N.M., and Shivashankar, G.V. (2010). Chapter 10 - Prestressed Nuclear Organization in Living Cells. In Methods in Cell Biology, G.V. Shivashankar, ed. (Academic Press), pp. 221-239.

McClintock, D., Gordon, L.B., and Djabali, K. (2006). Hutchinson–Gilford progeria mutant lamin A primarily targets human vascular cells as detected by an anti-Lamin A

G608G antibody. Proceedings of the National Academy of Sciences of the United States of America *103*, 2154-2159.

McClintock, D., Ratner, D., Lokuge, M., Owens, D.M., Gordon, L.B., Collins, F.S., and Djabali, K. (2007). The mutant form of lamin A that causes Hutchinson-Gilford Progeria is a biomarker of cellular aging in human skin. PLoS ONE *2*, e1269.

McConnell, B.B., Starborg, M., Brookes, S., and Peters, G. (1998). Inhibitors of cyclin-dependent kinases induce features of replicative senescence in early passage human diploid fibroblasts. Current Biology *8*, 351-354.

McKeon, F.D., Kirschner, M.W., and Caput, D. (1986). Homologies in both primary and secondary structure between nuclear envelope and intermediate filament proteins. Nature *319*, 463-468.

Mehta, I.S., Eskiw, C.H., Arican, H.D., Kill, I.R., and Bridger, J.M. (2011). Farnesyltransferase inhibitor treatment restores chromosome territory positions and active chromosome dynamics in Hutchinson-Gilford progeria syndrome cells. Genome Biology *12*, R74-R74.

Méndez-López, I., and Worman, H.J. (2012). Inner nuclear membrane proteins: Impact on human disease. Chromosoma *121*, 153-167.

Merideth, M.A., Gordon, L.B., Clauss, S., Sachdev, V., Smith, A.C.M., Perry, M.B., Brewer, C.C., Zalewski, C., Kim, H.J., Solomon, B.*, et al.* (2008). Phenotype and course of Hutchinson–Gilford progeria syndrome. The New England Journal of Medicine *358*, 592-604.

Metcalf, T.U., Cubas, R.A., Ghneim, K., Cartwright, M.J., Grevenynghe, J.V., Richner, J.M., Olagnier, D.P., Wilkinson, P.A., Cameron, M.J., Park, B.S.*, et al.* (2015).

Global analyses revealed age-related alterations in innate immune responses after stimulation of pathogen recognition receptors. Aging Cell *14*, 421-432.

Meyer, N., and Penn, L.Z. (2008). Reflecting on 25 years with MYC. Nat Rev Cancer *8*, 976-990.

Meyer, R.C., Giddens, M.M., Schaefer, S.A., and Hall, R.A. (2013). GPR37 and GPR37L1 are receptors for the neuroprotective and glioprotective factors prosaptide and prosaposin. Proceedings of the National Academy of Sciences *110*, 9529-9534.

Michaloglou, C., Vredeveld, L.C.W., Soengas, M.S., Denoyelle, C., Kuilman, T., Van Der Horst, C.M.A.M., Majoor, D.M., Shay, J.W., Mooi, W.J., and Peeper, D.S. (2005). BRAFE600-associated senescence-like cell cycle arrest of human naevi. Nature *436*, 720-724.

Michaud, K., Solomon, D.A., Oermann, E., Kim, J.-S., Zhong, W.-Z., Prados, M.D., Ozawa, T., James, C.D., and Waldman, T. (2010). Pharmacologic inhibition of cdk4/6 arrests the growth of glioblastoma multiforme intracranial xenografts. Cancer Research *70*, 3228-3238.

Minamino, T., and Komuro, I. (2007). Vascular cell senescence: Contribution to atherosclerosis. Circulation Research *100*, 15-26.

Minamino, T., Orimo, M., Shimizu, I., Kunieda, T., Yokoyama, M., Ito, T., Nojima, A., Nabetani, A., Oike, Y., Matsubara, H.*, et al.* (2009). A crucial role for adipose tissue p53 in the regulation of insulin resistance. Nat Med *15*, 1082-1087.

Minamino, T., Yoshida, T., Tateno, K., Miyauchi, H., Zou, Y., Toko, H., and Komuro, I. (2003). Ras induces vascular smooth muscle cell senescence and inflammation in human atherosclerosis. Circulation *108*, 2264-2269.

Mineta, K., Yamamoto, Y., Yamazaki, Y., Tanaka, H., Tada, Y., Saito, K., Tamura, A., Igarashi, M., Endo, T., Takeuchi, K*., et al.* (2011). Predicted expansion of the claudin multigene family. FEBS Letters *585*, 606-612.

Minetti, C., Bado, M., Broda, P., Sotgia, F., Bruno, C., Galbiati, F., Volonte, D., Lucania, G., Pavan, A., Bonilla, E*., et al.* (2002). Impairment of caveolae formation and T-system disorganization in Human Muscular Dystrophy with caveolin-3 eficiency. The American Journal of Pathology *160*, 265-270.

Mitrophanov, A.Y., and Groisman, E.A. (2008). Positive feedback in cellular control systems. BioEssays : news and reviews in molecular, cellular and developmental biology *30*, 542-555.

Mobasheri, A., and Marples, D. (2004). Expression of the AQP-1 water channel in normal human tissues: A semiquantitative study using tissue microarray technology. American Journal of Physiology - Cell Physiology *286*, C529-C537.

Moir, R.D., Montag-Lowy, M., and Goldman, R.D. (1994). Dynamic properties of nuclear lamins: lamin B is associated with sites of DNA replication. The Journal of Cell Biology *125*, 1201-1212.

Moir, R.D., Spann, T.P., Herrmann, H., and Goldman, R.D. (2000). Disruption of Nuclear Lamin Organization Blocks the Elongation Phase of DNA Replication. The Journal of Cell Biology *149*, 1179-1192.

Moiseeva, O., Mallette, F.A., Mukhopadhyay, U.K., Moores, A., and Ferbeyre, G. (2006). DNA Damage Signaling and p53-dependent Senescence after Prolonged β-Interferon Stimulation. Molecular Biology of the Cell *17*, 1583-1592.

Molofsky, A.V., Slutsky, S.G., Joseph, N.M., He, S., Pardal, R., Krishnamurthy, J., Sharpless, N.E., and Morrison, S.J. (2006). Increasing p16(INK4a) expression decreases forebrain progenitors and neurogenesis during ageing. Nature *443*, 448-452.

Mooney, M., Bond, J., Monks, N., Eugster, E., Cherba, D., Berlinski, P., Kamerling, S., Marotti, K., Simpson, H., Rusk, T.*, et al.* (2013). Comparative RNA-Seq and Microarray Analysis of Gene Expression Changes in B-Cell Lymphomas of Canis familiaris. PLoS ONE *8*, e61088.

Morita, K., Sasaki, H., Fujimoto, K., Furuse, M., and Tsukita, S. (1999). Claudin-11/OSP-based tight junctions of myelin sheaths in brain and Sertoli cells in testis. Journal of Cell Biology *145*, 579-588.

Mortazavi, A., Williams, B.A., McCue, K., Schaeffer, L., and Wold, B. (2008). Mapping and quantifying mammalian transcriptomes by RNA-Seq. Nat Meth *5*, 621-628.

Mougeolle, A., Poussard, S., Decossas, M., Lamaze, C., Lambert, O., and Dargelos, E. (2015). Oxidative stress induces Caveolin 1 degradation and impairs caveolae functions in skeletal muscle cells. PLoS ONE *10*, e0122654.

Muchir, A., Bonne, G., Van Der Kool, A.J., Van Meegen, M., Baas, F., Bolhuis, P.A., De Visser, M., and Schwartz, K. (2000). Identification of mutations in the gene encoding lamins A/C in autosomal dominant limb girdle muscular dystrophy with atrioventricular conduction disturbances (LGMD1B). Human Molecular Genetics *9*, 1453-1459.

Mun, G.I., Lee, S.J., An, S.M., Kim, I.K., and Boo, Y.C. (2009). Differential gene expression in young and senescent endothelial cells under static and laminar shear stress conditions. Free Radical Biology and Medicine *47*, 291-299.

Muñoz-Espín, D., Cañamero, M., Maraver, A., Gómez-López, G., Contreras, J., Murillo-Cuesta, S., Rodríguez-Baeza, A., Varela-Nieto, I., Ruberte, J., Collado, M*., et al.* (2013). Programmed cell senescence during mammalian embryonic development. Cell *155*, 1104-1118.

Muñoz-Espín, D., and Serrano, M. (2014). Cellular senescence: From physiology to pathology. Nature Reviews Molecular Cell Biology *15*, 482-496.

Munro, J., Barr, N.I., Ireland, H., Morrison, V., and Parkinson, E.K. (2004). Histone deacetylase inhibitors induce a senescence-like state in human cells by a p16-dependent mechanism that is independent of a mitotic clock. Experimental Cell Research *295*, 525-538.

Murayama, K.S., Kametani, F., Saito, S., Kume, H., Akiyama, H., and Araki, W. (2006). Reticulons RTN3 and RTN4-B/C interact with BACE1 and inhibit its ability to produce amyloid β-protein. European Journal of Neuroscience *24*, 1237-1244.

Musich, P.R., and Zou, Y. (2009). Genomic Instability and DNA Damage Responses in Progeria Arising from Defective Maturation of Prelamin A. Aging (Albany NY) *1*, 28-37.

Nacher, V., Carretero, A., Navarro, M., Armengol, C., Llombart, C., Rodríguez, A., Herrero-Fresneda, I., Ayuso, E., and Ruberte, J. (2006). The Quail Mesonephros: A New Model for Renal Senescence? Journal of Vascular Research *43*, 581-586.

Naetar, N., Korbei, B., Kozlov, S., Kerenyi, M.A., Dorner, D., Kral, R., Gotic, I., Fuchs, P., Cohen, T.V., Bittner, R*., et al.* (2008). Loss of nucleoplasmic LAP2α-lamin A complexes causes erythroid and epidermal progenitor hyperproliferation. Nature Cell Biology *10*, 1341-1348.

Nagata, S. (1997). Apoptosis by Death Factor. Cell *88*, 355-365.

Nair, R.R., Bagheri, M., and Saini, D.K. (2015). Temporally distinct roles of ATM and ROS in genotoxic-stress-dependent induction and maintenance of cellular senescence. Journal of Cell Science *128*, 342-353.

Nakakuki, M., Shimano, H., Inoue, N., Tamura, M., Matsuzaka, T., Nakagawa, Y., Yahagi, N., Toyoshima, H., Sato, R., and Yamada, N. (2007). A transcription factor of lipid synthesis, sterol regulatory element-binding protein (SREBP)-1a causes G1 cell-cycle arrest after accumulation of cyclin-dependent kinase (cdk) inhibitors. FEBS Journal *274*, 4440-4452.

Nakamura, A.J., Chiang, Y.J., Hathcock, K.S., Horikawa, I., Sedelnikova, O.A., Hodes, R.J., and Bonner, W.M. (2008). Both telomeric and non-telomeric DNA damage are determinants of mammalian cellular senescence. Epigenetics & Chromatin *1*, 6-18.

Nalaskowski, M.M., Fliegert, R., Ernst, O., Brehm, M.A., Fanick, W., Windhorst, S., Lin, H., Giehler, S., Hein, J., Lin, Y.-N.*, et al.* (2011). Human Inositol 1,4,5-Trisphosphate 3-Kinase Isoform B (IP3KB) Is a Nucleocytoplasmic Shuttling Protein Specifically Enriched at Cortical Actin Filaments and at Invaginations of the Nuclear Envelope. The Journal of Biological Chemistry *286*, 4500-4510.

Nambiar, R., McConnell, R.E., and Tyska, M.J. (2009). Control of cell membrane tension by myosin-I. Proceedings of the National Academy of Sciences of the United States of America *106*, 11972-11977.

Nardella, C., Clohessy, J.G., Alimonti, A., and Pandolfi, P.P. (2011). Pro-senescence therapy for cancer treatment. Nat Rev Cancer *11*, 503-511.

Narita, M., Nuñez, S., Heard, E., Narita, M., Lin, A.W., Hearn, S.A., Spector, D.L., Hannon, G.J., and Lowe, S.W. (2003). Rb-mediated heterochromatin formation and silencing of E2F target genes during cellular senescence. Cell *113*, 703-716.

Nathan, C. (2002). Points of control in inflammation. Nature *420*, 846-852.

Naugler, W.E., and Karin, M. (2008). NF-κB and Cancer — Identifying Targets and Mechanisms. Current opinion in genetics & development *18*, 19-26.

Navarro, C.L., Cau, P., and Lévy, N. (2006). Molecular bases of progeroid syndromes. Human Molecular Genetics *15*, R151-R161.

Navarro, C.L., De Sandre-Giovannoli, A., Bernard, R., Boccaccio, I., Boyer, A., Geneviève, D., Hadj-Rabia, S., Gaudy-Marqueste, C., Smitt, H.S., Vabres, P.*, et al.* (2004). Lamin A and ZMPSTE24 (FACE-1) defects cause nuclear disorganization and identify restrictive dermopathy as a lethal neonatal laminopathy. Human Molecular Genetics *13*, 2493-2503.

Nejat, E.J., Szmyga, M.J., Zapantis, G., and Meier, U.T. (2014). Progesterone Threshold Determines Nucleolar Channel System Formation in Human Endometrium. Reproductive Sciences *21*, 915-920.

Nelson, G., Wordsworth, J., Wang, C., Jurk, D., Lawless, C., Martin-Ruiz, C., and von Zglinicki, T. (2012). A senescent cell bystander effect: senescence-induced senescence. Aging Cell *11*, 345-349.

Nesic, O., Lee, J., Unabia, G.C., Johnson, K., Ye, Z., Vergara, L., Hulsebosch, C.E., and Perez-Polo, J.R. (2008). Aquaporin 1 - A novel player in spinal cord injury. Journal of Neurochemistry *105*, 628-640.

Nielsen, G.P., Stemmer-Rachamimov, A.O., Shaw, J., Roy, J.E., Koh, J., and Louis, D.N. (1999). Immunohistochemical survey of p16(INK4A) expression in normal human adult and infant tissues. Laboratory Investigation *79*, 1137-1143.

Nihal, M., Wu, J., and Wood, G.S. (2014). Methotrexate inhibits the viability of human melanoma cell lines and enhances Fas/Fas-ligand expression, apoptosis and

response to interferon-alpha: Rationale for its use in combination therapy. Archives of Biochemistry and Biophysics *563*, 101-107.

Nishida, M., Kasahara, K., Kaneko, M., Iwasaki, H., and Hayashi, K. (1985). Establishment of a new human endometrial adenocarcinoma cell line, Ishikawa cells, containing estrogen and progesterone receptors. Acta Obstetrica et Gynaecologica Japonica *37*, 1103-1111.

Noppe, G., Dekker, P., de Koning-Treurniet, C., Blom, J., van Heemst, D., Dirks, R.W., Tanke, H.J., Westendorp, R.G.J., and Maier, A.B. (2009). Rapid flow cytometric method for measuring senescence associated β-galactosidase activity in human fibroblasts. Cytometry Part A *75A*, 910-916.

Novakova, Z., Hubackova, S., Kosar, M., Janderova-Rossmeislova, L., Dobrovolna, J., Vasicova, P., Vancurova, M., Horejsi, Z., Hozak, P., Bartek, J.*, et al.* (2010). Cytokine expression and signaling in drug-induced cellular senescence. Oncogene *29*, 273-284.

Novelli, G., Muchir, A., Sangiuolo, F., Helbling-Leclerc, A., D'Apice, M.R., Massart, C., Capon, F., Sbraccia, P., Federici, M., Lauro, R.*, et al.* (2002). Mandibuloacral dysplasia is caused by a mutation in LMNA-encoding lamin A/C. American Journal of Human Genetics *71*, 426-431.

Nyren-Erickson, E.K., Jones, J.M., Srivastava, D.K., and Mallik, S. (2013). A disintegrin and metalloproteinase-12 (ADAM12): Function, roles in disease progression, and clinical implications. Biochimica et Biophysica Acta - General Subjects *1830*, 4445-4455.

O'Bryan, J.M., Potts, J.A., Bonkovsky, H.L., Mathew, A., Rothman, A.L., and for the, H.-C.T.G. (2011). Extended Interferon-Alpha Therapy Accelerates Telomere Length Loss in Human Peripheral Blood T Lymphocytes. PLoS ONE *6*, e20922.

Oertle, T., and Schwab, M.E. (2003). Nogo and its paRTNers. Trends in Cell Biology *13*, 187-194.

Ohtani, N., Yamakoshi, K., Takahashi, A., and Hara, E. (2004). The p16INK4a-RB pathway: molecular link between cellular senescence and tumor suppression. The Journal of Medical Investigation *51*, 146-153.

Ohtani, N., Yamakoshi, K., Takahashi, A., and Hara, E. (2010). Real-time in vivo imaging of p16(Ink4a)gene expression: a new approach to study senescence stress signaling in living animals. Cell Division *5*, art. no. 1.

Olive, M., Harten, I., Mitchell, R., Beers, J.K., Djabali, K., Cao, K., Erdos, M.R., Blair, C., Funke, B., Smoot, L.*, et al.* (2010). Cardiovascular pathology in Hutchinson-Gilford progeria: Correlation with the vascular pathology of aging. Arteriosclerosis, Thrombosis, and Vascular Biology *30*, 2301-2309.

Oliver, J.J., Webb, D.J., and Newby, D.E. (2005). Stimulated tissue plasminogen activator release as a marker of endothelial function in humans. Arteriosclerosis, Thrombosis, and Vascular Biology *25*, 2470-2479.

Olivieri, F., Rippo, M.R., Monsurrò, V., Salvioli, S., Capri, M., Procopio, A.D., and Franceschi, C. (2013). MicroRNAs linking inflamm-aging, cellular senescence and cancer. Ageing Research Reviews *12*, 1056-1068.

Ori, A., Toyama, Brandon H., Harris, Michael S., Bock, T., Iskar, M., Bork, P., Ingolia, Nicholas T., Hetzer, Martin W., and Beck, M. (2015). Integrated transcriptome and proteome analyses reveal organ-specific proteome deterioration in old rats. Cell Systems *1*, 224-237.

Orjalo, A.V., Bhaumik, D., Gengler, B.K., Scott, G.K., and Campisi, J. (2009). Cell surface-bound IL-1 is an upstream regulator of the senescence-associated IL-6/IL-8

cytokine network. Proceedings of the National Academy of Sciences *106*, 17031-17036.

Osorio, F.G., Bárcena, C., Soria-Valles, C., Ramsay, A.J., de Carlos, F., Cobo, J., Fueyo, A., Freije, J.M.P., and López-Otín, C. (2012). Nuclear lamina defects cause ATM-dependent NF-κB activation and link accelerated aging to a systemic inflammatory response. Genes and Development *26*, 2311-2324.

Ouellet, S., Vigneault, F., Lessard, M., Leclerc, S., Drouin, R., and Guérin, S.L. (2006). Transcriptional regulation of the cyclin-dependent kinase inhibitor 1A (p21) gene by NFI in proliferating human cells. Nucleic Acids Research *34*, 6472-6487.

Ovadya, Y., and Krizhanovsky, V. (2014). Senescent cells: SASPected drivers of age-related pathologies. Biogerontology *15*, 627-642.

Padiath, Q.S. (2006). Lamin B1 duplications cause autosomal dominant leukodystrophy. Nature Genet *38*, 1114-1123.

Palade, G.E. (1953). Fine Structure of Blood Capillaries. Journal of Applied Physics *24*, 1424–1436.

Pallone, T.L., Kishore, B.K., Nielsen, S., Agre, P., and Knepper, M.A. (1997). Evidence that aquaporin-1 mediates NaCl-induced water flux across descending vasa recta. American Journal of Physiology - Renal Physiology *272*, F587-F596.

Park, W.-Y., Park, J.-S., Cho, K.-A., Kim, D.-I., Ko, Y.-G., Seo, J.-S., and Park, S.C. (2000). Up-regulation of caveolin attenuates epidermal growth factor signaling in senescent cells. Journal of Biological Chemistry *275*, 20847-20852.

Parrinello, S., Coppe, J.P., Krtolica, A., and Campisi, J. (2005). Stromal-epithelial interactions in aging and cancer: Senescent fibroblasts alter epithelial cell differentiation. Journal of Cell Science *118*, 485-496.

Parry, D.A.D., Conway, J.F., and Steinert, P.M. (1986). Structural studies on lamin. Similarities and differences between lamin and intermediate-filament proteins. Biochemical Journal *238*, 305-308.

Parton, R.G., and del Pozo, M.A. (2013). Caveolae as plasma membrane sensors, protectors and organizers. Nat Rev Mol Cell Biol *14*, 98-112.

Passos, J.F., Nelson, G., Wang, C., Richter, T., Simillion, C., Proctor, C.J., Miwa, S., Olijslagers, S., Hallinan, J., Wipat, A.*, et al.* (2010). Feedback between p21 and reactive oxygen production is necessary for cell senescence. Molecular Systems Biology *6*, 347.

Passos, J.F., Saretzki, G., Ahmed, S., Nelson, G., Richter, T., Peters, H., Wappler, I., Birket, M.J., Harold, G., Schaeuble, K.*, et al.* (2007). Mitochondrial Dysfunction Accounts for the Stochastic Heterogeneity in Telomere-Dependent Senescence. PLoS Biology *5*, e110.

Passos, J.F., Simillion, C., Hallinan, J., Wipat, A., and von Zglinicki, T. (2009). Cellular senescence: unravelling complexity. Age *31*, 353-363.

Patel, H.H., and Insel, P.A. (2009). Lipid rafts and caveolae and their role in compartmentation of redox signaling. Antioxidants & Redox Signaling *11*, 1357-1372.

Pawlikowski, J.S., Adams, P.D., and Nelson, D.M. (2013). Senescence at a glance. Journal of Cell Science *126*, 4061-4067.

Pazolli, E., Alspach, E., Milczarek, A., Prior, J., Piwnica-Worms, D., and Stewart, S.A. (2012). Chromatin remodeling underlies the senescence- associated secretory phenotype of tumor stromal fibroblasts that supports cancer progression. Cancer Research *72*, 2251-2261.

Pekovic, V., Gibbs-Seymour, I., Markiewicz, E., Alzoghaibi, F., Benham, A.M., Edwards, R., Wenhert, M., von Zglinicki, T., and Hutchison, C.J. (2011). Conserved

cysteine residues in the mammalian lamin A tail are essential for cellular responses to ROS generation. Aging Cell *10*, 1067-1079.

Pelkmans, L., and Helenius, A. (2002). Endocytosis via caveolae. Traffic *3*, 311-320.

Pendas, A.M. (2002). Defective prelamin A processing and muscular and adipocyte alterations in Zmpste24 metalloproteinase-deficient mice. Nature Genet *31*, 94-99.

Penning, T.M., Burczynski, M.E., Jez, J.M., Hung, C.F., Lin, H.K., Ma, H., Moore, M., Palackal, N., and Ratnam, K. (2000). Human 3alpha-hydroxysteroid dehydrogenase isoforms (AKR1C1-AKR1C4) of the aldo-keto reductase superfamily: functional plasticity and tissue distribution reveals roles in the inactivation and formation of male and female sex hormones. Biochemical Journal *351*, 67-77.

Pereira, S., Bourgeois, P., Navarro, C., Esteves-Vieira, V., Cau, P., De Sandre-Giovannoli, A., and Lévy, N. (2008). HGPS and related premature aging disorders: From genomic identification to the first therapeutic approaches. Mechanisms of Ageing and Development *129*, 449-459.

Peter, A., and Stick, R. (2012). Evolution of the lamin protein family: what introns can tell. Nucleus *3*, 44-59.

Peter, A., and Stick, R. (2015). Evolutionary aspects in intermediate filament proteins. Current Opinion in Cell Biology *32*, 48-55.

Peter, M. (1989). Cloning and sequencing of cDNA clones encoding chicken lamins A and B1 and comparison of the primary structures of vertebrate A- and B-type lamins. J Mol Biol *208*, 393-404.

Pilling, L.C., Joehanes, R., Melzer, D., Harries, L.W., Henley, W., Dupuis, J., Lin, H., Mitchell, M., Hernandez, D., Ying, S.-X.*, et al.* (2015). Gene expression markers of age-related inflammation in two human cohorts. Experimental Gerontology *70*, 37-45.

Pinti, M., Troiano, L., Nasi, M., Bellodi, C., Ferraresi, R., Mussi, C., Salvioli, G., and Cossarizza, A. (2004). Balanced regulation of mRNA production for Fas and Fas Ligand in lymphocytes from centenarians: how the immune system starts its second century. Circulation *110*, 3108-3114.

Polvani, S., Tarocchi, M., and Galli, A. (2012). PPARγ and oxidative stress: Con(β) catenating NRF2 and FOXO. PPAR Research *2012*, 641087.

Pombo, A., and Dillon, N. (2015). Three-dimensional genome architecture: Players and mechanisms. Nature Reviews Molecular Cell Biology *16*, 245-257.

Pongratz, R.L., Kibbey, R.G., Shulman, G.I., and Cline, G.W. (2007). Cytosolic and Mitochondrial Malic Enzyme Isoforms Differentially Control Insulin Secretion. Journal of Biological Chemistry *282*, 200-207.

Preisser, L., Teillet, L., Aliotti, S., Gobin, R., Berthonaud, V., Chevalier, J., Corman, B., and Verbavatz, J.M. (2000). Downregulation of aquaporin-2 and -3 in aging kidney is independent of V2 vasopressin receptor. American Journal of Physiology - Renal Physiology *279*, F144-F152.

Prelog, M. (2006). Aging of the immune system: A risk factor for autoimmunity? Autoimmunity Reviews *5*, 136-139.

Pribluda, A., Elyada, E., Wiener, Z., Hamza, H., Goldstein, Robert E., Biton, M., Burstain, I., Morgenstern, Y., Brachya, G., Billauer, H.*, et al.* (2013). A Senescence-Inflammatory Switch from Cancer-Inhibitory to Cancer-Promoting Mechanism. Cancer Cell *24*, 242-256.

Pricola, K.L., Kuhn, N.Z., Haleem-Smith, H., Song, Y., and Tuan, R.S. (2009). Interleukin-6 Maintains Bone Marrow-Derived Mesenchymal Stem Cell Stemness by an ERK1/2-Dependent Mechanism. Journal of cellular biochemistry *108*, 577-588.

Prieur, A., and Peeper, D.S. (2008). Cellular senescence in vivo: a barrier to tumorigenesis. Current Opinion in Cell Biology *20*, 150-155.

Probin, V., Wang, Y., Bai, A., and Zhou, D. (2006). Busulfan Selectively Induces Cellular Senescence but Not Apoptosis in WI38 Fibroblasts via a p53-Independent but Extracellular Signal-Regulated Kinase-p38 Mitogen-Activated Protein Kinase-Dependent Mechanism. Journal of Pharmacology and Experimental Therapeutics *319*, 551-560.

Prokocimer, M., Barkan, R., and Gruenbaum, Y. (2013). Hutchinson–Gilford progeria syndrome through the lens of transcription. Aging Cell *12*, 533-543.

Prunuske, A.J., and Ullman, K.S. (2006). The nuclear envelope: form and reformation. Current Opinion in Cell Biology *18*, 108-116.

Pryse-Davies, J., Ryder, T.A., and Lynn MacKenzie, M. (1979). In vivo production of the nucleolar channel system in post menopausal endometrium. Cell and Tissue Research *203*, 493-498.

Puente, X.S., Quesada, V., Osorio, F.G., Cabanillas, R., Cadiñanos, J., Fraile, J.M., Ordóñez, G.R., Puente, D.A., Gutiérrez-Fernández, A., Fanjul-Fernández, M.*, et al.* (2011). Exome sequencing and functional analysis identifies BANF1 mutation as the cause of a hereditary progeroid syndrome. American Journal of Human Genetics *88*, 650-656.

Purcell, M., Kruger, A., and Tainsky, M.A. (2014). Gene expression profiling of replicative and induced senescence. Cell Cycle *13*, 3927-3937.

Puzianowska-Kuznicka, M., and Kuznicki, J. (2005). Genetic alterations in accelerated ageing syndromes: Do they play a role in natural ageing? The International Journal of Biochemistry & Cell Biology *37*, 947-960.

Quijano-Roy, S., Mbieleu, B., Bönnemann, C.G., Jeannet, P.Y., Colomer, J., Clarke, N.F., Cuisset, J.M., Roper, H., De Meirleir, L., D'Amico, A*., et al.* (2008). De novo LMNA mutations cause a new form of congenital muscular dystrophy. Annals of Neurology *64*, 177-186.

Quijano, C., Cao, L., Fergusson, M.M., Romero, H., Liu, J., Gutkind, S., Rovira, I.I., Mohney, R.P., Karoly, E.D., and Finkel, T. (2012). Oncogene-induced senescence results in marked metabolic and bioenergetic alterations. Cell Cycle *11*, 1383-1392.

Rader, J., Russell, M.R., Hart, L.S., Nakazawa, M.S., Belcastro, L.T., Martinez, D., Li, Y., Carpenter, E.L., Attiyeh, E.F., Diskin, S.J*., et al.* (2013). Dual CDK4/CDK6 Inhibition Induces Cell-Cycle Arrest and Senescence in Neuroblastoma. Clinical Cancer Research *19*, 6173-6182.

Ragnauth, C.D., Warren, D.T., Liu, Y., McNair, R., Tajsic, T., Figg, N., Shroff, R., Skepper, J., and Shanahan, C.M. (2010). Prelamin A acts to accelerate smooth muscle cell senescence and is a novel biomarker of human vascular aging. Circulation *121*, 2200-2210.

Rajagopalan, S., and Long, E.O. (2012). Cellular senescence induced by CD158d reprograms natural killer cells to promote vascular remodeling. Proceedings of the National Academy of Sciences *109*, 20596-20601.

Rak, J., Milsom, C., May, L., Klement, P., and Yu, J. (2006). Tissue factor in cancer and angiogenesis: The molecular link between genetic tumor progression, tumor

neovascularization, and cancer coagulopathy. Seminars in Thrombosis and Hemostasis *32*, 54-69.

Ranuncolo, S.M., Wang, L., Polo, J.M., Dell'Oso, T., Dierov, J., Gaymes, T.J., Rassool, F., Carroll, M., and Melnick, A. (2008). BCL6-mediated Attenuation of DNA Damage Sensing Triggers Growth Arrest and Senescence through a p53-dependent Pathway in a Cell Context-dependent Manner. The Journal of Biological Chemistry *283*, 22565-22572.

Ratajczak, P., Damy, T., Heymes, C., Oliviéro, P., Marotte, F., Robidel, E., Sercombe, R., Boczkowski, J., Rappaport, L., and Samuel, J.-L. (2003). Caveolin-1 and -3 dissociations from caveolae to cytosol in the heart during aging and after myocardial infarction in rat. Cardiovascular Research *57*, 358-369.

Rattan, S.I.S. (2014). Aging is not a disease: Implications for intervention. Aging and Disease *5*, 196-202.

Rawlings, J.S., Rosler, K.M., and Harrison, D.A. (2004). The JAK/STAT signaling pathway. Journal of Cell Science *117*, 1281-1283.

Ray, B.K., Dhar, S., Shakya, A., and Ray, A. (2011). Z-DNA-forming silencer in the first exon regulates human ADAM-12 gene expression. Proceedings of the National Academy of Sciences *108*, 103-108.

Reimand, J., Kull, M., Peterson, H., Hansen, J., and Vilo, J. (2007). g:Profiler—a web-based toolset for functional profiling of gene lists from large-scale experiments. Nucleic Acids Research *35*, W193-W200.

Ren, J.-L., Pan, J.-S., Lu, Y.-P., Sun, P., and Han, J. (2009). Inflammatory signaling and cellular senescence. Cellular Signalling *21*, 378-383.

Renou, L., Stora, S., Yaou, R.B., Volk, M., Šinkovec, M., Demay, L., Richard, P., Peterlin, B., and Bonne, G. (2008). Heart-hand syndrome of Slovenian type: A new kind of laminopathy. Journal of Medical Genetics *45*, 666-671.

Ressler, S., Bartkova, J., Niederegger, H., Bartek, J., Scharffetter-Kochanek, K., Jansen-Dürr, P., and Wlaschek, M. (2006). p16INK4A is a robust in vivo biomarker of cellular aging in human skin. Aging Cell *5*, 379-389.

Ridderstråle, W., Ulfhammer, E., Jern, S., and Hrafnkelsdóttir, T. (2006). Impaired capacity for stimulated fibrinolysis in primary hypertension is restored by antihypertensive therapy. Hypertension *47*, 686-691.

Rinaldo, P., Matern, D., and Bennett, M.J. (2002). Fatty acid oxidation disorders. In Annual review of physiology, pp. 477-502.

Robbins, E., Levine, E.M., and Eagle, H. (1970). MORPHOLOGIC CHANGES ACCOMPANYING SENESCENCE OF CULTURED HUMAN DIPLOID CELLS. The Journal of Experimental Medicine *131*, 1211-1222.

Rober, R.A., Weber, K., and Osborn, M. (1989). Differential timing of lamin A/C expression in the various organs of the mouse embryo and the young animal: a developmental study. Development *105*, 365-378.

Roberts, S., Evans, E.H., Kletsas, D., Jaffray, D.C., and Eisenstein, S.M. (2006). Senescence in human intervertebral discs. European Spine Journal *15*, 312-316.

Roblek, M., Schüchner, S., Huber, V., Ollram, K., Vlcek-Vesely, S., Foisner, R., Wehnert, M., and Ogris, E. (2010). Monoclonal antibodies specific for disease-associated point-mutants: Lamin A/C R453W and R482W. PLoS ONE *5*, e10604.

Rock, K.L., and Kono, H. (2008). The Inflammatory Response to Cell Death. Annual Review of Pathology: Mechanisms of Disease *3*, 99-126.

Rodier, F., and Campisi, J. (2011). Four faces of cellular senescence. The Journal of Cell Biology *192*, 547-556.

Rodier, F., Coppé, J.P., Patil, C.K., Hoeijmakers, W.A.M., Muñoz, D.P., Raza, S.R., Freund, A., Campeau, E., Davalos, A.R., and Campisi, J. (2009). Persistent DNA damage signalling triggers senescence-associated inflammatory cytokine secretion. Nature Cell Biology *11*, 973-979.

Rodier, F., Muñoz, D.P., Teachenor, R., Chu, V., Le, O., Bhaumik, D., Coppé, J.-P., Campeau, E., Beauséjour, C.M., Kim, S.-H.*, et al.* (2011). DNA-SCARS: distinct nuclear structures that sustain damage-induced senescence growth arrest and inflammatory cytokine secretion. Journal of Cell Science *124*, 68-81.

Romanov, V.S., Abramova, M.V., Svetlikova, S.B., Bykova, T.V., Zubova, S.G., Aksenov, N.D., Fornace, A.J., Pospelova, T.V., and Pospelov, V.A. (2010). p21Waf1 is required for cellular senescence but not for cell cycle arrest induced by the HDAC inhibitor sodium butyrate. Cell Cycle *9*, 3945-3955.

Rombouts, C., Aerts, A., Quintens, R., Baselet, B., El-Saghire, H., Harms-Ringdahl, M., Haghdoost, S., Janssen, A., Michaux, A., Yentrapalli, R.*, et al.* (2014). Transcriptomic profiling suggests a role for IGFBP5 in premature senescence of endothelial cells after chronic low dose rate irradiation. International Journal of Radiation Biology *90*, 560-574.

Rothberg, K.G., Heuser, J.E., Donzell, W.C., Ying, Y.S., Glenney, J.R., and Anderson, R.G.W. (1992). Caveolin, a protein component of caveolae membrane coats. Cell *68*, 673-682.

Roux, K.J., Kim, D.I., Raida, M., and Burke, B. (2012). A promiscuous biotin ligase fusion protein identifies proximal and interacting proteins in mammalian cells. J Cell Biol *196*, 801-810.

Rowat, A.C., Lammerding, J., Herrmann, H., and Aebi, U. (2008). Towards an integrated understanding of the structure and mechanics of the cell nucleus. BioEssays *30*, 226-236.

Roy, R., Wewer, U.M., Zurakowski, D., Pories, S.E., and Moses, M.A. (2004). ADAM 12 cleaves extracellular matrix proteins and correlates with cancer status and stage. Journal of Biological Chemistry *279*, 51323-51330.

Ruddy, M.J., Wong, G.C., Liu, X.K., Yamamoto, H., Kasayama, S., Kirkwood, K.L., and Gaffen, S.L. (2004). Functional Cooperation between Interleukin-17 and Tumor Necrosis Factor-α Is Mediated by CCAAT/Enhancer-binding Protein Family Members. Journal of Biological Chemistry *279*, 2559-2567.

Ruf, W. (2007). Tissue factor and PAR signaling in tumor progression. Thrombosis Research *120*, S7-S12.

Ryan, J.M., and Cristofalo, V.J. (1972). Histone acetylation during aging of human cells in culture. Biochemical and Biophysical Research Communications *48*, 735-742.

Saal, L., Troein, C., Vallon-Christersson, J., Gruvberger, S., Borg, A., and Peterson, C. (2002). BioArray Software Environment (BASE): a platform for comprehensive management and analysis of microarray data. Genome Biology *3*, software0003.0001 - software0003.0006.

Saccani, S., Pantano, S., and Natoli, G. (2002). p38-dependent marking of inflammatory genes for increased NF-[kappa]B recruitment. Nat Immunol *3*, 69-75.

Salama, R., Sadaie, M., Hoare, M., and Narita, M. (2014). Cellular senescence and its effector programs. Genes & Development *28*, 99-114.

Salminen, A., Kauppinen, A., and Kaarniranta, K. (2012). Emerging role of NF-κB signaling in the induction of senescence-associated secretory phenotype (SASP). Cellular Signalling *24*, 835-845.

Salminen, A., Ojala, J., and Kaarniranta, K. (2011a). Apoptosis and aging: Increased resistance to apoptosis enhances the aging process. Cell Mol Life Sci *68*, 1021-1031.

Salminen, A., Ojala, J., Kaarniranta, K., Haapasalo, A., Hiltunen, M., and Soininen, H. (2011b). Astrocytes in the aging brain express characteristics of senescence-associated secretory phenotype. European Journal of Neuroscience *34*, 3-11.

Sansoni, P., Vescovini, R., Fagnoni, F., Biasini, C., Zanni, F., Zanlari, L., Telera, A., Lucchini, G., Passeri, G., Monti, D.*, et al.* (2008). The immune system in extreme longevity. Experimental Gerontology *43*, 61-65.

Sarati, L.I., Toblli, J.E., Martinez, C.R., Uceda, A., Feldman, M., Balaszczuk, A.M., and Fellet, A.L. (2013). Nitric oxide and AQP2 in hypothyroid rats: A link between aging and water homeostasis. Metabolism: Clinical and Experimental *62*, 1287-1295.

Saretzki, G., and Von Zglinicki, T. (2002). Replicative Aging, Telomeres, and Oxidative Stress. Annals of the New York Academy of Sciences *959*, 24-29.

Sarkar, D., Emdad, L., Lee, S.G., Yoo, B.K., Su, Z.Z., and Fisher, P.B. (2009). Astrocyte elevated gene-1: Far more than just a gene regulated in astrocytes. Cancer Research *69*, 8529-8535.

Sarkar, D., and Fisher, P.B. (2006). Molecular mechanisms of aging-associated inflammation. Cancer Letters *236*, 13-23.

Scaffidi, P., and Misteli, T. (2006). Lamin A-dependent nuclear defects in human aging. Science *312*, 1059-1063.

Scaffidi, P., and Misteli, T. (2008). Lamin A-dependent misregulation of adult stem cells associated with accelerated ageing. Nat Cell Biol *10*, 452-459.

Schena, M., Shalon, D., Davis, R.W., and Brown, P.O. (1995). Quantitative Monitoring of Gene Expression Patterns with a Complementary DNA Microarray. Science *270*, 467-470.

Scherer, P.E., Tang, Z., Chun, M., Sargiacomo, M., Lodish, H.F., and Lisanti, M.P. (1995). Caveolin Isoforms Differ in Their N-terminal Protein Sequence and Subcellular Distribution: Identification and epitope mapping of an isoform-specific monoclonal antibody probe. Journal of Biological Chemistry *270*, 16395-16401.

Schieven, G.L. (2009). The p38α kinase plays a central role in inflammation. Current Topics in Medicinal Chemistry *9*, 1038-1048.

Schirmer, E.C., and Foisner, R. (2007). Proteins that associate with lamins: Many faces, many functions. Experimental Cell Research *313*, 2167-2179.

Schmidt, S., Essmann, F., Cirstea, I.C., Kuck, F., Thakur, H.C., Singh, M., Kletke, A., Jänicke, R.U., Wiek, C., Hanenberg, H.*, et al.* (2010). The centrosome and mitotic spindle apparatus in cancer and senescence. Cell Cycle *9*, 4469-4473.

Schmitt, C.A., Fridman, J.S., Yang, M., Lee, S., Baranov, E., Hoffman, R.M., and Lowe, S.W. (2002). A Senescence Program Controlled by p53 and p16INK4a Contributes to the Outcome of Cancer Therapy. Cell *109*, 335-346.

Schnabl, B., Purbeck, C.A., Choi, Y.H., Hagedorn, C.H., and Brenner, D. (2003). Replicative senescence of activated human hepatic stellate cells is accompanied by a pronounced inflammatory but less fibrogenic phenotype. Hepatology *37*, 653-664.

Schott, J., and Stoecklin, G. (2010). Networks controlling mRNA decay in the immune system. Wiley Interdisciplinary Reviews: RNA *1*, 432-456.

Schreiber, K.H., and Kennedy, B.K. (2013). When lamins go bad: nuclear structure and disease. Cell *152*, 1365-1375.

Sedelnikova, O.A., Horikawa, I., Zimonjic, D.B., Popescu, N.C., Bonner, W.M., and Barrett, J.C. (2004). Senescing human cells and ageing mice accumulate DNA lesions with unrepairable double-strand breaks. Nat Cell Biol *6*, 168-170.

Sedelnikova, O.A., Redon, C.E., Dickey, J.S., Nakamura, A.J., Georgakilas, A.G., and Bonner, W.M. (2010). Role of oxidatively induced DNA lesions in human pathogenesis. Mutation research *704*, 152-159.

Seidler, S., Zimmermann, H.W., Bartneck, M., Trautwein, C., and Tacke, F. (2010). Age-dependent alterations of monocyte subsets and monocyte-related chemokine pathways in healthy adults. BMC Immunology *11*, 30-30.

Serrano, M., Hannon, G.J., and Beach, D. (1993). A new regulatory motif in cell-cycle control causing specific inhibition of cyclin D/CDK4. Nature *366*, 704-707.

Serrano, M., Lin, A.W., McCurrach, M.E., Beach, D., and Lowe, S.W. (1997). Oncogenic ras provokes premature cell senescence associated with accumulation of p53 and p16INK4a. Cell *88*, 593-602.

Severino, V., Alessio, N., Farina, A., Sandomenico, A., Cipollaro, M., Peluso, G., Galderisi, U., and Chambery, A. (2013). Insulin-like growth factor binding proteins 4 and 7 released by senescent cells promote premature senescence in mesenchymal stem cells. Cell Death and Disease *4*, e913.

Shah, P.P., Donahue, G., Otte, G.L., Capell, B.C., Nelson, D.M., Cao, K., Aggarwala, V., Cruickshanks, H.A., Rai, T.S., McBryan, T.*, et al.* (2013). Lamin B1 depletion in

senescent cells triggers large-scale changes in gene expression and the chromatin landscape. Genes & Development *27*, 1787-1799.

Sharpless, N.E., and DePinho, R.A. (2007). How stem cells age and why this makes us grow old. Nat Rev Mol Cell Biol *8*, 703-713.

Sharpless, N.E., and Sherr, C.J. (2015). Forging a signature of in vivo senescence. Nature Reviews Cancer *15*, 397-408.

Shay, J.W., Pereira-Smith, O.M., and Wright, W.E. (1991). A role for both RB and p53 in the regulation of human cellular senescence. Experimental Cell Research *196*, 33-39.

Shay, J.W., and Wright, W.E. (2000). Hayflick, his limit, and cellular ageing. Nat Rev Mol Cell Biol *1*, 72-76.

Shelton, D.N., Chang, E., Whittier, P.S., Choi, D., and Funk, W.D. (1999). Microarray analysis of replicative senescence. Current Biology *9*, 939-945.

Shen, L., Zhang, H., Yan, T., Zhou, G., and Liu, R. (2015). Association between interleukin 17A polymorphisms and susceptibility to rheumatoid arthritis in a Chinese population. Gene *566*, 18-22.

Shen, X.H., Xu, S.J., Jin, C.Y., Ding, F., Zhou, Y.C., and Fu, G.S. (2013). Interleukin-8 prevents oxidative stress-induced human endothelial cell senescence via telomerase activation. International Immunopharmacology *16*, 261-267.

Sherr, C.J., and DePinho, R.A. (2000). Cellular Senescence: Minireview Mitotic Clock or Culture Shock? Cell *102*, 407-410.

Sherr, C.J., and McCormick, F. (2002). The RB and p53 pathways in cancer. Cancer Cell *2*, 103-112.

Shi, Z., Xu, W., Loechel, F., Wewer, U.M., and Murphy, L.J. (2000). ADAM 12, a disintegrin metalloprotease, interacts with insulin-like growth factor-binding protein-3. Journal of Biological Chemistry *275*, 18574-18580.

Shibata, Y., Shemesh, T., Prinz, W.A., Palazzo, A.F., Kozlov, M.M., and Rapoport, T.A. (2010). Mechanisms determining the morphology of the peripheral ER. Cell *143*, 774-788.

Shimi, T., Butin-Israeli, V., Adam, S.A., Hamanaka, R.B., Goldman, A.E., Lucas, C.A., Shumaker, D.K., Kosak, S.T., Chandel, N.S., and Goldman, R.D. (2011). The role of nuclear lamin B1 in cell proliferation and senescence. Genes & Development *25*, 2579-2593.

Shimi, T., Kittisopikul, M., Tran, J., Goldman, A.E., Adam, S.A., Zheng, Y., Jaqaman, K., and Goldman, R.D. (2015). Structural organization of nuclear lamins A, C, B1, and B2 revealed by superresolution microscopy. Molecular Biology of the Cell *26*, 4075-4086.

Shimi, T., Pfleghaar, K., Kojima, S.-i., Pack, C.-G., Solovei, I., Goldman, A.E., Adam, S.A., Shumaker, D.K., Kinjo, M., Cremer, T.*, et al.* (2008). The A- and B-type nuclear lamin networks: microdomains involved in chromatin organization and transcription. Genes & Development *22*, 3409-3421.

Shlush, L., Itzkovitz, S., Cohen, A., Rutenberg, A., Berkovitz, R., Yehezkel, S., Shahar, H., Selig, S., and Skorecki, K. (2011). Quantitative digital in situ senescence-associated beta-galactosidase assay. BMC Cell Biology *12*, 16-26.

Shoeman, R.L., and Traub, P. (1990). The in vitro DNA-binding properties of purified nuclear lamin proteins and vimentin. Journal of Biological Chemistry *265*, 9055-9061.

Shumaker, D.K., Dechat, T., Kohlmaier, A., Adam, S.A., Bozovsky, M.R., Erdos, M.R., Eriksson, M., Goldman, A.E., Khuon, S., Collins, F.S*., et al.* (2006). Mutant nuclear lamin A leads to progressive alterations of epigenetic control in premature aging. Proceedings of the National Academy of Sciences *103*, 8703-8708.

Shumaker, D.K., Solimando, L., Sengupta, K., Shimi, T., Adam, S.A., Grunwald, A., Strelkov, S.V., Aebi, U., Cardoso, M.C., and Goldman, R.D. (2008). The highly conserved nuclear lamin Ig-fold binds to PCNA: Its role in DNA replication. Journal of Cell Biology *181*, 269-280.

Shvarts, A. (2002). A senescence rescue screen identifies BCL6 as an inhibitor of anti-proliferative p19ARF-p53 signaling. Genes & Development *16*, 681-686.

Signer, Robert A.J., and Morrison, Sean J. (2013). Mechanisms that Regulate Stem Cell Aging and Life Span. Cell Stem Cell *12*, 152-165.

Silva, M., do Vale, A., and dos Santos, N.N. (2008). Secondary necrosis in multicellular animals: an outcome of apoptosis with pathogenic implications. Apoptosis *13*, 463-482.

Simon, D.N., and Wilson, K.L. (2011). The nucleoskeleton as a genome-associated dynamic 'network of networks'. Nat Rev Mol Cell Biol *12*, 695-708.

Simon, D.N., and Wilson, K.L. (2013). Partners and post-translational modifications of nuclear lamins. Chromosoma *122*, 13-31.

Sinensky, M. (1994). The processing pathway of prelamin A. J Cell Sci *107*, 61-67.

Sinha, B. (2011). Cells respond to mechanical stress by rapid disassembly of caveolae. Cell *144*, 402-413.

Sitte, N., Merker, K., Von Zglinicki, T., Grune, T., and Davies, K.J.A. (2000). Protein oxidation and degradation during cellular senescence of human BJ fibroblasts: Part I - Effects of proliferative senescence. FASEB Journal *14*, 2495-2502.

Smogorzewska, A., and De Lange, T. (2002). Different telomere damage signaling pathways in human and mouse cells. EMBO Journal *21*, 4338-4348.

Snel, B., Lehmann, G., Bork, P., and Huynen, M.A. (2000). STRING: a web-server to retrieve and display the repeatedly occurring neighbourhood of a gene. Nucleic Acids Research *28*, 3442-3444.

Solana, R., Tarazona, R., Gayoso, I., Lesur, O., Dupuis, G., and Fulop, T. (2012). Innate immunosenescence: Effect of aging on cells and receptors of the innate immune system in humans. Seminars in Immunology *24*, 331-341.

Song, Y.S., Lee, B.Y., and Hwang, E.S. (2005). Dinstinct ROS and biochemical profiles in cells undergoing DNA damage-induced senescence and apoptosis. Mechanisms of Ageing and Development *126*, 580-590.

Sonoda, H., Yokota-Ikeda, N., Oshikawa, S., Kanno, Y., Yoshinaga, K., Uchida, K., Ueda, Y., Kimiya, K., Uezono, S., Ueda, A.*, et al.* (2009). Decreased abundance of urinary exosomal aquaporin-1 in renal ischemia-reperfusion injury. American Journal of Physiology - Renal Physiology *297*, F1006-F1016.

Spallarossa, P., Altieri, P., Aloi, C., Garibaldi, S., Barisione, C., Ghigliotti, G., Fugazza, G., Barsotti, A., and Brunelli, C. (2009). Doxorubicin induces senescence or apoptosis in rat neonatal cardiomyocytes by regulating the expression levels of the telomere binding factors 1 and 2. American Journal of Physiology - Heart and Circulatory Physiology *297*, H2169-H2181.

Stähli, B.E., Camici, G.G., Steffel, J., Akhmedov, A., Shojaati, K., Graber, M., Lüscher, T.F., and Tanner, F.C. (2006). Paclitaxel enhances thrombin-induced endothelial tissue factor expression via c-Jun terminal NH 2 kinase activation. Circulation Research *99*, 149-155.

Stanfel, M.N., Shamieh, L.S., Kaeberlein, M., and Kennedy, B.K. (2009). The TOR pathway comes of age. Biochimica et Biophysica Acta (BBA) - General Subjects *1790*, 1067-1074.

Starr, D.A., and Fridolfsson, H.N. (2010). Interactions Between Nuclei and the Cytoskeleton Are Mediated by SUN-KASH Nuclear-Envelope Bridges. Annual review of cell and developmental biology *26*, 421-444.

Stein, G.H., Drullinger, L.F., Soulard, A., and Dulić, V. (1999). Differential Roles for Cyclin-Dependent Kinase Inhibitors p21 and p16 in the Mechanisms of Senescence and Differentiation in Human Fibroblasts. Molecular and Cellular Biology *19*, 2109-2117.

Stewart, C., and Burke, B. (1987). Teratocarcinoma stem cells and early mouse embryos contain only a single major lamin polypeptide closely resembling lamin B. Cell *51*, 383-392.

Stewart, C.L., Roux, K.J., and Burke, B. (2007). Blurring the Boundary: The Nuclear Envelope Extends Its Reach. Science *318*, 1408-1412.

Stierlé, V., Couprie, J., Östlund, C., Krimm, I., Zinn-Justin, S., Hossenlopp, P., Worman, H.J., Courvalin, J.C., and Duband-Goulet, I. (2003). The carboxyl-terminal region common to lamins A and C contains a DNA binding domain. Biochemistry *42*, 4819-4828.

Storch, K., Taatjes, D., Bouffard, N., Locknar, S., Bishop, N., and Langevin, H. (2007). Alpha smooth muscle actin distribution in cytoplasm and nuclear invaginations of connective tissue fibroblasts. Histochemistry and cell biology *127*, 523-530.

Storer, M., and Keyes, W.M. (2014). Developing senescence to remodel the embryo. Communicative & Integrative Biology *7*, 1-4.

Storer, M., Mas, A., Robert-Moreno, A., Pecoraro, M., Ortells, M.C., Di Giacomo, V., Yosef, R., Pilpel, N., Krizhanovsky, V., Sharpe, J.*, et al.* (2013). Senescence Is a Developmental Mechanism that Contributes to Embryonic Growth and Patterning. Cell *155*, 1119-1130.

Strelkov, S.V., Schumacher, J., Burkhard, P., Aebi, U., and Herrmann, H. (2004). Crystal structure of the human lamin A coil 2B dimer: implications for the head-to-tail association of nuclear lamins. J Mol Biol *343*, 1067-1080.

Stuurman, N., Heins, S., and Aebi, U. (1998). Nuclear lamins: Their structure, assembly, and interactions. Journal of Structural Biology *122*, 42-66.

Subramanian, A., Tamayo, P., Mootha, V.K., Mukherjee, S., Ebert, B.L., Gillette, M.A., Paulovich, A., Pomeroy, S.L., Golub, T.R., Lander, E.S.*, et al.* (2005). Gene set enrichment analysis: A knowledge-based approach for interpreting genome-wide expression profiles. Proceedings of the National Academy of Sciences *102*, 15545-15550.

Sulston, J.E., Schierenberg, E., White, J.G., and Thomson, J.N. (1983). The embryonic cell lineage of the nematode Caenorhabditis elegans. Developmental Biology *100*, 64-119.

Sun, P., Yoshizuka, N., New, L., Moser, B.A., Li, Y., Liao, R., Xie, C., Chen, J., Deng, Q., Yamout, M.*, et al.* (2007). PRAK Is Essential for ras-Induced Senescence and Tumor Suppression. Cell *128*, 295-308.

Sun, Y., Campisi, J., Higano, C., Beer, T.M., Porter, P., Coleman, I., True, L., and Nelson, P.S. (2012). Treatment-induced damage to the tumor microenvironment promotes prostate cancer therapy resistance through WNT16B. Nat Med *18*, 1359-1368.

Suram, A., Kaplunov, J., Patel, P.L., Ruan, H., Cerutti, A., Boccardi, V., Fumagalli, M., Di Micco, R., Mirani, N., Gurung, R.L.*, et al.* (2012). Oncogene-induced telomere dysfunction enforces cellular senescence in human cancer precursor lesions. The EMBO Journal *31*, 2839-2851.

Suzuki, Y., Mogami, H., Ihara, H., and Urano, T. (2009). Unique secretory dynamics of tissue plasminogen activator and its modulation by plasminogen activator inhibitor-1 in vascular endothelial cells. Blood *113*, 470-478.

Takahashi, A., Ohtani, N., Yamakoshi, K., Iida, S.-i., Tahara, H., Nakayama, K., Nakayama, K.I., Ide, T., Saya, H., and Hara, E. (2006). Mitogenic signalling and the p16INK4a-Rb pathway cooperate to enforce irreversible cellular senescence. Nat Cell Biol *8*, 1291-1297.

Takai, H., Smogorzewska, A., and de Lange, T. (2003). DNA Damage Foci at Dysfunctional Telomeres. Current Biology *13*, 1549-1556.

Taniura, H., Glass, C., and Gerace, L. (1995). A chromatin binding site in the tail domain of nuclear lamins that interacts with core histones. J Cell Biol *131*, 33-44.

Taş, U., Çayli, S., Inanir, A., Özyurt, B., Ocakli, S., Karaca, Z.I., and Sarsilmaz, M. (2012). Aquaporin-1 and aquaporin-3 expressions in the intervertebral disc of rats with aging. Balkan Medical Journal *29*, 349-353.

Taylor, M.R.G., Slavov, D., Gajewski, A., Vlcek, S., Ku, L., Fain, P.R., Carniel, E., Di Lenarda, A., Sinagra, G., Boucek, M.M.*, et al.* (2005). Thymopoietin (lamina-associated polypeptide 2) gene mutation associated with dilated cardiomyopathy. Human Mutation *26*, 566-574.

Tchkonia, T., Zhu, Y., Van Deursen, J., Campisi, J., and Kirkland, J.L. (2013). Cellular senescence and the senescent secretory phenotype: Therapeutic opportunities. Journal of Clinical Investigation *123*, 966-972.

Terman, A., and Brunk, U.T. (2004). Lipofuscin. The International Journal of Biochemistry & Cell Biology *36*, 1400-1404.

Terzakis, J.A. (1965). The nucleolar channel system of the human endometrium. The Journal of Cell Biology *27*, 293-304.

Thangavel, C., Dean, J.L., Ertel, A., Knudsen, K.E., Aldaz, C.M., Witkiewicz, A.K., Clarke, R., and Knudsen, E.S. (2011). Therapeutically activating RB: reestablishing cell cycle control in endocrine therapy-resistant breast cancer. Endocrine-Related Cancer *18*, 333-345.

The Gene Ontology Consortium (2010). The Gene Ontology in 2010: extensions and refinements. Nucleic Acids Research *38*, D331-D335.

Thuahnai, S.T., Lund-Katz, S., Williams, D.L., and Phillips, M.C. (2001). Scavenger Receptor Class B, Type I-mediated Uptake of Various Lipids into Cells: INFLUENCE OF THE NATURE OF THE DONOR PARTICLE INTERACTION WITH THE RECEPTOR. Journal of Biological Chemistry *276*, 43801-43808.

Tighe, P., Negm, O., Todd, I., and Fairclough, L. (2013). Utility, reliability and reproducibility of immunoassay multiplex kits. Methods *61*, 23-29.

Tomicic, M.T., and Kaina, B. (2013). Topoisomerase degradation, DSB repair, p53 and IAPs in cancer cell resistance to camptothecin-like topoisomerase I inhibitors. Biochimica et Biophysica Acta - Reviews on Cancer *1835*, 11-27.

Tominaga-Yamanaka, K., Abdelmohsen, K., Martindale, J.L., Yang, X., Taub, D.D., and Gorospe, M. (2012). NF90 coordinately represses the senescence-associated secretory phenotype. Aging (Albany NY) *4*, 695-708.

Torres, R.A., and Lewis, W. (2014). Aging and HIV/AIDS: Pathogenetic role of therapeutic side effects. Laboratory Investigation *94*, 120-128.

Toth, J.I., Yang, S.H., Qiao, X., Beigneux, A.P., Gelb, M.H., Moulson, C.L., Miner, J.H., Young, S.G., and Fong, L.G. (2005). Blocking protein farnesyltransferase improves nuclear shape in fibroblasts from humans with progeroid syndromes. Proceedings of the National Academy of Sciences of the United States of America *102*, 12873-12878.

Tran, N.D., Kim, S., Vincent, H.K., Rodriguez, A., Hinton, D.R., Bullock, M.R., and Young, H.F. (2010). Aquaporin-1-mediated cerebral edema following traumatic brain injury: Effects of acidosis and corticosteroid administration. Journal of Neurosurgery *112*, 1095-1104.

Trinchieri, G. (2010). Type I interferon: friend or foe? The Journal of Experimental Medicine *207*, 2053-2063.

Trujillo, E., González, T., Marín, R., Martín-Vasallo, P., Marples, D., and Mobasheri, A. (2004). Human articular chrondrocytes, synoviocytes and synovial microvessels express aquaporin water channels; upregulation of AQP1 in rheumatoid arthritis. Histology and Histopathology *19*, 435-444.

Trushina, E., Du Charme, J., Parisi, J., and McMurray, C.T. (2006). Neurological abnormalities in caveolin-1 knock out mice. Behavioural Brain Research *172*, 24-32.

Tzur, Y.B., Wilson, K.L., and Gruenbaum, Y. (2006). SUN-domain proteins: 'Velcro' that links the nucleoskeleton to the cytoskeleton. Nature Reviews Molecular Cell Biology *7*, 782-788.

Ugalde, A.P., Español, Y., and López-Otín, C. (2011a). Micromanaging aging with miRNAs: New messages from the nuclear envelope. Nucleus *2*, 549-555.

Ugalde, A.P., Ramsay, A.J., de la Rosa, J., Varela, I., Marino, G., Cadinanos, J., Lu, J., Freije, J.M.P., and Lopez-Otin, C. (2011b). Aging and chronic DNA damage response activate a regulatory pathway involving miR-29 and p53. EMBO J *30*, 2219-2232.

Umezu-Goto, M., Kishi, Y., Taira, A., Hama, K., Dohmae, N., Takio, K., Yamori, T., Mills, G.B., Inoue, K., Aoki, J.*, et al.* (2002). Autotaxin has lysophospholipase D activity leading to tumor cell growth and motility by lysophosphatidic acid production. Journal of Cell Biology *158*, 227-233.

Urano, T., Sumiyoshi, K., Pietraszek, M.H., Takada, Y., and Takada, A. (1991). PAI-1 play an important role in the expression of t-PA activity in the euglobulin clot lysis by controlling the concentration of free t-PA. Thrombosis and Haemostasis *66*, 474-478.

Vallabhapurapu, S., and Karin, M. (2009). Regulation and function of NF-κB transcription factors in the immune system. In Annual Review of Immunology, pp. 693-733.

Van Den Berg, Y.W., Osanto, S., Reitsma, P.H., and Versteeg, H.H. (2012). The relationship between tissue factor and cancer progression: Insights from bench and bedside. Blood *119*, 924-932.

Van Deursen, J.M. (2014). The role of senescent cells in ageing. Nature *509*, 439-446.

Van Itallie, C.M., and Anderson, J.M. (2013). Claudin interactions in and out of the tight junction. Tissue Barriers *1*, e25247.

Varga, T., Czimmerer, Z., and Nagy, L. (2011). PPARs are a unique set of fatty acid regulated transcription factors controlling both lipid metabolism and inflammation. Biochimica et biophysica acta *1812*, 1007-1022.

Vasto, S., Candore, G., Balistreri, C.R., Caruso, M., Colonna-Romano, G., Grimaldi, M.P., Listi, F., Nuzzo, D., Lio, D., and Caruso, C. (2007). Inflammatory networks in ageing, age-related diseases and longevity. Mechanisms of Ageing and Development *128*, 83-91.

Vasto, S., Carruba, G., Lio, D., Colonna-Romano, G., Di Bona, D., Candore, G., and Caruso, C. (2009). Inflammation, ageing and cancer. Mechanisms of Ageing and Development *130*, 40-45.

Velarde, M.C., Flynn, J.M., Day, N.U., Melov, S., and Campisi, J. (2012). Mitochondrial oxidative stress caused by Sod2 deficiency promotes cellular senescence and aging phenotypes in the skin. Aging (Albany NY) *4*, 3-12.

Velculescu, V.E., Zhang, L., Vogelstein, B., and Kinzler, K. (1995). Serial analysis of gene expression. Science *270*, 484-487.

Venable, M.E., Webb-Froehlich, L.M., Sloan, E.F., and Thomley, J.E. (2006). Shift in sphingolipid metabolism leads to an accumulation of ceramide in senescence. Mechanisms of Ageing and Development *127*, 473-480.

Ventura, A., Kirsch, D.G., McLaughlin, M.E., Tuveson, D.A., Grimm, J., Lintault, L., Newman, J., Reczek, E.E., Weissleder, R., and Jacks, T. (2007). Restoration of p53 function leads to tumour regression in vivo. Nature *445*, 661-665.

Verstraeten, V.L.R.M., Broers, J.L.V., van Steensel, M.A.M., Zinn-Justin, S., Ramaekers, F.C.S., Steijlen, P.M., Kamps, M., Kuijpers, H.J.H., Merckx, D., Smeets, H.J.M.*, et al.* (2006). Compound heterozygosity for mutations in LMNA causes a progeria syndrome without prelamin A accumulation. Human Molecular Genetics *15*, 2509-2522.

Vigouroux, C., and Capeau, J. (2005). A-type lamin-linked lipodystrophies. Novartis Foundation Symposium *264*, 166-177.

Viteri, G., Chung, Y.W., and Stadtman, E.R. (2010). Effect of progerin on the accumulation of oxidized proteins in fibroblasts from Hutchinson Gilford progeria patients. Mechanisms of Ageing and Development *131*, 2-8.

Voeltz, G.K., Prinz, W.A., Shibata, Y., Rist, J.M., and Rapoport, T.A. (2006). A Class of Membrane Proteins Shaping the Tubular Endoplasmic Reticulum. Cell *124*, 573-586.

Volonte, D., Zou, H., Bartholomew, J.N., Liu, Z., Morel, P.A., and Galbiati, F. (2015). Oxidative stress-induced inhibition of Sirt1 by caveolin-1 promotes p53-dependent premature senescence and stimulates the secretion of interleukin 6 (IL-6). Journal of Biological Chemistry *290*, 4202-4214.

von Zglinicki, T. (2002). Oxidative stress shortens telomeres. Trends in Biochemical Sciences *27*, 339-344.

Vorburger, K., Lehner, C.F., Kitten, G.T., Eppenberger, H.M., and Nigg, E.A. (1989). A second higher vertebrate B-type lamin. cDNA sequence determination and in vitro processing of chicken lamin B2. J Mol Biol *208*, 405-415.

Waaijer, M.E.C., Parish, W.E., Strongitharm, B.H., van Heemst, D., Slagboom, P.E., de Craen, A.J.M., Sedivy, J.M., Westendorp, R.G.J., Gunn, D.A., and Maier, A.B. (2012). The number of p16INK4a positive cells in human skin reflects biological age. Aging Cell *11*, 722-725.

Wajapeyee, N., Serra, R.W., Zhu, X., Mahalingam, M., and Green, M.R. (2008). Oncogenic BRAF Induces Senescence and Apoptosis through Pathways Mediated by the Secreted Protein IGFBP7. Cell *132*, 363-374.

Walesch, S.K., Richter, A.M., Helmbold, P.H., and Dammann, R.H. (2015). Claudin11 promoter hypermethylation is frequent in malignant melanoma of the skin, but uncommon in nevus cell nevi. Cancers *7*, 1233-1243.

Wang, C., Gong, B., Bushel, P.R., Thierry-Mieg, J., Thierry-Mieg, D., Xu, J., Fang, H., Hong, H., Shen, J., Su, Z.*, et al.* (2014). The concordance between RNA-seq and microarray data depends on chemical treatment and transcript abundance. Nat Biotech *32*, 926-932.

Wang, C., Jurk, D., Maddick, M., Nelson, G., Martin-Ruiz, C., and Von Zglinicki, T. (2009). DNA damage response and cellular senescence in tissues of aging mice. Aging Cell *8*, 311-323.

Wang, F., and Zhu, Y. (2011). Aquaporin-1: A potential membrane channel for facilitating the adaptability of rabbit nucleus pulposus cells to an extracellular matrix environment. Journal of Orthopaedic Science *16*, 304-312.

Wang, J., Duncan, D., Shi, Z., and Zhang, B. (2013a). WEB-based GEne SeT AnaLysis Toolkit (WebGestalt): update 2013. Nucleic Acids Research *41*, W77-W83.

Wang, K., Das, A., Xiong, Z.-M., Cao, K., and Hannenhalli, S. (2013b). Identification of gene clusters with phenotype-dependent expression with application

to normal and premature ageing. In Proceedings of the International Conference on Bioinformatics, Computational Biology and Biomedical Informatics (Wshington DC, USA, ACM), pp. 377-383.

Wang, M.C., O'Rourke, E.J., and Ruvkun, G. (2008). Fat Metabolism Links Germline Stem Cells and Longevity in C. elegans. Science *322*, 957-960.

Warde-Farley, D., Donaldson, S.L., Comes, O., Zuberi, K., Badrawi, R., Chao, P., Franz, M., Grouios, C., Kazi, F., Lopes, C.T.*, et al.* (2010). The GeneMANIA prediction server: biological network integration for gene prioritization and predicting gene function. Nucleic Acids Research *38*, W214-W220.

Waterham, H.R., Koster, J., Mooyer, P., Van Noort, G., Kelley, R.I., Wilcox, W.R., Wanders, R.J.A., Hennekam, R.C.M., and Oosterwijk, J.C. (2003). Autosomal recessive HEM/Greenberg skeletal dysplasia is caused by 3β-hydroxysterol Δ14-reductase deficiency due to mutations in the lamin B receptor gene. American Journal of Human Genetics *72*, 1013-1017.

Weber, K., Plessmann, U., and Traub, P. (1989). Maturation of nuclear lamin A involves a specific carboxy-terminal trimming, which removes the polyisoprenylation site from the precursor; implications for the structure of the nuclear lamina. FEBS Letters *257*, 411-414.

Weber, K., Riemer, D., and Dodemont, H. (1991). Aspects of the evolution of the lamin/intermediate filament protein family: A current analysis of invertebrate intermediate filament proteins. Biochemical Society Transactions *19*, 1021-1023.

Weinstein, J.N., Myers, T.G., O'Connor, P.M., Friend, S.H., Fornace, A.J., Kohn, K.W., Fojo, T., Bates, S.E., Rubinstein, L.V., Anderson, N.L.*, et al.* (1997). An

Information-Intensive Approach to the Molecular Pharmacology of Cancer. Science *275*, 343-349.

West, M.D., Shay, J.W., Wright, W.E., and Linskens, M.H.K. (1996). Altered expression of plasminogen activator and plasminogen activator inhibitor during cellular senescence. Experimental Gerontology *31*, 175-193.

Weyemi, U., Lagente-Chevallier, O., Boufraqech, M., Prenois, F., Courtin, F., Caillou, B., Talbot, M., Dardalhon, M., Al Ghuzlan, A., Bidart, J.M.*, et al.* (2012). ROS-generating NADPH oxidase NOX4 is a critical mediator in oncogenic H-Ras-induced DNA damage and subsequent senescence. Oncogene *31*, 1117-1129.

Wheaton, K., Sampsel, K., Boisvert, F.-M., Davy, A., Robbins, S., and Riabowol, K. (2001). Loss of functional caveolae during senescence of human fibroblasts. Journal of Cellular Physiology *187*, 226-235.

Williams, T.M., and Lisanti, M.P. (2004). The caveolin proteins. Genome Biology *5*, 214.

Wolda, S.L., and Glomset, J.A. (1988). Evidence for modification of lamin B by a product of mevalonic acid. J Biol Chem *263*, 5997-6000.

Wolstein, J.M., Lee, D.H., Michaud, J., Buot, V., Stefanchik, B., and Plotkin, M.D. (2010). INK4a knockout mice exhibit increased fibrosis under normal conditions and in response to unilateral ureteral obstruction. American Journal of Physiology - Renal Physiology *299*, F1486-F1495.

Worman, H.J., and Schirmer, E.C. (2015). Nuclear membrane diversity: underlying tissue-specific pathologies in disease? Current Opinion in Cell Biology *34*, 101-112.

Wu, G., Dawson, E., Duong, A., Haw, R., and Stein, L. (2014). ReactomeFIViz: a Cytoscape app for pathway and network-based data analysis. F1000Research *3*, 146.

Wu, G.S., Burns, T.F., McDonald, E.R., Jiang, W., Meng, R., Krantz, I.D., Kao, G., Gan, D.-D., Zhou, J.-Y., Muschel, R.*, et al.* (1997). KILLER/DR5 is a DNA damage-inducible p53-regulated death receptor gene. Nat Genet *17*, 141-143.

Wynn, R.M. (1967). Intrauterine Devices: Effects on Ultrastructure of Human Endometrium. Science *156*, 1508-1510.

Xie, H., Liu, F., Liu, L., Dan, J., Luo, Y., Yi, Y., Chen, X., and Li, J. (2013). Protective role of AQP3 in UVA-induced NHSFs apoptosis via Bcl2 up-regulation. Archives of Dermatological Research *305*, 397-406.

Xue, W., Zender, L., Miething, C., Dickins, R.A., Hernando, E., Krizhanovsky, V., Cordon-Cardo, C., and Lowe, S.W. (2007). Senescence and tumour clearance is triggered by p53 restoration in murine liver carcinomas. Nature *445*, 656-660.

Yamakoshi, K., Takahashi, A., Hirota, F., Nakayama, R., Ishimaru, N., Kubo, Y., Mann, D.J., Ohmura, M., Hirao, A., Saya, H.*, et al.* (2009). Real-time in vivo imaging of p16Ink4a reveals cross talk with p53. The Journal of Cell Biology *186*, 393-407.

Yamamoto, M., Clark, J.D., Pastor, J.V., Gurnani, P., Nandi, A., Kurosu, H., Miyoshi, M., Ogawa, Y., Castrillon, D.H., Rosenblatt, K.P.*, et al.* (2005). Regulation of Oxidative Stress by the Anti-aging Hormone Klotho. Journal of Biological Chemistry *280*, 38029-38034.

Yamashita, D., Kondo, T., Ohue, S., Takahashi, H., Ishikawa, M., Matoba, R., Suehiro, S., Kohno, S., Harada, H., Tanaka, J.*, et al.* (2015). miR340 suppresses the stem-like cell function of glioma-initiating cells by targeting tissue plasminogen activator. Cancer Research *75*, 1123-1133.

Yang, G., Rosen, D.G., Zhang, Z., Bast, R.C., Mills, G.B., Colacino, J.A., Mercado-Uribe, I., and Liu, J. (2006). The chemokine growth-regulated oncogene 1 (Gro-1) links RAS signaling to the senescence of stromal fibroblasts and ovarian tumorigenesis. Proceedings of the National Academy of Sciences of the United States of America *103*, 16472-16477.

Yang, J., Liu, X., Yuan, X., and Wang, Z. (2015). MiR-99b promotes metastasis of hepatocellular carcinoma through inhibition of claudin 11 expression and may serve as a prognostic marker. Oncology Reports *34*, 1415-1423.

Yang, T., Espenshade, P.J., Wright, M.E., Yabe, D., Gong, Y., Aebersold, R., Goldstein, J.L., and Brown, M.S. (2002a). Crucial step in cholesterol homeostasis: Sterols promote binding of SCAP to INSIG-1, a membrane protein that facilitates retention of SREBPs in ER. Cell *110*, 489-500.

Yang, Y.H., Dudoit, S., Luu, P., Lin, D.M., Peng, V., Ngai, J., and Speed, T.P. (2002b). Normalization for cDNA microarray data: a robust composite method addressing single and multiple slide systematic variation. Nucleic Acids Research *30*, e15.

Yepuri, G., Velagapudi, S., Xiong, Y., Rajapakse, A.G., Montani, J.-P., Ming, X.-F., and Yang, Z. (2012). Positive crosstalk between arginase-II and S6K1 in vascular endothelial inflammation and aging. Aging Cell *11*, 1005-1016.

Yoneyama, M., Kikuchi, M., Natsukawa, T., Shinobu, N., Imaizumi, T., Miyagishi, M., Taira, K., Akira, S., and Fujita, T. (2004). The RNA helicase RIG-I has an essential function in double-stranded RNA-induced innate antiviral responses. Nat Immunol *5*, 730-737.

Young, A.P., Schlisio, S., Minamishima, Y.A., Zhang, Q., Li, L., Grisanzio, C., Signoretti, S., and Kaelin, W.G. (2008). VHL loss actuates a HIF-independent senescence programme mediated by Rb and p400. Nat Cell Biol *10*, 361-369.

Young, A.R.J., and Narita, M. (2009). SASP reflects senescence. EMBO Reports *10*, 228-230.

Young, A.R.J., and Narita, M. (2010). Connecting autophagy to senescence in pathophysiology. Current Opinion in Cell Biology *22*, 234-240.

Young, A.R.J., Narita, M., Ferreira, M., Kirschner, K., Sadaie, M., Darot, J.F.J., Tavaré, S., Arakawa, S., Shimizu, S., Watt, F.M.*, et al.* (2009). Autophagy mediates the mitotic senescence transition. Genes & Development *23*, 798-803.

Yu, C.-E., Oshima, J., Fu, Y.-H., Wijsman, E.M., Hisama, F., Alisch, R., Matthews, S., Nakura, J., Miki, T., Ouais, S.*, et al.* (1996). Positional Cloning of the Werner's Syndrome Gene. Science *272*, 258-262.

Yu, J.L., May, L., Lhotak, V., Shahrzad, S., Shirasawa, S., Weitz, J.I., Coomber, B.L., Mackman, N., and Rak, J.W. (2005). Oncogenic events regulate tissue factor expression in colorectal cancer cells: Implications for tumor progression and angiogenesis. Blood *105*, 1734-1741.

Yu, Q., Katlinskaya, Yuliya V., Carbone, Christopher J., Zhao, B., Katlinski, Kanstantsin V., Zheng, H., Guha, M., Li, N., Chen, Q., Yang, T.*, et al.* (2015). DNA-Damage-Induced Type I Interferon Promotes Senescence and Inhibits Stem Cell Function. Cell Reports *11*, 785-797.

Zhang, J., Pickering, C.R., Holst, C.R., Gauthier, M.L., and Tlsty, T.D. (2006). p16INK4a Modulates p53 in Primary Human Mammary Epithelial Cells. Cancer Research *66*, 10325-10331.

Zhang, Q., Bethmann, C., Worth, N.F., Davies, J.D., Wasner, C., Feuer, A., Ragnauth, C.D., Yi, Q., Mellad, J.A., Warren, D.T.*, et al.* (2007). Nesprin-1 and -2 are involved in the pathogenesis of Emery - Dreifuss muscular dystrophy and are critical for nuclear envelope integrity. Human Molecular Genetics *16*, 2816-2833.

Zhang, R., Poustovoitov, M.V., Ye, X., Santos, H.A., Chen, W., Daganzo, S.M., Erzberger, J.P., Serebriiskii, I.G., Canutescu, A.A., Dunbrack, R.L.*, et al.* (2005). Formation of MacroH2A-containing Senescence-Associated Heterochromatin Foci and senescence driven by ASF1a and HIRA. Developmental Cell *8*, 19-30.

Zhu, F., Li, Y., Zhang, J., Piao, C., Liu, T., Li, H.-H., and Du, J. (2013). Senescent Cardiac Fibroblast Is Critical for Cardiac Fibrosis after Myocardial Infarction. PLoS ONE *8*, e74535.

Zhu, J., Woods, D., McMahon, M., and Bishop, J.M. (1998). Senescence of human fibroblasts induced by oncogenic Raf. Genes Dev *12*, 2997-3007.

Zhu, Y., Armstrong, J.L., Tchkonia, T., and Kirkland, J.L. (2014). Cellular senescence and the senescent secretory phenotype in age-related chronic diseases. Current Opinion in Clinical Nutrition and Metabolic Care *17*, 324-328.

Zhu, Y., Tchkonia, T., Pirtskhalava, T., Gower, A., Ding, H., Giorgadze, N., Palmer, A.K., Ikeno, Y., Borden, G., Lenburg, M.*, et al.* (2015). The Achilles' heel of senescent cells: from transcriptome to senolytic drugs. Aging Cell *14*, 644-658.

Zindy, F., Quelle, D.E., Roussel, M.F., and Sherr, C.J. (1997). Expression of the p16INK4a tumor suppressor versus other INK4 family members during mouse development and aging. Oncogene *15*, 203-211.

Zou, H., Stoppani, E., Volonte, D., and Galbiati, F. (2011). Caveolin-1, cellular senescence and age-related diseases. Mechanisms of Ageing and Development *132*, 533-542.